



UNIVERSITY OF SOUTHERN QUEENSLAND
Faculty of Engineering and Surveying

**Investigation of Stormwater Particles Generated From
Common Urban Surfaces**

A Dissertation Submitted by

Ian Malcolm Brodie

For the Award of

Doctor of Philosophy

2007

Principal Supervisor

Dr Mark Porter

Associate Supervisor

Dr David Thorpe

ABSTRACT

Pollution due to urban stormwater runoff is a significant environmental issue. Large regional devices including sediment ponds and constructed wetlands are common features in the urban landscape to treat runoff. In keeping with this approach, data requirements to evaluate stormwater impacts have mainly been met by the monitoring of sizeable urban catchments, typically greater than 10ha in area. Urban runoff characteristics have thus been conventionally linked with broadly defined catchment attributes. Land use, as defined by zonings such as Residential, Commercial and Industrial, is an attribute often used to evaluate stormwater runoff from urban catchments.

The emergence of Water Sensitive Urban Design (WSUD) in Australia is changing the management focus from the reliance on a small number of large-scale devices to many smaller-scale source controls distributed throughout the catchment. This paradigm shift in stormwater management places greater emphasis on small-scale processes within urban areas. Subsequently there is a need for more knowledge about stormwater generated from specific urban surfaces (roads, roofs, grassed areas etc).

The objective of this study was to demonstrate how urban stormwater quality can be managed on the basis of urban surfaces. The study involved the collection of data for typical urban surfaces and the development of predictive models to estimate stormwater quality. A series of case studies is provided to illustrate the use of surface-related data and modelling tools in stormwater management, particularly in the context of WSUD.

Non-Coarse Particles (NCP), defined as suspended solids less than 500 μ m in size, was selected as the stormwater pollutant under consideration. NCP is divided into the following particle size classes; Very Fine Particles (VFP, <8 μ m), Fine Particles (FP, 8-63 μ m) and Medium Particles (MP, 63-500 μ m). Laboratory methods to determine the concentration of these particle classes within stormwater runoff were adapted and refined from current standard methods. Organic content of each stormwater particle class was also determined.

An innovative device, the flow splitter, was developed to collect runoff samples from urban surfaces. The flow splitter was designed to obtain a composite flow-proportional sample, necessary to derive the Event Mean Concentration of

stormwater particles. Hydraulic and sediment testing of a prototype flow splitter confirmed that the device is an accurate and unbiased sampling method.

Flow splitters were installed at five monitoring sites within inner city Toowoomba, Australia. The sites have small catchments (50 to 450m² area) representative of urban impervious areas (galvanized iron roof, concrete carpark and bitumen road pavement) and pervious areas (grassed and exposed bare soil). Overall, runoff from 40 storms with rainfalls from 2.5mm to 64.3mm was sampled during the period December 2004 to January 2006.

A scatter plot analysis identified potential correlations between measured NCP loads and basic rainfall parameters such as rainfall depth and intensity. An exponential-type trend, consistent with many washoff models, is evident between load and average rainfall intensity for all surfaces. A composite index, referred to as the Rainfall Detachment Index (RDI), was found to be better than average rainfall intensity in explaining a relationship between NCP load and storm rainfall characteristics.

The insight gained from the RDI led to the development of a particle Mass Balance Model for impervious surfaces. Depending on the surface type, the model was able to provide reasonable estimates ($R^2 = 0.74$ to 0.97) against the measured NCP loads. Simpler analytical methods for particle load estimation were also developed in the study. A total of five methods were produced. An error analysis was conducted to compare the performance of each method to accurately reproduce the measured NCP loads. The analysis also included three methods used in current practice, which performed poorly compared to the new modelling techniques.

The analytical methods provide useful tools in urban stormwater planning. The Mass Balance Model and measured surface-specific data were used in a number of case study examples to demonstrate possible applications. The applications included assessments of 1) the relative contribution that different urban surfaces make to the particle load in runoff; 2) how surface-specific data can be directly transferred to represent a large-scale urban catchment located in a different climate; 3) the particle loads generated from Residential and Commercial land uses; 4) the effect of exposed areas of bare soil on the particle loads from a Residential catchment; 5) the effect that widespread adoption of rainwater tanks may have on particle concentration in Residential urban runoff and 6) the particle load reductions by the use of a grass swale to treat road runoff.

CERTIFICATION OF DISSERTATION

I certify that the ideas, experimental work, results, analyses and conclusions reported in this dissertation are entirely my own effort, except where otherwise acknowledged. I also certify that the work is original and has not been previously submitted for any other award, except where otherwise acknowledged.

Signature of Candidate

Date

ENDORSEMENT

Signature of Principal Supervisor

Date

Signature of Associate Supervisor

Date

ACKNOWLEDGEMENTS

This investigation involved a number of research activities including stormwater monitoring, laboratory analysis of samples and data modelling and analysis. Several people have made valuable contributions to these research activities during the course of the project.

Firstly, the support and guidance provided by my supervisors, Dr Mark Porter and Dr David Thorpe, has been excellent and contributed to the success of the project. The research was financially supported by the Condamine Alliance and I am grateful to Penny Cook and Mark Schuster for this assistance.

Members of the technical staff at USQ provided practical inputs to the project. Glen Bartkowski applied his considerable carpentry skills in fabricating the prototype sampling devices and associated testing rigs. Bernhard Black and Kim Larsen provided much appreciated support in the laboratory analysis of the stormwater samples. Chris Galligan built the five flow splitters that were used in the stormwater monitoring.

Toowoomba City Council also had a significant involvement in the project. Due to the concerted efforts of Sri Vigneswaran and Peter Lembo, the road sampling device was installed in a very timely fashion to sample a number of summer storms. Peter Keane provided rainfall and water quality data available from the Council monitoring system.

Other organisations provided data to complement the research project. Don Neale from the Queensland Environmental Protection Agency provided historical air quality data for Toowoomba. Alastair McHaig and Lucy Peljo made available data from the Brisbane City Council stormwater monitoring network for my use.

Finally, this dissertation would not have been completed without the care and support provided by my wife, Lyn, and my daughters, Ellen and Megan.

ASSOCIATED PUBLICATIONS

Brodie, I. and M. Porter (2004) *Use of Passive Stormwater Samplers in Water Sensitive Urban Design*. 'WSUD2004 Cities as Catchments' 2004 International Conference, Adelaide, Australia, 21-25 November 2004.

Brodie, I. (2005) *Stormwater Particles and Their Sampling Using Passive Devices*. 10th International Conference on Urban Drainage, Copenhagen, Denmark, 21-26 August 2005.

Brodie, I. (2005) *Suspended Solids in Stormwater Runoff from Various Urban Surfaces*. USQ Faculty of Engineering and Surveying Report to Condamine Alliance, September 2005.

Porter, M., **I. Brodie**, M. Achmad and V. Aravinthan (2005) *Researching Sustainable Future Urban Water Supplies*. Engineers Australia Southern Engineering Conference 2005 'Managing Resources for a Sustainable Future', Toowoomba, Australia, 15 October 2005.

Brodie, I. (2005) *Monitoring of Particle Washoff from Five Different Urban Surfaces*. Presentation to 15th Queensland Water Symposium, Brisbane, Australia, 23-24 November 2005.

Brodie, I. and M. Porter (2006) *Stormwater Particle Characteristics of Five Different Urban Surfaces*. 7th International Conference on Urban Drainage Modelling in conjunction with 4th International Conference on Water Sensitive Urban Design, Melbourne, Australia, 3-7 April 2006.

Brodie, I. (2006) *Prediction of Stormwater Particle Loads from Impervious Urban Surfaces Based on a Rainfall Detachment Index*. 7th International Conference on Urban Drainage Modelling in conjunction with 4th International Conference on Water Sensitive Urban Design, Melbourne, Australia, 3-7 April 2006.

Brodie, I. and M. Porter (2006) *Error Analysis of Methods to Estimate Suspended Solids Loads in Urban Stormwater*. Australian Journal of Water Resources (Accepted for publication).

Brodie, I., Rosewell, C. (2007) *Theoretical Relationships Between Rainfall Intensity and Kinetic Energy Variants Associated With Stormwater Particle Washoff*. Journal of Hydrology. Vol 340, No 1-2, pp 40-47, doi:10.1016/j.jhydrol.2007.03.019

Brodie, I., (2007) *Prediction of Stormwater Particle Loads from Impervious Urban Surfaces Based on a Rainfall Detachment Index*, Water Science and Technology. Vol 55, No 4, pp 49-56, doi:10.2166/wst.2007.094

GLOSSARY OF TERMS

Abbreviations

Abbreviation	Description
ARI	Average Recurrence Interval
CP	Coarse Particles (greater than 500µm in size)
DCIA	Directly Connected Impervious Area
EMC	Event Mean Concentration
FIP	Fine Inorganic Particles
FOP	Fine Organic Particles
FP	Fine Particles (8 to 63µm in size)
ICIA	Indirectly Connected Impervious Area
LID	Low Impact Development
MIP	Medium Inorganic Particles
MOP	Medium Organic Particles
MP	Medium Particles (63 to 500µm in size)
NCP	Non-Coarse Particles (less than 500µm in size)
NPDES	United States National Pollutant Discharge Elimination System
NSQD	United States National Stormwater Quality Database
NTU	Nephelometric Turbidity Units
NURP	United States Nationwide Urban Runoff Program
PSD	Particle Size Distribution
SAAEL	Sustainable Average Annual Export Load
SFVR	Sample Flow Volume Ratio
SSC	Suspended Sediment Concentration
SUDS	Sustainable Urban Drainage Systems
TMDL	Total Maximum Daily Loads
TSS	Total Suspended Solids
USGS	United States Geological Survey
USLE	Universal Soil Loss Equation
VFIP	Very Fine Inorganic Particles
VFOP	Very Fine Organic Particles
VFP	Very Fine Particles (less than 8µm in size)
VSS	Volatile Suspended Solids
WSUD	Water Sensitive Urban Design

Parameters

Symbol	Parameter	Units
$\sum I_6^2$	Sum of six-minute rainfall intensity squared	mm ² /hr ²
A	Surface catchment area	m ²
ADP	Antecedent dry period	hr
AMC	Antecedent moisture conditions	mm
AP	Antecedent rainfall depth	mm
AR _{DPdry}	Dry weather accumulation rate of detained particles on the surface before the storm	mg/m ² /hr
AR _{FPdry}	Dry weather accumulation rate of free particles on the surface before the storm	mg/m ² /hr
AR _{FPwet}	Wet weather accumulation rate of free particles on the surface during the storm	mg/m ² /hr
C	Runoff coefficient	-
C(t)	Particle concentration in stormwater at time <i>t</i>	mg/L
CLE	Cumulative load error	%
C _P	Adjustment factor to L _{drain} for very small rainfalls less than 3 to 5mm	%
D	Rainfall duration	hr
d _S	Representative particle size	µm
DT	Dry time during storm	hr
EI ₃₀	Rainfall erosivity index	-
e _K	Kinetic energy per unit rainfall depth	J/m ² /mm
E _K	Total rainfall kinetic energy for storm	J/m ²
F _{IC}	Adjustment factor to allow for indirectly connected impervious areas in urban catchments	-
h	Flow depth in grass channel	m
I	Average rainfall intensity	mm/hr
IBT	Interburst time during storm	hr
I _C	Critical average rainfall intensity for initiation of particle washoff	mm/hr
I _o	Average rainfall intensity corresponding to complete washoff of L _o	mm/hr
I _{tc}	Rainfall intensity for storm corresponding to time of concentration of the catchment	mm/hr
k	Decay coefficient for pollutant washoff	/s
K	Washoff coefficient in exponential washoff function	varies

L	Net particle load at point of discharge.	mg, kg, mg/m ²
<i>l</i>	Grass channel length	m
L _{DPdrain}	Detained particle load washed to the lateral drain during storm from surface	mg/m ²
L _{drain}	Total particle load in lateral drain available for mobilisation to point of discharge	mg/m ²
L _{FPdrain}	Free particle load washed to the lateral drain during storm from surface	mg/m ²
L _{RPdrain}	Retained particle load within the lateral drain at the end of the storm	mg/m ²
L _{DPsurf}	Detained particle load available for washoff on the surface during the storm	mg/m ²
L _{FPi}	Free particle load on the surface at the start of the storm	mg/m ²
L _{FPsurf}	Free particle load available for washoff on the surface during the storm	mg/m ²
L _i	Initial particle load on the surface that is easily washed off	mg/m ²
L _M	Measured load at point of discharge	mg/m ²
L _o	Particle load on surface available for washoff at start of storm	mg/m ²
L _P	Predicted load at point of discharge	mg/m ²
L _R	Particle load on surface available for washoff	mg/m ²
L _{RPSurf}	Free particle load retained on the surface at the end of the storm	mg/m ²
LR _{RPdrain}	Dry weather loss rate of retained particles in the drain before the storm.	%/hr
L _S	Surface length	m
Max _{DPdry}	Maximum detained particle load on surface prior to start of storm	mg/m ²
Max _{FPdry}	Maximum free particle load on surface prior to start of storm.	mg/m ²
Max _{FPwet}	Maximum free particle load on surface during the storm.	mg/m ²
MLE	Maximum load error	%
<i>n</i>	Number of events	count
N _{f,s}	Particle fall number	-
P	Rainfall depth	mm
Peak I ₆	Peak six-minute rainfall intensity	mm/hr
Peak I ₆ ²	Peak six-minute rainfall intensity squared	mm ² /hr ²

PI_{cr}	Peak I_6 resulting in 100% transport efficiency of net particles within lateral drain to point of discharge	mm/hr
PINT	Flow intensity of preceding storm	L/hr
PM_{10}	Concentration of airborne particles smaller than $10\mu\text{m}$	$\mu\text{g}/\text{m}^3$
q	Stormwater discharge per unit surface area	mm/s
Q	Stormwater peak discharge	L/s
$Q(t)$	Stormwater discharge at time t	L/s
R	Runoff depth	mm
R_C	Critical runoff rate for washoff for initiation of particle washoff	mm/hr
RDI	Rainfall detachment index	mm^3/hr^4
RDI_i	RDI corresponding to complete washoff of L_i	mm^3/hr^4
RDI_o	RDI corresponding to complete washoff of L_o	mm^3/hr^4
RP_{DPcr}	Critical threshold of rain power ($\sum I_6^2/D$) when complete washoff of detained particles occurs	mm^2/hr^3
RP_{FPcr}	Critical threshold of rain power ($\sum I_6^2/D$) when complete washoff of free particles occurs	mm^2/hr^3
R_{roof}	Roof runoff volume	kL
R_T	Total runoff volume for a storm event	L, m^3
S_a	Tank storage volume at end of previous storm	kL
S_c	Tank storage capacity	kL
S_D	Lateral drain slope	m/m
S_i	Tank storage volume at the start of the storm	kL
S_o	Water volume available for tank storage	kL
S_s	Surface slope to lateral drain	m/m
T	Trapping efficiency for d_s	-
TE_{drain}	Transport efficiency of net particles within lateral drain to point of discharge	%
U	Household demand for tank water	kL/ha/day
V	Average mean velocity between grass blades	m/s
VDS	Number of vehicles travelling on road surface during a storm	counts/event
VIDS	Vehicle traffic intensity on road surface during a storm	counts/mm/hr
V_s	Stoke's settling velocity for d_s	m/s

WE_{DP}	Washoff efficiency of detained particles to lateral drain	%
WE_{FP}	Washoff efficiency of free particles to lateral drain	%
W_S	Surface width	m
X	Rainfall or runoff parameter in exponential washoff function	-

TABLE OF CONTENTS

1	Introduction	1
1.1	Overview	1
1.2	Hypothesis and Objectives	4
1.3	Structure of the Thesis	4
2	Literature Review of Stormwater Particles from Established Urban Surfaces	8
2.1	Selected Stormwater Pollutant	8
2.2	TSS Sources and Processes in Urban Areas	9
2.3	Important Aspects of TSS Loads from Urban Surfaces	10
2.3.1	Event Mean Concentration as a Basis for TSS Loads	10
2.3.2	Urban Surface Type versus Land Use as a Basis for TSS Loads	11
2.3.3	Importance of Impervious Surfaces	13
2.3.4	Importance of Particle Size Characteristics	14
2.3.5	Importance of Organic Matter	17
2.3.6	Importance of Hydrological Factors	18
2.4	Runoff Quality from Urban Surfaces	19
2.4.1	Road Pavements	19
2.4.2	Car Parks and Driveways	21
2.4.3	Roofs	22
2.4.4	Grassed Areas	22
2.5	Methods to Measure TSS EMCs and Loads	23
2.5.1	Grab Sampling	23
2.5.2	Insitu Sampling – Automatic Pumping Samplers	23
2.5.3	Insitu Sampling - Passive Samplers	24
2.5.4	Turbidity Monitoring	26
2.5.5	Sampling Requirements	28
2.5.6	Sample Processing and Analysis	29
3	Current Context and Scope of Study	31
3.1	Current Context – Stormwater Runoff from Urban Surfaces	31
3.2	Current Context – Stormwater Infrastructure Planning Using Land Use Data versus Urban Surface Data	34
3.3	Scope of Study	38
3.3.1	Monitoring of Stormwater Runoff from Urban Surfaces	38
3.3.2	Application of Urban Surface Type as Basis for Stormwater Infrastructure Planning	39
4	Classification and Laboratory Analysis of Stormwater Particles	40
4.1	Stormwater Particle Classification	40
4.2	Laboratory Analysis of Stormwater Particles	41
5	Design and Testing of Passive Sampling Devices	45
5.1	Review of Passive Samplers	45
5.1.1	Gravity Flow Samplers	45
5.1.2	Siphon Flow Samplers	47
5.1.3	Rotational Flow Samplers	48

5.1.4	Flow Splitting Samplers	49
5.1.5	Direct Sieving Samplers	50
5.2	Selection of Passive Sampler Type	51
5.2.1	Flow Proportional Sampling	51
5.2.2	Catchment Area	52
5.2.3	Sample Capture and Isolation	52
5.2.4	Sample Volume	53
5.2.5	Selected Passive Sampler Type and Adopted Design Criteria	54
5.3	Concept Design of Selected Passive Samplers	55
5.3.1	Concept Design of Flow Splitter	55
5.3.2	Concept Design of Orifice-Weir	56
5.4	Hydraulic Testing of Passive Samplers	57
5.4.1	Hydraulic Testing Apparatus	57
5.4.2	Hydraulic Testing Procedures	58
5.4.3	Modifications to the Prototype Flow Splitter	58
5.4.4	Modifications to the Orifice-Weir	59
5.4.5	Hydraulic Test Results	60
5.5	Sediment Testing of Passive Samplers	60
5.5.1	Sediment Testing Apparatus	61
5.5.2	Sediment Testing Procedures	62
5.6	Sediment Test Results and Discussion	63
6	Collection of Stormwater Particle Data from Urban Surfaces	69
6.1	Location of Stormwater Monitoring	69
6.2	Description of Stormwater Monitoring Methods	69
6.3	Description of Stormwater Monitoring Sites	73
6.3.1	Description of Roof Monitoring Site	74
6.3.2	Description of Grassed and Bare Soil Monitoring Sites	76
6.3.3	Description of Carpark Monitoring Site	78
6.3.4	Description of Road Monitoring Site	80
6.4	Data Collected During Stormwater Monitoring	81
6.4.1	Rainfall Data	81
6.4.2	Stormwater Particle EMC Data	82
7	Analysis of Stormwater Particle Data	86
7.1	Summary of Data Analysis Methods	86
7.2	Hydrological Analysis using DRAINS	86
7.2.1	Description of DRAINS Model	86
7.2.2	Runoff Hydrograph Estimation Using DRAINS	87
7.2.3	Measured and Predicted Runoff Coefficients	89
7.2.4	Particle Load Estimates for Individual Storms	91
7.3	Box Plot Analysis of Particle EMC Data	93
7.3.1	Box Plots of Particle EMCs	93
7.3.2	Box Plots of Inorganic Content	94
7.3.3	Box Plots of Particle Size Composition	94
7.4	Scatter Plots of Impervious Surface NCP Load Data	98
7.4.1	Impervious Surface NCP Loads versus Rainfall Parameters	98
7.4.2	Impervious Surface Non-Coarse Particle Composition versus Average Intensity	108

7.5	Scatter Plots of Pervious Surface Non-Coarse Particle Load Data	112
7.5.1	Bare Surface Non-Coarse Particle Loads versus Rainfall Parameters	112
8	Relationships between Non-Coarse Particle Loads and Rainfall Parameters for Impervious Surfaces	116
8.1	Approach to Identify Relationships between Non-Coarse Particle Loads and Rainfall Parameters	116
8.2	General Form of Particle Washoff Relationship for Impervious Surfaces	116
8.3	Particle Washoff Relationships Using December 2004 to February 2005 Data	119
8.3.1	Use of Average Rainfall Intensity I	119
8.3.2	Identification of the Rainfall Detachment Index	122
8.4	Particle Washoff Relationships Using March 2005 to June 2005 Data	125
8.5	Particle Washoff Relationships Using July 2005 to January 2006 Data	129
8.6	Physical Basis of the Rainfall Detachment Index	132
8.6.1	General Form of Rainfall Detachment Index	132
8.6.2	Relationship between $\sum I_6^2$ and Rainfall Kinetic Energy E_K	133
8.7	Washoff Effects Unexplained by I and RDI	137
8.7.1	Effect of Dustfall on Roof Non-Coarse Particle Loads	137
8.7.2	Effect of Storm Duration and Rainfall Depth	139
8.8	Particle Washoff Relationships Using Selected December 2004 to January 2006 Data	145
9	Non-Coarse Particle Mass Balance Model for Impervious Urban Surfaces	151
9.1	Approach for Development of a Particle Mass Balance Model	151
9.2	Basic Conceptual Model of Particle Washoff Processes	151
9.2.1	Inclusion of Surface and Drainage System	152
9.2.2	Free and Detained Particles	152
9.2.3	Particle Detachment from the Surface Based on Rain Power	154
9.2.4	Particle Transport along the Lateral Drain Based on Peak Rainfall Intensity	155
9.3	Basic Conceptual Model of Particle Buildup Processes	156
9.3.1	Rapid Post-Storm Recovery of Free Particles	157
9.3.2	Relatively Constant Detained Particle Load	159
9.3.3	Particle Retention within the Lateral Drain	159
9.4	Initial Particle Mass Balance Model	160
9.4.1	Parameterisation of Initial Particle Mass Balance Model	160
9.4.2	Calibration of Initial Particle Mass Balance Model	162
9.5	Additional Particle Washoff and Buildup Processes	165
9.5.1	Particle Retention in Lateral Drain During Very Small Storms	167
9.5.2	Particle Loss in Drain After Storms	167
9.5.3	Wet Weather Particle Accumulation in Long Duration Storms	168
9.6	Refinement of Initial Particle Mass Balance Model	171
9.6.1	Parameterisation of Refined Particle Mass Balance Model	171
9.6.2	Calibration of Refined Particle Mass Balance Model	174
9.6.3	Validation of Refined Particle Mass Balance Model	176
9.6.4	Discussion on Parameter Selection for Refined Particle Mass Balance Model	179
10	Development of Planning Tools Based on Urban Surfaces	182
10.1	Planning to Achieve Water Quality Outcomes	182

10.2	Stormwater Particle Load Estimation Methods for Impervious Surfaces	182
10.3	Current EMC Based Methods for Particle Load Estimation	185
10.3.1	Arithmetic and Logarithmic Mean EMC Methods	185
10.3.2	Stochastic EMC Method	186
10.4	Proposed Methods for Particle Load Estimation	186
10.4.1	Rainfall Depth Adjusted EMC Method	186
10.4.2	Rainfall Intensity Adjusted EMC Method	189
10.4.3	Average I Method	193
10.4.4	RDI Method	193
10.4.5	Mass Balance Method	193
10.4.6	Particle Load Estimation Methods for Pervious Surfaces	194
10.5	Error Analysis of Stormwater Particle Load Estimation Methods for Impervious Surfaces	195
11	Application of Planning Tools	204
11.1	Approach to Application of Planning Tools	204
11.2	Relative Contribution of Urban Surfaces	204
11.3	Representation of Urban Land Use Based on Surface Composition	209
11.3.1	Description of Wynnum Stormwater Monitoring	210
11.3.2	Analysis of Stormwater Runoff Volumes for Wynnum	212
11.3.3	Analysis of Non-Coarse Particle Loads for Wynnum	213
11.4	Case Study Assessment of Stormwater Management Issues	217
11.4.1	Effect of Urban Land Use Type on Non-Coarse Particle Loads	217
11.4.2	Effect of Bare Soil Areas on Non-Coarse Particle Loads	221
11.4.3	Effect of Rainwater Tanks on Non-Coarse Particle Loads from Residential Areas	223
11.4.4	Effect of Grass Swales on Non-Coarse Particle Loads from Road Surfaces	227
12	Conclusions and Recommendations	233
12.1	Summary and Conclusions	233
12.1.1	Particle Classification and Laboratory Analysis	234
12.1.2	Design and Testing of Passive Sampling Devices	234
12.1.3	Collection and Analysis of Stormwater Particle Data from Urban Surfaces	236
12.1.4	Predictive Models to Estimate Particle Loads	237
12.1.5	Demonstration of Application of Stormwater Planning Tools	241
12.2	Recommendations for Further Research	244
13	References	246
Appendix A Stormwater Monitoring Data		269
Appendix B Mass Balance Model Calculations		278
Appendix C Case Study Calculations		287

LIST OF TABLES

■	Table 1.1 TSS concentrations (mg/L) in stormwater from urban land uses	2
■	Table 1.2 TSS concentrations (mg/L) in stormwater from urban surfaces	3
■	Table 1.3 Outlines of thesis chapters	5
■	Table 2.1 Grain size classification of sediments in the clay to sand range	15
■	Table 2.2 Pollutant fractions by weight associated with various particle sizes	16
■	Table 2.3 Requirements for representative event sampling	28
■	Table 3.1 Conventional planning process for urban stormwater quality management	35
■	Table 4.1 Examples of classifications used for stormwater particles	40
■	Table 4.2 Proposed classification of stormwater particles based on size range	40
■	Table 4.3 Features of the proposed particle classification scheme	41
■	Table 4.4 Adopted laboratory procedures for stormwater particle analysis	42
■	Table 5.1 Desirable attributes of a passive EMC sampler	51
■	Table 5.2 Adopted design criteria for passive EMC sampler	54
■	Table 5.3 Sediment test statistics normalised as a percentage of theoretical particle concentrations	65
■	Table 6.1 Basic properties of surface monitoring sites	74
■	Table 6.2 Definition of rainfall parameters	81
■	Table 6.3 Statistics of rainfall characteristics of storm events ($n=40$) during December 2004 to January 2006	82
■	Table 6.4 Arithmetic means and standard deviations of particle EMCs (mg/L) measured for December 2004 to January 2006 runoff events	83
■	Table 7.1 Soil type descriptions to define DRAINS Hortonian infiltration curves	88
■	Table 7.2 AMC starting points and preceding rainfalls	88
■	Table 7.3 Statistical means and standard deviations of runoff coefficients for December 2004 to February 2005 runoff events	90
■	Table 7.4 Statistical means and standard deviations of particle loads for December 2004 to January 2006 runoff events	93
■	Table 7.5 Definition of rainfall energy parameters	105
■	Table 7.6 Qualitative scale of degree of correlation	106
■	Table 7.7 Assessment of visual correlation between impervious surface Non-Coarse Particle loads and selected rainfall parameters	106
■	Table 7.8 Assessment of visual correlation between bare soil Non-Coarse Particle loads and selected rainfall parameters	112
■	Table 8.1 Exponential-type regression of Non-Coarse Particle loads against average rainfall intensity for December 2004 to February 2005 storm data	120
■	Table 8.2 Piecewise linear regression of Non-Coarse Particle loads against Rainfall Detachment Index for December 2004 to February 2005 storm data	125
■	Table 8.3 Regression of Non-Coarse Particle loads against I and RDI for selected December 2004 to January 2006 storm data	147
■	Table 9.1 Description of parameters used in initial particle Mass Balance Model	162

■	Table 9.2 Particle mass balance parameters calibrated against December 2004 to February 2005 Non-Coarse load data	163
■	Table 9.3 Description of parameters used in refined particle Mass Balance Model	174
■	Table 9.4 Refined particle mass balance parameters calibrated against March 2005 to June 2005 Non-Coarse load data	175
■	Table 10.1 Selected examples of planning approaches to manage stormwater pollutant loads	183
■	Table 10.2 Data requirements of Non-Coarse Particle load estimation methods	184
■	Table 10.3 Mean Non-Coarse Particle EMCs for December 2004 to January 2006 runoff events	185
■	Table 10.4 Arithmetic Mean Non-Coarse Particle EMCs for impervious surfaces based on discrete rainfall ranges for December 2004 to January 2006 runoff events	189
■	Table 11.1 Non-Coarse Particle load statistics (mg/m ² /storm) for monitored surfaces based on December 2004 to January 2006 runoff events	205
■	Table 11.2 Cumulative Non-Coarse Particle loads and runoff volumes from each surface for December 2004 to January 2006 storms, expressed as a ratio of the roof estimates	208
■	Table 11.3 Statistics of rainfall characteristics of selected Wynnum storms(<i>n</i> =27) during 1999	214
■	Table 11.4 TSS EMC statistics for Residential, Commercial and Industrial land uses from various stormwater monitoring studies	218
■	Table 11.5 Adopted surface composition (%) for hypothetical Residential and Commercial land uses	219
■	Table 11.6 Results of Non-Coarse Particle load analysis for hypothetical Residential and Commercial land uses based on Toowoomba December 2004 to January storms, on a per hectare basis	220
■	Table 11.7 Results of Non-Coarse Particle load analysis for hypothetical Residential land use with 10% bare soil based on Toowoomba December 2004 to January 2006 storms, on a per hectare basis	223
■	Table 11.8 Results of Non-Coarse Particle load analysis for hypothetical Residential land use with rainwater tank strategy based on Toowoomba December 2004 to January 2006 storms, on a per hectare basis	227
■	Table 11.9 Results of Non-Coarse Particle load analysis for 450m ² Toowoomba road surface with existing kerb and hypothetical grass swale based on December 2004 to January storms	231
■	Table 12.1 Brief descriptions of NCP load estimation methods for impervious surfaces	240
■	Table 12.2 Brief descriptions of examples and case studies to demonstrate application of stormwater planning tools	242

LIST OF FIGURES

■	Figure 5.1 Gravity flow sampler by Waschbusch <i>et al.</i> (1999)	45
■	Figure 5.2 Gravity flow sampler by Stein <i>et al.</i> (1998)	46
■	Figure 5.3 Siphon sampler used by Gray & Frisk (1992)	47
■	Figure 5.4 Flume and Coshocton wheel	48
■	Figure 5.5 Flow splitting sampler used by Clarke <i>et al.</i> (1981)	50
■	Figure 5.6 Side view of direct sieving sampler used by Pratt & Adams (1981)	50
■	Figure 5.7 Diagram showing the cross section and long section views of the flow splitter	55
■	Figure 5.8 Diagram showing the cross section and long section views of the orifice-weir sampling device	56
■	Figure 5.9 Flow diagram of hydraulic testing apparatus	57
■	Figure 5.10 Photograph of hydraulic testing apparatus in operation	58
■	Figure 5.11 Measured SVFR for prototype passive samplers based on hydraulic testing	60
■	Figure 5.12 Diagram showing the layout of the sediment testing apparatus	61
■	Figure 5.13 Photograph of sediment testing area	61
■	Figure 5.14 Theoretical particle concentrations of channel flow during the sediment tests	64
■	Figure 5.15 Individual sediment test results for MP, FP, VFP and FP+VFP normalised as a percentage of theoretical particle concentrations	65
■	Figure 6.1 Mean monthly rainfall and temperature for Toowoomba	69
■	Figure 6.2 Aerial view of monitoring sites showing individual catchments and sampler locations	70
■	Figure 6.3 Site layout plan of residential allotment showing location of monitored surfaces, samplers and rainfall instrumentation	72
■	Figure 6.4 Physical components of each surface monitoring site and definition of geometric parameters	73
■	Figure 6.5 Photograph of the roof sampler installation	75
■	Figure 6.6 Photograph of the roof sampling device	75
■	Figure 6.7 Photograph of the grassed and bare soil plots and installed samplers	76
■	Figure 6.8 Photograph of the carpark sampler installation	78
■	Figure 6.9 Site layout plan of carpark showing surface diverted to sampler	79
■	Figure 6.10 Photograph of the road sampler being installed	80
■	Figure 6.11 Plots of Non-Coarse Particle EMC against Rainfall Depth for December 2004 to January 2006 runoff events	85
■	Figure 7.1 Adopted Horton infiltration curves for grass and bare soil surfaces	89
■	Figure 7.2 Box plots of measured and estimated runoff coefficients for December 2004 to February 2005 runoff events	90
■	Figure 7.3 Plots of Non-Coarse Particle load versus rainfall depth for December 2004 to January 2006 runoff events	92
■	Figure 7.4 Box plots of EMCs for MPs, FPs, VFPs and Non-Coarse Particles for December 2004 to January 2006 runoff events	95
■	Figure 7.5 Box plots of inorganic content for MPs, FPs, VFPs and Non-Coarse Particles for December 2004 to January 2006 runoff events	96

■	Figure 7.6 Box plots of particle size composition of MPs, FPs and VFPs for December 2004 to January 2006 runoff events	97
■	Figure 7.7 Comparison of road mean particle size distribution for Non-Coarse Particles with Australian and Overseas envelopes for road and highway runoff	98
■	Figure 7.8 Scatter plots of roof Non-Coarse Particle loads against rainfall parameters for December 2004 to January 2006 runoff events – Antecedent and event rainfall parameters	99
■	Figure 7.9 Scatter plots of roof Non-Coarse Particle loads against rainfall parameters for December 2004 to January 2006 runoff events – Rainfall intensity and energy parameters	100
■	Figure 7.10 Scatter plots of carpark Non-Coarse Particle loads against rainfall parameters for December 2004 to January 2006 runoff events – Antecedent and event rainfall parameters	101
■	Figure 7.11 Scatter plots of carpark Non-Coarse Particle loads against rainfall parameters for December 2004 to January 2006 runoff events – Rainfall intensity and energy parameters	102
■	Figure 7.12 Scatter plots of road Non-Coarse Particle loads against rainfall parameters for December 2004 to January 2006 runoff events – Antecedent and event rainfall parameters	103
■	Figure 7.13 Scatter plots of road Non-Coarse Particle loads against rainfall parameters for December 2004 to January 2006 runoff events – Rainfall intensity and energy parameters	104
■	Figure 7.14 Scatter plots for roof particle compositions against average rainfall intensity for December 2004 to January 2006 runoff events	109
■	Figure 7.15 Scatter plots for carpark particle compositions against average rainfall intensity for December 2004 to January 2006 runoff events	110
■	Figure 7.16 Scatter plots for road particle compositions against average rainfall intensity for December 2004 to January 2006 runoff events	111
■	Figure 7.17 Scatter plots of bare soil Non-Coarse Particle loads against rainfall parameters for December 2004 to January 2006 runoff events – Antecedent and event rainfall parameters	113
■	Figure 7.18 Scatter plots of bare soil Non-Coarse Particle loads against rainfall parameters for December 2004 to January 2006 runoff events – Rainfall intensity and energy parameters	114
■	Figure 8.1 Exponential type form of particle washoff relationships	118
■	Figure 8.2 Roof, carpark and road Non-Coarse Particle loads plotted against average rainfall intensity based on December 2004 to February 2005 data	121
■	Figure 8.3 Roof, carpark and road Non-Coarse Particle loads plotted against RDI based on December 2004 to February 2005 data	123
■	Figure 8.4 Piecewise linear form of particle washoff relationships	124
■	Figure 8.5 Roof, carpark and road Non-Coarse Particle loads plotted against average rainfall intensity based on March 2005 to June 2005 data	126
■	Figure 8.6 Roof, carpark and road Non-Coarse Particle loads plotted against RDI based on March 2005 to June 2005 data	127
■	Figure 8.7 Storm durations and rainfall depths for December 2004 to February 2005 events compared with March 2005 to June 2005 events and July 2005 to January 2006 events	128
■	Figure 8.8 Roof, carpark and road Non-Coarse Particle loads plotted against average rainfall intensity based on July 2005 to January 2006 data	130
■	Figure 8.9 Roof, carpark and road Non-Coarse Particle loads plotted against RDI based on July 2005 to January 2006 data	131
■	Figure 8.10 Kinetic energy contents relationships based on Equations 8.5 and 8.6	134
■	Figure 8.11 Plot of E_K against $\sum I_6^2$ for December 2004 to February 2005 storm events	135
■	Figure 8.12 Plot of E_K/D against average rainfall intensity I for December 2004 to February 2005 storm events	136

■	Figure 8.13 Maximum daily PM ₁₀ for February 2005 recorded at Toowoomba	138
■	Figure 8.14 Maximum daily PM ₁₀ for October 2005 recorded at Toowoomba	138
■	Figure 8.15 Road Non-Coarse Particle loads plotted against I and RDI using December 2004 to January 2006 data grouped based on rainfall characteristics	141
■	Figure 8.16 Carpark Non-Coarse Particle loads plotted against I and RDI using December 2004 to January 2006 data grouped based on rainfall characteristics	143
■	Figure 8.17 Roof Non-Coarse Particle loads plotted against I and RDI using December 2004 to January 2006 data grouped based on rainfall characteristics	144
■	Figure 8.18 Road Non-Coarse Particle loads plotted against I and RDI using selected December 2004 to January 2006 data and showing fitted regression curves	148
■	Figure 8.19 Carpark Non-Coarse Particle loads plotted against I and RDI using selected December 2004 to January 2006 data and showing fitted regression curves	149
■	Figure 8.20 Roof Non-Coarse Particle loads plotted against I and RDI using selected December 2004 to January 2006 data and showing fitted regression curves	150
■	Figure 9.1 Conceptual model of basic washoff processes for urban impervious surfaces	152
■	Figure 9.2 Free and detained particles on impervious surfaces	153
■	Figure 9.3 Conceptual model of basic buildup processes for urban impervious surfaces	157
■	Figure 9.4 Parameterisation of initial particle Mass Balance Model for urban impervious surfaces	161
■	Figure 9.5 Regression plots of Average rainfall intensity I, $\sum I_6^2/D$ and Peak I ₆ based on December 2004 to February 2005 storm data	163
■	Figure 9.6 Washoff and transport efficiency curves (WE _{FP} , WE _{DP} and TE _{drain}) for roof, carpark and road surfaces used in initial Mass Balance Model	164
■	Figure 9.7 Plots of predicted and measured Non-Coarse loads using basic mass balance analysis of December 2004 to February 2005 storm data	166
■	Figure 9.8 Additional processes to the conceptual model of particle buildup and washoff for urban impervious surfaces	167
■	Figure 9.9 Definition of rainfall bursts and interburst period (IBP) and dry period (DP) using the 15/06/05 storm temporal pattern as an example	170
■	Figure 9.10 Parameterisation of refined particle Mass Balance Model	171
■	Figure 9.11 Washoff and transport efficiency curves (WE _{FP} and TE _{drain}) for roof, carpark and road surfaces used for in refined Non-Coarse Particle Mass Balance Model	176
■	Figure 9.12 Plots of predicted and measured Non-Coarse particle loads (mg/m ²) using refined mass balance analysis of December 2004 to June 2005 storm data	178
■	Figure 9.13 Plot of wet weather fine particle load (mg/m ²) on road surface used in refined mass balance analysis against the duration that rainfall intensity is within the range of 0.5 to 2mm/hr for December 2004 to January 2006 storm data	181
■	Figure 10.1 Relative position of stormwater pollutant estimation methods on a scale of increasing accuracy, data inputs and complexity	184
■	Figure 10.2 Daily rainfall frequency curve for Toowoomba based on 1980 to 2004 data	187
■	Figure 10.3 Box plots of Non-Coarse Particle EMCs in various rainfall ranges for impervious surfaces for December 2004 to June 2005 runoff events	188
■	Figure 10.4 Plot of road Non-Coarse EMCs against Rainfall Depth with interpolated contours based on average rainfall intensity	190
■	Figure 10.5 Plot of Peak I ₆ against Average Intensity I for December 2004 to January 2006 storms longer than 5 hours duration	192

■	Figure 10.6 Regression line of bare soil Non-Coarse Particle load against runoff depth for December 2004 to January 2006 runoff events	194
■	Figure 10.7 Plots of predicted EMC using EMC based methods and measured EMC for road surface and December 2004 to January 2006 runoff events	197
■	Figure 10.8 Plots of predicted EMC using Average I, RDI and Particle Mass Balance methods and measured EMC for road surface and December 2004 to January 2006 runoff events	198
■	Figure 10.9 Cumulative Load Error (CLE) using each estimation method for road surface and December 2004 to January 2006 runoff events	199
■	Figure 10.10 Maximum Load Error (MLE) for each estimation method for road surface and December 2004 to January 2006 runoff events	200
■	Figure 10.11 Error curves for each EMC and load estimation method for road surface and December 2004 to January 2006 runoff events	203
■	Figure 11.1 Mean runoff in response to rainfall for each surface based on December 2004 to January 2006 runoff events	206
■	Figure 11.2 Mean Non-Coarse Particle load in mg against rainfall ranges	207
■	Figure 11.3 Mean Non-Coarse Particle load as percentage of the total of the five surface loads against rainfall ranges	207
■	Figure 11.4 Distribution of roofs, roads, other impervious and pervious surfaces in Wynnum catchment from Ahlman & Fletcher (2003)	210
■	Figure 11.5 Plot of predicted and measured runoff volume at Wynnum monitoring site for 1999 to 2003 storms	213
■	Figure 11.6 Plot of $\sum I_6^2$ against rainfall depth for Wynnum 1999 storms and Toowoomba December 2004 to June 2005 storms	214
■	Figure 11.7 Plot of predicted Non-Coarse Particle EMC and measured TSS EMC at Wynnum monitoring site for 1999 storms	215
■	Figure 11.8 Plots of Non-Coarse Particle load contribution, runoff contribution and mean Non-Coarse Particle EMC for various rainfall ranges for hypothetical 1 ha Residential and Commercial areas and December 2004 to January 2006 storms	222
■	Figure 11.9 Plots of Non-Coarse Particle load contribution, runoff contribution and mean Non-Coarse Particle EMC for various rainfall ranges for hypothetical 1 ha Residential and Residential +10% Bare Soil areas and December 2004 to January 2006 storms	224
■	Figure 11.10 Plots of Non-Coarse Particle load contribution, runoff contribution and mean Non-Coarse Particle EMC for various rainfall ranges for hypothetical 1 ha Residential and Residential +Rainwater Tanks areas and December 2004 to January 2006 storms	228
■	Figure 11.11 Transport efficiency (TE_{drain}) curve for hypothetical grass swale based on Particle Fall Number ($N_{f,s}$) assuming no infiltration compared with curve for road kerb	230

1 Introduction

1.1 Overview

Stormwater runoff from urban areas conveys a wide range of pollutants including sediments, litter, trash, organic matter, nutrients, heavy metals, oils, surfactants and greases. The solid particles transported by stormwater runoff comprise both inorganic matter (from eroded sediments, deposits of airborne dust, road pavement wear etc) and organic matter (from vegetation, sewage overflows, litter, grass clippings etc). **Total Suspended Solids (TSS)** is the term used to describe the solid particles that are mobilised in runoff during a storm event.

Heavy metal (including lead, copper, cadmium and zinc) are often present in urban runoff in a dissolved form or adsorbed onto mainly inorganic sediments. Sediment particles also adsorb nutrients such as phosphorus. Hazardous pollutants including polycyclic aromatic hydrocarbons are mainly attached to suspended organic matter (Schueler 1987).

If not adequately managed, urban stormwater can detrimentally impact downstream receiving environments. Long term degradation of receiving waters can occur when pollutants adsorbed onto suspended solids accumulate in the sediments and subsequently dissolve into the water column under anoxic or low-pH conditions (Marsalek *et al.* 1997). Turbid waters often reflect the presence of suspended solids. A high level of turbidity limits light penetration in water and affects aquatic plant growth as well as reducing the aesthetic appeal of waterways.

To mitigate these impacts, many local government authorities have responded by placing greater emphasis on reducing or treating stormwater from urban areas. The issue is significant, as suspended sediment concentrations in urban stormwater are typically two to ten times greater than runoff from undisturbed non-urban catchments (Chiew *et al.* 1997b).

A key aspect of stormwater management is to understand the quantum of pollutant loads generated from urban areas. Traditionally, such understanding has been gained by stormwater monitoring of catchments that have a dominant land use or the land use composition is known. This approach follows from the common planning

classification of urban areas in terms of broad land use zones such as Residential, Commercial and Industrial areas.

Pollutant load can be expressed in several ways and **Event Mean Concentration (EMC)** is a common term in stormwater practice. The EMC is the flow-weighted concentration of a pollutant derived for an individual storm or statistically averaged over a number of storms. TSS concentrations, including EMCs, measured by selected studies of urban catchments are summarised in **Table 1.1**.

■ **Table 1.1 TSS concentrations (mg/L) in stormwater from urban land uses**

Study	Residential	Commercial	Industrial
Statistical mean of EMCs from worldwide review of literature by Duncan (1999)	141	133	150
Annual mean EMC for Brisbane, Australia from BCC (2003)	151	145	83
Median of EMCs from USA National Urban Runoff Program from Athayde <i>et al.</i> (1983)	101	69	-
Typical concentrations for Florida USA from Harper (1998)	72	94	94

An alternative to the land use-based approach is to view an urban area as comprising various types of surface, each with specific pollutant generation characteristics. These surfaces can include road pavements, paved and unpaved carparks, roofs, grassed areas and other discrete surfaces that form the mosaic of urban development. Conceptualising urban areas as being made up of various component surfaces has developed with the emergence of **Water Sensitive Urban Design**. WSUD involves management practices (e.g. rainwater tanks and grass swales) that can be implemented at a small scale within individual lots.

Significant amounts of EMC data are available for individual types of urban surfaces, especially road and highway pavements. Published studies have compiled and statistically analysed data to derive expected values of EMC for various urban surfaces. TSS concentrations from some of these studies are compiled in **Table 1.2**.

■ **Table 1.2 TSS concentrations (mg/L) in stormwater from urban surfaces**

Study	Roofs	Roads	Landscaped
Statistical mean of EMCs from worldwide review of literature by Duncan (1999)	36	257 ¹ , 69 ²	-
Residential area, Canada from Pitt & McLean (1986)	13	242	100
Central Paris, France from Gromaire-Mertz <i>et al.</i> (1999) – median EMCs	29	93	74 ³
Monroe, Wisconsin, USA from Wachbusch <i>et al.</i> (1999) – median EMCs	18	60 ⁴ , 64 ⁵	75 ⁶

Notes:

1. Classed as 'High' urban – greater than 67% residential development
2. Classed as 'Low' urban – less than 67% residential development
3. Landscaped areas included grassed and paved yards
4. Classed as 'Feeder' street – pavement runoff excluding kerb flow
5. Classed as 'Arterial' street – pavement runoff excluding kerb flow
6. Landscaped areas include lawns only

Only a limited number of studies have recognised that urban areas consist of a range of discrete surface types and then attempted to measure EMCs for these surfaces within the same geographical region. This is the intent of this study, with a focus on South East Queensland, Australia.

Monitoring of the quantity and quality of stormwater runoff from the basic surface types is required in order to apply this alternative approach. Simple and cost-effective sampling methods are needed to enable local government authorities to determine the pollutant generation characteristics for their geographical area. This aspect is addressed in the initial data collection and analysis phases of the dissertation.

The later phases of the thesis will describe how information relating to basic surface types can be applied in the planning of stormwater infrastructure within urban areas.

Currently our knowledge about the source of urban stormwater pollutants is mainly confined to broad land use categories. More detailed information is needed regarding the individual surfaces that collectively contribute to stormwater pollution in order to more effectively plan and design management strategies. Methods to analyse and model the pollutant loads generated from urban surfaces as inputs into the stormwater planning process are investigated. This aspect includes the analysis of the

collected data and the development of a suite of methods to predict stormwater particle loads at an individual surface scale.

The use of brand names in this dissertation is for explanatory purposes only and should not be interpreted as endorsement of any particular product.

1.2 Hypothesis and Objectives

The research hypothesis addressed in this dissertation is that “management of **urban stormwater quality** can be better planned on the basis of identification and analysis of the pollutant load from **component surfaces** than it can through conventional methods using a more aggregated **land use based** approach”.

The thesis is presented in several phases to achieve the following objectives:

- To establish a particle classification system and associated laboratory procedures suitable for the determination of suspended solids concentrations in urban runoff
- To develop a robust and cost effective sampling technique that can be used to measure stormwater pollutant loads generated from urban surfaces
- To monitor runoff from typical urban surfaces and characterise the amount and concentration of generated stormwater particles
- To develop predictive models that estimate the stormwater particle loads produced from urban surfaces
- To demonstrate approaches based on urban surfaces that can be applied to stormwater infrastructure planning in urban areas, in order to more effectively deliver improvements in water quality

The outcomes of this work represent an original contribution to knowledge in that they include new sampling techniques for the monitoring of stormwater runoff from urban surfaces and provide a better understanding of factors effecting stormwater quality. Innovative predictive models and methods to aggregate stormwater data from urban surfaces were established to assess the impacts of urban development and to evaluate management measures.

1.3 Structure of the Thesis

The structural development of the thesis is outlined in **Table 1.3**.

■ **Table 1.3 Outlines of thesis chapters**

Chapter 2 Literature Review of Stormwater Particles From Established Urban Surfaces

A review of literature concerning stormwater particles generated from urban surfaces is provided in Chapter 2 as background to the thesis. The review covers various aspects including particle sources and washoff processes, particle size characteristics, organic content, runoff qualities from various urban surfaces and land uses, sampling methods and laboratory analyses.

Chapter 3 Current Context and Scope of Study

The current context of the measurement and application of stormwater particle loads is described in Chapter 3. This material provided a basis to define the scope of the dissertation and to establish an appropriate methodology. It was identified that sampling techniques for stormwater runoff from small areas could be improved and a critical aspect of the thesis is the design and testing of an innovative runoff sampling device. A clear need exists for data and planning tools based on urban surfaces for use in stormwater management including **Water Sensitive Urban Design (WSUD)**.

Chapter 4 Classification and Laboratory Analysis of Stormwater Particles

A particle classification system as a basis for data collection and analysis is documented in Chapter 4. The system divides suspendable particles into four size classes; Very Fine, Fine, Medium and Coarse. Collectively the first three size classes are referred to as **Non-Coarse Particles (NCP)**. Each class is further subdivided into its organic and inorganic fractions, yielding a total of eight particle subclasses. Laboratory techniques to measure the concentration of each particle class in stormwater runoff samples are developed and developed in this Chapter.

Chapter 5 Design and Testing of Passive Sampling Devices

A description of the concept design and development of two passive sampling devices (a flow splitter and an orifice-weir device) is provided in Chapter 5. Hydraulic testing of both types of sampler was undertaken to determine their performance in obtaining a sample volume suitable for laboratory analysis. Sediment testing was also conducted to determine the ability of the devices to capture unbiased Non-Coarse Particle samples.

Chapter 6 Collection of Stormwater Particle Data from Urban Surfaces

Data collection procedures related to stormwater runoff from urban surfaces are documented in Chapter 6. Five flow splitters were constructed and installed at selected urban surfaces ranging from 50 to 450 m² in area. The sites included a road pavement, a carpark, a galvanised roof, a grassed area and a bare soil area located in Toowoomba, Queensland. Samples were collected for a total of 40 storms during the period from November 2004 to January 2006. Laboratory analysis was conducted to determine particle EMCs and inorganic contents.

Chapter 7 Analysis of Stormwater Particle Data

A hydrological model, DRAINS, described by O'Loughlin & Stack (2003), was used to predict runoff volumes from each surface during individual storms. Particle load, expressed as mg/m², was derived from the product of the measured EMC and estimated runoff volume. Box plots of particle EMCs were prepared to make comparisons between the monitored surfaces. Scatter plots of particle loads were generated to assess potential correlations between particle loads and various hydrological parameters.

Chapter 8 Relationships Between Non-Coarse Particle Loads and Rainfall Parameters for Impervious Surfaces

An exponential regression relationship between Non-Coarse Particle load and average rainfall intensity was found to provide a reasonable match to measured data, particularly for storm durations less than 5 hours. A composite index, referred to as the **Rainfall Detachment Index** (RDI), was identified as a basis to further explain the relationship between Non-Coarse Particle load and storm characteristics. RDI utilizes 6-minute rainfall intensities and is a variant to the well known Rainfall Erosivity Index (EI₃₀) used in soil erosion estimation.

Chapter 9 Non-Coarse Particle Mass Balance Model for Impervious Urban Surfaces

A conceptual model of particle load generation from impervious surfaces was postulated to provide a descriptive view of physical processes represented by the RDI. The conceptual model was then used to develop a predictive model of particle mass balance on impervious surfaces in response to rainfall. Refinements were made to the Mass Balance Model to allow for traffic-related particle accumulation during long duration storms.

Chapter 10 Development of Planning Tools Based on Urban Surfaces

A range of methods to estimate stormwater particle loads are described in Chapter 10. The methods developed as part of the thesis involve varying levels of data needs, complexity and subsequent accuracy of results. Eight methods were evaluated, including five new methods based on the regression relationships and Mass Balance Model developed in Chapters 8 and 9. An error analysis highlights the capabilities and limitations of each method as planning tools to estimate particle loads and concentrations.

Chapter 11 Application of Planning Tools

Specific examples of the application of the methods to predict particle loads are described in Chapter 11. The examples include an assessment of the relative contribution of urban surfaces to particle load, the representation of urban land use based on surface composition and the effect of stormwater measures such as grass swales and rainwater tanks. The case studies demonstrate how the urban surface based methods can be applied to a range of stormwater management and WSUD issues.

Chapter 12 Conclusions and Recommendations

The main conclusions of the thesis are summarised in Chapter 12 and recommendations for further research are also provided.

2 Literature Review of Stormwater Particles from Established Urban Surfaces

2.1 Selected Stormwater Pollutant

Stormwater from urban areas can convey a wide range of pollutants including sediments, litter, organic matter, nutrients, pathogens, heavy metals, oils and greases.

Total Suspended Solids (TSS) is often regarded as a generic or surrogate indicator of urban stormwater pollution. Heavy metals, hydrocarbons and phosphorus are closely associated with TSS as these pollutants are adsorbed onto fine particles (Chebbo & Bachoc 1992; Thomson *et al.* 1997; Urbonas 1991). TSS is also a key pollutant as deposition of suspended solids can cause blockage of stormwater infrastructure, modify flow conditions in open channels and disrupt aquatic habitats. Turbidity due to fine particles remaining in suspension also reduces light penetration in water bodies.

The terms suspended sediments, total solids, suspended solids, suspended material and nonsettleable solids have been used interchangeably with TSS to describe the suspended solid-phase material in stormwater (James 2003).

The USGS and US Federal Highway Administration conducted an extensive study of the use of TSS to characterise suspended sediments in runoff. In November 2000, the USGS issued a policy (US GS 2000a) that established the Suspended Sediment Concentration (SSC) method of analysis as the preferred standard for runoff analysis. James (2003) also questions the reliability of TSS as suitable measure for stormwater particles.

*On the basis that it is a generic measure of urban stormwater quality, suspended solids was selected as the main pollutant to be considered by the study. The SSC method of analysis was selected as the preferred technique to analytically measure suspended solids in stormwater runoff. A further discussion in relation to the TSS and SSC analytical methods is provided in **Section 2.5.6** of this Chapter. It should be noted that the vast majority of previous studies in this field have adopted TSS as a measure of suspended solids.*

2.2 TSS Sources and Processes in Urban Areas

In general terms, sources of TSS include wet and dry atmospheric deposition, wear of road surfaces and from vehicles, soil disturbance due to construction activities and erosion of pervious areas by wind and water (Pitt 1979).

The processes of buildup and washoff generally describe the introduction of TSS and other pollutants into stormwater, especially from impervious surfaces.

Buildup is the accumulation of particles that are deposited onto surfaces during dry weather. Using roads as an example, vehicle motion and atmospheric fallout leads to continuous deposition of particles onto road pavements. Sources of particles or 'road dust' include material arising from wear of the pavement, tyres, brake linings, corrosion of vehicle bodywork and soil eroded from adjacent surfaces.

The mass of road dust increases with time during dry weather periods, but the accumulation rate may be irregular and non-linear (Birch & Scollen 2003). A maximum or equilibrium limit of sediment accumulation generally applies, as removal and dispersal processes such as street cleaning and wind action tend to offset deposition processes (Ball *et al.* 1996).

Washoff is the process of deposited material being removed in wet weather by rainfall and runoff. Duncan (1995) concluded that washoff is driven by rainfall energy. The energy of falling raindrops dislodges surface particles, which are suspended within the surface water film. As the water film builds up and flows downslope, the energy to retain the particles in suspension is provided by the moving water. Both surface dislodgment and overland flow processes are governed by rainfall intensity.

Construction activity and other forms of soil disturbance can have a major effect on washoff quality. Washoff loads of TSS can be increased by a factor of 100 or more by soil disturbance in a catchment (Pisano 1976). In this respect, water quality is affected by two distinct phases of urbanisation (Schueler 1992). During construction, erosion of disturbed surfaces and sedimentation are key issues. After development is established, the accumulation and washoff of deposits, mainly from impervious surfaces, becomes a major water quality issue.

Buildup and washoff are key processes that act on urban surfaces that directly introduce TSS into stormwater runoff. There are additional processes downstream of these surfaces that further add to TSS load from urban areas. Erosion of degraded, unstable waterways may lead to high rates of sediment loads. For example, Trimble (1997) found that erosion of the San Diego Creek in California represented about two-thirds of the total sediment yield generated from an urbanising catchment.

*The focus of the thesis is the contribution of washoff from primarily **established** urban surfaces to the TSS load in stormwater runoff. Although important, the investigation of runoff from temporary construction sites and other sources such as waterway erosion is not within the scope of this study.*

2.3 Important Aspects of TSS Loads from Urban Surfaces

2.3.1 Event Mean Concentration as a Basis for TSS Loads

The simplest method for estimating stormwater TSS loads is based on the **Event Mean Concentration** (EMC). The EMC is defined as the total mass L discharged during a runoff event divided by the total runoff volume R_T discharged during the event (Huber 1993). Mathematically, EMC is a flow-weighted average as shown in **Equation 2.1**.

$$EMC = \frac{L}{R_T} = \frac{\int C(t)Q(t)dt}{\int Q(t)dt} \quad [2.1]$$

where $C(t)$ is the TSS concentration at time t and $Q(t)$ is the discharge at time t .

An EMC may be determined by collecting a bulk sample, by physically combining a number of discrete samples into a composite sample, or by mathematically calculating a flow-weighted composite value from analysis of multiple discrete samples taken during the runoff period (Bent *et al.* 2001).

Monitoring of urban catchments suggest that EMC varies from one storm to another, following a log-normal distribution (Athayde *et al.* 1983; Driscoll 1986; Sharpin 1995). It is important to monitor a number of storm events to capture this variability. Leecaster *et al.* (2002) recommend that seven storms is the minimum number to be

monitored. WSDE (2002) in their guidelines for evaluating emerging stormwater treatment technologies suggest that from 12 to 35 events should be sampled.

In practice, the product of EMC and runoff volume R_T is used to determine the pollutant mass loading L . This calculation can be done for individual storms and then annualised to derive an average annual load (expressed in kg/year). Local government authorities and other agencies commonly use annual load estimates to quantify the water quality impacts of urban runoff in receiving waters.

A key part of the thesis is to measure EMCs for a range of storm events in order to characterise its variability and also to provide a basis to determine mean annual load or other statistical measures that can be used to quantify TSS loads from various urban surface types.

2.3.2 Urban Surface Type versus Land Use as a Basis for TSS Loads

The export of TSS loads from urban catchments is often specified in terms of land use zoning (e.g. Residential, Commercial and Industrial) as this type of broad town planning data is readily available.

The USEPA Nationwide Urban Runoff Program (NURP) measured runoff qualities from 81 sites within the USA, divided into Residential, Mixed, Commercial, Industrial and Open/Non-urban land use categories (Athayde *et al.* 1983). Differences between the runoff qualities of the various land uses were found to be not significant, except for the Open/Non-urban land use types.

Contrary to the NURP results, Brezonik & Stadelmann (2002) found significant differences in event mean concentrations (EMCs) among land use groups within the Twin Cities Metropolitan Area of Minnesota. However, the correlation of EMC values to catchment attributes such as land use composition and impervious area was found to be weak. In Australia, local stormwater monitoring by Brisbane City Council also suggests that EMCs differ between certain types of land use such as Residential and Industrial (City Design 2000).

Both the Twin Cities and Brisbane studies used data specific to a geographical region. This may partly explain why these local studies found differences in EMCs amongst land use groups, whereas the wider NURP study, which pooled data from a

number of climatic regions, found no such trends. This observation is corroborated by the work of Duncan (1995) who found that the runoff quality from various land use types were not significantly different when 21 water quality parameters from 508 sites pooled from technical literature world-wide were analysed. In contrast, highly significant differences in stormwater quality among urban surface types (roof, pavement, roads, etc) were identified.

Despite the potential lack of differentiation, using land use zoning as a means of determining TSS load characteristics is common practice in Australia and elsewhere. Users of catchment-based models such as AQUALM, EMSS and MUSIC generally apply land use as a basis to estimate pollutant loads as this data directly relates to the management question that is frequently posed: “What is the expected change in stormwater quality if land use within a catchment is modified?” At a catchment scale (greater than 10 ha), using land use as a basis to estimate stormwater loads is a simple and convenient approach.

Recognition is emerging in Australia that the type of urban surface may be superior to the land use category as a basis of determining stormwater loads. The draft Chapter 3 of Australian Runoff Quality (IEAust 2003) outlines the limitations of using land use zoning and offers a method to estimate stormwater loads from ungauged catchments using surface characteristics (from Phillips & Thompson 2002).

There is also an emerging trend of applying management practices distributed throughout a catchment in preference to a smaller number of large “end of pipe” systems such as constructed wetlands and detention basins. These distributed practices can be applied at a lot scale (less than 1 ha) and are referred to as Low Impact Development (LID), Sustainable Urban Drainage Systems (SUDS) or Water Sensitive Urban Design (WSUD). It is considered that stormwater loads based on specific land surfaces, rather than the more broadly defined land use, would be required to more effectively assess the performance of these types of small-scale measures.

*The thesis will investigate the TSS washoff from specific types of **surfaces** that occur in urban areas, as distinct to runoff from areas of homogeneous land use.*

2.3.3 Importance of Impervious Surfaces

TSS load from an urban surface is a function of both the quantity and quality of stormwater runoff. The amount and frequency of surface runoff is thus a key factor in governing stormwater loads. On this basis, hydrological behaviour is an important aspect and it is for this reason that urban surfaces are generally grouped as being impervious or pervious.

- **Impervious** – Urban surfaces including roofs, paved car parks, footpaths and roadways that allow no or minimal infiltration of rainfall into the ground. A high proportion of rainfall directly runs off these surfaces. Impervious surfaces are often directly connected to the stormwater drainage system, referred to as Directly Connected Impervious Area (DCIA). Alternatively, Indirectly Connected Impervious Area (ICIA) describes surfaces where there is no direct link to the stormwater drainage. An example of ICIA is a roof surface that drains to a downpipe connected to a backyard bubbler outlet.
- **Pervious** – Urban surfaces such as lawns, landscaped areas and road verges that allow infiltration of rainfall into the underlying soil. Due to this infiltration capacity, pervious areas have a rainfall- runoff response that is markedly different to those of impervious areas.

In comparison to other surface types, impervious surfaces yield greater stormwater volumes and peak runoff rates and also provide a site for traffic-generated residues and airborne pollutants to accumulate. The hard nature of most impervious surfaces means that a proportion of residue buildup is efficiently washed off by even very minor rainfall events. It is for these reasons that the amount of DCIA within a catchment is a key factor in poor urban runoff quality.

A study in the USA (Beach 2003) concluded that the biological condition of downstream streams are likely to be degraded due to increased flows, higher temperatures and poor water quality in catchments where as little as 10% of the area consists of impervious surfaces. Recent research in Australia (Ladson *et al.* 2003) suggests that a degraded ecological condition of streams is highly correlated to Drainage Connection, defined as the proportion of impervious areas in a catchment that is directly connected to a stream by a stormwater pipe or sealed drain.

Small, frequent rainfall events are important in stormwater quality management as they may contribute the bulk of pollutant loads over time. Guo & Urbonas (1996) demonstrated that nearly 95 percent of runoff-producing events at Denver, Colorado are smaller than a two-year Average Recurrence Interval (ARI) storm. An analysis of a Malaysian urban area with 50% DCIA indicated that 95% of the annual runoff volume was generated by storms of 6 month ARI or less (MDID 2001). Analyses of Australian urban catchments indicate that the sum of the stormwater flows up to the 1 year ARI can represent greater than 95% of the mean annual runoff volume (IEAust 2003).

Most runoff from urban catchments for minor, frequent storms is generally derived from impervious surfaces. Infiltration into pervious areas means that runoff is typically generated from these surfaces only during rainfalls greater than at least 5 to 10mm. For smaller rain depths, almost all the runoff and pollutants originate from impervious surfaces (Pitt & Voorhees 2000).

Impervious surfaces can be the dominant generator of surface runoff as this type of surface initiates runoff more frequently than pervious surfaces. For example, Lee & Heaney (2003) predicted over a 52 year simulation period that DCIA covering 44% of a residential catchment situated in Boulder, California contributed 72% of the total runoff volume. The relative importance of the different surfaces is, however, highly dependent on the specific land use and rainfall patterns (Pitt & Voorhees 2000).

An understanding of the runoff generation characteristics of both impervious and pervious urban surfaces, including knowing when runoff is initiated, is considered to be an important aspect of the proposed research. Impervious surfaces, especially DCIA, have the highest potential to cause frequent water quality impacts to downstream waters and this is a key factor in selecting the dominant types of surfaces investigated in this study. Minor storms less than 6 months to 1 year ARI magnitude should be targeted in terms of stormwater runoff monitoring.

2.3.4 Importance of Particle Size Characteristics

A classification of particles based on grain size is shown in **Table 2.1** (from Bent *et al.* 2001). It should be noted that several particle classification systems are available. Dense mineral particles generally only remain in suspension if within the silt range

or smaller ($<62\mu\text{m}$), but sand-sized particles can be temporarily suspended by flowing waters (Davies-Colley & Smith 2001).

■ **Table 2.1 Grain size classification of sediments in the clay to sand range**

Clay Range (0.5 to 4 μm)		Silt Range (4 to 62 μm)		Sand Range (62 to 2000 μm)	
Class	Particle Size	Class	Particle Size	Class	Particle Size
Very fine clay	0.24 – 0.50	Very fine silt	4 - 8	Very fine sand	62 - 125
Fine clay	0.50 – 1.0	Fine silt	8 - 16	Fine sand	125 - 250
Medium clay	1 - 2	Medium silt	16 - 31	Medium sand	250 - 500
Coarse clay	2 - 4	Coarse silt	31 - 62	Coarse sand	500 - 1000
				Very coarse sand	1000 - 2000

Medium sand up to 500 μm maximum size may be accepted as an upper limit for suspended matter as larger particles tend to be conveyed in stormwater as bedload (Lloyd & Wong 1999). Protocols developed by the Washington State Department of Ecology (WSDE 2002) for the testing of new stormwater treatment technologies also define TSS as matter smaller than 500 μm in diameter.

Research by Muthukaruppan *et al.* (2002) suggests that the particle size distribution (PSD) within urban runoff varies with catchment geology. Stormwater samples from four sedimentary catchments in Melbourne exhibited a coarser PSD compared to samples from a basaltic catchment in Brisbane. Within each catchment, there were minimal differences in the PSDs for different storms. Sampling within storm events found that PSD became finer through the event, with the larger particles dominating the rising limb of single peak events. This outcome is similar to findings by Furumai *et al.* (2001) who investigated the washoff behaviour of coarse and fine particle fractions within the overall TSS load generated from an urban catchment near Tokyo, Japan.

Particles smaller than 100 μm made up between 60 to 95% by mass of the TSS load in the Melbourne study. This outcome is consistent with Lloyd & Wong (1999) who concluded that runoff from road and highway surfaces in Australia have a relatively high proportion of finely graded sediments. Results from a small number of

Australian studies show that 65% or more of the TSS were finer than 100 μm , compared to less than 25% based on similar studies in Europe and USA.

Particles deposited on road surfaces tend to be coarser than the sediment material in washoff samples. Less than 15% of dry samples collected manually from an urban road surface in Melbourne were finer than 100 μm (Vaze & Chiew 2002). This is mainly due to the ease at which rain and flow can transport the finer particles and the dissolution of the coarser particles during storm events.

Many contaminants are closely associated with suspended sediments. Metals, hydrocarbon by-products, nutrients and pesticides readily attach to sediments finer than 63 μm due to the higher specific surface area that is available (DeGroot 1995; Greb & Bannerman 1997; Randall *et al.* 1982). Simple relationships are available to predict the association of contaminants with specific surface area, including those by Ball (2000) derived for heavy metals and phosphorus.

As indicated in **Table 2.2**, contaminants can also be associated with coarser particles. Biological and chemical oxygen demand, volatile solids and nitrogen are largely associated with sand sized particles (Sartor *et al.* 1974).

■ **Table 2.2 Pollutant fractions by weight associated with various particle sizes¹**

Pollutant	Fraction of Total (% by weight)		
	<43 μm	43-246 μm	>246 μm
Total solids	5.9	37.5	56.5
Biological oxygen demand	24.3	32.5	43.2
Chemical oxygen demand	22.7	57.4	19.9
Volatile solids	25.6	34.0	40.4
Kjeldahl nitrogen	18.7	39.8	41.5
All heavy metals		51.2 ²	48.7
All pesticides		73.0 ²	27.0

Notes:

1. Sourced from Sartor *et al.* (1974)
2. Data provided for particle size less than 246 μm

Heavy metals tend to be equally associated with clay, silt and sand particles. Similar results were obtained by Regenmorter *et al.* (2002) in their study of highway runoff near Lake Tahoe, California. This pattern may be due to the various forms of heavy metals that are available including adsorbed onto fine sediments, as intact metal

particulates and as inclusions in or on inert compounds (Birch & Scollen 2003). Phosphates and pesticides are associated with silts and clays.

A particle size of 500 μm (medium sand) was adopted as the upper limit for suspended sediments in stormwater for the purpose of this thesis. Contaminant associations can be present over the full spectrum of particle size from clay, silts to sands. On this basis, stormwater sampling methods were aimed at obtaining representative samples of TSS size gradations smaller than 500 μm . Ideally, it would be useful to subdivide the TSS sample at least into coarse and fine fractions, as washoff behaviour is different for these particle size ranges. It is recognised that most of the TSS washed from roads and other impervious surfaces could be finely graded and less than 100 μm in size.

2.3.5 Importance of Organic Matter

Gross organic matter that may be mobilised by stormwater runoff, such as grass clippings and leaves, can release significant amounts of nutrients when decomposing under wet conditions (McCann & Michael 1999; Strynchuk *et al.* 1999). Organic matter washed into receiving waters can lead to oxygen depletion and eutrophication effects such as algal blooms.

Sansalone & Tittlebaum (2001) investigated particulates washed from a major road overpass in Louisiana, USA and found that organic matter represented 29%, on average, of the TSS concentration. The organic fraction of suspended solids collected in Paris, France varied from 40 to 70% in street runoff to 14 to 68% in roof runoff (Gromaire-Mertz *et al.* 1999).

Organic particles typically have low relative densities and remain suspended, even at macroscopic sizes (> 1mm). Studies of highway runoff have found that many of the particles finer than 40 μm are organic with specific gravities less than 1.5 (Sansalone & Buchberger 1997). By comparison, the specific gravity of inorganic sediments typically ranges from 2.6 to 2.8 (US ACE 1995).

The fraction of stormwater particles that are in an organic form has important management implications. Treatment processes such as settling are not as effective for organic matter compared to the heavier inorganic sediments. Organic matter

can also lead to significant water quality impacts to downstream waterways. The determination of the organic fraction of stormwater particles is considered to be an important aspect of the research.

2.3.6 Importance of Hydrological Factors

Apart from the physical characteristics of the surface, hydrological parameters such as rainfall intensity, rainfall depth, runoff volume and antecedent dry period are anticipated to influence the TSS loads washed from urban surfaces.

At a broad level, some studies suggest that the runoff volume is more critical than pollutant EMC in the determination of TSS load. Charbeneau & Barrett (1998) demonstrated that simply using a constant EMC applied to all types of land use was adequate to predict TSS load to a preliminary screening level. Differences in TSS load estimates were then solely due to the runoff generation characteristics of each land use, but even so, the predicted loads reasonably matched the measured loads. Some studies (Haster & James 1994; Rushton 2001) have considered that the TSS loads contributed from pervious grassed surfaces as being insignificant due to their low runoff characteristics.

Using regression methods, Irish & Barrett (1998) determined that more than 90% of the variation in TSS load from an expressway site in Austin, Texas could be explained by four hydrologic variables. These variables were the runoff volume, the flow intensity (runoff volume/storm duration), the duration of the antecedent dry period (ADP), and the flow intensity of the preceding storm (PINT). The last two variables were found to be significant. TSS load was found to increase with an increase in the ADP and decrease with an increase in the PINT.

Using stochastic modelling, Le Boutillier *et al.* (2000) established a reasonable correlation ($R^2=0.80$) between TSS load from a residential catchment in Saskatchewan and two hydrological parameters; the average five-minute rainfall intensity and the rainfall depth. However, significant errors (up to 88%) were found if this correlation was used to predict the TSS load from individual storm events.

Some studies (e.g. Chiew *et al.* 1997a) place a greater importance on washoff processes rather than buildup of pollutants during dry weather, as individual storms remove only a small proportion of the surface load that is available. Pollutant

washoff thus can be limited by the capacity of rainfall and runoff to mobilise and transport pollutants from the surface (i.e. transport limiting rather than source limiting). Tomanovic & Maksimovic (1996) also found for an asphalt street surface that buildup is a less important process compared to washoff.

Field and laboratory experiments by Vaze & Chiew (2003) suggest that the turbulence and energy due to falling raindrops and the shear stress imparted by surface runoff are both important washoff processes. This was based on rainfall simulator tests on small impervious plots that were screened to dissipate raindrop impact. The washoff loads from the screened plots were a significant proportion (of the order of 50%) of the unscreened loads. As part of their study, characteristic curves were produced that related TSS areal loading (in mg/m^2) to rainfall duration and intensity.

The importance of raindrop energy in the detachment of particles and subsequent entrainment in overland surface flow has its precedence in soil erosion studies, such as Tan (1989) and Proffitt & Rose (1991).

Hydrological parameters are very significant in terms of the generation of TSS loads from urban surfaces. On this basis, hydrological data collection of at least the duration, intensity and total rainfall depth of storm events and antecedent dry periods is considered an important aspect of the thesis.

2.4 Runoff Quality from Urban Surfaces

TSS concentrations from urban surfaces, particularly roads and streets, have been measured by numerous studies. A summary of outcomes from selected investigations is provided in the following sections.

2.4.1 Road Pavements

As part of a synopsis of sediment monitoring issues for the USGS, Bent *et al.* (2001) undertook a review of studies from the USA, Australia, Canada, France, Sweden and the United Kingdom over the past 25 years. Sampled TSS concentrations from highway and street pavements varied from 4 to 129 000 mg/L , with mean values falling in the range of 29 to 18 000 mg/L . The median particle size of sediments

collected in these studies range from 13 to 1000 μm (medium silt to very coarse sand).

A similar review of available literature by Duncan (1995) used 37 sets of suspended solids data to estimate a mean road runoff concentration of 193 mg/L. Roads situated in highly urbanised areas had a higher mean concentration (257 mg/L) than the mean derived for low-density urban areas (69 mg/L). A weak correlation ($R^2=0.16$) was found for an inverse relationship between suspended solids concentration and annual rainfall.

Crabtree *et al.* (2005) measured pollutant concentrations in runoff from six UK motorway sites during 10 storms. The mean TSS EMC based on the results for all measured data was 114 mg/L, reaching a maximum EMC of 1350 mg/L.

Drapper *et al.* (1999) investigated the quality of road runoff from 21 sites in South East Queensland over an 18-month period. In-situ grab samplers were installed at road bridges and 20 L composite water samples were collected. Median EMC concentration for TSS ranged from 60 to 1925 mg/L, indicating a large variability between sites. Based on size distributions by volume, the median particle size was less than 100 μm at most sites. No statistical relationships between TSS concentration and other factors, such as traffic volume, were found.

Based on TSS data from 31 USA states, Driscoll *et al.* (1990) reported an overall mean concentration of 142 mg/L for runoff from roads with traffic volumes exceeding 30,000 vehicles per day (compared to 41 mg/L for rural roads with less than 30,000 vehicles per day). Sansalone & Tittlebaum (2001) measured TSS concentrations from a major road overpass in Louisiana, USA and reported a median of 225 mg/L. The road had a traffic flow of 70,400 vehicles per day.

Lloyd & Wong (1999) sampled runoff from Dandenong Road, Melbourne during two storm events. The road carries approximately 32,000 vehicles per day. The TSS EMC for the first storm was 441 mg/L. A significantly lower EMC of 129 mg/L was measured for a smaller storm that occurred seven days after the first event. Instantaneous TSS concentrations measured during runoff ranged from 14 to 2267 mg/L. Based on size distributions by weight, the median particle size ranged from

30 to 70 μm , with the coarser material being associated with samples taken during the rising limb of the runoff hydrograph. Organic matter represented between 60 to 100% of particles larger than 118 μm .

2.4.2 Car Parks and Driveways

Rushton (2001) monitored runoff from various parking lots, each about 0.1 ha in area, located at the Florida Aquarium, Tampa, USA. TSS data was collected for 30 storms during a twelve-month period. Average EMC values of two lots with asphalt pavement were determined to be 11.2 and 13.5 mg/L. The introduction of vegetated swales and porous pavements was found to significantly reduce TSS load from the car park areas.

Pitt & Voorhees (2000) summarised USA data from five studies of paved parking areas and reported mean TSS concentrations that ranged from 41 to 1660 mg/L. Reported mean TSS concentrations for two paved driveway sites in Toronto were 373 and 440 mg/L. Sampling of parking area runoff at Alabama by Pitt *et al.* (1995) detected a mean TSS concentration of 110 mg/L (range from 9 to 750 mg/L).

Rabanal & Grizzard (1995) monitored runoff from an office parking area, a commercial fuelling station and a fast-food restaurant parking lot over a fifteen-month period. All sites were located in Washington D.C. A flow-weighted composite sample was taken at each site for a total of 123 storm events. The office parking area generated the lowest median TSS EMC (10.6 mg/L) and the highest (38 mg/L) was produced by the fuelling station. The median EMC for the fast food parking area was 20.8 mg/L TSS. EMC values for individual storms ranged from 1.0 to 271 mg/L.

Stormwater runoff from parking lot catchments located in Cookeville, Tennessee was monitored by Neary *et al.* (2002). EMC values that were derived for seven storms recorded for a 2.4 ha parking lot ranged from 15 to 124 mg/L. The EMC range for a smaller 0.1 ha lot was 2.0 to 91 mg/L.

Gnecco *et al.* (2005) sampled runoff from a 5000 m² fuel station and a 6500 m² auto recycler and dismantling facility in the Liguria region of Italy. Both sites are subject to significant commercial activities. The fuel station, for example, is located on a

major highway and includes refuelling stations, a parking lot for trucks and buses and a restaurant. EMCs of TSS for the fuel station ranged from 44 to 193 mg/L (mean 125 mg/L, $n=5$ storms). Higher TSS EMCs ranging from 187 mg/L to 894 mg/L (mean 378 mg/L, $n=15$ storms) were measured at the auto recycler and dismantling facility.

Monitoring of runoff from a paved parking lot located in Kongju, Korea was conducted for 7 storms by Kim *et al.* (2005). Rainfall varied from 8.1mm to 45.3mm and EMC values for TSS in runoff from the parking lot ranged from 12.0 mg/L to 37.4 mg/L.

2.4.3 Roofs

Pitt & Voorhees (2000) summarised USA data from two studies of roof washoff. The reported range of mean TSS concentration was 4 to 22 mg/L. Sampling of roof runoff at Alabama, USA by Pitt *et al.* (1995) detected a statistical mean TSS concentration of 14 mg/L (range from 0.5 to 92 mg/L). Duncan (1995) derived a mean roof runoff concentration of 26 mg/L based on statistical analysis of 11 datasets obtained from a worldwide literature review.

2.4.4 Grassed Areas

Barten & Jahnke (1997) installed lawn runoff samplers on 29 turf areas in the Twin Cities Metropolitan Area of Minneapolis and St. Paul. Turf quality varies from bare soil to total grass cover up to a golf course green standard. A total of 113 TSS samples were collected during a two year monitoring period. The statistical mean TSS concentration was 925 mg/L (range from 2 to 11,900 mg/L).

A large variation in TSS concentration between different sites of similar surface type is apparent from the literature review. Similarly, significant variability exists between TSS concentrations measured for different storms at the same location. Road pavements tend to generate TSS concentrations that are substantially higher than those from roof surfaces.

2.5 Methods to Measure TSS EMCs and Loads

2.5.1 Grab Sampling

Grab sampling is the manual collection of water samples by onsite personnel during the monitoring event. It requires minimal equipment but has several disadvantages. Obtaining grab samples is labour-intensive and safety risks to personnel may be present in taking the sample. Access to the sampling site may be difficult, the response time for personnel to start sampling may be slow and human errors may occur (Bent *et al.* 2001).

Multiple grab samples and flow measurements are required over the duration of runoff events to determine EMC values. This may not be practical in small urban catchments where the runoff response to rainfall is very fast. As an alternative to multiple grab sampling, Ma *et al.* (2002) demonstrated that taking a single grab sample at a certain time during a storm event provides a reasonable basis to derive oil and grease EMC values.

Pitt *et al.* (1995) describes grab sampling methods that were used to collect sheet flow samples from a various urban surfaces in Birmingham, Alabama. For deep flows, samples were collected directly into sample bottles. For shallow flows, a peristaltic hand operated vacuum pump created a weak vacuum in the sample bottle, which then gently drew the water sample directly into the container through a tube. A sampling location free of debris and a slow sampling rate was used to avoid capture of particles not flowing in the water. For pervious areas, a small clean plate (preferably glass) was placed on the ground to allow the water to flow onto it and to reduce this contamination risk. Approximately one-litre sample volumes were obtained using this technique.

2.5.2 Insitu Sampling – Automatic Pumping Samplers

Automatic pumping samplers have been generally used to collect urban runoff samples. For example, most of the extensive dataset collected by the US National Urban Runoff Program (NURP) was obtained using automatic samplers (Athayde *et al.* 1983). A typical automatic sampler installation uses a peristaltic pump to suction a water sample from the stormwater flow into sample containers.

Recent studies suggest that automatic samplers may not provide representative TSS concentrations when sand-sized material is present (Bent *et al.* 2001). The location and orientation of the sampling tube within the water flow, in addition to the sample intake velocity relative to the water flow velocity (isokinetics) are important factors that influence the PSD of the samples being collected.

2.5.3 Insitu Sampling - Passive Samplers

Passive samplers are typically installed in the flow path and control the sampling rate by the placement, orientation and design of the sampler intake. Bent *et al.* (2001) provide a summary of various types of passive samplers that are available. They are generally designed to collect a proportion of the stormwater flow as it submerges or flows over the sampler intake. Passive samplers may apply the following methods:

- A steep inclined channel to cause supercritical flow that is then split by baffles to obtain a flow-proportional sample (Clarke *et al.* 1981). Flume testing by Hwang *et al.* (1997) found that the flow splitting characteristics of this type of device are influenced by the channel roughness.
- Mesh screens or sieve trays that are installed in road inlet pits or catch-basins (Ellis & Harrop 1984; Pratt & Adams 1981). Sediments are retained on the screens and estimating the total flow volume passing through the screens during the monitoring event derives the particle concentrations.
- A vertical array of sample bottles with intake tubes which are arranged to siphon water samples when the flow reaches a sufficient depth (Gray & Fisk 1992).
- A double ball valve to ensure that the sampler is only open during flow immersion and is closed when the sample bottle is full. This type of sampler was used by Dudley (1995) to take samples within stormwater pipes and at roadside kerbs.
- A sheet-flow collection system that concentrates flow through a Parshall flume to measure flow volume and into a 2000 L storage tank (Sansalone *et al.* 1998).
- Sample pots that are installed directly into the pavement. The sampler intake is in the form of a small hole recessed just below the pavement surface with a setscrew to regulate the inflow volume. Waschbusch *et al.* (1999) describe

similar designs for sampling of driveways, lawns, roof, parking lots and storm-sewer outfalls.

- Barten & Jahnke (1997) used a simple device to sample lawn runoff at sites in Minneapolis and St Paul. Two lengths of PVC pipe were placed flush with the ground surface and splayed at an angle of 150 degrees. Slits were cut into the pipe to allow the entry of sheet flow, which was then collected at the end of both pipes by a one-litre bottle. A small tube was used to regulate the amount of water discharged into the bottle.
- A plastic, low-cost device was developed by USA company GKY to collect and retain a representative sample of up to five litres in volume. It consists of a small container installed below ground and a surface cover to intercept sheet flows. Entry of water into the container is controlled by a number of open ports. A buoyant flap closes off the ports and isolates the sample when the container is full. This type of sampler, mounted flush with the pavement surface, is also described by Stein, Graziano *et al.* (1998).
- A rotation flow sampler, referred to as a Coshocton wheel, combined with a flume and a multi-slot splitting device was used by Rabanal & Grizzard (1995) to collect composite EMC samples for urban sites in Washington D.C.

Passive samplers may have a number of technical limitations including (from Bent *et al.* 2001):

- Provision may not be made for recording the period of flow sampled. Sample pots, for example, installed in road surfaces may fill quickly and may not provide a representative sample of the full runoff event (Bannerman *et al.* 1993).
- Debris buildup on the sampler intake could alter water and sediment flows resulting in blockage or unrepresentative sampling.
- Relatively small flow-contributing areas may not be representative of larger areas of the same surface type and may suffer from the effects of bypass flows and surcharging effects.
- Samples collected by passive samples installed on road pavements may be difficult to retrieve during heavy traffic.

- Passive samplers that are open to the atmosphere may collect debris, sediments and atmospheric dust.

2.5.4 Turbidity Monitoring

Turbidity is associated with the 'cloudiness' of water, as caused by the light scattering of suspended particles. Nephelometric turbidimeters measure light scattered at an angle (commonly 90 or 180 degrees) to the beam. The turbidity measured by these devices is in nephelometric turbidity units (NTU). Turbidity measurements typically have a standard error of 10 percent at 1 NTU which is consistent with an indicative standard error of 10 percent for TSS laboratory analysis (APHA 1998).

The major advantage of turbidimeters over the sampling and laboratory-based measurement of TSS is the potential for continuous monitoring. Studies have shown that insitu measurement of turbidity, in conjunction with discrete TSS sampling, provides an efficient and accurate method to determine event loads (Lewis 1996). Turbidity provides a surrogate measure of TSS but suffers from a number of deficiencies. Factors such as variations in particle size, particle composition and water colour may potentially confound a relationship between turbidity and TSS.

A turbidity-TSS relationship is necessary in order to determine TSS concentrations as turbidity is not a direct measure of TSS. Based on a review of a number of studies, the best correlations were obtained in areas where the sediment properties were likely to be relatively constant (such as oceanic environments and small catchments), where field instruments were used and where the TSS concentrations covered a wide range (Gippel 1989). These conditions are anticipated to prevail in the washoff from urban surfaces.

A simple linear regression of TSS on turbidity for each site and storm event is usually adequate to estimate TSS load (Lewis 1996). Load estimates could be further improved with curvilinear fits or individual fits for the rising and recession phases of a runoff event. Gippel (1995) also used a linear regression to fit turbidity to TSS for data collected in the Latrobe River and from a forested catchment near Eden, Australia.

A simple linear TSS-turbidity regression was also used by Furumai *et al.* (2001) based on stormwater monitoring data from an urban residential area near Tokyo, Japan. A high correlation ($R^2 = 0.93$) was obtained between the fine size fraction (less than 45 μm) of TSS and turbidity. The turbidity correlation to particle sizes greater than 45 μm was considered to be poor ($R^2 = 0.68$). It was concluded that continuous monitoring with a turbidity sensor would be useful to measure the washoff behaviour of fine TSS particles.

Different types of turbidimeters can produce different numerical values of NTU measurement. These differences are introduced by variations in design features such as light source, spectral sensitivity of the detector and the light beam configuration (Davies-Colley & Smith 2001). It is thus important to establish a turbidity-TSS calibration to the specific instrument that is used in the monitoring work.

A simple and inexpensive attenuation turbidimeter was developed by Lawler & Brown (1992). It cost less than ten percent of the price of commercially available devices and used a green light-emitting diode as a light source. The more costly infra-red source is generally used in commercial devices. The Lawlor & Brown turbidimeter was deployed to measure highly turbid flows in a glacial river in southern Iceland and it captured two large sediment pulses, which were unrelated to discharge variations. It is unlikely the pulse events would have been detected by automatic sampling methods.

Spanberg & Niemczynowicz (1992) used a turbidity meter deployed in a road gully pit to monitor pollutant washoff from an asphalt surface in Sweden. The meter was installed in a specially designed chamber that included a funnel inlet, a sediment sampling port and a v-notch weir for flow measurement. Substantial variations in turbidity were recorded over about one minute timescales and these were found to be related to variations in flow. A similar monitoring system was used by Tomanovic & Maksimovic (1996) to record runoff from an asphalt area in Belgrade, Yugoslavia.

Although turbidimeters can be useful in filling in the temporal gaps between discrete TSS sampling, turbidity is considered by some as, at best, a qualitative indication of sediment concentration. For example, based on data for 1135 runoff samples collected in a highway drainage pipe in Massachusetts, Smith (2000) found a large

scatter between turbidity and SSC measurements. This variability may be due to the turbidity measurement which depends on many factors including the particle size distribution of the sediment flow, the quality and maintenance of the probe, the effects of fouling of the optics by oils, greases and biofilms, and the temperature of the probe (Bent *et al.* 2001).

2.5.5 Sampling Requirements

Stormwater sampling to determine EMC values may involve taking a number of individual aliquots on a flow-proportioned basis throughout the runoff event. These aliquots can be combined to form a composite sample. Two measures were developed in California to determine whether a composite sample might be deemed to be adequately representative of the runoff event (Caltrans 2000). The first measure is a minimum number of sample aliquots to be collected for the event based on total rainfall. A minimum percent capture is also specified and this is defined as the percent of the total event runoff flow during which composite sample collection occurred. Recommended measures are provided in **Table 2.3**.

■ Table 2.3 Requirements for representative event sampling¹

Total Event Rainfall (mm)	Minimum Number of Aliquots	Minimum Percent Capture
0 – 6 mm	6	85
6 – 12.5mm	8	80
12.5 – 25 mm	10	80
>25 mm	12	75

Note: 1. Sourced from Caltrans (2000)

Based on statistical analysis of TSS and flow data measured for the Santa Ana River in California, Leecaster *et al.* (2002) determined an optimal sampling strategy in order to derive annual loads for a large watercourse. Single storms were most efficiently characterised by taking 12 flow-based samples. This is similar to recommendations by Caltrans (2000). Sampling of a minimum of seven storms was found to be adequate to determine annual TSS load trends to within acceptable accuracy limits.

High pollutant concentrations can occur at the beginning of the storm event. This first flush effect has been observed in many stormwater runoff studies (Barrett *et al.* 1998a; Sansalone & Buchberger 1997), although it is a highly variable process that

may not occur consistently. Based on a review of published literature in urban stormwater quality processes, Duncan (1995) refers to first flush as when the incremental pollutant load exceeds the incremental flow at the start of a runoff event, when both flow and load are expressed as a fraction of the event total. First flush becomes less detectable if the time of concentration of the catchment is relatively long relative to the storm duration, and is thus a characteristic of small catchments.

The sample volume that should be collected depends on the expected suspended sediment concentration. The precision of SSC analysis (refer **Section 2.5.6**) is limited mainly by the amount of residue that is retained after filtration. A minimum residue amount of 100 mg has been suggested by Davies-Colley & Smith (2001). If stormwater runoff has low suspended sediment concentrations (less than 10 mg/L), a minimum sample volume of 10 L is required.

Representative sampling to establish EMC values should maximise the number of flow-proportioned aliquots to be taken over as much of the full duration of the runoff event as is practical. This includes the start of a storm event when first flush effects may occur. Also, the composite sample volume should be at least 10 L if low TSS concentrations are expected. These requirements have significant implications to the design and use of the stormwater sampling method.

2.5.6 Sample Processing and Analysis

Analytical methods to obtain solid-phase concentrations include the suspended sediment concentration (SSC) method (ASTM 2002) and the total suspended solids (TSS) method (APHA 1998).

The SSC method is considered to be a better analysis for stormwater runoff than the TSS method for several reasons (from Gray *et al.* 2000):

- The SSC method uses standardised procedures that process the entire sample received by the laboratory. These procedures include evaporation, filtration or wet sieving of the whole sample volume.
- The TSS method requires analysis of a subsample extracted from the original sample. The subsample volume is 100 mL, unless more than 200 mg of residue is expected to collect on the filter, in which case a smaller volume is extracted.

Subsampling procedures, such as pouring or pipetting, appear not to obtain an aliquot that is representative of the sediment concentration and particle size distribution of the original sample. As a result, the subsample is usually deficient in sand size particles.

- The percentage of sand-size and finer material can be determined by the SSC method, but not by the TSS method.
- The TSS method originated as an analytical method for wastewater, presumably for samples collected after a settling step at a wastewater treatment facility. It is considered fundamentally unreliable for the analysis of natural water samples.

The TSS method of analysis was found to produce concentration data that are negatively biased (i.e. tend to underestimate) by 25 to 34% with respect to the SSC method. Discrepancies between the two methods were attributed to the procedures in the TSS method to obtain aliquots or sub samples, particularly if very fine sands and larger particles are present (Gray *et al.* 2000). The TSS method provided unbiased results when less than 25% of the sample material was finer than 62 μm .

For the purpose of this study, the SSC analytical method was selected as the basis of determining the concentration of suspended solids in preference to the TSS analytical method.

3 Current Context and Scope of Study

3.1 Current Context – Stormwater Runoff from Urban Surfaces

A review of published literature relating to stormwater particle loads from urban surfaces is provided in **Chapter 2**. The following important aspects from the literature review underpin the methodology developed for this thesis:

- EMCs in stormwater runoff vary from one storm to another, but the values are positively skewed and typically follow a lognormal distribution. It is thus necessary to monitor a number of storm events to quantify this distribution. Recommendations on the minimum number of monitored storms to capture the variability of EMC ranges from at least seven to up to 35 events (refer Section 2.3.1). *In this thesis, stormwater monitoring was conducted over a 13 month period and captured data for 40 rainfall events.*
- Impervious surfaces including roofs, paved car parks, footpaths and roadways dominate urban landscapes and typically generate the majority of runoff volume, especially in small storms. This is an important implication for the management of stormwater quality as TSS load is a function of both the runoff volume and EMC. *An understanding of runoff generation characteristics of urban surfaces is a fundamental requirement of the research.*
- Small, frequent rainfall events generally contribute to the bulk of particle washoff loads over time. *Minor storms less than 6 months to 1 year average recurrence interval (ARI) were targeted by the stormwater runoff monitoring conducted during the project.*
- The TSS load includes a mix of particle sizes from clay-size (0.5 to 4µm in size), silt-size (4 to 62µm) and sand-size (62 to 2000µm). There are various systems to classify particle size ranges, but published studies may not always indicate which system has been adopted and this makes comparisons between studies difficult. *A particle size classification scheme was devised as part of the study, expanding on size classes for sediment analysis recommended by Bent et al. (2001).*
- Standard TSS analysis provides no information regarding the relative composition of clay, silt or sand-size particles within a stormwater sample, unless a particle size distribution (PSD) analysis is conducted. Washoff

behaviour, contaminant associations such as heavy metal adsorption and stormwater treatment processes are closely allied with particle size. A sample having a small number of coarse particles can theoretically have the same TSS concentration as a sample with a large number of fine particles, but their physical properties, turbidity, water quality characteristics and ability to be treated would be very different. *It is considered important to obtain a breakdown of TSS samples into at least its coarse and fine size fractions to establish particle characteristics.*

- A standardised TSS laboratory analysis method is available, but may not give a consistently reliable measure of suspended solids concentration in stormwater samples. An alternative method, the suspended sediment concentration (SSC) method, is preferred (Gray *et al.* 2000). *This study modified the SSC method to suit the specific particle characteristics of urban runoff.*
- Dense mineral particles generally only remain in suspension if within the silt range or smaller (<62µm), but sand-sized particles can be temporarily suspended by flowing waters (refer Section 2.3.4). *For the purpose of this thesis, medium sand (500µm maximum) is adopted as the upper particle size limit.* Inorganic particles larger than this size are easily removed by sedimentation within stormwater treatment systems.
- Urban stormwater may also contain significant amounts of organic particles. These particles are generally less dense than inorganic sediments and also can potentially cause adverse water quality impacts such as oxygen depletion and nutrient release. *The thesis also investigates the organic content of stormwater particles.*
- Apart from the physical characteristics of the surface, hydrological parameters including rainfall intensity, storm rainfall volumes and the time period of dry weather between storms (antecedent dry period) all influence the TSS load washed from urban surfaces. These hydrological aspects vary geographically so extrapolating TSS load characteristics measured from other regions is expected to introduce uncertainty. *On this basis, local monitoring of urban surfaces was undertaken and relevant hydrological parameters were recorded in this study.*

Various techniques are available to sample stormwater flows. A focus of the thesis is to investigate simple and cost-effective methods that can be easily employed to measure the washoff characteristics of local urban surfaces. Existing sampling methods include:

- **Grab sampling** which involves the manual collection of water samples by onsite personnel during a rainfall event. It requires minimal equipment but has the disadvantages of being labour-intensive. Safety risks may be present, site access may be difficult and the response time for personnel to start sampling may be slow. Sampling by suitably trained volunteers may reduce labour costs. *Grab sampling was not conducted in the project as the hydrologic response of urban impervious surfaces to rainfall is very fast and thus difficult to sample manually.*
- **In-situ automatic pumping samplers** typically use a peristaltic pump to suction a water sample from the runoff flow into sample containers. These samplers are installed at the monitoring site and pumping is usually triggered electronically by rainfall or water depth sensors. This type of sampler is popular as it overcomes many of the disadvantages associated with grab sampling. *As automatic pumping samplers are relatively costly to deploy and have the potential to obtain non-representative samples of the coarser fractions of TSS, this type of in-situ sampling was not used in the thesis.*
- **Turbidimeters** are devices that detect the light scattering of suspended particles and hence obtain a measure of the ‘cloudiness’ or turbidity of the water. By correlating turbidity with TSS concentration, a TSS measurement can be derived thus avoiding the need for collecting a water sample and conducting laboratory analysis. This approach has been used in many studies but often with mixed results as the TSS-turbidity correlation is often poor. However, the application of turbidimeters offers the substantial benefit of continuous, cost effective monitoring. *The use of turbidimeters offers the significant benefit of continuous monitoring of stormwater flows, but there are a number of limitations in applying turbidity measurements to derive TSS concentrations. The application of turbidimeters in urban stormwater monitoring has significant potential, but due to resource limitations, was not investigated as part of this thesis.*
- **In-situ passive samplers** include a wide range of devices that are typically installed in the runoff flow path and collect a proportion of the flow as the

sampler intake is submerged. Most passive samplers are based on simple storage containers. They may have a mechanical device (such as a valve) to regulate the sample flow or to isolate the sample when the container is full. Passive samplers are prone to a number of technical limitations, such as rapid filling, which means that a representative sample over the full rainfall event may not be obtained.

Passive samplers offer a simple and cost effective method to collect samples washed off from urban surfaces, but are prone to a number of technical limitations. A key part of the study was to develop a passive sampler that would overcome many of these limitations.

3.2 Current Context – Stormwater Infrastructure Planning Using Land Use Data versus Urban Surface Data

Stormwater infrastructure and non-structural controls are used to manage the environmental impacts resulting from urban stormwater. Identifying a management strategy for stormwater quality requires a high level of planning during all phases of urbanisation. Planning procedures vary considerably, but a sequential process is conventionally used as broadly defined in **Table 3.1** and adapted from Planning Plus (2003b). These procedures follow the normal development sequence in Australia starting with the initial release of land to the setting out of urban subdivisions and subsequent development of individual allotments.

This sequential planning process has evolved to define stormwater infrastructure requirements, mainly situated within public land, prior to the development phase. This infrastructure typically involves stormwater conveyance systems, (pipes, channels and waterways), discharge reduction systems (detention basins, infiltration basins) and treatment systems (sediment ponds, constructed wetlands).

Collectively, these systems can be referred to as the ‘subdivisional drainage system’ and reside generally within public lands including open space corridors, roadways and drainage reserves. If incorporated, measures such as detention basins, urban ponds and wetlands tend to be large-scale landscape features concentrated at a few locations within the overall drainage corridor. As such, these measures are often referred to as ‘end of pipe’ or ‘regional’ solutions installed to meet stormwater quality objectives set at the discharge outlet of the subdivision.

■ **Table 3.1 Conventional planning process for urban stormwater quality management (adapted from Planning Plus 2003b)**

Planning Phase	Issues Addressed	Scale of Development Addressed	Types of Planning Studies
Strategic Phase (Prior to any development of an urban release area)	Setting broad visions, goals, targets, desired water quality outcomes and setting the direction of urban development	Broad-scale greenfield land or redevelopment of existing urban areas	Local environment plans, urban release studies, local environmental plans
Subdivision Phase (Prior to development of a portion or stage of an urban release area)	Definition of major stormwater and waterway corridors, requirements for large-scale structural controls, mainly within public land	Subcatchments, individual subdivisions or stages of development	Development control plans, Stormwater management plans, Water and soil management plans
Development Phase (Prior to development of an individual allotment)	Requirements for connection of individual lots to the stormwater system, requirements for small-scale controls within private land	Individual allotments within a subdivision	Development control plans, planning codes.

A feature of conventional planning is that most major components of the stormwater infrastructure are strategically located and sized during the subdivision phase. The details of individual lot development are usually not known at this phase, except for the spatial extent of various generic land use zones within the subdivision.

In order to design the subdivisional drainage system, it is generally assumed that hydrologic properties, such as the fraction imperviousness of lots, are homogeneous across each single land use area. As a consequence of this approach, data collection to support the drainage design has traditionally focussed on the monitoring of catchments that have a single dominant land use or the land use composition is known.

The focus of stormwater management in the development phase has traditionally involved the simple connection of individual lots to the pre-established subdivisional drainage system as the lots are progressively developed. The opportunity to reduce stormwater flows and loads by incorporating measures within individual lots (referred to as ‘source’ controls) has historically been ignored, as the stormwater infrastructure is generally predetermined during the subdivision phase.

Recent trends are leading to the greater use of source controls within individual lots, in conjunction with measures within the subdivisional system, to reduce stormwater impacts. These measures are referred to as Low Impact Development (LID) in the USA, Sustainable Urban Drainage Systems (SUDS) in Europe and Water Sensitive Urban Design (WSUD) in Australia. All of these emerging approaches incorporate “a system of strategically placed smaller-scale and distributed stormwater management techniques in order to better replicate, replace or mimic the filtering, storage and infiltration processes that are critical for maintaining the function of the catchment” (Virginia DEQ 2003).

WSUD, and its overseas counterparts, employs a wide range of structural practices including detention devices, filtration and bioretention devices, grassed swales, infiltration devices, porous paving and roof water tanks (Planning Plus 2003a). Site planning techniques such as minimising the spatial extent of impervious surfaces, are also applied. Some of these measures can be deployed within the subdivisional drainage system and at a smaller-scale within individual lots.

It is becoming recognised that there are significant opportunities within lots to reduce stormwater discharges and hence reduce the size and cost of the downstream subdivisional drainage system. These opportunities include the reduction of impervious surfaces, onsite reuse of stormwater and roofwater, and disposal by infiltration.

A common WSUD theme is the recognition that management opportunities within urban lots should be integrated within the overall planning framework, rather than as an afterthought at the end of a sequential planning process. In this way, stormwater infrastructure within the subdivision can be reduced in scale. On this basis, WSUD approaches are questioning the conventional planning practice used in urban development, but are faced with a number of challenges. Some of these challenges include:

- A lack of data relating to the stormwater runoff behaviour of the various surfaces within individual lots. This data is required to assess the performance of lot-based WSUD measures in reducing discharge and improving runoff quality. *This aspect is the focus of the first phase of this thesis.*

- A lack of performance data relating to specific WSUD measures and guidance on the detail design of these measures. There is also limited information on the community acceptance of these practices.
- Local governments, and others, have concerns regarding the long-term maintenance of WSUD practices, particularly measures that are situated within privately-owned lots (i.e. outside of the subdivisional drainage system maintained by local governments).
- WSUD needs to be fully integrated into the planning framework at all phases of development. A difficulty is that lot-based WSUD measures may be administered at the end of the development approval process and this leads to uncertainty as to whether desired environmental outcomes (usually expressed as water quality targets at the subdivision drainage outlet) will ultimately be met. This is especially the case if WSUD measures are not fully implemented within the majority of lots of the subdivision.
- How lot-based WSUD is administered at the development approval stage may also be difficult and raises a number of questions. Should measures such as rainwater tanks and onsite infiltration be compulsory? Should performance indicators be set for each lot with a requirement that lot-based WSUD meet this performance objective? How much of the obligation to treat and reduce stormwater runoff should be placed within privately owned and maintained assets?
- The nexus between lot-based WSUD measures, similar measures within the subdivisional drainage system and achieving water quality objectives at the drainage outlet needs to be demonstrated for each urban development proposal. This usually requires predictive modelling to select and optimise a total management system that achieves the desired objectives. The modelling is often more complex than that required for conventional stormwater drainage design. Models are available (e.g. MUSIC, AQUALM) and their application in development assessment is growing rapidly, but often in the absence of validation of predicted results.
- The traditional method of assessing the water quality impacts of proposed development based on mean or long-term averages is also being questioned (Phillips & Thompson 2002). This approach ignores the inherent variability of

water quality under natural conditions. A preferred approach is to apply continuous modelling (daily estimates over a simulation period of several years) to predict this statistical variability, although it greatly increases the analysis work required for development assessment.

- There is also an emerging desire to integrate stormwater as a valued resource into the overall water supply and usage within urban areas (referred to as total water cycle or integrated water management). Stormwater re-use offers significant benefits in reducing flows discharging from urban areas and the water quality and quantity implications to downstream receiving waters are currently not often recognised.

Many of these challenges are currently being actively addressed (Lloyd 2001) and it is not the intent of the study to respond to all of the challenges that are listed above.

A major aim of the thesis is to investigate ways that information relating to urban surfaces can be applied within a development planning context that is increasing influenced by WSUD principles and practices.

3.3 Scope of Study

3.3.1 Monitoring of Stormwater Runoff from Urban Surfaces

The subject of the first phase of this project (**Chapters 4 to 7**) is the contribution from primarily **established** urban surfaces to the particle load in stormwater runoff. A main goal is to develop a robust and cost effective sampling technique that can be used by local government to measure stormwater pollutant loads generated from urban surfaces. Passive samplers offer significant potential to realise this outcome and are used in the study.

A key part of the thesis is the development and testing of a passive stormwater sampler devised to overcome the technical limitations associated with this type of device. A stormwater monitoring program was designed that applied the passive sampler to obtain data for a range of urban surfaces. These surfaces included a roof, a road pavement, a carpark, a bare soil area and a grassed area. The collected data were analysed to establish EMC statistics and to define stormwater runoff characteristics for each surface type.

3.3.2 Application of Urban Surface Type as Basis for Stormwater Infrastructure Planning

The definition of urban areas by surface composition provides a potentially useful basis for stormwater infrastructure planning. It allows the estimation of stormwater discharges and qualities to be conducted at a sub-lot scale. By aggregating surface areas together, larger urban areas such as subdivisions and suburbs can also be simply represented.

The scope of the second phase of the thesis (**Chapters 8 to 11**) is to investigate and develop ways that the collected data based on urban surfaces can be applied in stormwater infrastructure planning. It is intended that the monitoring data collected as part of the first study phase will provide an insight into key processes that influence the buildup and washoff of particles from urban surfaces. Relationships between particle loads and rainfall characteristics will be explored. A suite of methods to predict the particle load generated from urban surfaces is planned to be a major product of the research work.

The application of selected surface-based models to stormwater management, particularly in the context of Water Sensitive Urban Design, will be demonstrated by a series of case studies. The analysis of these case studies has a basis founded on discrete urban surfaces, rather than the more broadly defined land use that is generally used in current practice.

4 Classification and Laboratory Analysis of Stormwater Particles

4.1 Stormwater Particle Classification

Various researchers have separated TSS into individual particle size ranges for their urban stormwater studies. Examples of different particle classifications used in this way are provided in **Table 4.1**. Currently there is no consistent approach to dividing TSS into particle size classes, which makes data comparisons between studies very difficult.

■ **Table 4.1 Examples of classifications used for stormwater particles**

Source	Description of Particle Classification
Ball <i>et al.</i> (1994)	Three size classes; 0.45-37 μ m, 37-62 μ m, >62 μ m
Characklis & Wiesner (1997)	Three size classes; < 0.45 μ m, 0.45-20 μ m, > 20 μ m
Madge (2004)	Five size classes; <0.4 μ m, 0.4-5 μ m, 5-20 μ m, 20-80 μ m, >80 μ m

Table 4.2 shows the particle classification system that was developed and adopted in this thesis as the most appropriate one to evaluate stormwater runoff from urban surfaces. It divides suspendable particles into four classes according to size; Very Fine, Fine, Medium and Coarse. Each class is further subdivided into its organic and inorganic fractions, yielding a total of eight particle subclasses.

■ **Table 4.2 Proposed classification of stormwater particles based on size range**

Class	Range (μ m)	Inorganic Particle	Organic Particle
Very Fine (VFP)	0.45 – 8	Very Fine Inorganic (VFIP)	Very Fine Organic (VFOP)
Fine (FP)	8 – 63	Fine Inorganic (FIP)	Fine Organic (FOP)
Medium (MP)	63-500	Medium Inorganic (MIP)	Medium Organic (MOP)
Coarse (CP)	>500	Coarse Inorganic (CIP)	Coarse Organic (COP)

The objective of the stormwater monitoring was to obtain representative samples of the Non-Coarse Particles in urban stormwater, namely the Very Fine, Fine and Medium classes. Features of these particle classes are outlined in **Table 4.3**.

Approximately an 8-fold increase in particle size defines the boundary of each class.

With the exception of Very Fine silt, which is included in the Very Fine class, the classes can be separated as Clays, Silts or Sands under the system described by Bent *et al.* (2001). The upper size limit for Fine particles is consistent with that specified by ASTM (2002) for ‘fines’ sediment concentration in water.

■ **Table 4.3 Features of the proposed particle classification scheme (Non-Coarse Particles only)**

Feature	Very Fine	Fine	Medium
Upper limit of particle size	8µm	63µm (7.9 x VFP limit)	500µm (7.9 x FP limit)
Corresponding grain sizes in particle class ¹	Fine clay, Medium clay, Coarse clay, Very Fine silt	Fine silt, Medium silt, Coarse silt	Very Fine sand, Fine sand, Medium sand

Note: 1. Based on classification system described by Bent *et al.* (2001).

The proposed classification system assumes that suspended particles consist of Non-Coarse Particles smaller than 500 µm. Dense mineral particles generally only remain in suspension if smaller than sand (<63 µm), but sand-sized particles can be temporarily suspended by flowing waters (Davies-Colley & Smith 2001). Medium sand up to 500µm maximum size may be considered to be an upper limit for suspended matter as larger particles tends to be conveyed in stormwater as bedload (Lloyd & Wong 1999). This 500µm definition of suspended matter has also been used in the performance testing of stormwater treatment devices, e.g. by Washington State Department of Ecology (WSDE 2002).

4.2 Laboratory Analysis of Stormwater Particles

Laboratory procedures were required to determine the concentrations of the MP, FP and VFP size classes of stormwater particles in addition to their organic and inorganic fractions.

As acknowledged in Section 2.5.6 of this thesis, the testing method that is considered to be most suitable for the determination of the solid-phase concentration of suspended particles in water samples is the Suspended Sediment Concentration (SSC) Method - ASTM D 3977-97 (Reapproved 2002). A wet sieving and filtration method (Test Method C) is incorporated into the SSC standard that allows the concentration of ‘coarse’ sediments (>63µm) and ‘fine’ sediments (<63µm) to be determined. ‘Fine’ particles include cohesive clays that may not be settleable.

The SSC Test Method C was adapted by introducing additional filtration and screening steps to obtain the necessary partitioning into VFPS (<8µm), FPS (8-63µm) and MPs (63-500µm). Specifically, this involved a 500µm screen to separate particles in the MP size range from the ‘coarse’ particles, and an 8µm filter to isolate the VFPS from the ‘fine’ particles.

The APHA Standard Method 2540-E and US EPA Method 1684 (EPA 2001) for volatile suspended solids were used to determine the organic fraction of each particle class.

The laboratory procedures for sample handling, screening, filtering, drying and ignition are outlined in **Table 4.4**. Analysis of subsample duplicates were conducted, providing sample volumes were sufficient. Sample volumes were occasionally insufficient to subsample for separate FP and VFP analysis; in these cases a combined FP and VFP determination was made (referred to as the FP+VFP concentration). A key feature of the laboratory procedure is the use of a churn splitter to ensure full mixing during subsampling. Alternative methods such as manual shaking have been found to bias sediment concentrations (de Ridder *et al.* 2002).

■ **Table 4.4 Adopted laboratory procedures for stormwater particle analysis**

Description of Procedure
<p>Step A. Sample Handling Bulk stormwater samples up to 80L in volume were analysed. The sample containers were plastic and sealed to avoid contamination. Samples were refrigerated at 4 °C up to the time of analysis to minimise microbial decomposition of solids. Before analysis, samples were brought to room temperature and weighed to determine the net weight (gross weight minus the container weight).</p>
<p>Step B. Coarse and Medium Screening of Whole of Sample The entire sample was poured through two 30 cm diameter screens. The initial screen was a 500µm sieve to trap CPs. Particles retained on this screen were discarded. A 63µm sieve was used as the second screen to trap MPs which were washed from the sieve into a preweighed porcelain crucible. The filtrate from the screening process was retained in a clean container for subsampling and filtering.</p>

Step C. Subsampling

The filtrate from the above screening process contains particles less than 63 μ m (FPs and VFPs). Determination of FP and VFP concentrations requires a filtering technique that aims to yield a dried residue of between 10 to 200 mg retained on the filter medium. Subsampling was frequently required in order to limit the filter residue. A churn splitter based on a USGS design (Horowitz *et al.* 2001) was used to obtain duplicate subsamples for further analysis. These subsamples were typically 1L in volume. For low concentration samples such as roof water, no subsampling was undertaken as this would have left inadequate residue mass after filtering. The volume of each subsample was measured and recorded.

Step D. Fine Filtering of Subsamples

A reusable nylon fine-mesh filter (8 μ m SpectraMesh ®) was used to capture FPs. The subsample was filtered under vacuum through the SpectraMesh and frequent washing off of the retained FPs into a clean glass flask was performed during the filtering process. The filtrate that passed through the SpectraMesh was also stored in a clean container for further filtering. Using this technique, particles within each subsample were physically separated into FPs and VFPs.

Step E. Very Fine Filtering of Subsamples

A second filtering pass was required to isolate and weigh the FPs and VFPs. In this case, a 1.5 μ m 90mm-diameter glass fibre filter (Whatman 934-AH ®) was selected for this purpose. The filtrate passing through the SpectraMesh was sequentially filtered through the glass fibre filter to obtain VFPs. Similarly, the retained particles washed from the SpectramMesh were also filtered to obtain FPs.

Step F. Drying of MPs, FPs and VFPs

The crucible containing MPs from Step B and the glass filters with FPs and VFPs were placed in an oven to dry. Temperature was set at 105 °C for a minimum of 1 hour. After drying, the samples were placed in a desiccator to return to room temperature. The samples were weighed to determine the net weight of the dried residue (gross weight minus weight of filter or crucible).

The particle concentration in each MP, FP and VFP class was derived by dividing the net weight of dried residue (in mg) by the subsample volume (in L).

Step G. Ignition of MPs, FPs and VFPs

The glass filters were placed on crucibles and, together with the MPs crucible, were inserted into a preheated furnace set at 550 °C. The crucibles were kept in the furnace for at least one hour to ensure ignition and volatilisation of organic particles. The crucibles were let to partially cool in air and then transferred to a dessicator for final cooling to room temperature. The samples were weighed to determine the net weight of residue after ignition (gross weight minus weight of filter and crucible).

Step H. Determination of Particle Concentrations

Organic particles concentrations (MOP, FOP and VFOP) were derived by:

Organic particle concentration = (Net weight of dried residue – Net weight of residue after ignition) divided by Subsample Volume

The concentration of inorganic particles (MIP, FIP and VFIP) were derived by:

Inorganic particle concentration = Net weight of residue after ignition divided by Subsample Volume

The concentration of particle classes (MP, FP and VFP) were derived by summing the organic and inorganic components (e.g. MP = MOP+MIP). Non-Coarse Particle (NCP) concentration was derived by summing the component particle classes (i.e. NCP = MP+FP+VFP)

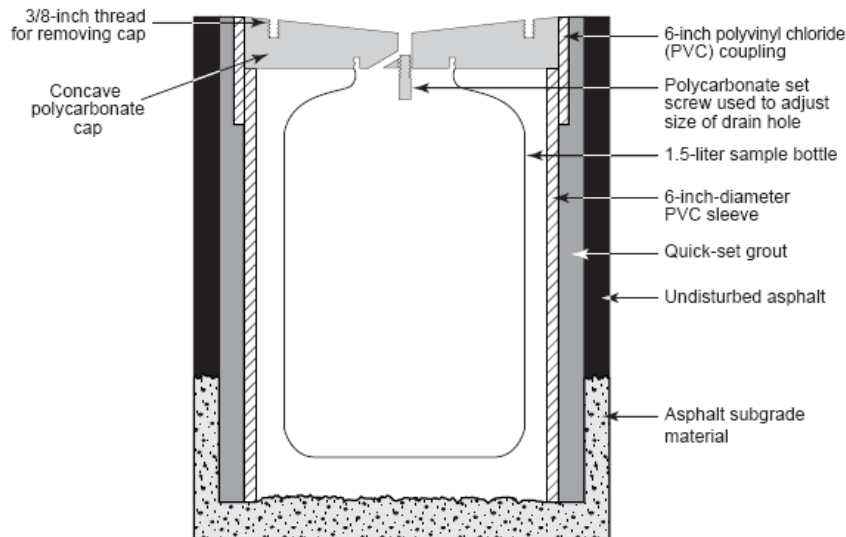
5 Design and Testing of Passive Sampling Devices

5.1 Review of Passive Samplers

Bent *et al.* (2001) provides a summary of passive samplers that were used in previous studies to sample urban runoff. Many of these samplers, and others, are discussed below in terms of the main hydraulic principle in their design: gravity flow, siphon flow, rotational flow, flow splitting and direct sieving.

5.1.1 Gravity Flow Samplers

Gravity flow samplers are simply designed to collect and store stormwater flow as it submerges or flows over the sampler intake. **Figure 5.1** shows an example used by Waschbusch *et al.* (1999) to sample road runoff. The device is installed flush to the road surface so that a portion of the stormwater flow drains into the sample bottle through a small hole shown at the top. The size of the drain hole, which can be adjusted by a set screw, regulates the flow into the bottle.

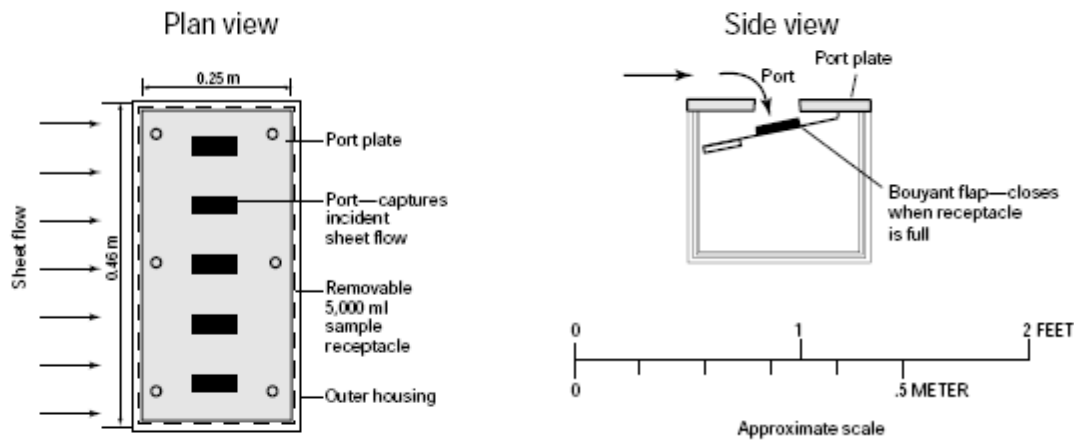


- **Figure 5.1 Gravity flow sampler by Waschbusch *et al.* (1999). Extracted from Brent *et al.* (2001).**

Similar products are commercially available with larger storage capacity (typically 5L). They have the capability to isolate the sample container when full by means of a

ball valve. Dudley (1995) had used this approach in installing a sampling device within a grated road gully pit.

Figure 5.2 shows a gravity flow sampler used by Stein *et al.* (1998) to sample stormwater flows from a road pavement. The design includes a 5L storage container housed within the pavement surface. A number of ports capture stormwater as it flows over the top of the device. A buoyant flap closes off the ports when the container is full.



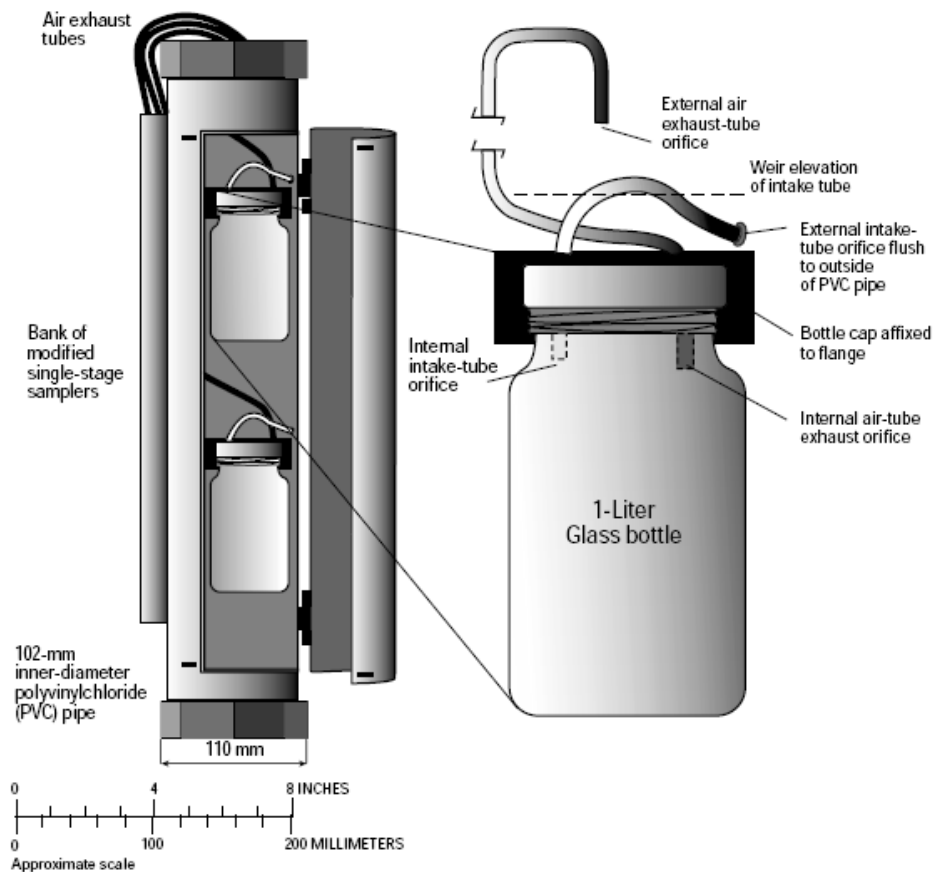
- **Figure 5.2 Gravity flow sampler by Stein *et al.* (1998). Extracted from Bent *et al.* (2001).**

A limitation of this type of device is that the sample containers may completely fill before stormwater runoff has ceased. Under such conditions, it is difficult to ascertain what portion of the event hydrograph has been sampled. Their main application is generally restricted to the capture of initial or first flush samples. Debris may also fully block the sampler intake or restrict the amount of stormwater entering the storage container.

These devices are typically installed within an urban surface to sample the shallow overland flow that is generated during storm events. In some circumstances, the catchment area that drains to the sampler may be difficult to accurately determine or the site could be subject to bypass flows from adjacent areas.

5.1.2 Siphon Flow Samplers

An example of a siphon flow sampler is shown in **Figure 5.3**, from Gray & Fisk (1992). This device, also referred to as a ‘single stage sampler’, relies on the formation of a siphon action as the water level rises above the intake tube into the sample bottle. Water is siphoned into the container until it is filled.



- **Figure 5.3** Siphon sampler used by Gray & Frisk (1992). Extracted from Bent *et al.* (2001).

A number of siphon flow samplers can be stacked vertically to collect samples throughout the rising part of the runoff event and this technique has been used in several river studies (Newham *et al.* 2001; USGS 2000b). Once the siphon action is initiated, rapid filling of the sample container generally occurs and so the technique is suitable for obtaining discrete or ‘grab’ samples at specific stages of the runoff event.

Siphon flow samplers provide a reliable basis to sample water, providing that most suspended sediment particles are in the silt to clay size range (less than 62 μ m).

Larger particles may not be consistently captured, depending on the location of the intake tube relative to the channel bed and the amount of suction that is available.

A major limitation of siphon flow samplers is that they are unable to operate when water levels are falling and thus do not capture samples during the recession part of a runoff event. These devices are mainly deployed within open channels and waterways where water depth ranges over a few metres. A reliable siphon action is unlikely to form under shallow water conditions, as is the case of stormwater flowing over urban surfaces.

5.1.3 Rotational Flow Samplers

An example of a sampler that applies rotational flow is the Coshocton wheel sampler originally developed by the US Department of Agriculture to capture sediment samples from field plots (US DA 1979). A typical installation consists of a flume and a Coshocton wheel as shown in **Figure 5.4**.

The flume, usually an H-flume, provides a measurement of peak runoff discharge and also jets the flow of water onto the face of the Coshocton wheel. The wheel is inclined slightly from the horizontal and the impact of the water causes the wheel to rotate. An elevated sampling slot mounted on the face of the wheel extracts a water sample when it rotates through the flow jet. The sample is then routed through the base of the wheel to a sample storage tank.



■ **Figure 5.4** Flume and Coshocton wheel reproduced from www.rickly.com and accessed on 1 March 2004.

Samples are continuously taken by a Coshocton wheel and flow-weighted, providing representative sampling of the entire storm flow. The device is widely used in the USA for research monitoring of soil erosion and agricultural runoff. Rabanal & Grizzard (1995) used an H-flume and Coshocton wheel to obtain samples from four small impervious urban catchments in Washington D.C.

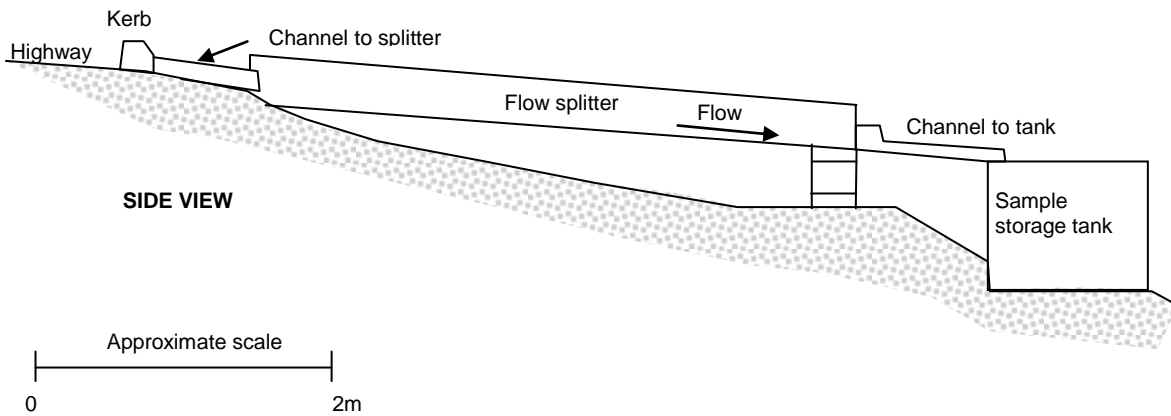
A limitation of the device is that a vertical drop is required to form a flow jet from the flume onto the Coshocton wheel and this may not be possible in flat terrain. At high flows when the speed of wheel rotation exceeds 35 RPM, the rotation may become irregular and stall the wheel (Bonta 2001).

Other types of rotational flow samplers are available. Researchers from the University of Idaho have developed a hybrid passive-automatic sampler based on a pumping sampler (IDF 1999). A diaphragm pump that extracts the water sample is self-powered by flowing water driving a set of rotational impellers. The rate of sampling is proportional to flow rate and the impeller speed also provides a measure of flow velocity.

5.1.4 Flow Splitting Samplers

A flow splitting sampler relies on the diversion of a small portion of the stormwater flow. An example as used by Clarke *et al.* (1981) to obtain composite samples of highway runoff is presented in **Figure 5.5**. The device consists of a 3.7m long, steep chute with a series of vertical baffles at the lower end. These baffles act to split off a constant proportion of the stormwater flow, which is channeled into a storage tank.

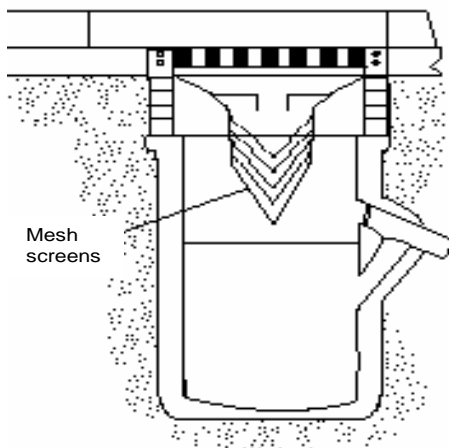
The sampler is relatively large in size and this aspect is a constraint where available space is limited. Supercritical flows are required in order for the device to function hydraulically. To achieve this flow regime, the chute needs to be inclined at a steep gradient of up to 9%. This requirement may be a problem in flat terrain or roads that are located in a cutting. The sampler also has a large open surface that may collect debris and atmospheric dust that can be washed into the storage tank.



■ **Figure 5.5** Flow splitting sampler used by Clarke *et al.* (1981). Reproduced from Bent *et al.* (2001).

5.1.5 Direct Sieving Samplers

Direct sieving samplers are used specifically for the determination of sediment concentration in stormwater runoff. An example applied by Pratt & Adams (1981) is shown in **Figure 5.6**. It uses a number of conical-shaped mesh screens that are nested vertically. Stormwater flows are directed onto the top screen. Mesh openings decrease in size such that coarse material is retained in the top screen and progressively finer particles are collected on the subsequent screens. The process is analogous to laboratory techniques using screens to determine sediment particle size distributions.



■ **Figure 5.6** Side view of direct sieving sampler used by Pratt & Adams (1981), installed in a road stormwater pit.

The device relies on capturing sediment particles as distinct from other types of passive sampler that aim to capture a representative sample of the stormwater flow. Determination of sediment concentrations requires an estimate or measurement of the total flow volume passing through the screens.

5.2 Selection of Passive Sampler Type

WSUD at a lot scale requires information on the quantity and quality of stormwater washed from urban surfaces. The **Event Mean Concentration** (EMC) provides a practical basis to characterize these stormwater loads and EMC is defined as the total pollutant mass discharged during a runoff event divided by the total runoff volume. In practice the product of EMC and runoff volume R_T gives the mass load L for a specific storm event, as demonstrated in **Equation 5.1**.

$$L = \frac{EMC \times R_T}{1000} \quad [5.1]$$

where L is the mass load in kg, EMC is the event mean concentration in mg/L and R_T is the total runoff volume in m^3 .

Passive samplers have a major role in obtaining EMC data providing several factors in their design are met. Desirable attributes of a passive sampler are listed in **Table 5.1** under two headings; the physical features of the sampler and its ability to obtain representative sampling. Some of these attributes are discussed in more detail in this Chapter.

■ Table 5.1 Desirable attributes of a passive EMC sampler

Physical Features	Representative Sampling
<ul style="list-style-type: none"> ■ Compact and easy to install ■ Not highly visible to reduce incidence of vandalism ■ Easily retrieved sample container ■ Clogging by debris is prevented or reduced ■ Adequate hydraulic capacity to handle the design flow ■ Limited exposed surfaces that may accumulate pollutants ■ Able to be installed in a defined flowpath ■ Able to be installed in low slope conditions 	<ul style="list-style-type: none"> ■ Able to obtain a flow-proportional sample over full duration of runoff event ■ Able to capture, store and isolate a sample for subsequent retrieval and laboratory analysis ■ Able to service a catchment area that is representative of the selected urban surface ■ Able to obtain a sample that is representative of the particle size distribution of the runoff flow

5.2.1 Flow Proportional Sampling

EMC and runoff volume are measurement outcomes of a sampling program intended to estimate the pollutant mass generated for an individual storm. Laboratory analysis

of a flow-weighted composite sample provides a reliable EMC value. The sample can be obtained by using sample aliquots that are proportional to the instantaneous stormwater discharge throughout the full duration of the storm runoff event. Sampling can be continuous or at frequent time intervals during the runoff event.

If continuous sampling is conducted and the ratio of sample discharge to stormwater flow discharge remains constant throughout the event, then the sample volume represents a direct measure of the total runoff volume. This provides a simple basis to determine runoff volume (R_T in **Equation 5.1**). Estimates of runoff volume based on recorded rainfall data would also provide a useful verification of the monitoring equipment.

5.2.2 Catchment Area

In order to measure the stormwater characteristics from a specific type of surface, the catchment to be sampled should be homogeneous and have well-defined boundaries. Ideally, the site should have a single discharge outlet and not be affected by bypass flows from adjacent areas.

The size of the catchment is limited by the capacity of the passive sampler to capture and store the stormwater sample. The catchment should be as large as practical to ensure that small-scale variations in the urban surface do not unduly influence the sampling outcomes.

5.2.3 Sample Capture and Isolation

Water samples should be physically captured and stored within a container that can be easily retrieved after each storm event. This allows laboratory analysis of water quality determinants to be conducted specifically to meet the needs of the study.

It should be noted that direct sieving samplers and other flow independent techniques (such as the use of turbidimeters) provide a basis for suspended sediment measurement. However, they do not physically obtain a water sample and are thus restricted in their usefulness.

An important objective of the passive sampler design is to ensure that the sample container is isolated from further stormwater entry when it is full. This issue has been resolved in previous designs by the use of ball valves, floating flaps and other

simple mechanical devices to seal off or close the sampler intake.

5.2.4 Sample Volume

The volume of the collected sample should be as large as practical to provide maximum integration of pollutant variations throughout the runoff event. Sample storage volume is dependent on the proportion of total runoff volume that is captured and the magnitude of the storm event that is targeted.

In practice, the sample flow volume ratio (abbreviated in this thesis as SFVR and defined as the ratio of the sample volume to the event runoff volume) can cover a wide range depending on the mode of sampling. For example, if the bulk of the runoff is collected in a 2000L tank as done by Sansalone *et al.* (1998) in their investigation of road runoff then the SFVR may be close to 1:1.

At the opposite end of the range, the US EPA (1999) suggests that sampling by automatic pumping samplers using 500mL bottles may have a SFVR as low as 1:70,000. A more typical SFVR range for continuous flow samplers (e.g. Coshocton wheel and flow splitting devices) is of the order of 1:100 to 1:1000.

For ease of installation and sample container retrieval, handling and transport, a reasonable maximum volume of the sample container would be 50L. The minimum sample volume could be dictated by laboratory analysis requirements. For example, the precision of TSS analysis is limited by the amount of residue retained after filtration. Based on a minimum residue mass of 100 mg (from Davies-Colley & Smith, 2001), the corresponding minimum sample volume is of the order of 10L if the stormwater runoff has low TSS concentrations (less than 10 mg/L). Smaller storage volumes are also expected to have a low SFVR and a higher potential to be filled prior to the end of the runoff event.

Analysis of Australian urban catchments indicates that the sum of all stormwater flows up to the 1-year Average Recurrence Interval (ARI) can represent more than 95 percent of the mean annual runoff volume (IEAust 2003). From this basis, it was decided to adopt a sample container size that captures at least the runoff from a 1-year ARI design storm. Selection of appropriate storm duration should be based on site access and other factors that may affect the timing and ability to retrieve samples, but is anticipated to fall in the range of 12 to 24 hours in South East

Queensland.

5.2.5 Selected Passive Sampler Type and Adopted Design Criteria

The hydraulic principles of rotational flow or flow splitting appear to offer the best outcomes in terms of sampler performance. Direct sieving was excluded on the basis that it is restricted to sediment capture and no water sample is obtained. Siphon flow samplers are expected to have limited application in shallow flow conditions and may not be reliable in obtaining unbiased samples of particles larger than silt size. Gravity flow samplers are useful for first flush sampling but need to be substantially modified to ensure consistent flow-weighted sampling over the full duration of a runoff event.

Flow splitting with vertical baffles extracts samples over the full depth of water flow and thus provides a method to collect particles that are conveyed as bedload, washload or floating on the surface. It was decided to design a new flow splitter that overcomes some of the limitations of devices reported in previous studies while ensuring acceptable sampling performance. The limitations of previous sampler designs include the relatively large size of the device, exposure of a large surface to the open air and the requirement to be installed at a steep incline (refer **Section 5.1.4**). A gravity flow sampler based on an orifice and weir arrangement was also developed for comparison with the flow splitter.

In addition to the desirable attributes listed in **Table 5.1**, specific criteria were established for the design of a passive EMC sampler for use in the monitoring of urban surfaces. The design criteria are summarised in **Table 5.2**.

■ **Table 5.2 Adopted design criteria for passive EMC sampler**

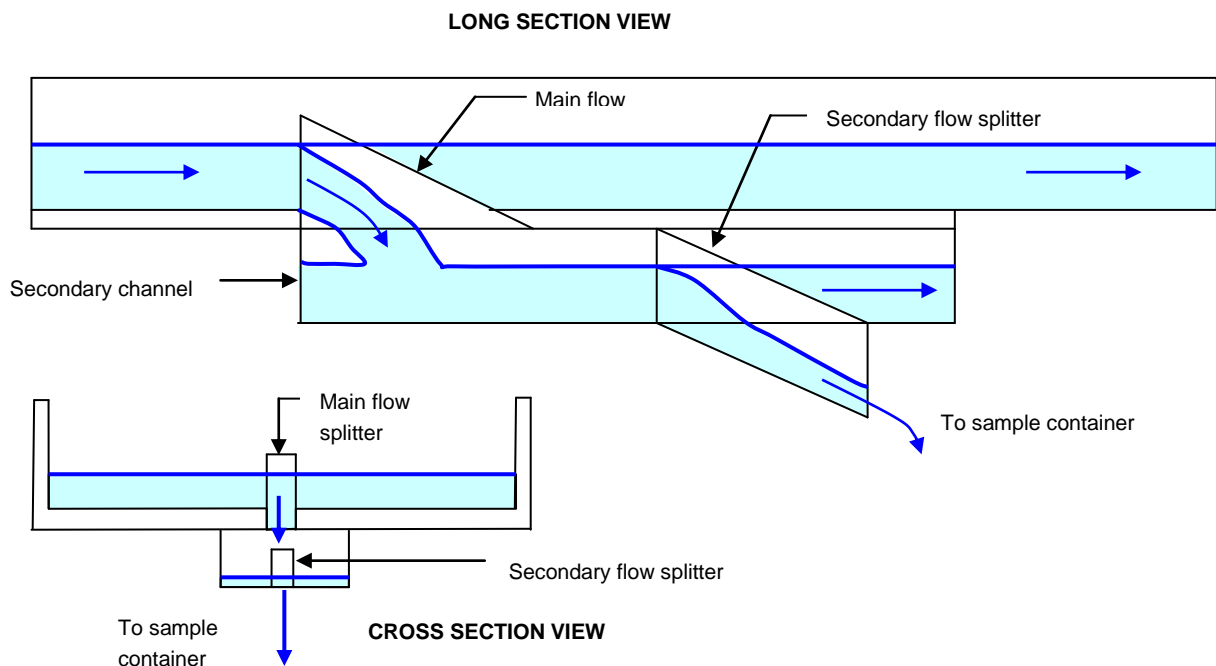
Design Criteria
<ul style="list-style-type: none"> ■ Able to service an impervious catchment area of at least 200 m² ■ Hydraulic capacity to handle 1 year ARI 12 hour duration storm runoff ■ SFVR in an indicative range of 1:100 to 1:1000, depending on application ■ Sample storage volume in the range of 10L to 50L, depending on storm magnitude ■ Able to continuously collect and flow-weight samples ■ Able to take representative samples of organic and inorganic particles less than 500µm in size

5.3 Concept Design of Selected Passive Samplers

5.3.1 Concept Design of Flow Splitter

Figure 5.7 shows the concept design of the proposed flow splitter for use in the monitoring of small urban areas. For clarity, elements including the sample storage container, inlet and outlet transitions to train water into and out of the device and a rack or screen to intercept debris are not shown.

The basis of the device is the sequential operation of two flow splitters. Stormwater flow is directed into a 150mm wide rectangular channel. The channel is set at a grade such that a subcritical flow regime is maintained with a velocity that provides mobilisation of particles less than 500 μ m (greater than 0.5 m/s). Faster, supercritical flow regimes were not used because they introduce hydraulic effects that could impair the sampler performance (e.g. oblique standing waves within the channel). It was intended that, when installed, the bed of the channel would match the existing ground surface.



- **Figure 5.7 Diagram showing the cross section and long section views of the flow splitter**

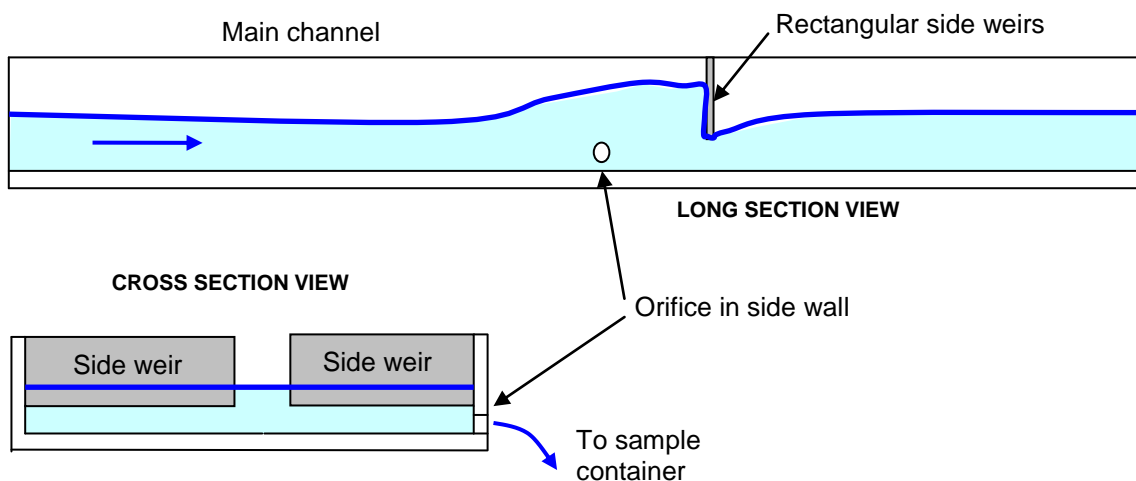
A horizontal slot parallel to the flow direction is provided midway in the main channel base. Vertical walls either side of the slot split the flow and direct a portion of the discharge through the slot. The spacing between the walls controls the amount

of water that is delivered through the slot to a secondary channel that is fitted to the underside of the channel bed. The SVFR associated with this first flow splitter was designed to be of the order of 1:20.

The split flow is conveyed in the secondary channel and passes another slot arrangement, similar in design to the flow splitter located in the main channel. The SVFR of this second flow splitter was designed to be of the order of 1:10, giving an overall device SVFR of approximately 1:200. Sampled flows are drained off and collected in a storage container located under the device. Excess flows pass through the main and secondary channels to the exit of the passive sampler.

5.3.2 Concept Design of Orifice-Weir

A diagram of the orifice and weir concept is presented in **Figure 5.8**. This device incorporates an orifice located on the side wall of the rectangular channel to drain off a continuous sample from the stormwater flow. A downstream weir, consisting of two rectangular side plates, acts as a flow constriction and regulates water depth and the hydraulic head on the orifice. This alternative design was investigated as the sample extraction point is located at the side of the channel. It was recognised that this approach could potentially be less prone to debris blockage than the flow splitter, which is centrally located within the channel.



- **Figure 5.8** Diagram showing the cross section and long section views of the orifice-weir sampling device

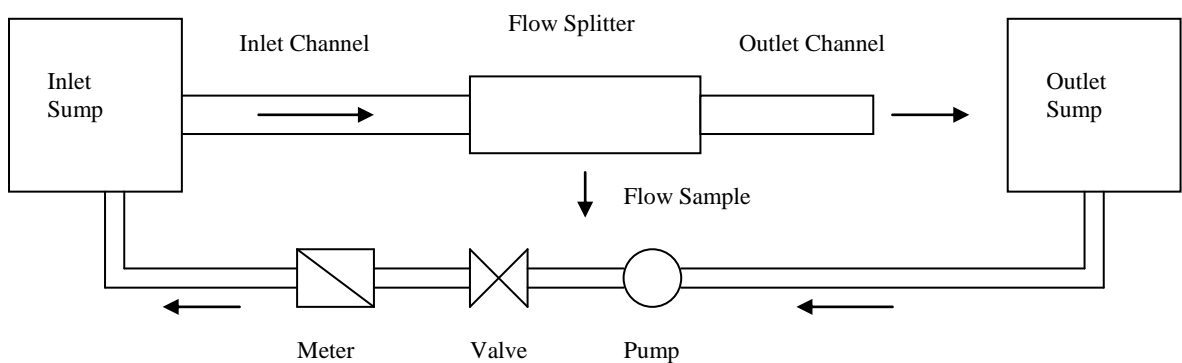
5.4 Hydraulic Testing of Passive Samplers

Prototypes of the flow splitter and orifice-weir passive samplers were constructed and hydraulically tested. The purpose of the testing was to determine the efficacy in obtaining a constant SFVR over a range of stormwater flows. Modifications to the sampler designs were made during the testing to optimise the hydraulic performance.

5.4.1 Hydraulic Testing Apparatus

A diagram of the flume testing apparatus is shown in **Figure 5.9**. A pump delivers water to an inlet sump that drains into a 1500mm long by 150mm wide plywood channel. The purpose of the inlet channel is to provide normal flow conditions prior to entry into the flow splitter. The bulk of the flow passes through the flow splitter and is directed via the outlet channel into the downstream outlet sump. A proportion of the flow is diverted by the flow splitter and is collected by a bucket. The pump extracts water from the outlet sump to form a closed reticulated flow system. An electromagnetic meter provides a reading of the water flow directed to the inlet sump. A hand-operated valve allows the rate of flow to be adjusted.

A photo of the testing apparatus in operation is shown as **Figure 5.10**. The channel and flow splitter are elevated by wooden supports, which can be adjusted to change the channel slope.



■ **Figure 5.9 Flow diagram of hydraulic testing apparatus**



■ **Figure 5.10 Photograph of hydraulic testing apparatus in operation**

5.4.2 Hydraulic Testing Procedures

The flow splitter and orifice-weir were tested separately for discharges ranging from 1.0 to 5.0 L/s as measured by the flow meter ('Rosemount' magnetic flow meter, 4-20mA). The testing was conducted under steady flow conditions when the flow rate as measured by the meter reached a constant value. A plastic bucket collected the sample flow diverted by the prototype sampler. The time taken to fill the bucket was measured. An electronic scale was then used to measure the net weight of the collected water and hence the sampled discharge (in L/s). The test was replicated and the results were averaged. In the final testing of the flow splitter, the tests were done in triplicate.

The SFVR was calculated as a ratio of the total discharge as measured by the flow meter and the sample discharge.

5.4.3 Modifications to the Prototype Flow Splitter

In order to obtain a consistent SFVR over the desired flow range (1 to 5 L/s), several modifications to the flow splitter were made during testing. Initially, the vertical walls that form the main flow splitter were made from 2mm thick Perspex ®. The walls acted as a significant flow obstruction and generated bow-type waves at the flow opening between the walls, which affected the amount of flow that was

diverted. This effect was minimised by using thinner wall material (1mm thick Perspex).

In the prototype design, the vertical walls that form the secondary flow splitter terminated flush with the underside of the secondary channel. During low flows (less than 1 L/s), the sample flow would not freely discharge from the splitter and would attach to the underside of the channel due to surface tension. This effect was minimised by continuing the vertical walls such that they protruded beneath the channel.

Initially, the vertical walls of the main flow splitter were triangular, with the top of the splitter tapering into the main channel bed. At high flows (greater than 3 L/s), the top of the splitter would impinge against the flow and affect the amount of flow being diverted. Using rectangular-shaped walls instead of the triangular walls reduced this effect.

5.4.4 Modifications to the Orifice-Weir

Flow through an orifice is non-linear as the discharge is proportional to the square root of the flow depth. In order to maintain a consistent SFVR over the desired range of discharges, a weir is required to increase the normal flow depth in the channel. A special weir is needed to force the inherently non-linear characteristics of orifice flow to act in a linear response to the channel flow. In practice, this weir configuration is difficult to achieve.

Eight different configurations of orifice diameter and height above the channel bed were tested, in combination with weir geometry. The orifice diameter, elevation above the channel bed and weir geometry varied between each configuration. The final configuration was a 6mm diameter orifice located in an aluminium plate set at a 45 degree angle to the flow direction and 4mm above the channel bed. Flow depths at this point were controlled by two side weirs, each encroaching 50mm into the channel.

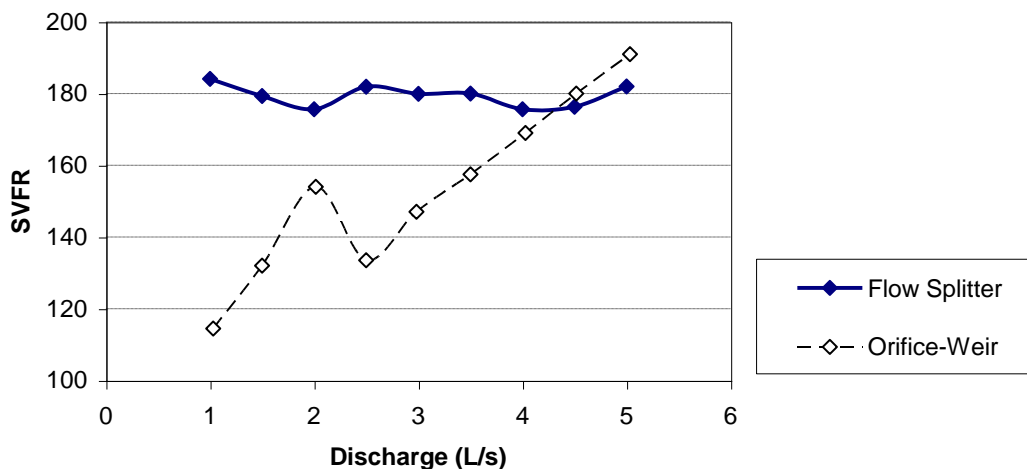
A vertical gap of 20mm was retained between the underside of the side weirs and the channel bed. This gap allowed low flows less than 1 L/s to be unaffected by the weir control. The main function of the weir is to elevate the depth of flow for higher rates of flow.

5.4.5 Hydraulic Test Results

The measured SVFR values for the prototype samplers are plotted as **Figure 5.11** for discharges ranging from 1 to 5 L/s in 0.5 L/s increments.

Experimentally determined SVFR values for the flow splitter fell in a narrow range from 1:174.6 to 1:184.1 (mean 179.4 ± 3.0), consistent with the relatively constant SVFR that is desirable to obtain accurate EMC data. By comparison, the SFVR values for the orifice-weir ranged widely from 1:114.5 to 1:191 (mean 153.2 ± 24.5). If used for collecting EMC samples, the potential sampling error in the orifice-weir device would be of the order of $\pm 15\%$ compared with $\pm 2\%$ for the flow splitter.

The measured performance of the flow splitter in obtaining a constant SVFR is substantially better than that from the flow splitting device previously shown in **Figure 5.5**, based on flume testing of a number of configurations by Hwang *et al.* (1997). Variations in SVFR up to 30% from the mean were recorded by these researchers.



■ **Figure 5.11 Measured SVFR for prototype passive samplers based on hydraulic testing**

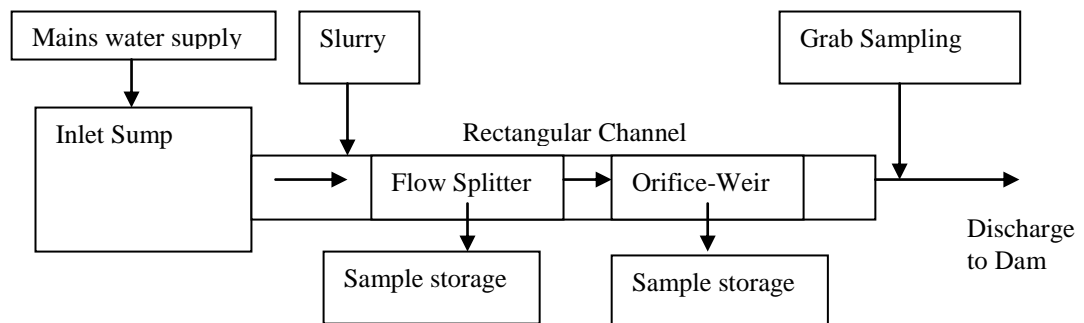
5.5 Sediment Testing of Passive Samplers

The efficacy of the two types of passive samplers in capturing representative concentrations of suspended particles was also evaluated. A sediment testing rig was established to simultaneously test the flow splitter and the orifice-weir device. Grab samples at the outlet of the testing rig were taken for comparative purposes.

The testing investigated Non-Coarse Particles (NCP including MP, FP and VFP as defined previously in **Table 4.2**) with three test replications.

5.5.1 Sediment Testing Apparatus

A diagram of the testing apparatus is shown in **Figure 5.12** and a photograph of the testing area is presented as **Figure 5.13**. The testing rig was installed at a USQ field site adjacent to a small storage dam. Mains water was delivered by a flexible hose to an inlet sump and the flow rate was adjusted by use of a gate valve. Water is released from the sump into a 150mm wide plywood channel which housed the flow splitter and the orifice-weir device.



■ **Figure 5.12** Diagram showing the layout of the sediment testing apparatus



■ **Figure 5.13** Photograph of sediment testing area

A pre-prepared slurry mixture of soil and water was added to the channel flow immediately downstream of the inlet sump. The mixture was contained in a 40L slurry drum and was released into the flowing water by a small plastic tap. Initial mixing of the slurry was promoted by the use of side weirs which induced local turbulence and higher water depths at the entry point of slurry into the channel. An inclined sheet metal plate assisted in spreading the slurry mixture across the full width of the channel and prevented the slurry from being concentrated midstream.

A proportion of the flow was diverted by both the flow splitter and the orifice-weir located downstream of the slurry release point. The sampled flows were captured by 20L drums located under the channel. The bulk of the water exited the flow channel and discharged to the dam. Grab sampling was conducted at the channel outlet prior to release to the dam.

5.5.2 Sediment Testing Procedures

The slurry mixture was prepared before each sediment test run. Slurry preparation involved mixing 500g dry weight of a black soil material with approximately 40L of mains water, producing a suspended particle concentration of approximately 13,000 mg/L. The slurry was mixed and stored for a minimum of three days to ensure wetting of the soil particles. After remixing, determinations of MP, FP and VFP concentrations in the slurry mixture were made. Generally, each slurry mixture was dominated by particles less than 63 μ m (FPs and VFPS). These particles represented 85% to 92% of the total particle mass.

The slurry was wet-sieved through a 500 μ m screen to remove Coarse Particles (CP) followed by a 63 μ m screen to retain MPs. MP concentration was determined by drying and weighing as specified by ASTM (2002). The dried MPs were returned to the slurry mixture. Determination of FP and VFP concentrations involved a sequential filtration procedure that initially used cellulose filter paper (8 μ m rating) and glass fibre filters. The screening and filtration procedures were also used in the analysis of the sediment test samples and are detailed in **Section 4.2**. The cellulose filter paper was replaced by SpectraMesh® nylon fine-mesh filters in later laboratory analysis work.

After preparation of the slurry mixture, samplers were tested using the following procedures:

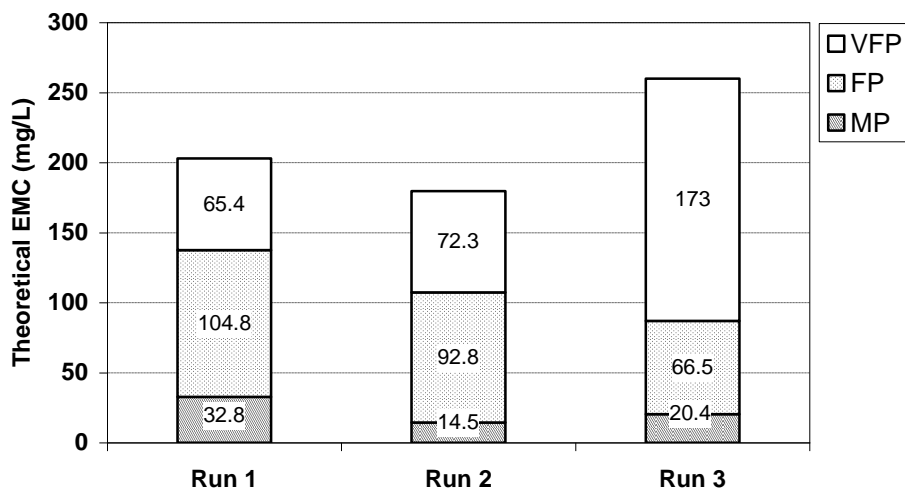
- Mains water flow into the channel was adjusted to steady state flow conditions of about 3 L/s by use of a gate valve. The measured time to fill a 200L plastic drum positioned at the channel outlet was used to determine the water discharge for each test.
- The slurry was released into the channel flow downstream of the inlet sump. As noted in the description of the testing apparatus, measures were taken to promote full mixing of the slurry with the flowing water. At the same time as the slurry flow was initiated, 20L drums were positioned to capture the continuous flow sample extracted by the flow splitter and the orifice-weir devices.
- A 1L grab sample was taken at the channel outlet at one minute intervals. The grab samples were added to a separate 20L drum to form a composite sample of the test.
- During the course of the test, the contents of the 40L slurry drum were manually mixed using a churn. The elapsed time to fully drain the slurry mixture into the channel was measured. When the slurry drum was empty, sample capture by the passive samplers and the collection of grab samples also ceased. The duration of the sediment tests were generally in the range of 12 to 13 minutes.
- The elapsed duration and the steady state discharge used in each test were recorded.

5.6 Sediment Test Results and Discussion

For each test run, numerical estimates were made of the theoretical particle concentrations following dilution of the slurry within the channel flow. These estimates are based on conservation of mass principles using **Equation 5.2**. The theoretical MP, FP and VFP concentrations are given in **Figure 5.14** for each of the three test runs. For Run 3, the VFP concentration was significantly higher than previous runs due to sonification of the slurry mixture prior to laboratory analysis.

$$EMC_{test} = \frac{L_{slurry}}{Q_{test} \times D_{test}} \quad [5.2]$$

where EMC_{test} is the theoretical diluted EMC of the slurry particles in the channel flow (mg/L), L_{slurry} is the measured particle mass in the slurry (mg), Q_{test} is the steady state flow in the channel during the test (L/s) and D_{test} is the elapsed duration of the sediment test (s).



- Figure 5.14 Theoretical particle concentrations of channel flow during the sediment tests. The Run 3 slurry mixture was sonified prior to laboratory analysis.

After each test run, the MP, FP and VFP concentrations of the three collected samples were analysed in the laboratory. Particle concentrations were normalised as a percentage of the theoretical value to allow comparisons of the performance of each sampling technique. The test results expressed as percentages are presented in **Figure 5.15**. Means and standard deviations of the normalised values were calculated and are provided in **Table 5.3** and the means are also plotted on **Figure 5.15**.

The percentage mean value can be interpreted as a measure of sampling accuracy; that is, the capability of matching the theoretical particle concentration. Also, the percentage standard deviation indicates the consistency of sampling performance over the range of test runs.

Table 5.3 Sediment test statistics normalised as a percentage of theoretical particle concentrations

Particle Class	% of Theoretical Concentration (Mean ± Standard Deviation)		
	Grab Sampling	Flow Splitter	Orifice-Weir
MP	25 ± 23	29 ± 11	31 ± 24
FP	91 ± 34	85 ± 42	84 ± 36
VFP	122 ± 29	129 ± 40	111 ± 43
<63µm FP+VFP	100 ± 8	98 ± 2	91 ± 7
<500µm MP+FP+VFP	88 ± 11	91 ± 6	84 ± 10

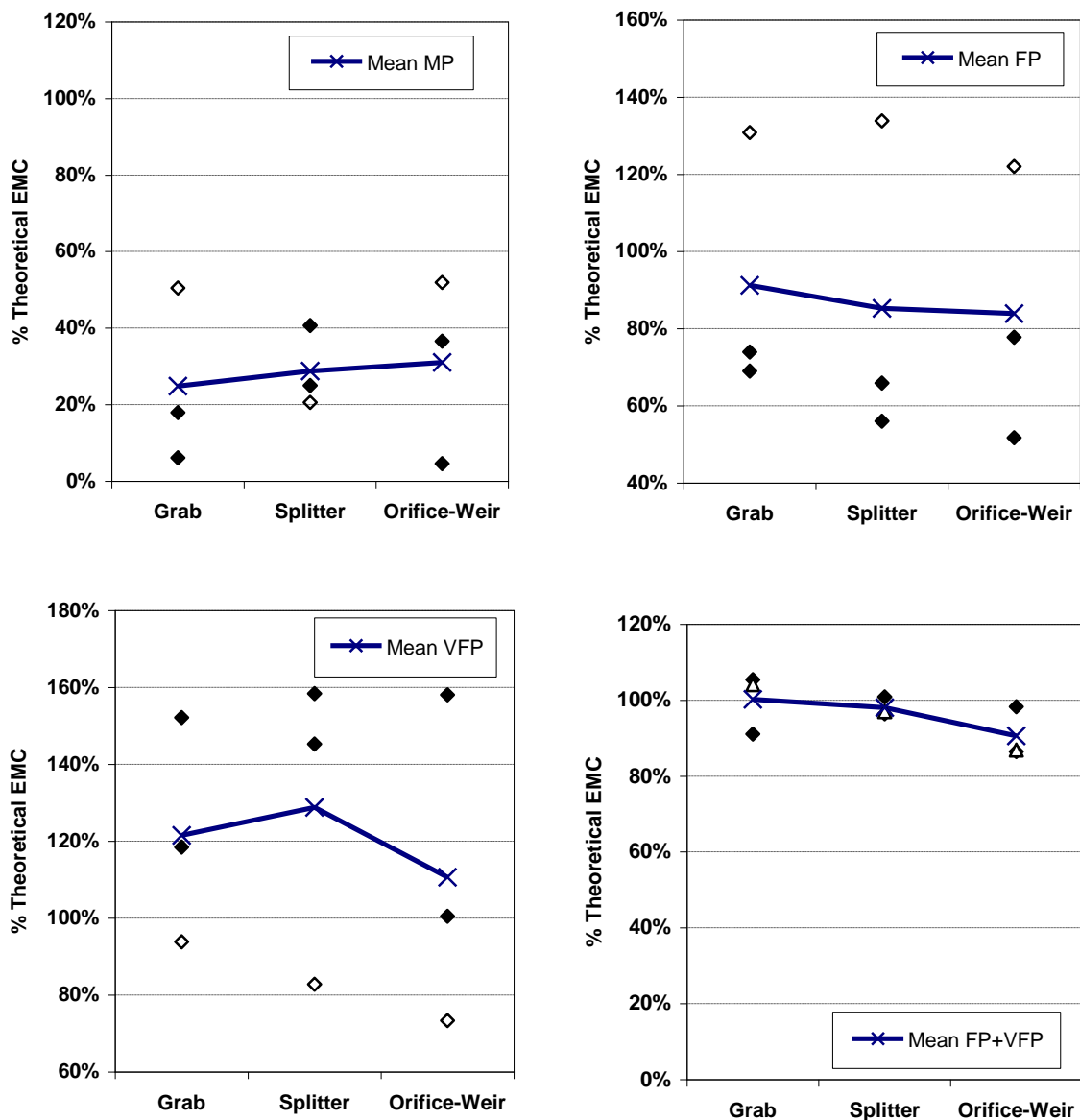


Figure 5.15 Individual sediment test results for MP, FP, VFP and FP+VFP normalised as a percentage of theoretical particle concentrations. Run 3 data is plotted as \diamond . The mean of the three test runs is also plotted as X.

The sediment test statistics in **Table 5.3** indicate that all sampling methods significantly underestimated the MP concentration. These sand-sized particles corresponding to 63 to 500 μm particle size are unlikely to be evenly distributed across the channel bed, making accurate sampling very difficult. In addition to this spatial variability, the poor performance of the relatively frequent grab sampling suggests that there are also significant temporal fluctuations in the movement of MPs within the channel. The relatively low mass of MPs in the slurry mixture may have also introduced inaccuracies during laboratory analysis.

All sampling methods gave lower FP and higher VFP concentrations, on average, relative to the theoretical values. As shown in **Figure 5.15**, there is a significant disparity in the Run 3 results (shown as \diamond) with respect to the first two runs. The FP concentrations for both Runs 1 and 2 for all sampling techniques were consistently below the theoretical EMCs. Also, their respective VFP concentrations were above the theoretical EMCs. This outcome suggests that a bias may have been introduced in the laboratory analysis of the slurry.

ASTM (2002) recommends that filtration methods be used for samples containing less than 10,000 mg/L. As the slurry mixture had sediment concentrations of the order of 13,000 mg/L, filter blockage is of concern. Cellulose filter paper was used to separate the VFPs from the FPs and blockage of this filter media would tend to overestimate the FP mass and underestimate the VFP mass in the slurry mixture. This blockage effect possibly explains the trends evident in the results for Runs 1 and 2.

To confirm whether the slurry testing procedure had introduced a bias, the subsample aliquot from the Run 3 slurry mixture was sonified prior to laboratory analysis. As evident in **Figure 5.15**, this resulted in trends that are opposite to the results of the first two runs, that is, FP concentrations for all sampling methods were above the theoretical EMC and the VFPs were all below the theoretical values. This result suggests that the laboratory methods used for the high-concentration slurry mixture have introduced uncertainty in the partitioning of particles less than 63 μm into their VFP and FP size fractions.

Filter blockage effects should not be as pronounced in the analysis of urban stormwater samples, which have particle concentrations substantially less than the recommended 10,000 mg/L filtration limit. However, the filtration methods used to separate VFPs were modified in response to the outcomes of the slurry analysis. The cellulose filter paper was replaced with SpectraMesh® nylon fine-mesh filters. These filters are more durable than the cellulose filters, are reusable and regular removal of filter residue from this product during the filtration process reduces blockage potential.

Because of the uncertainty in the theoretical values based on the slurry concentrations, the combined sum of FPs and VFPs (FP+VFP in **Table 5.3**) was introduced as a more reliable measure of sampling performance. This combination represents the total particles passing through the 63µm screen, and is not subject to potential errors introduced by the filtration separation of VFPs from FPs. Based on FP+VFP, grab sampling is shown to be a highly accurate method, closely followed by the flow splitter. The orifice-weir is the least accurate method, but this device nevertheless provides a reasonable basis of sampling (approximately 10% under-estimation of theoretical concentrations). The flow splitter gives the most consistent performance over the range of test runs.

In the case of total particles less than 500µm (NCP or MP+FP+VFP in **Table 5.3**), the accuracy of the flow splitter is similar to the frequent grab sampling and is potentially a more consistent method. The orifice-weir device appears to be the least accurate method. The three methods under-estimated particle concentration by 9% to 16% and this inaccuracy was mainly introduced by the poor sampling capture of MPs.

To summarise the hydraulic and sediment testing, the flow splitter accuracy ($\pm 2\%$ error) in obtaining a flow-proportional sample is significantly better than the orifice-weir ($\pm 15\%$ error). Generally, the accuracy of the flow splitter in sampling stormwater particles is similar to frequent grab sampling and is potentially a more consistent method. The orifice-weir device appears to be the least accurate sampling method.

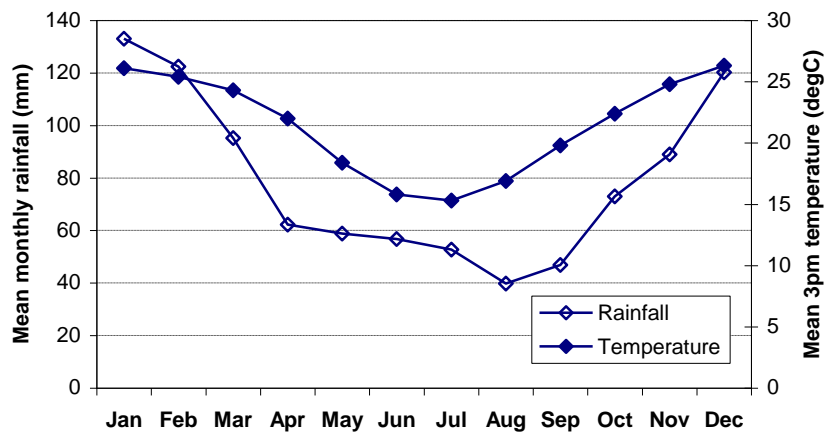
In the case of sampling particles less than 63 μ m (FP+VFP), the flow splitter is highly accurate (98% match with theoretical concentrations) and is considered to be a suitable sampling method for this size range. All sampling methods failed to obtain fully representative samples of MPs. This poor performance is attributed to spatial and temporal fluctuations in the transport of MPs within the flow channel.

*The flow splitter was selected as the preferred sampling device for the monitoring of urban surfaces in this project. This was based on the consistent performance of the device under laboratory testing to collect a fixed proportion of a range of water discharges (to within $\pm 2\%$ accuracy). Continuously dividing a sample from the water flow and accumulating it into storage provides a composite sample that can be used for EMC determination. The sediment testing of the flow splitter indicates that this device provides a representative EMC sample that is comparable with, if not more consistent, than very frequent (1 minute) grab sampling. **Chapter 6** describes the installation of five flow splitters to obtain stormwater runoff samples from different urban surfaces.*

6 Collection of Stormwater Particle Data from Urban Surfaces

6.1 Location of Stormwater Monitoring

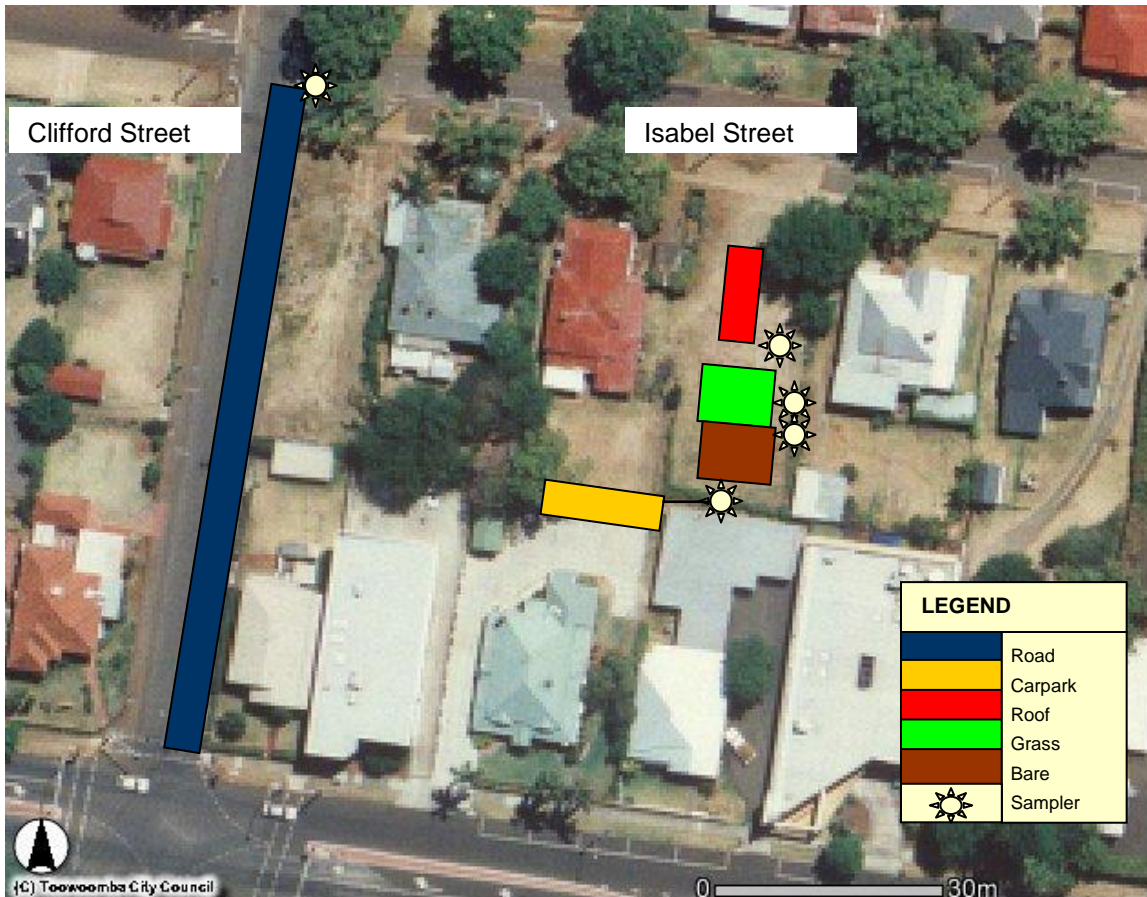
A network of five stormwater monitoring sites was established within the inner city area of Toowoomba, Queensland. Toowoomba is Australia's largest inland city after Canberra with a population of 92,500 people. It is situated 700m above sea level on the Great Dividing Range. The climate of Toowoomba is temperate and is characterised by dry winters and wet summers. Average annual rainfall is 950 mm/year typically over 106 raindays. Monthly patterns of mean monthly rainfalls and temperature are provided in **Figure 6.1**.



■ **Figure 6.1 Mean monthly rainfall and temperature for Toowoomba**

6.2 Description of Stormwater Monitoring Methods

Five types of urban surfaces were selected for monitoring stormwater runoff. These surfaces include a galvanised iron roof, a concrete carpark, an asphalt roadway, a grassed area and an exposed area of bare soil. These surfaces are typical of the range of impervious and pervious surfaces commonly present within urban areas in Australia. All five monitoring sites were established within a 70m radius to reduce variability in runoff due to spatial differences in rainfall. An aerial photograph of the monitoring area (refer **Figure 6.2**) indicates the close proximity of the sites to each other. The roof, grassed and bare surfaces are situated within an 800m² allotment.



■ **Figure 6.2 Aerial view of monitoring sites showing individual catchments and sampler locations**

Stormwater from a neighbouring carpark surface was diverted to a sampling device installed at the rear of the allotment. A separate sampler was installed west of the allotment to collect runoff from a section of road pavement on nearby Clifford Street.

A flow splitter sampler was fabricated and installed at each monitoring site. The sample volume flow ratio SVFR of each sampler varied with the peak stormwater discharge anticipated for each site. SVFR values equal to 1:20 were used for the design of the grass and bare soil samplers, 1:40 was used for the roof and carpark samplers and 1:200 was adopted for the larger road catchment. After installation, flow tests were conducted to confirm the actual SVFR of each flow splitter.

Each flow splitter was housed in a box lined with form-ply to protect against weathering and vandalism. The box for the roof sampler was set above ground and the boxes for the other samplers were installed partly or fully below ground. Each sampler had an 80L plastic container to store the collected stormwater sample.

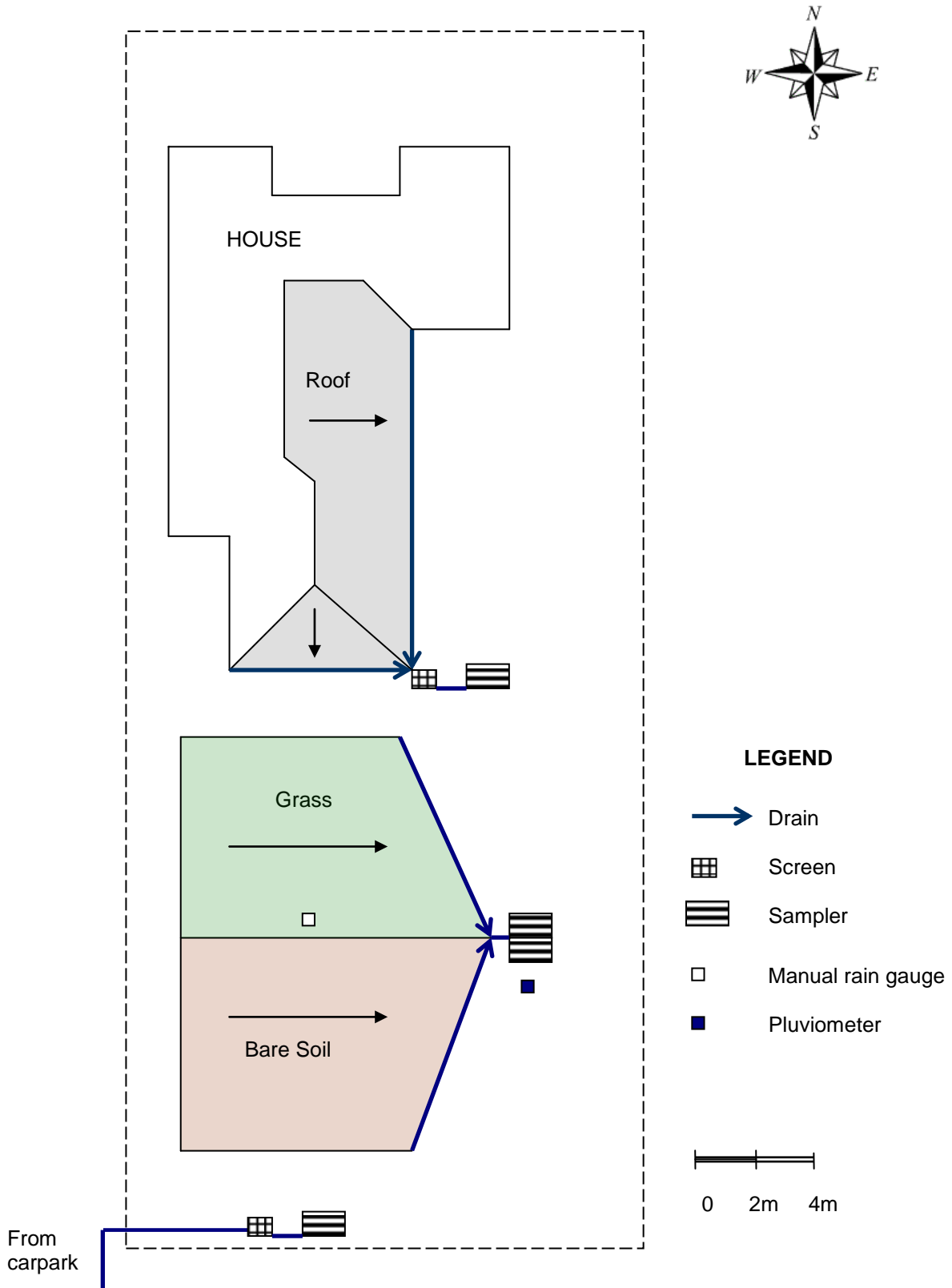
Following sample retrieval, laboratory analysis was undertaken to determine particle concentrations.

A tipping bucket pluviometer was installed at ground level at the rear of the allotment, adjacent to the grass and bare soil plots. The time of 0.25mm rainfall increments was recorded using a Hobo ® event logger. A manually read rain gauge was also installed nearby to measure total rainfall depths in case of failure of the tipping bucket pluviometer. A layout plan showing the roof, grassed and bare soil surfaces located within the residential allotment is provided as **Figure 6.3**. The locations of samplers and rainfall instrumentation are also indicated on the plan.

The monitoring program was initially conducted over a 3-month summer period from December 2004 to end February 2005. Data from this initial period was used to develop a conceptual model of particle generation processes (refer **Chapter 9** for details). A sequence of 14 storms, ranging in rainfall depth from 2.5mm to 48.5mm, was sampled during this period. Some storms early in the sequence were not sampled at the road site as the flow splitter was installed in late December 2004. Rainfall hyetographs and total rainfall depths were recorded for the full period of testing.

Monitoring continued during the succeeding 4-month period from March 2005 to the end of June 2005. This monitoring encapsulated the autumn and start of winter seasons which tend to be drier periods for Toowoomba. This period of data was applied to refine the particle washoff model. A total of 10 storms, varying from 2.5mm to 28.25mm rainfall, were sampled.

Monitoring was conducted over a further 6-month period from July 2005 to mid-January 2006. The winter months of July and August 2005 were characterised by very low rainfalls, with a total of 15.2mm being recorded for this period. Runoff events that were sampled mainly incorporated the spring and early-summer seasonal periods. These data were used to further refine and enhance the particle washoff model. A total of 16 storms, ranging in rainfall depth from 5mm to 64.25mm were sampled.

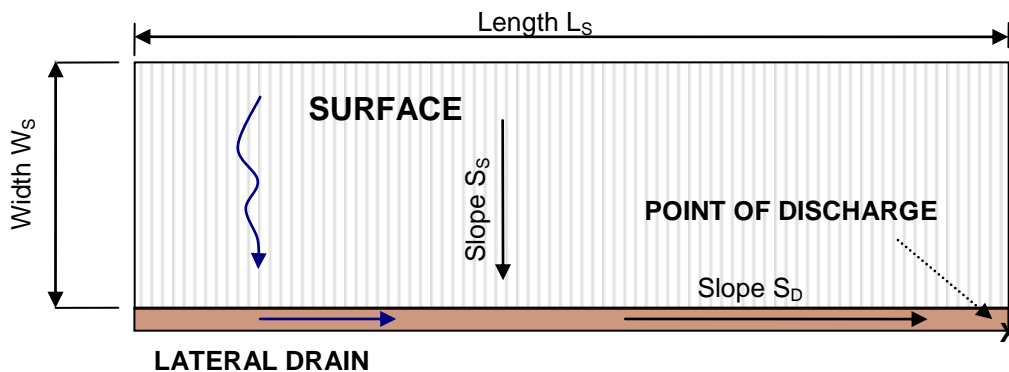


■ Figure 6.3 Site layout plan of residential allotment showing location of monitored surfaces, samplers and rainfall instrumentation

All available data were used to derive storm characteristics including average and peak rainfall intensities. Laboratory determinations were made of the sample volume and EMCs of Non-Coarse Particles, including organic and inorganic fractions and yielding MIP, MOP, FIP, FOP, VFIP and VFOP concentrations.

6.3 Description of Stormwater Monitoring Sites

As indicated in **Figure 6.4**, the physical components of each monitoring site include the surface itself (e.g. road pavement) and the drainage system (e.g. road gutter) that laterally collects and conveys the surface runoff to the stormwater sampling device located at a single point of discharge.



- **Figure 6.4 Physical components of each surface monitoring site and definition of geometric parameters**

The basic geometry of each surface is defined by the length (L_S) and width (W_S) with the width being in the direction of surface, or overland, flow. Surface gradient is defined by slope S_S . The lateral drain gradient along the length L_S of the surface is also described by a slope S_D . **Table 6.1** lists the basic geometric properties of each of the five surfaces. All surface areas fall in the 50 to 60 m² range with the exception of the road pavement which covered an area of 450 m².

The length and width of the roof, grassed and bare soil plots are indicative as these catchments are non-rectangular in shape. W_S provides an indication of the average travel distance that surface runoff makes to reach the lateral drain and L_S is the average travel distance along the drain to the point of discharge.

■ **Table 6.1 Basic properties of surface monitoring sites**

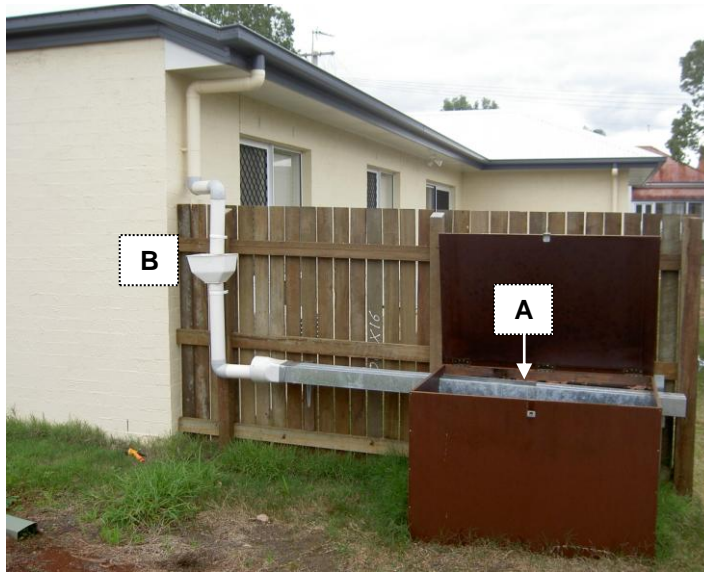
Site	Description of surface and lateral drain	Length L _s	Width W _s	Slopes S _s , S _D
Roof	51.8 m ² corrugated galvanised iron roof with Colorbond ® gutter	16.6m	3.1m	47%, <0.1%
Road	450 m ² asphalt pavement with concrete kerb, no gutter	75m	6.0m	5.0%, 0.9%
Carpark	56.2 m ² four-bay concrete carpark with concrete kerb	4.8m	11.7m	6.3%, 0.8%
Grassed	55.6 m ² couch turf lawn with roof gutter providing lateral drainage	6.5m	8.6m	1%, 0.4%
Bare soil	58.8 m ² bare krasnozem soil with roof gutter providing lateral drainage	7.1m	8.3m	1%, 0.4%

6.3.1 Description of Roof Monitoring Site

Construction of a residential house at the allotment was completed in October 2004, shortly before the start of stormwater monitoring. The roof is therefore a new surface in good condition. Roof material is corrugated galvanised iron sheeting with a Colorbond Quad ® gutter nominally 150mm wide. The roof pitch is 25° and the slope of the gutter to the roof downpipe is negligible. Some ponding of water occurs in the gutter after rain.

A photograph of the roof sampler installation is shown in **Figure 6.5**. The roof surface is located on the eastern side of the house. A downpipe was disconnected and a new PVC pipe section was installed to divert roof water to the sampler. A leaf screen was installed to reduce debris blocking the flow splitter. The flow splitter and an 80L plastic container for sample collection are housed within an aboveground form-ply box. A photograph of the roof sampling device is presented in **Figure 6.6**.

The roof sampler was operational from 9 December 2004.



LEGEND

A Flow Splitter

B Screen

- Figure 6.5 Photograph of the roof sampler installation



LEGEND

A Flow Splitter

B Sample Container

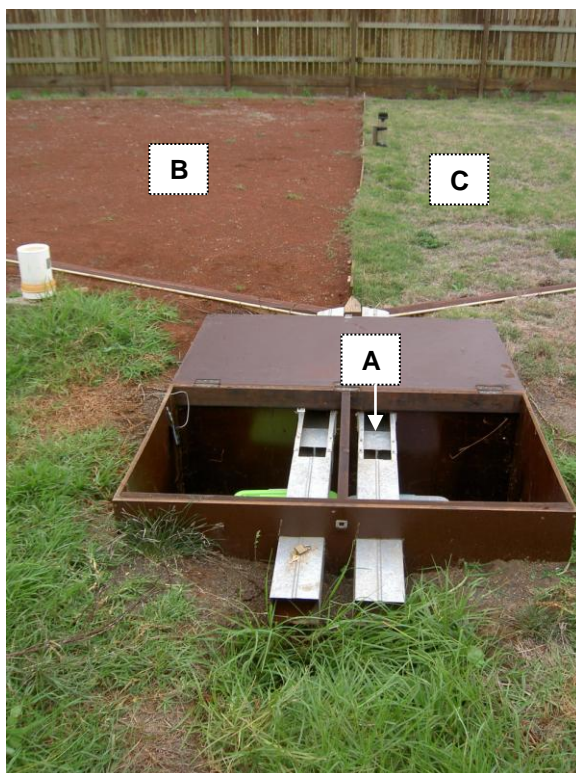
- Figure 6.6 Photograph of the roof sampling device

6.3.2 Description of Grassed and Bare Soil Monitoring Sites

During house construction, cut earthworks provided a relatively flat building platform that covered most of the allotment. Average depth of cut was approximately 0.3m. Plots for the grassed and bare surfaces were established at the rear of the house.

Soil testing was conducted as part of the house footings design and a borehole analysis indicated a surface layer of silty clay loam to 0.6m depth. This dark brown to black material had a high content of ironstone gravel (exceeding 20%) and overlaid strata layers of moist, highly plastic and reactive clays.

A photograph of the grassed and bare soil plots is provided as **Figure 6.7**. To construct the plots, red kraznozom soil was imported to the site and spread to form a single, uniformly graded surface. The depth of the imported soil material varies from less than 5cm to 15cm. The surface was graded at 1% slope and divided into two plots of equal size. Final surface levels and slopes were checked by survey. Timber edging was installed to define the perimeter of each plot.



LEGEND

- A Flow Splitter
- B Bare Soil Plot
- C Grassed Plot

- Figure 6.7 Photograph of the grassed and bare soil plots and installed samplers

The northern plot was turfed on 22 December 2004 with couch lawn and the adjacent plot was left bare with an exposed soil surface. Roof guttering was installed in the ground to drain the surface flows from each plot to the sampler. Care was taken to ensure that the lip of the gutter was flush with the plot surface to minimise ponding effects. A leaf mesh was installed in the gutters to capture debris that may block the flow splitter.

Each plot drained to a flow splitter and both of these devices were housed in a form-ply box set in the ground. A manually read raingauge and a pluviometer were installed close to the box.

It has been established that overland flow due to intense rainfall can be a dominant process in removing and transporting particles for exposed land surfaces steeper than 3%. For slopes less than 3%, raindrop splash is expected to be the main process in soil particle mobilisation (Turner *et al.* 1985). Little or no rill erosion occurs on surfaces with low slopes (McCool *et al.* 1987). Gilley *et al.* (1985) also determined that an overland slope of 1% was just sufficient to initiate transport of detached soil to the outlet of a bare soil plot.

As the slope of the bare soil plot in this study is 1%, it was anticipated that no or limited amounts of Coarse soil particles would be washed to the sampling device and that rills would not be formed during storm events. This was confirmed by inspections of the bare soil plot which show no evidence of rilling. Thus, the main form of particle mobilisation is due to ‘interill’ erosion which is governed by the kinetic energy of rainfall.

Once rilling occurs, as may be the case for steeper soil plots, there is a significant increase in soil movement. The relationship between soil erosion and ground slope is non-linear. For example, Zingg (1940) found that erosion is proportional to $(\text{Slope})^{1.49}$ comparable to $(\text{Slope})^{1.35}$ as identified by Musgrave (1947). Using these power relationships suggest that soil loss from, for example, a 4% slope is up to eight times the loss from a 1% slope.

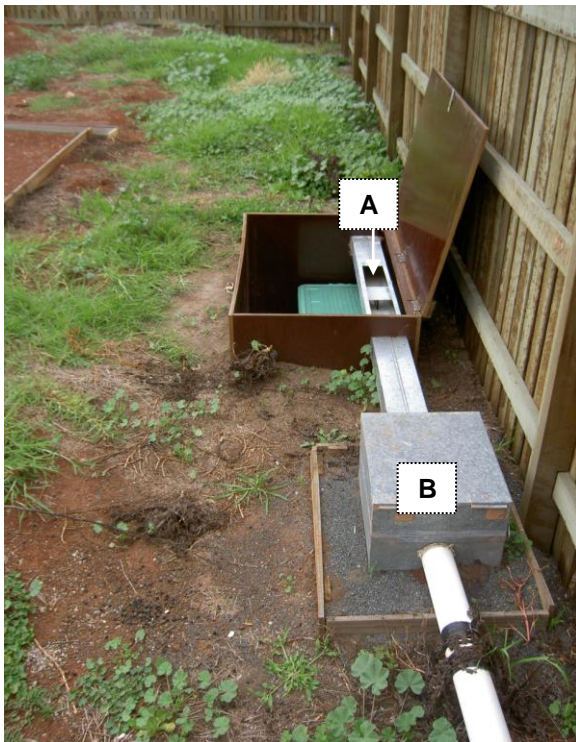
Based on these published figures, the data obtained for the 1% bare soil plot can be considered representative only of exposed, flatly graded bare soil surfaces at a physical scale of approximately 10m in length. In an urban context, this

configuration is typical of the cut-and-fill earthworks used to form a building pad within a residential lot. The particle EMCs that have been measured from the bare soil plot relate to the absence of any surface rilling, which may occur at steeper ground slopes.

6.3.3 Description of Carpark Monitoring Site

Commercial businesses including an orthodontic surgery are situated adjacent to the southern side of the allotment. A rear carpark that services these premises is close to and is elevated above the allotment boundary. On this basis, it was feasible to divert a portion of the carpark surface to a sampling device installed at the rear of the allotment.

The carpark drains to a kerb on its eastern side which directs stormwater south to an inlet pit. A small section of the kerb was removed and a PVC pipe installed to divert runoff to a flow splitter installed within the allotment. As shown in **Figure 6.8** photograph, the sampling device is housed in a form-ply box set partially in the ground next to the rear fence of the allotment. A grate installed in a metal box intercepts debris before entry into the sampler.

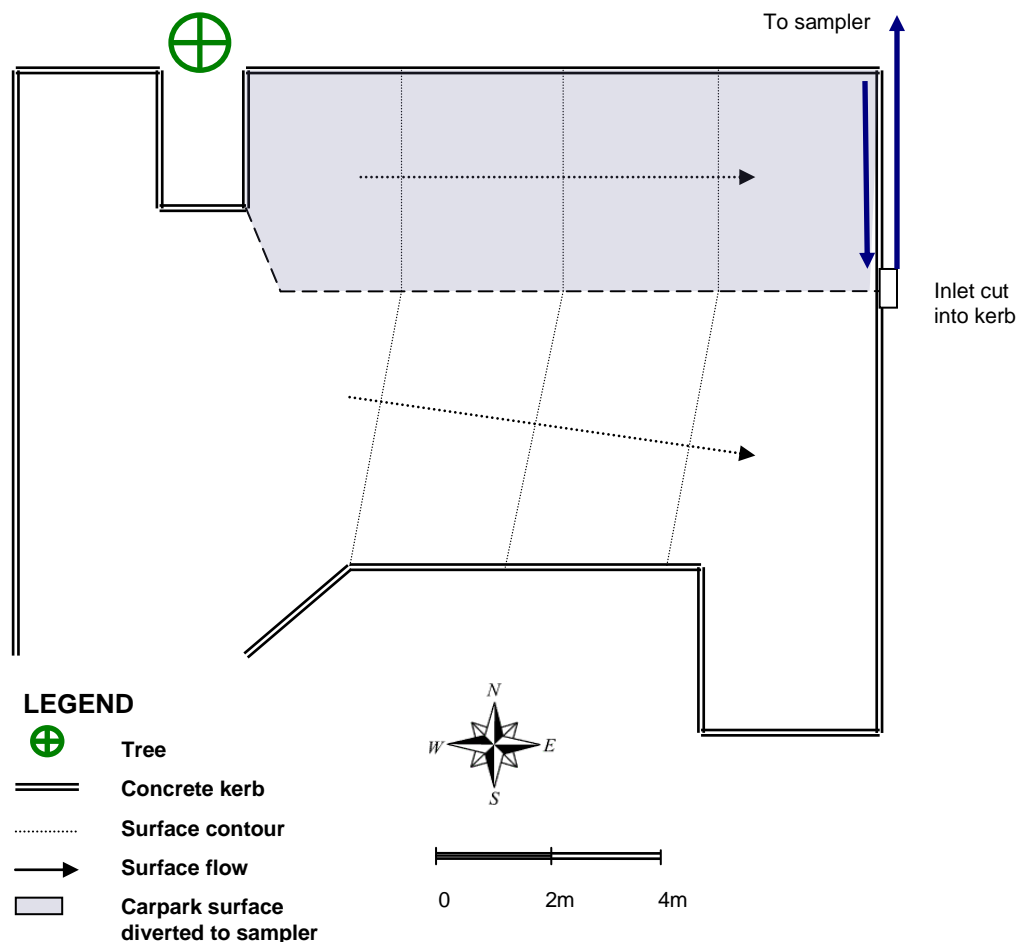


LEGEND

- A Flow Splitter
- B Screen

■ **Figure 6.8 Photograph of the carpark sampler installation**

A site plan showing the carpark site is included as **Figure 6.9**. A 56 m² portion of the carpark area is diverted that includes four parking bays. Several factors contribute to less than ideal conditions for stormwater monitoring, but the close proximity of the carpark provided an excellent opportunity to measure an additional type of urban surface. A large tree sheltered some of the carpark area from rainfall and also dropped leaves and berries during autumn. An industrial waste bin servicing the orthodontic surgery is often kept in the carpark. As a result, debris loadings are relatively high.



■ **Figure 6.9** Site layout plan of carpark showing surface diverted to sampler

As indicated in **Figure 6.9**, the diverted surface is well defined by a concrete kerb on the northern side but the southern boundary is not as clearly delineated as it is based on the carpark surface topography. The potential for uncontrolled entry and egress

of surface flows is high and the physical extent of the carpark contributing to runoff at high rainfall intensities is uncertain. The diversion of the carpark and sampler installation was completed on 11 December 2004.

6.3.4 Description of Road Monitoring Site

As indicated previously on **Figure 6.2**, a road pavement also formed a key stormwater monitoring site. The drainage area includes Clifford Street which is part of the inner city residential street system within Toowoomba. Clifford Street is a one way, northbound roadway that handles approximately 3500 vehicles/day.

The road pavement has a two way crossfall and a sampler was located at the intersection of Clifford Street and Isabel Street to collect runoff from the eastern side of the street. Stormwater is directed in a northerly direction by a concrete kerb. There is no gutter or stormwater pipe along Clifford Street and the longitudinal grade of the kerb is relatively low at less than 1%. A sampler, as shown in **Figure 6.10**, was installed on 21 December 2004.



■ **Figure 6.10** Photograph of the road sampler being installed

Installation involved making a one metre long cutting into the existing kerb and installing a kerb inlet flush with the existing road pavement. A pit, fabricated from mild steel, was built in to collect the road runoff and direct the flow into a pipe to the sampling device. A removable mesh screen was inserted into the pit to intercept leaves and debris.

The device was of similar design to the other samplers and included a flow splitter and a plastic container for sample storage housed within a form-ply box. As the device is situated within a road reserve, the sampler box was designed to withstand vehicle loading and has a lockable steel plate lid to prevent vandalism. It was also designed to have no surface obstructions that may cause a tripping hazard for pedestrians using the adjacent footpath.

6.4 Data Collected During Stormwater Monitoring

6.4.1 Rainfall Data

Data were collected for a total of 40 storms during a 13-month period from December 2004 to January 2006. In some events, especially in the initial phase after the samplers were first installed, data collection was partly incomplete due to equipment malfunction. Determinations were made of several rainfall characteristics for each event, as summarised in **Table 6.2**.

■ Table 6.2 Definition of rainfall parameters

Parameter	Basis	Symbol	Units
Rainfall Depth	Total rainfall (precipitation) measured during storm	P	mm
Rainfall Duration	Time period during storm when rainfall intensity exceeded 0.25 mm/hr	D	hr
Average Rainfall Intensity	Rainfall depth/ Rainfall duration	I	mm/hr
Peak 6 minute Rainfall Intensity	Maximum rainfall intensity during 6 minute time increment	Peak I_6	mm/hr
Antecedent Dry Period	Time period elapsed since cessation of rainfall of previous storm and start of rainfall of the sampled event	ADP	hr
Antecedent Rainfall Depth	Total rainfall of previous storm	AP	mm

During a sampling event, rainfall may occur as a series of bursts separated by periods of no rainfall or very low intensity rainfall. To provide a representative measure of rainfall duration, the cumulative time period in which the intensity of rainfall exceeded a nominal 0.25 mm/hr was adopted.

The rainfall data for storm events during the period December 2004 to January 2006 are compiled in **Appendix A**. A statistical summary of rainfall characteristics for the monitored storms is provided in **Table 6.3**. It is important to note that the rainfall statistics are defined by the operational period of sample collection for each event. Some sampling events were separated by a relatively short period of dry weather, giving an ADP value of a few hours. In hydrological terms, these samples may be considered to be the outcome of the same weather pattern, but are included in the statistics as two sets of data. This was done to ensure that the rainfall characteristics directly correspond with the stormwater particle concentrations and loads that were measured.

Additional terms (Dry Period DP and Interburst Period IBP) are introduced in Section 9.5.3 of this thesis to accommodate the effect of relatively short ADPs in predicting particle loads from impervious surfaces.

■ **Table 6.3 Statistics of rainfall characteristics of storm events ($n=40$) during December 2004 to January 2006**

Statistic	P (mm)	D (hr)	I (mm/hr)	Peak I_6 (mm/hr)	ADP (hrs)	AP (mm)
Maximum	64.3	21.3	40.0	72.1	363.5	43.0
Minimum	2.5	0.2	1.0	3.8	1.3	0.8
Median	14.4	2.7	3.7	20.1	76.3	7.0
Mean \pm S.D	17.4 \pm 13.6	5.0 \pm 5.1	6.3 \pm 7.1	23.5 \pm 15.8	106 \pm 101	11.5 \pm 11.6
Coeff. Of Variation	0.79	1.02	1.12	0.67	0.95	1.02

Mean = Arithmetic mean, S.D = Standard Deviation

6.4.2 Stormwater Particle EMC Data

Samples captured by the flow splitters were retrieved following each storm and laboratory analysed to determine particle concentrations. EMC data for all particle classes are compiled in **Appendix A**. Arithmetic means and standard deviations of particle EMCs for each urban surface are provided in **Table 6.4**. Logarithmic means are also provided as previous studies have identified that a log-normal distribution

often applies to TSS EMC data for urban surfaces (refer Section 2.3.1). As a measure of central tendency, the logarithmic mean values are consistently less than the arithmetic means.

- **Table 6.4 Arithmetic means and standard deviations of particle EMCs (mg/L) measured for December 2004 to January 2006 runoff events. Logarithmic means included in brackets.**

Particle Class	Particle EMC (mg/L)				
	Roof	Carpark	Road	Grass ¹	Bare
Number of runoff events, <i>n</i>	35	32	35	2	5
Non-Coarse NCP	16.3±26.4 (9.3)	64±75 (39)	229±150 (190)	40	736±486 (555)
MP	2.8±3.4 (1.9)	29±45 (12)	56±50 (38)	15.5	228±152 (186)
MIP	1.9±2.9 (1.0)	27±40 (12)	42±40 (28)	11.9	173±126 (134)
MOP	1.2±1.3 (0.70)	14±13 (8)	17±13 (12)	3.6	55±27 (50)
FP	11.3±20.7 (5.6)	34±33 (23)	174±143 (122)	21.0	324±323 (195)
FIP	8.4±17.3 (3.7)	25±26 (16)	138±120 (92)	12.6	260±265 (148)
FOP	2.8±3.5 (1.8)	12±8 (10)	36±24 (28)	7.9	63±59 (41)
VFP	3.7±7.9 (1.9)	7.9±4.7 (6.4)	26±16 (21)	13.6	121±80 (77)
VFIP	2.7±6.8 (0.9)	4.2±2.9 (3.3)	19±13 (14)	6.3	97±67 (46)
VFOP	1.1±1.4 (0.8)	4.3±3.1 (3.6)	7.6±4.2 (6.2)	7.2	24±14 (19)

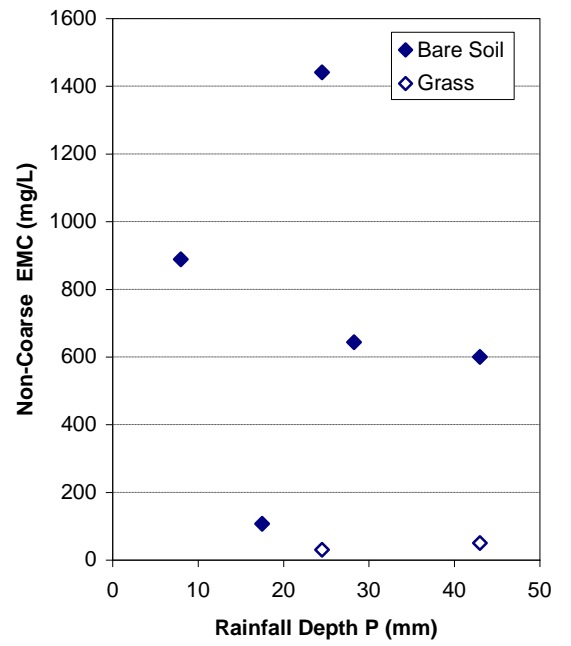
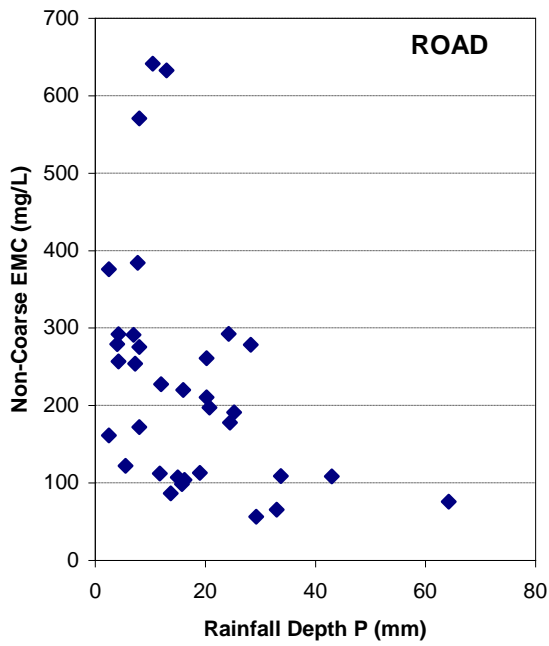
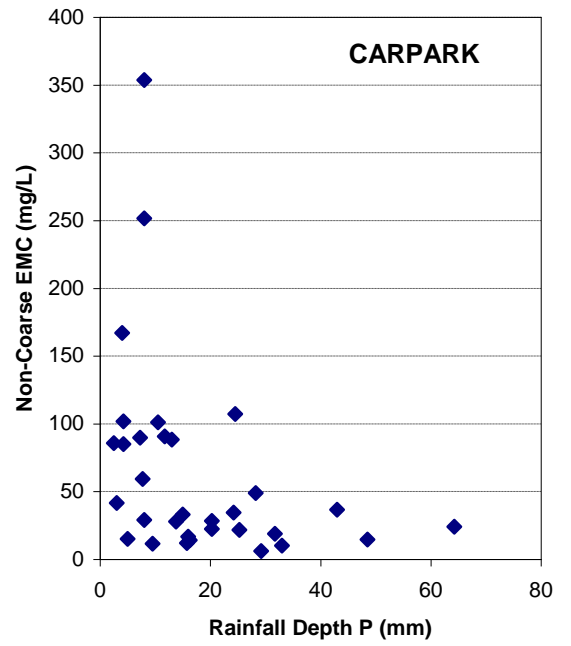
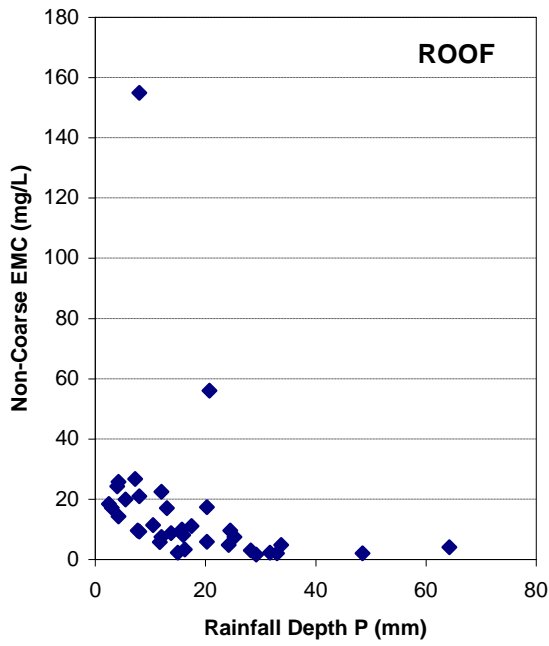
Notes:

1. No standard deviation and logarithmic mean provided for Grass as data for 2 storms only

The statistics are provided for events when runoff occurred and a sample with adequate volume was obtained for laboratory analysis. Particle concentration data was obtained for up to 88% of rainfall events from the impervious roof, carpark and road surfaces. Runoff from the pervious bare and grassed plots occurred in a small number of storms, generally when rainfall exceeded 20mm depth.

Plots of Non-Coarse Particle EMCs against rainfall depth showing all data collected for the period December 2004 to January 2006 are provided as **Figure 6.11**. A pattern of decreasing EMC with higher rainfall is evident for the impervious roof, carpark and road surfaces. This may indicate a dilution effect; the runoff volume generated from the surface in response to rainfall becomes proportionally larger than the particle mass washed off the surface. No discernable trend between rainfall depth and EMC is present in the bare soil concentration data.

*The particle EMCs and loads obtained over the 13 month period from December 2004 to January 2006 provides a comprehensive set of data suitable to describe the stormwater runoff characteristics especially for the impervious surfaces. Data was obtained for a total of 40 storms, including the detailed measurement of rainfall parameters. Comparisons of runoff characteristics between different surfaces and potential correlations with key rainfall parameters are described in **Chapter 7** of this thesis.*



■ Figure 6.11 Plots of Non-Coarse Particle EMC against Rainfall Depth for December 2004 to January 2006 runoff events

7 Analysis of Stormwater Particle Data

7.1 Summary of Data Analysis Methods

The dataset described in **Chapter 6** was analysed using several methods. Firstly, a hydrological analysis was undertaken to predict the runoff generated from each surface during individual storms. The estimated runoff volume was applied to check the sampling performance of the flow splitters.

Box plots of particle concentration data were prepared to make comparisons between the different urban surfaces. In many cases, differences between surfaces were significant. Estimates of the inorganic content of Medium Particles (MP), expressed as a mass percentage, were determined as the ratio of the Medium Inorganic Particle (MIP) concentration to the MP concentration. The inorganic contents of Fine Particles (FP) and Very Fine Particles (VFP) were similarly derived from the FIP and VFIP concentration data. Box plots of inorganic contents were also produced to compare the results across the range of urban surfaces.

The runoff volume estimates and concentration data were used to compute particle loads, expressed as mg/m^2 , from each surface.

Plots of particle load data against various rainfall parameters were produced. These scatter plots visually indicated potential correlations between particle loads generated from urban surfaces and hydrological parameters.

The hydrological analysis and plotting procedures are described in detail in this Chapter.

7.2 Hydrological Analysis using DRAINS

7.2.1 Description of DRAINS Model

DRAINS is a computer model first released in January 1998 by Watercom Pty Ltd and commonly used in Australia for the design and analysis of urban stormwater drainage systems. It converts rainfall patterns to stormwater runoff hydrographs which are then routed through a drainage network. DRAINS uses the ILSAX model (O'Loughlin 1993) for hydrological analysis, but it can also support other routing

models used in Australia such as RORB, RAFTS and WBNM (O'Loughlin & Stack 2003).

For impervious surfaces, an initial rainfall loss to account for depression storage is applied to estimate runoff. The Horton infiltration curve approach (Horton 1933), defined as **Equation 7.1**, is used to determine rainfall losses on pervious surfaces during a storm event. These losses differ depending on soil type and the antecedent moisture condition (AMC) prior to the storm.

$$f = f_c + (f_0 - f_c) e^{-K_f \cdot t} \quad [7.1]$$

where f is the infiltration capacity at time t (mm/hr), t is time after start of the storm (hours), f_0 is the infiltration capacity at time zero, f_c is the minimum infiltration capacity (mm/hr) and K_f is the curve shape factor.

7.2.2 Runoff Hydrograph Estimation Using DRAINS

A DRAINS model was constructed to represent each of the five urban surfaces. Each surface was modelled as a separate node using the catchment areas listed in **Table 6.1**. Due to the relatively small size of the monitored surfaces, a minimum time of concentration equal to 5 minutes was applied to each catchment (DNR 1992).

Rainfall pluviographs recorded onsite were downloaded from the data logger and converted into a timeseries of rainfall intensity values at 6-minute increments. This dataset was used by the DRAINS model to define rainfall patterns for each individual storm. Initial losses for the impervious surfaces were based on those published by Goyen & O'Loughlin (1999) and were set at 0.5mm for the roof and 1.0mm for the road and carpark surfaces. These adopted losses were used in the DRAINS model to simulate the peak stormwater discharge and runoff volume generated by the road, carpark and roof surfaces for each storm.

The Hortonian infiltration curves were used to model the rainfall losses for the pervious surfaces. DRAINS follows the soil classification system used by Terstriep & Stall (1974) in which the curves are divided into four types designated A, B, C and D. These types are described in **Table 7.1** as extracted from O'Loughlin & Stack (2003). In addition to soil infiltration loss, depression storage can also be applied to pervious surfaces in the DRAINS model.

■ **Table 7.1 Soil type descriptions to define DRAINS Hortonian infiltration curves**

Soil Type	Description
Type A	Low runoff potential with high infiltration rates, consisting of sands and gravels
Type B	Moderate infiltration rates and moderately well drained soils
Type C	Slow infiltration rates and may have layers that impede downward movement of water
Type D	High runoff potential with very slow infiltration rates, consisting of clays with a high water table and a high swelling potential

Antecedent moisture condition (AMC) is used by DRAINS to establish the infiltration capacity at the start of the storm. AMC is defined by four starting points on the Hortonian curves, denoted as 1, 2, 3, or 4. The starting points from O'Loughlin & Stack (2003) can be related to the total rainfall in the five days that preceded the storm, as indicated in **Table 7.2**.

■ **Table 7.2 AMC starting points and preceding rainfalls**

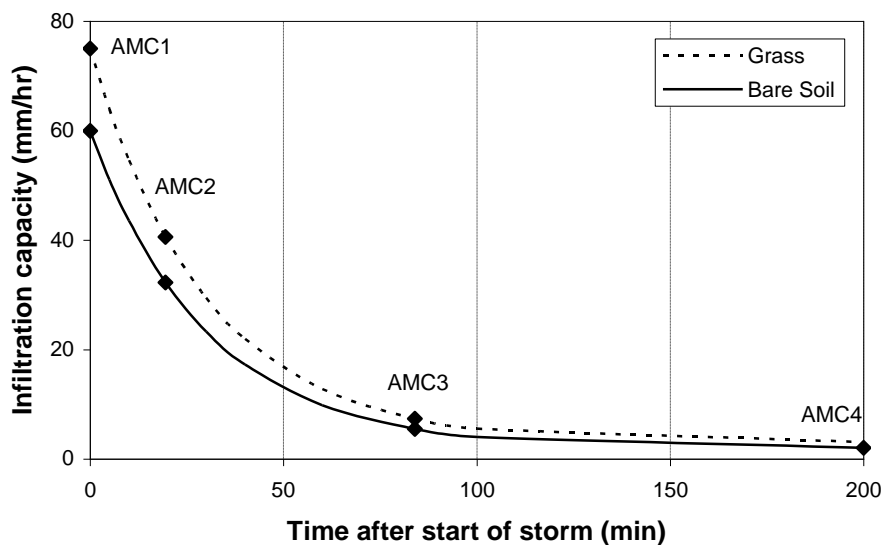
AMC Starting Point	Description	Total Rainfall in 5 days preceding storm (mm)
1	Completely dry	0
2	Moderately dry	0 to 12.5
3	Moderately wet	12.5 to 25
4	Saturated	>25

The pervious grass and bare soil plots only generated runoff during a small number of storm events, as the infiltration losses often exceeded the total rainfall. Runoff from the grass area occurred in three storms during December 2004 to June 2005 when rainfall depth exceeded 20 mm or high intensity rainfalls occurred (~ 40 mm/hr). Sample volumes for laboratory analysis were inadequate in most of these runoff events. In the case of the bare soil area, runoff occurred during five storms (typically exceeding 15mm rainfall depth).

Various soil types (listed in **Table 7.1**) were trialled in the DRAINS model to match the runoff characteristics of the pervious surfaces. By an iterative process, the runoff behaviour of the grass surface was best matched by using Soil Type D and a 1.5mm depression storage. A modified Soil Type D that had a reduced initial infiltration capacity and 1.5mm depression storage was found to be applicable to the bare soil

plot. The calibrated soil types are not consistent with the known soil description as higher infiltration rates were anticipated. The low infiltration properties that were adopted may be the result of soil compaction by machinery during construction of the house and formation of the plots.

The calibrated Hortonian infiltration curves for the bare and grassed surfaces are presented in **Figure 7.1**. The AMC starting points are also plotted on the curves. These values were used to derive the peak stormwater discharge and runoff volume produced from the grass and bare soil surfaces for each storm.



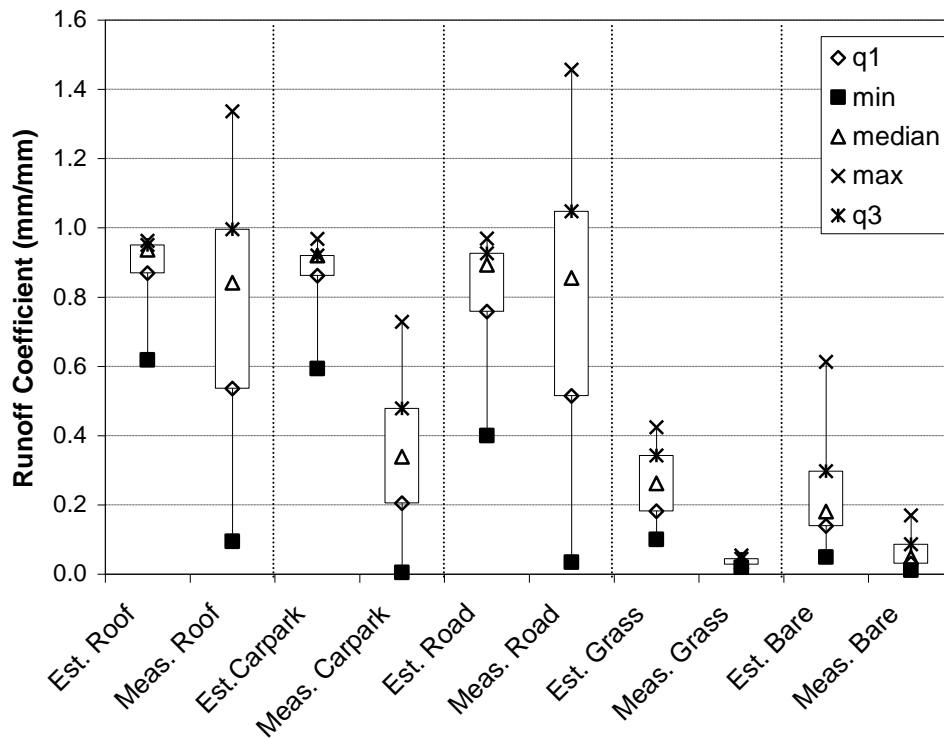
■ **Figure 7.1** Adopted Horton infiltration curves for grass and bare soil surfaces

7.2.3 Measured and Predicted Runoff Coefficients

The sample volume collected by each flow splitter, when multiplied by their respective sample flow volume ratio SVFR, provides an estimate of the total runoff volume for each storm event. A measured runoff coefficient, defined as the ratio of runoff volume to rainfall volume (or C), can be determined from this information. Statistical mean and standard deviations of C values were compared with runoff coefficients estimated from the DRAINS analysis as provided in **Table 7.3**. These statistics coincide with the initial start-up period of monitoring from December 2004 to February 2005. Box plots of C values are also presented as **Figure 7.2**.

■ **Table 7.3 Statistical means and standard deviations of runoff coefficients for December 2004 to February 2005 runoff events**

Parameter	Roof	Carpark	Road	Grass	Bare
Number of storms, n	13	13	11	2	4
Measured C	0.77±0.35	0.34±0.22	0.79±0.46	0.03±0.02	0.07±0.07
C Estimated by DRAINS	0.89±0.10	0.87±0.11	0.84±0.18	0.26±0.23	0.26±0.23



■ **Figure 7.2 Box plots of measured and estimated runoff coefficients for December 2004 to February 2005 runoff events. Note q1=first quartile value (25%), min = minimum value, max = maximum value and q3 = third quartile value (75%).**

The measured mean C for the roof is consistent with the mean predicted by DRAINS. Measured C values for the first few storms recorded for the roof were less than 0.5; significantly lower than expected values for an impervious surface. On inspection, some roof flow was being diverted to an adjacent downpipe due to the flat grading of the guttering system. Vertical plates were inserted into the gutter to isolate the roof runoff to flow to the sampling device. In storms subsequent to this gutter modification, the measured C values were higher (typically 0.9 to 1.0) as flow diversion was restricted. The inclusion of the measured C values for the initial storms results in the measured mean C for the roof being slightly less than the

predicted mean C and also increases the variance of measured C values (refer box plot **Figure 7.2**).

The mean C measured for the carpark is significantly less than the predicted mean. This is due to the high potential for stormwater flows to be diverted prior to the inlet of the sampling device (refer to **Section 6.3.3** for a discussion on this aspect). Due to this flow diversion effect, the actual SFVR for the carpark sampler is considered to be significantly less than the SFVR adopted to determine the measured runoff values.

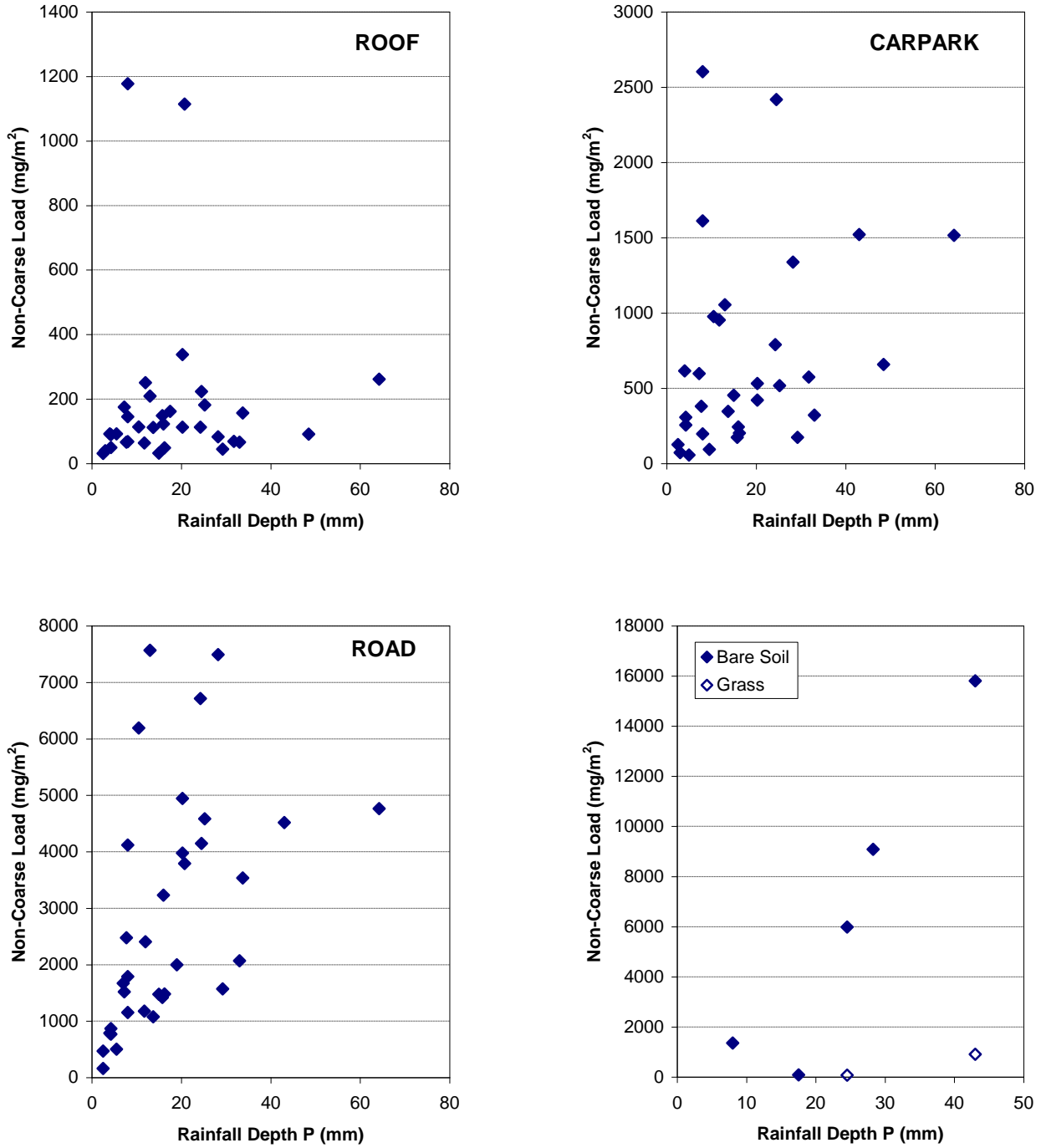
Measured and predicted mean C values for the road were found to be in close agreement, as was the case for the bare soil surface. The measured mean C value for the grass surface was less than the predicted value, but this outcome is based on a small number of runoff events.

During a single storm, the measured C value exceeded 1.0 for both the roof and road surfaces. These are outliers indicating measurement error as runoff volume can not exceed rainfall volume. During the storm of 18/1/2005, the pluviometer failed and so no rainfall temporal pattern was available for a DRAINS analysis. Rainfall data collected by Toowoomba City Council indicates that this storm had an approximate frequency corresponding to 2 year ARI which is significantly greater than the 6 month ARI used in the design of the sampling device. This exceeded the hydraulic capacity of the flow splitter channel, resulting in an overflow into the sample container.

Generally, the performance of the flow splitters in capturing a reasonable portion of the runoff hydrograph during the monitored storms is considered to be good.

7.2.4 Particle Load Estimates for Individual Storms

The load of each particle class generated by the urban surfaces on an individual storm basis was derived by multiplying the particle EMC by the runoff volume predicted by DRAINS analysis. Plots of Non-Coarse Particle load against rainfall depth showing data for December 2004 to January 2006 storms are provided as **Figure 7.3**. Statistical means and standard deviations of particle loads for each urban surface are provided in **Table 7.4**.



■ Figure 7.3 Plots of Non-Coarse Particle load versus rainfall depth for December 2004 to January 2006 runoff events

■ **Table 7.4 Statistical means and standard deviations of particle loads for December 2004 to January 2006 runoff events**

Particle Class	Particle Load (mg/m ² /storm)				
	Roof	Carpark	Road	Grass	Bare
Number of storms, <i>n</i>	35	32	35	2	5
Non-Coarse	180±255	691±651	3350±3290	490	6470±6350
MP	34±31	292±387	649±558	282	2470±2905
FP	101±157	361±274	2230±2800	383	3110±2200
VFP	35±60	91±63	316±293	247	1590±1520

Notes:

1. No standard deviation provided for Grass as data for 2 storms only

7.3 Box Plot Analysis of Particle EMC Data

7.3.1 Box Plots of Particle EMCs

Box plots of particle EMCs for all December 2004 to January 2006 storms were produced and are presented as **Figure 7.4**. The plots enable data for the different surfaces to be graphically compared and show various statistical parameters. These parameters include median, minimum (min), maximum (max), first quartile or 25 percentile (q1) and third quartile or 75 percentile values (q3). The box plots for the grass and bare surfaces are indicative due to the small number of sampled events (less than 6) and are included for completeness.

Box plots are shown for EMCs of MPs, FPs, VFPs and Non-Coarse Particles (or the sum of MPs, FPs and VFPs). Generally in all particle classes, the roof EMCs were the lowest, followed by the carpark EMCs and road EMCs in that order. The bare soil EMCs were the highest with the grass EMCs tending to be of similar magnitude as the carpark values. An exception is the grass VFP EMCs which were higher and of the same order as the road EMCs.

The box plots indicate a significant range of EMC values, typically a 10 to 100-fold difference between the minimum and maximum values that were measured. The road EMCs exhibited a narrower range; approximately a 5-fold difference. The measured range of grass EMCs was small due to the limited number of runoff events that were measured for this pervious surface.

7.3.2 Box Plots of Inorganic Content

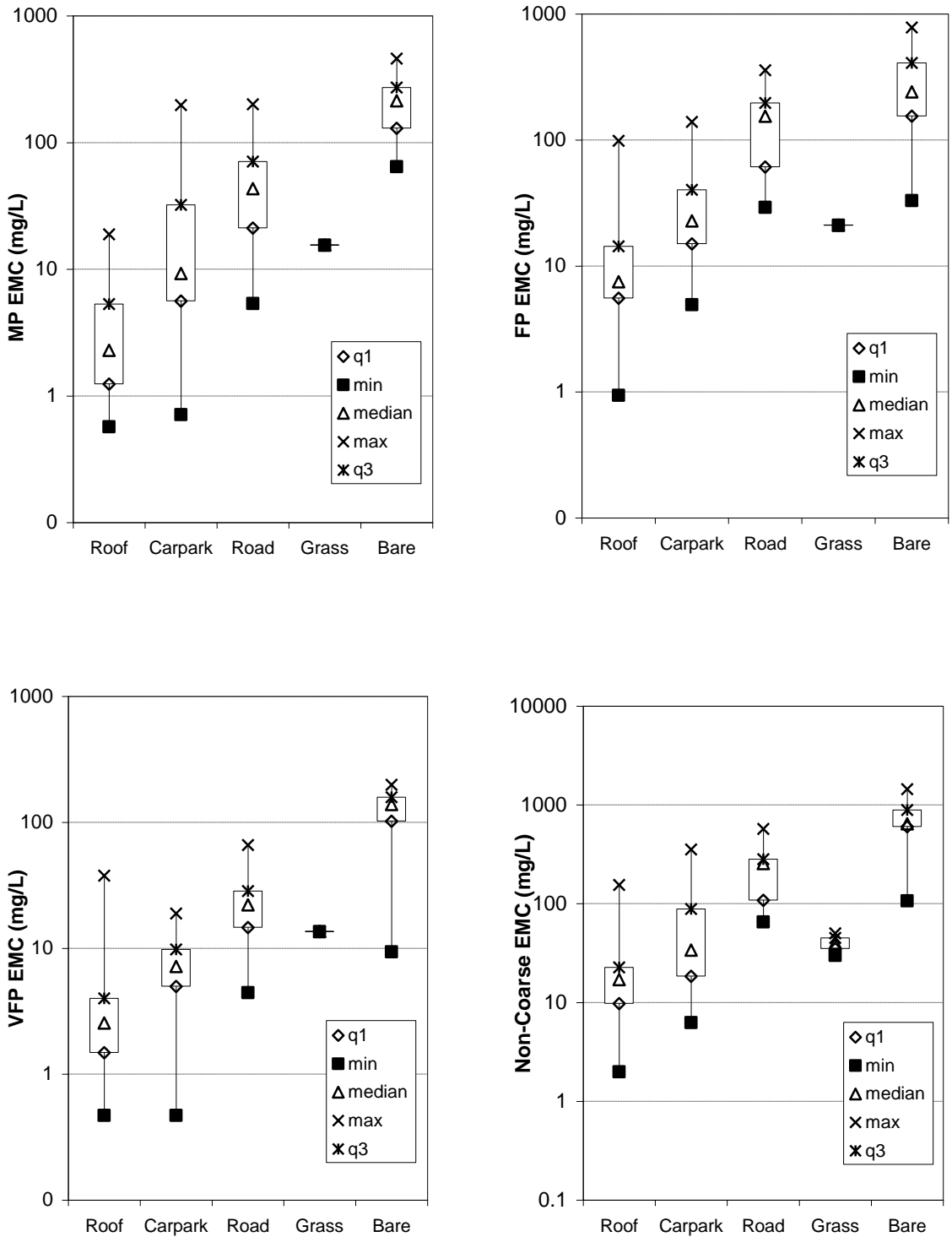
Box plots of the inorganic content of each particle class, expressed as a percentage by weight, are presented as **Figure 7.5**. These plots are based on the MIP, FIP and VFIP concentrations that were measured for each storm.

In all particle classes, most of the particle mass consists of inorganic matter (as % Inorganic generally exceeds 50%). Overall, for Non-Coarse Particles the inorganic content generally fell in a range between 55 to 85%. Inorganic content for the roof, carpark and grass were of similar magnitude with the road and bare soil values being slightly higher. This pattern was also present for the inorganic content of FPs and VFPs, but in the case of grass MPs the inorganic content was more consistent with road and bare soil values.

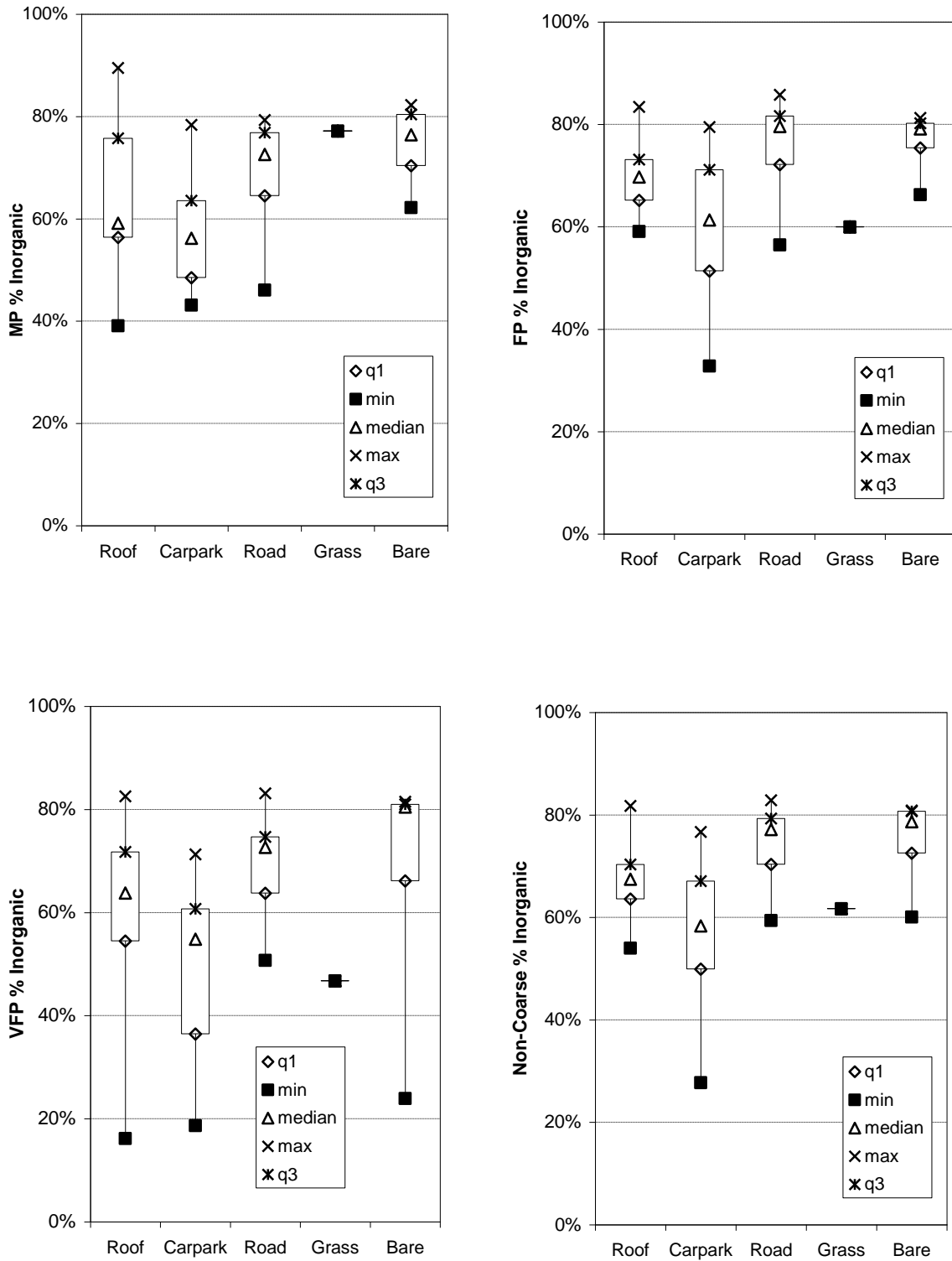
The median inorganic content for the road surface Non-Coarse Particles is 77%. This content is comparable with the 72% median based on TSS and VSS data for highway runoff measured from nine storms at Louisiana, USA (Sansalone & Tittlebaum 2001), but higher than the 45% median determined by Gromaire-Mertz *et al.* (1999) for street runoff from seven storms within central Paris, France. For the Paris study, a median inorganic content of 61% was determined for roof TSS which is slightly less than the 66% median for Non-Coarse Particles (refer **Figure 7.5**).

7.3.3 Box Plots of Particle Size Composition

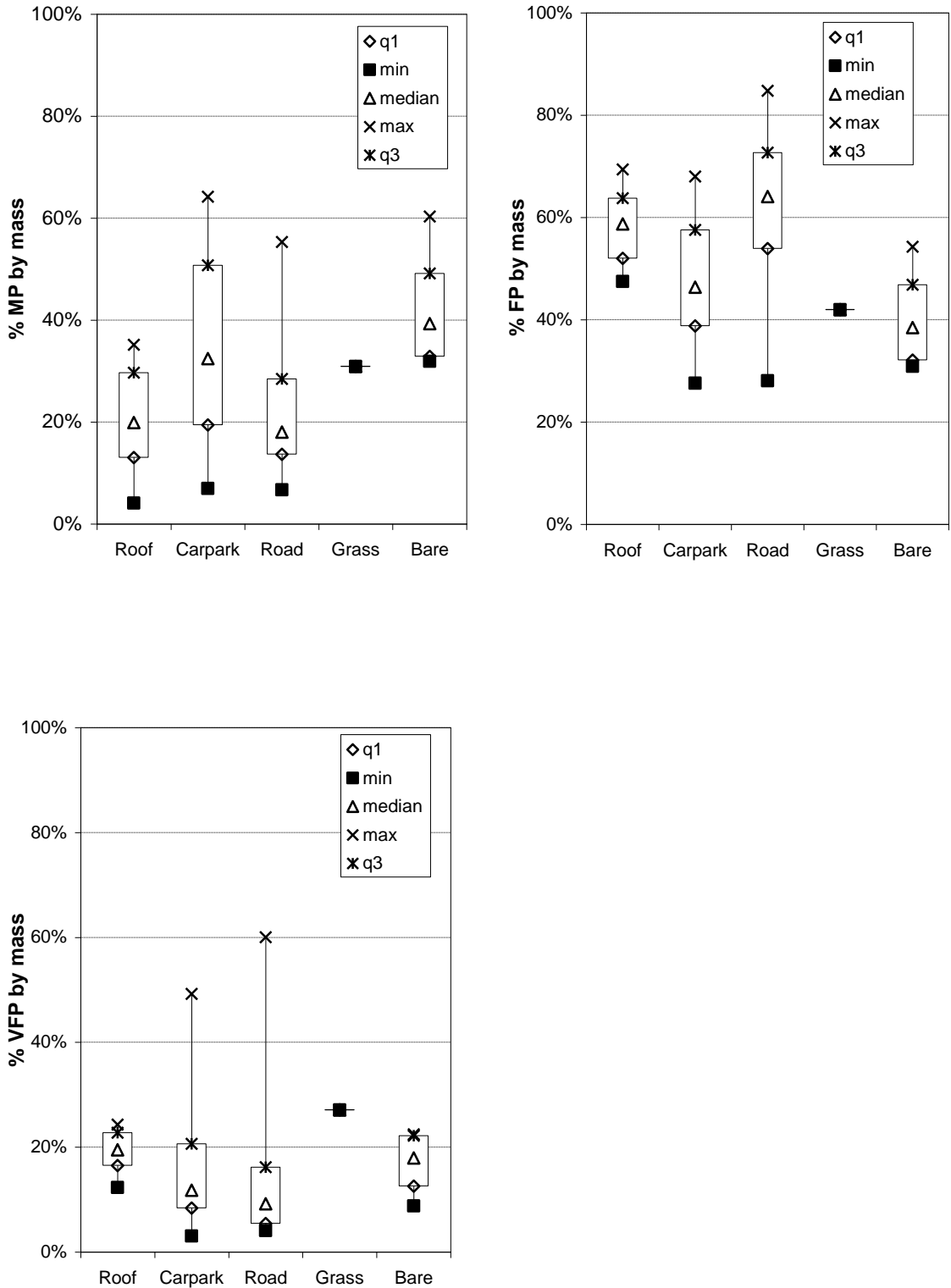
The distribution of particle size for the urban surfaces is indicated by the series of box plots presented in **Figure 7.6**. These plots show the mass of MPs, FPs and VFPs as a percentage of the overall Non-Coarse Particle mass. FPs tends to contribute the greatest particle mass in road and roof runoff with percentages generally in the 50 to 70% range. Bare soil runoff had near equal proportions, by mass, of FPs and MPs with median values of approximately 40%. By comparison, the percentage mass of MPs were generally less than 30% for roof, road and grass runoff and slightly higher than 30% for carpark runoff. The proportion of VFPs by mass tended to be relatively small at typically less than 20%.



■ **Figure 7.4** Box plots of EMCs for MPs, FPs, VFPs and Non-Coarse Particles for December 2004 to January 2006 runoff events. Note q1=first quartile value (25%), min = minimum value, max = maximum value and q3 = third quartile value (75%).

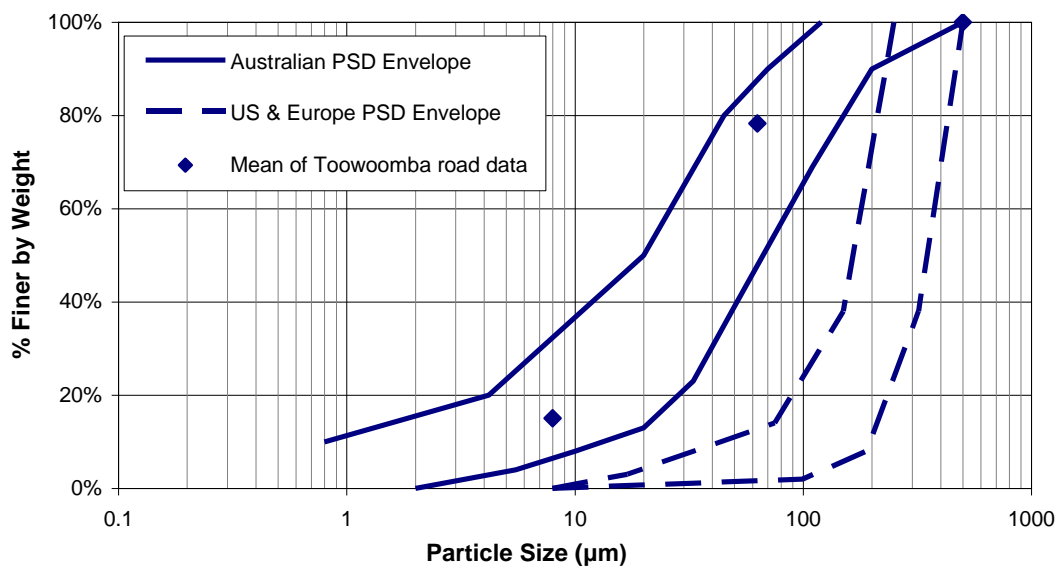


■ Figure 7.5 Box plots of inorganic content for MPs, FPs, VFPs and Non-Coarse Particles for December 2004 to January 2006 runoff events. Note q1=first quartile value (25%), min = minimum value, max = maximum value and q3 = third quartile value (75%).



■ **Figure 7.6 Box plots of particle size composition of MPs, FPs and VFPs for December 2004 to January 2006 runoff events. Note q1=first quartile value (25%), min = minimum value, max = maximum value and q3 = third quartile value (75%).**

Lloyd & Wong (1999) found that the size distribution of Non-Coarse Particles from Australian road runoff studies was distinctly different to data obtained from USA and Europe. **Figure 7.7** shows that the particle size distributions (PSDs) of three Australian studies (Ball & Abustan 1995; Drapper 1998; Lloyd & Wong 1999) can be contained within an envelope that has a relatively high proportion of finely graded particles. By comparison, the overseas PSDs have a smaller proportion of fine particles. The mean PSD of Non-Coarse Particles based on the VFP, FP and MP data obtained from the Toowoomba road site is also overlaid onto **Figure 7.7** and is consistent with the findings of Lloyd & Wong (1999).

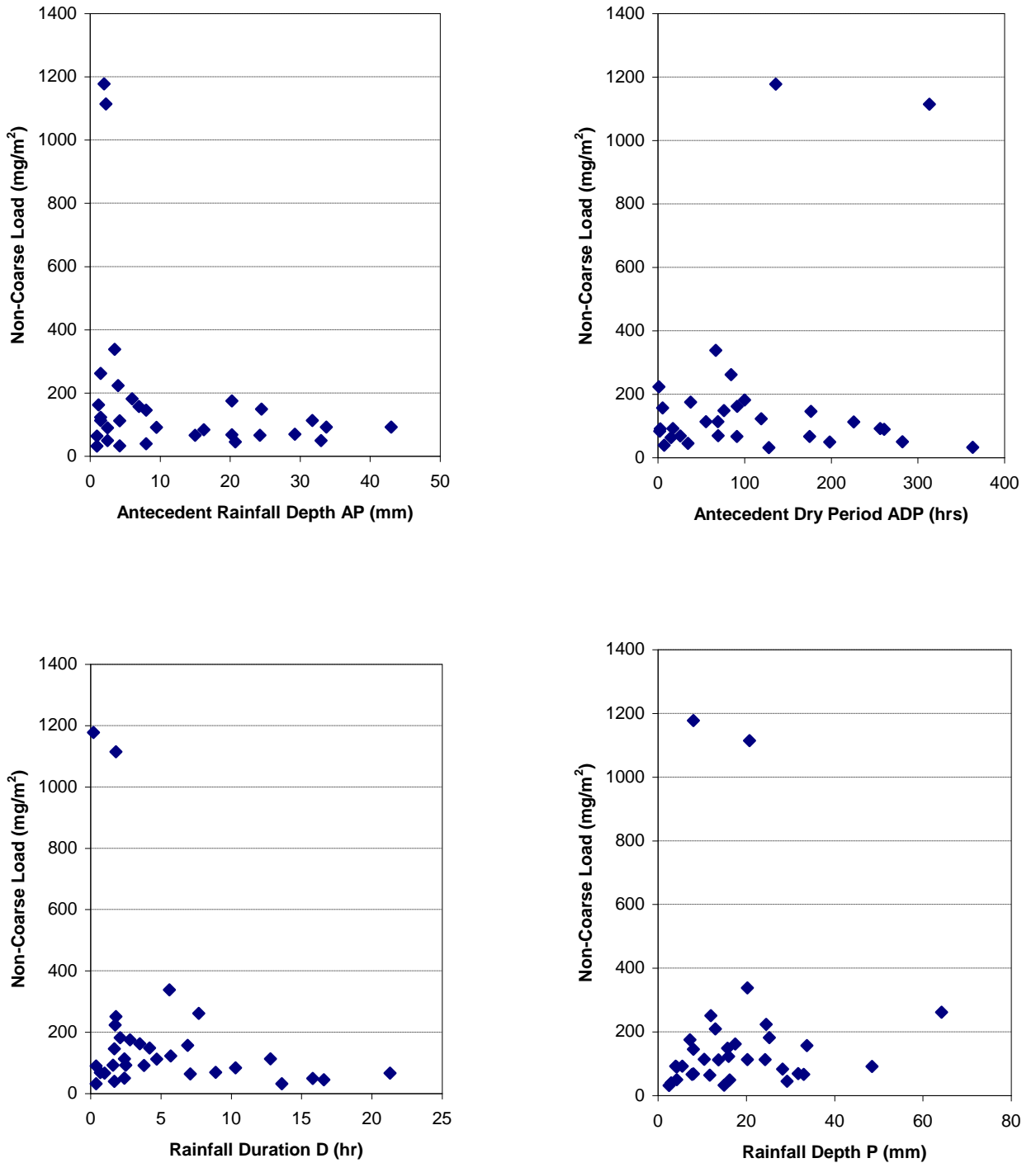


- **Figure 7.7 Comparison of road mean particle size distribution for Non-Coarse Particles with Australian and Overseas envelopes for road and highway runoff (from Lloyd & Wong 1999)**

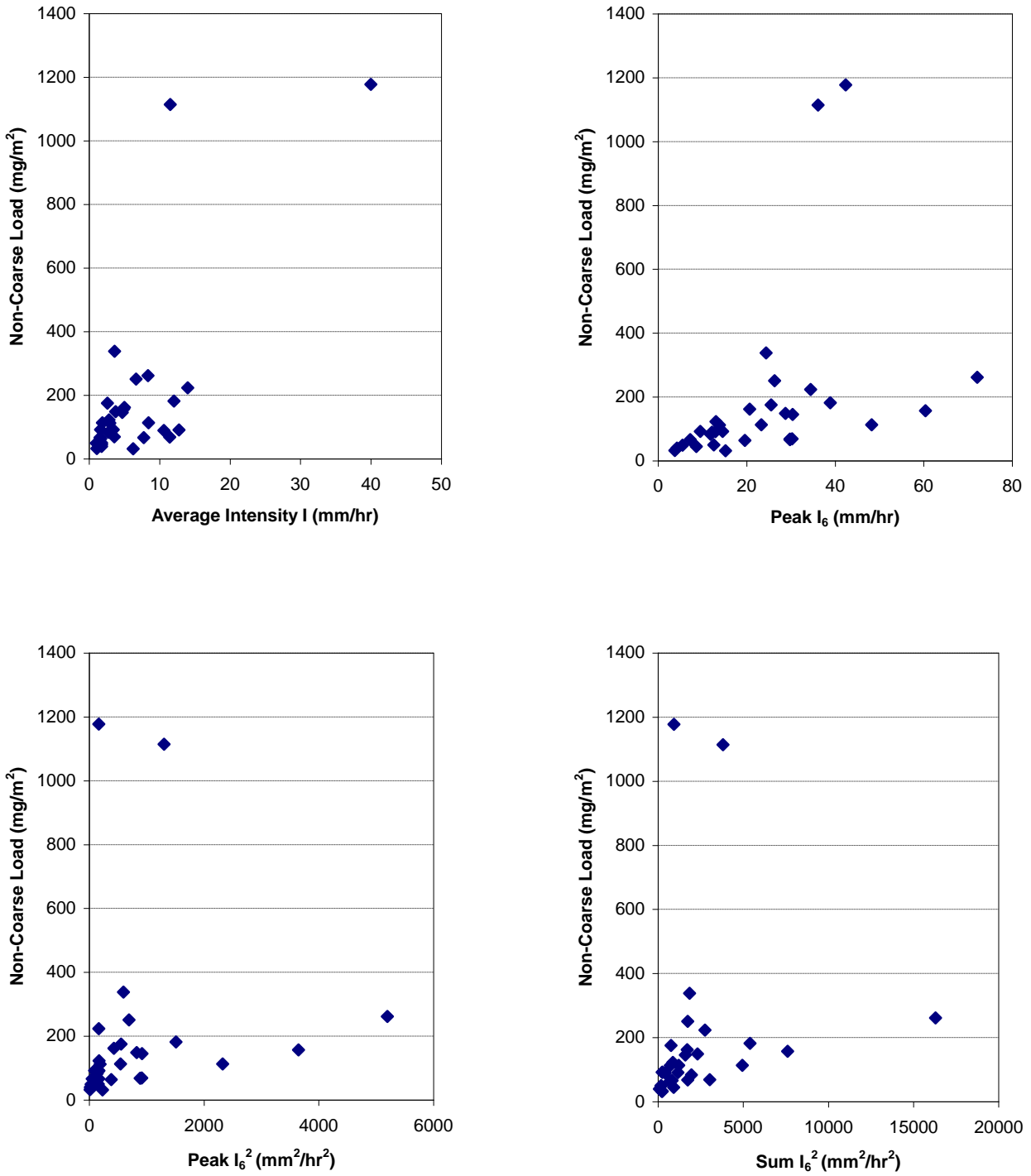
7.4 Scatter Plots of Impervious Surface NCP Load Data

7.4.1 Impervious Surface NCP Loads versus Rainfall Parameters

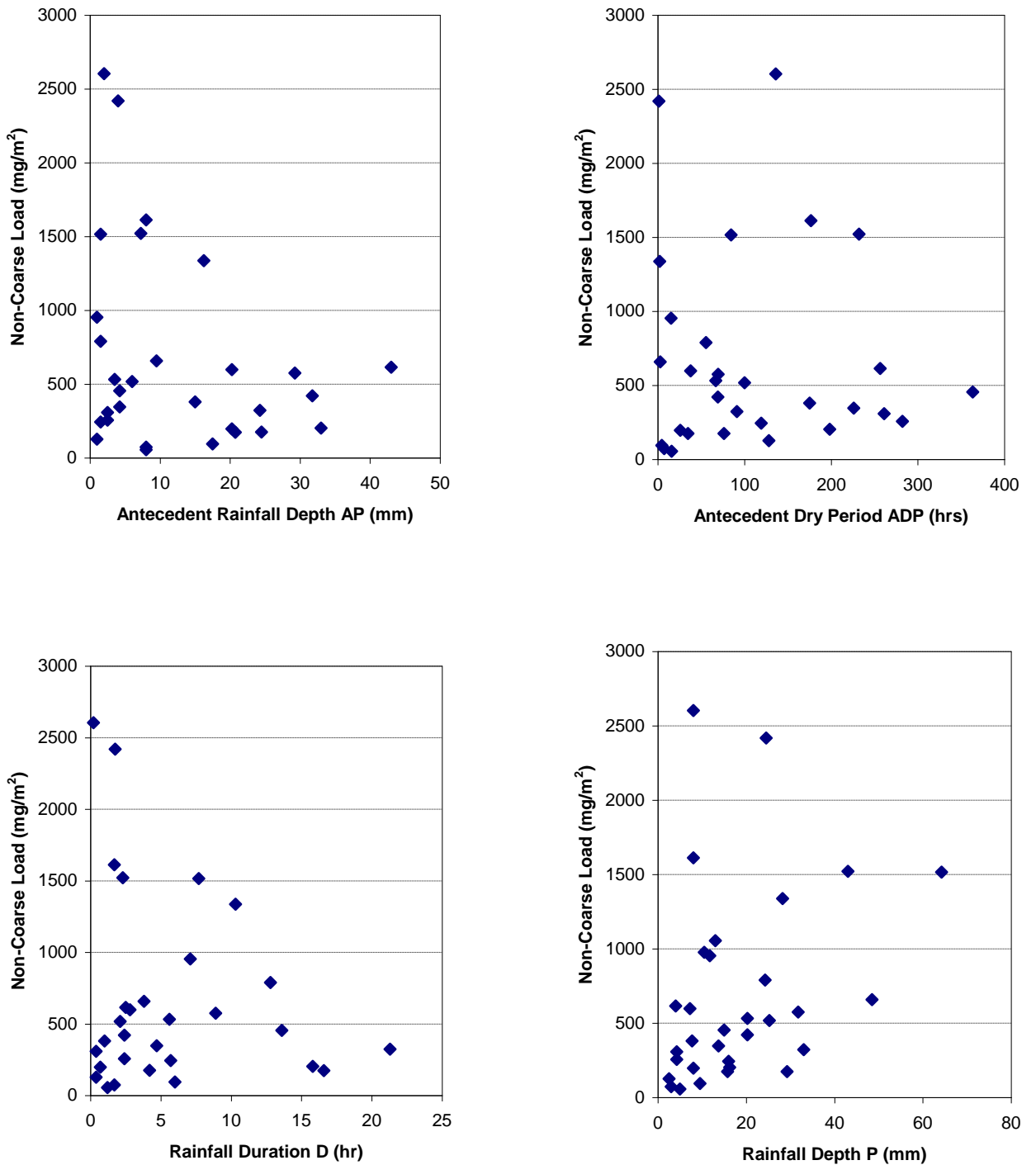
Scatter plots of Non-Coarse Particle loads measured for all December 2004 to January 2006 storms were prepared for a range of rainfall parameters. These rainfall parameters are previously listed and defined in **Table 6.2**. The scatter plots for the impervious roof, carpark and road surfaces are presented as **Figures 7.8 to 7.13**.



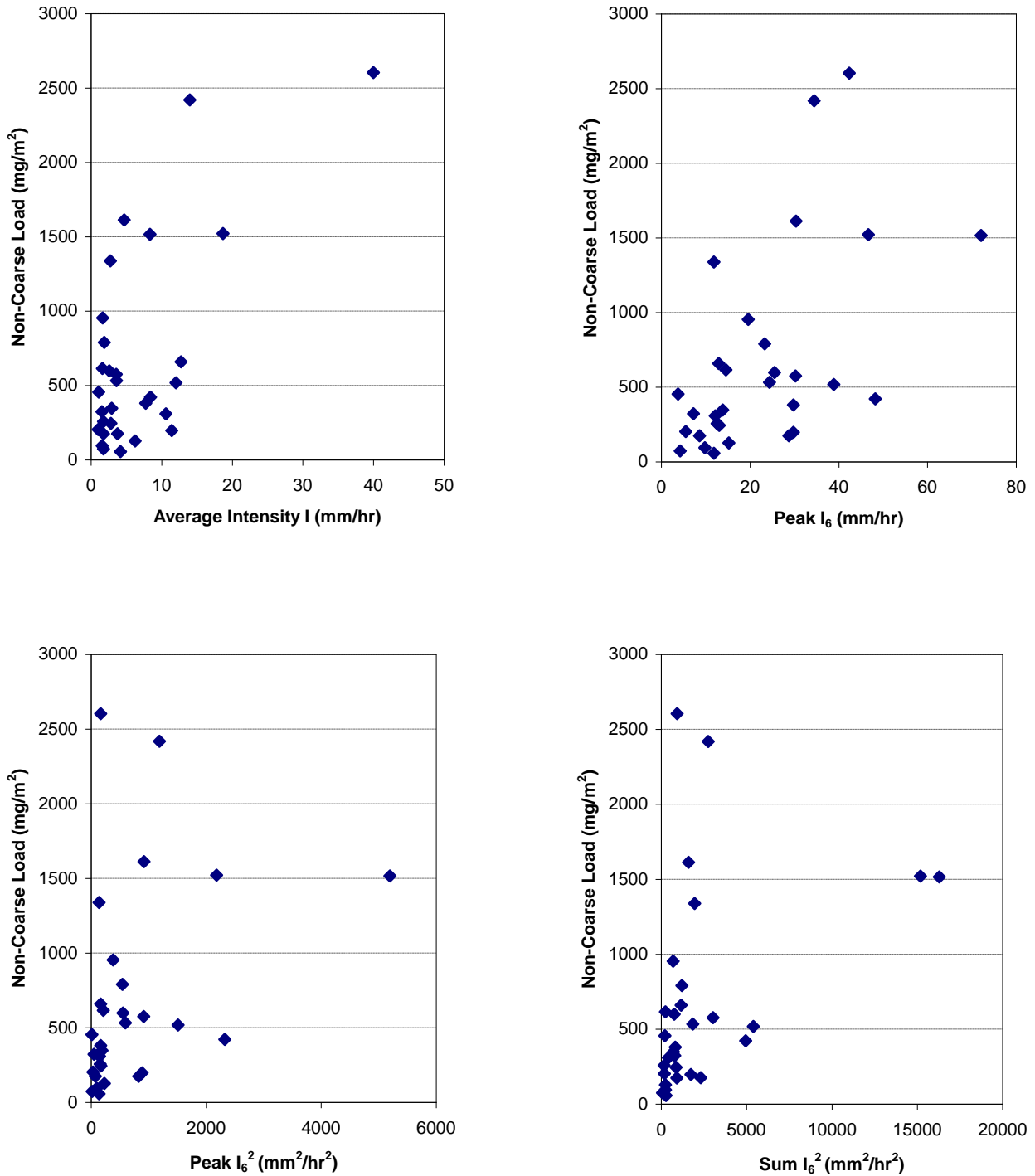
■ **Figure 7.8 Scatter plots of roof Non-Coarse Particle loads against rainfall parameters for December 2004 to January 2006 runoff events – Antecedent and event rainfall parameters**



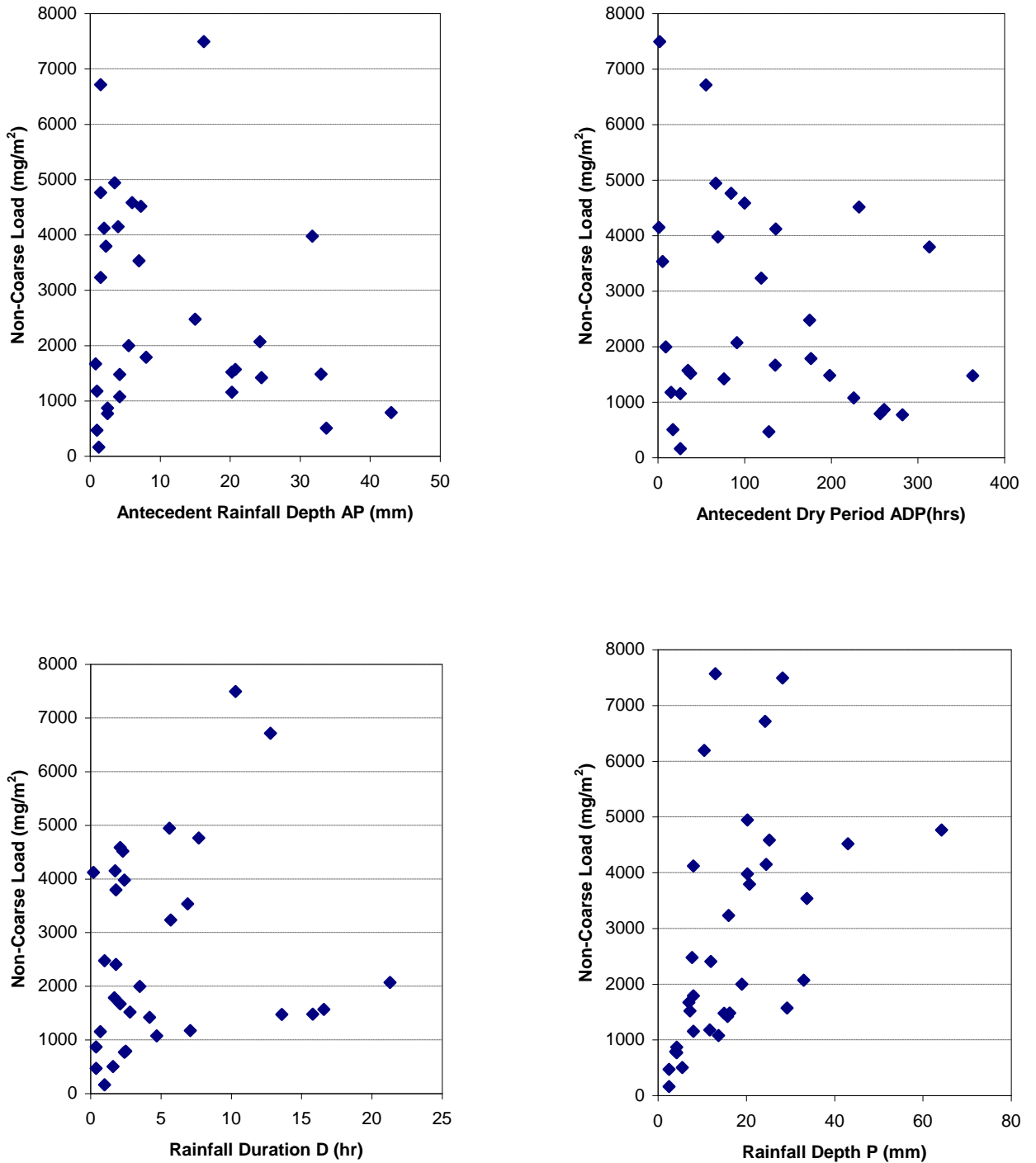
■ Figure 7.9 Scatter plots of roof Non-Coarse Particle loads against rainfall parameters for December 2004 to January 2006 runoff events – Rainfall intensity and energy parameters



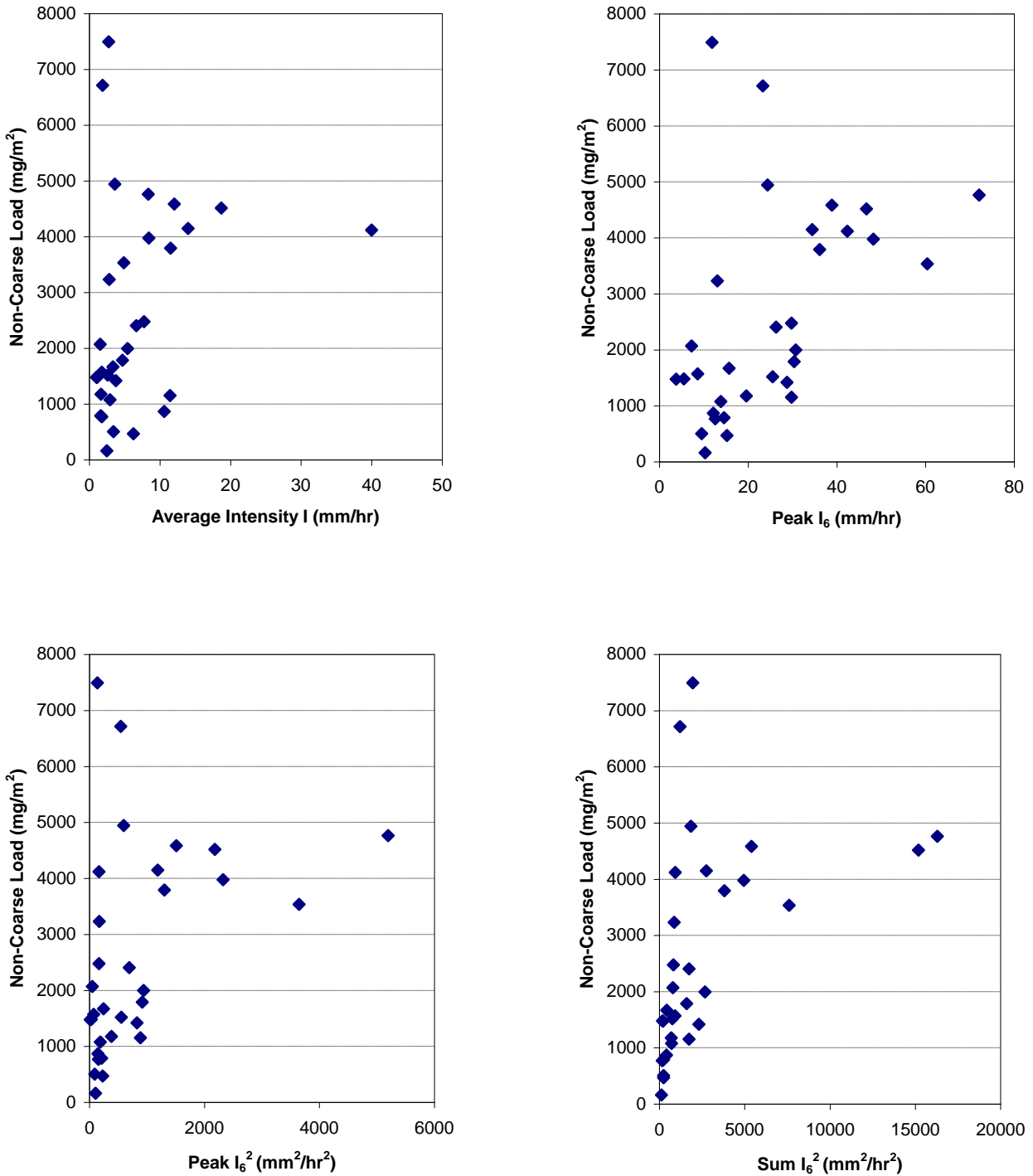
■ Figure 7.10 Scatter plots of carpark Non-Coarse Particle loads against rainfall parameters for December 2004 to January 2006 runoff events – Antecedent and event rainfall parameters



■ Figure 7.11 Scatter plots of carpark Non-Coarse Particle loads against rainfall parameters for December 2004 to January 2006 runoff events – Rainfall intensity and energy parameters



■ **Figure 7.12 Scatter plots of road Non-Coarse Particle loads against rainfall parameters for December 2004 to January 2006 runoff events – Antecedent and event rainfall parameters**



■ **Figure 7.13** Scatter plots of road Non-Coarse Particle loads against rainfall parameters for December 2004 to January 2006 runoff events – Rainfall intensity and energy parameters

In addition to the basic rainfall parameters, two extra parameters (Peak I_6^2 and $\sum I_6^2$) were also included in the scatter plots. These parameters are defined in **Table 7.5** and relate to particle detachment due to rainfall impact energy. Predicted washoff of soil particles from pervious surfaces commonly employ a relationship based on I^2 (Haster & James 1994; Meyer & Wischmeier 1969; Nearing *et al.* 1989; Rose 1960). Other researchers suggest that particle detachment due to rain splash is proportional to $I^{1.6}$ (Gabet & Dunne 2003; Meyer 1981) or $I^{1.5}$ (Ekern 1954).

Zug *et al.* (1999) applied a washoff function based on I^2 to reproduce TSS pollutographs measured from five French urban catchments. Chiew *et al.* (1997a) found that TSS loads estimated using $\sum I_6^2$ were better than those from other rainfall parameters in matching measured TSS loads from a 200 ha Melbourne catchment. Similar power functions based on I_6 have also been applied in estimating TSS, total nitrogen and total phosphorus loads washed from urban catchments in Melbourne and Brisbane (Francey *et al.* 2004; Francey *et al.* 2005).

Particle washoff from small urban catchments was assumed by Svensson (1987) to be proportional to $(I/I_d)^2$, where I_d is a rainfall intensity constant. A similar relationship was applied by Westerlund *et al.* (2005) to model suspended solid transport from a road in northern Sweden and also by Artina *et al.* (2005) to estimate TSS loads from a 1.15ha truck transit and parking area situated in Bologna, Italy.

■ **Table 7.5 Definition of rainfall energy parameters**

Parameter	Basis	Symbol	Units
Peak 6 minute Rainfall intensity squared	Maximum rainfall intensity during 6 minute time increment squared	Peak I_6^2	mm^2/hr^2
Sum of 6 minute Rainfall intensity squared	Sum of rainfall intensity at 6 minute increments squared during time period within storm when rainfall intensity exceeded 0.25 mm/hr	$\sum I_6^2$	mm^2/hr^2

The scatter plots provide a visual guide to possible correlations between loads generated from individual storms and various rainfall characteristics. Each plot was assessed and the degree of correlation was ranked according to the qualitative scale provided in **Table 7.6**.

■ **Table 7.6 Qualitative scale of degree of correlation**

Scale	Description
++	A positive correlation (load increases as rainfall parameter increases) is visually present
+	A positive correlation maybe present, but is not clearly evident in the scatter plot
NA	No correlation is visually apparent
-	A negative correlation maybe present, but is not clearly evident in the scatter plot
--	A negative correlation (load decreases as rainfall parameter increases) is visually present

The degrees of correlation based on the visual assessment of scatter plots are compiled in **Table 7.7**. A statistical correlation analysis was not conducted as this approach assumes a linear relationship is present, which may not be the case.

■ **Table 7.7 Assessment of visual correlation between impervious surface Non-Coarse Particle loads and selected rainfall parameters**

Rainfall Parameter	Roof Loads	Carpark Loads	Road Loads
Antecedent Rainfall Depth AP	--	--	-
Antecedent Dry Period ADP	-	-	-
Rainfall Duration D	--	--	NA
Rainfall Depth P	NA	NA	+
Average rainfall intensity I	++	++	+
Peak I_6	++	+	+
Peak I_6^2	+	+	+
$\sum I_6^2$	+	+	+

For all surfaces, a weak negative correlation is graphically present between antecedent dry period (ADP) and the Non-Coarse Particle load that is generated. The load tends to decrease with an increase in the antecedent rainfall depth (AP), although this trend is weaker for the road surface. A relationship between load and rainfall depth is generally not evident, except for a weak positive correlation for the road surface. The strongest positive trends are exhibited between loads and average rainfall intensity (I) and peak 6-minute intensity (Peak I_6).

Many stormwater models for impervious surfaces such as roads adopt a buildup-washoff concept that involves particle accumulation during dry weather and their subsequent removal by rainfall and runoff during storms. Examples of these models include SWMM (Huber & Dickinson 1988), STORM (Abbot 1977) and HSPF (Johanson *et al.* 1984). These, and other models, assume that the buildup of particles on a surface increases with the number of dry days that has elapsed since the previous storm. A linear or exponential function is typically used and defines the amount of particle load that is available for washoff at the start of the storm.

If buildup is a time dependent process then a positive correlation would be evident between load and antecedent dry period (ADP). As summarised in **Table 7.7**, no visual trend is present to indicate that a long extended dry period would consistently lead to a greater accumulation of particles compared to a shorter dry period.

Similarly, Deletic & Maksimovic (1998) found that there was no correlation between TSS concentration and ADP in their study of stormwater runoff from paved areas. Other studies of urban runoff have also found no relationship between TSS load and ADP (Charbeneau & Barrett 1998; Le Boutillier *et al.* 2000).

This observation is also consistent with Chiew *et al.* (1997a) who postulated that the accumulation of particles onto impervious surfaces is maintained relatively constant at all times. Buildup is viewed as a process of dynamic equilibrium whereby deposition by dustfall, vehicles and other means is offset by removal processes such as wind, vehicle induced eddies and particle decomposition. Particle buildup onto a washed surface following a storm event can occur rapidly to quickly restore the dynamic equilibrium (White 1989). Grottker (1987) also found that high rates of particle accumulation occurred on roads during a very short period after a rainfall, especially in the first day.

Desbordes & Servat (1987) found that rainfall intensity and storm volume were more important than particle buildup during dry weather. As indicated in **Table 7.7**, a positive correlation was visually present between Non-Coarse Particle load and rainfall intensity factors, in particular average rainfall intensity (I) and Peak I_6 . Other studies have also identified that rainfall intensity is a key determinant of particle washoff (Kuo *et al.* 1993; Yaziz *et al.* 1989).

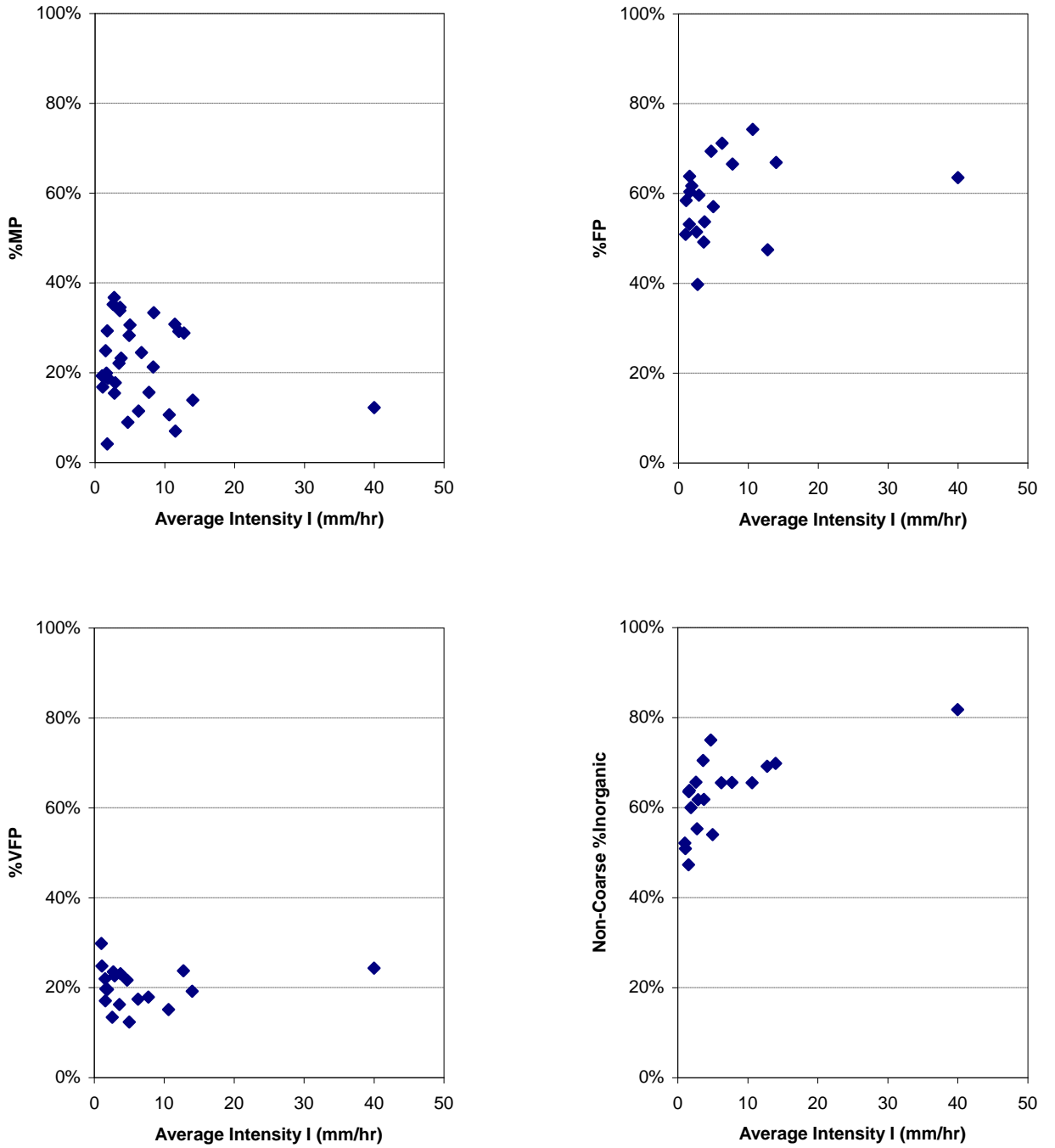
7.4.2 Impervious Surface Non-Coarse Particle Composition versus Average Intensity

Particle composition includes the mass distribution of particle size (% MP, %FP and %VFP) and the inorganic content of Non-Coarse Particles. Scatter plots of these composition parameters against average rainfall intensity for the impervious roof, carpark and road surfaces are provided as **Figures 7.14, 7.15 and 7.16**. The average rainfall intensity was selected as the independent variable as this rainfall parameter exhibited a positive correlation to particle loads, as indicated in **Table 7.7**.

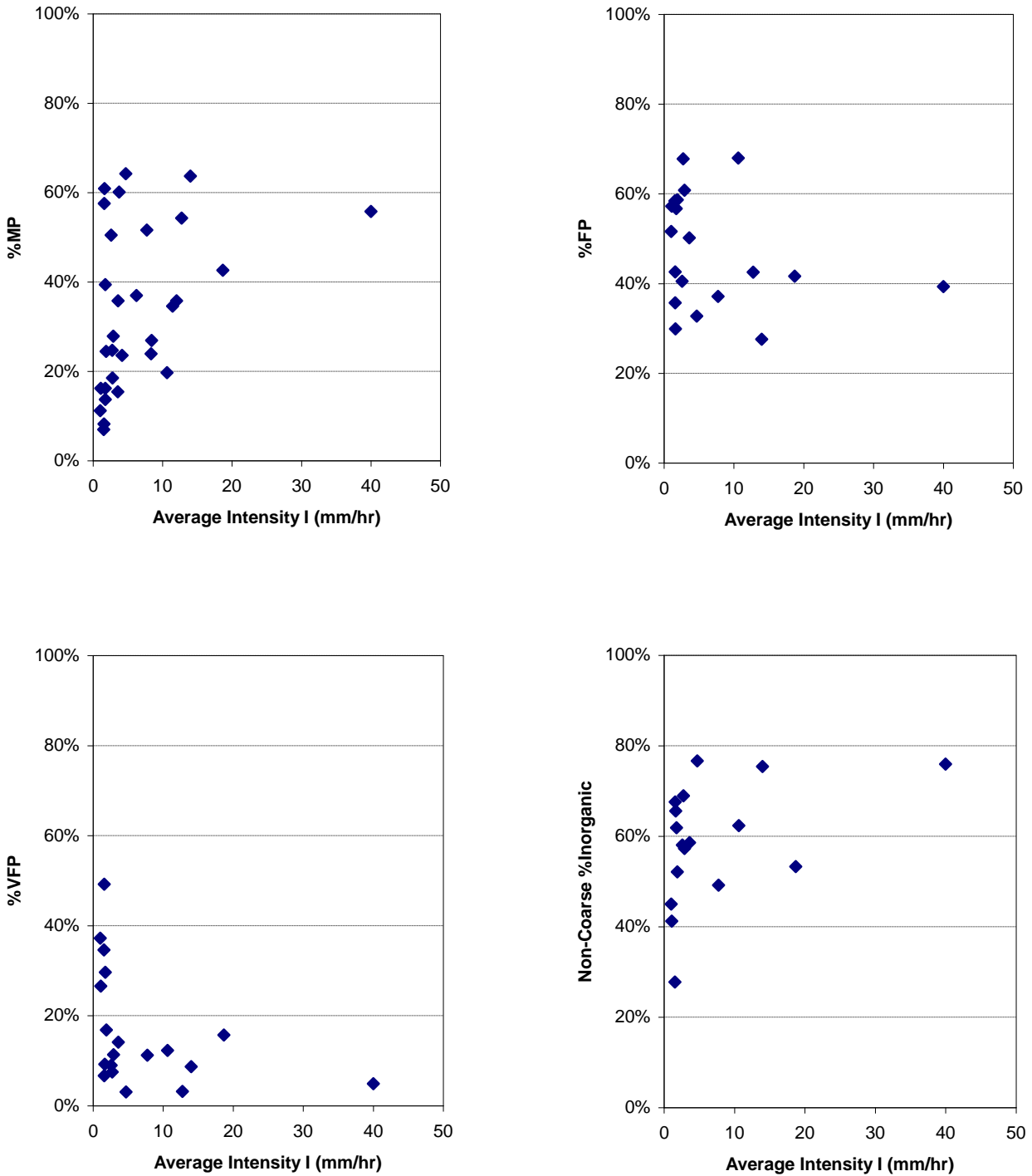
In the case of roof runoff (refer **Figure 7.14**), %MP, %FP and %VFP values tend to be scattered around constant values. These values are of the order of 15% for MP, 65% for FP and 20% for VFP. A positive or negative correlation with average rainfall intensity is not apparent. The data scatter for %MPs for storms less than 5 mm/hr is high in comparison to the %FP data, whilst the scatter in %VFP is low. A positive correlation between inorganic content and average rainfall intensity is visually evident in the roof scatter plot.

The %MP, %FP and %VFP values also tend to be scattered around constant proportions for the carpark runoff; of the order of 55% MP, 40% FP and less than 10% VFP (refer **Figure 7.15**). Carpark runoff has a coarser particle size distribution compared to roof runoff with a dominance of MP sized particles. For very low rainfall intensities (less than 2 mm/hr), there is a significant increase in the VFP content (up to 50%) with an attendant drop in MP content. This suggests that under these conditions, there is insufficient rainfall to fully mobilise MPs and there is preferential transport of the finer VFPs. A consistent trend is shown in the inorganic content with an increase in the proportion of less-dense organic particles being transported by these low intensity storms.

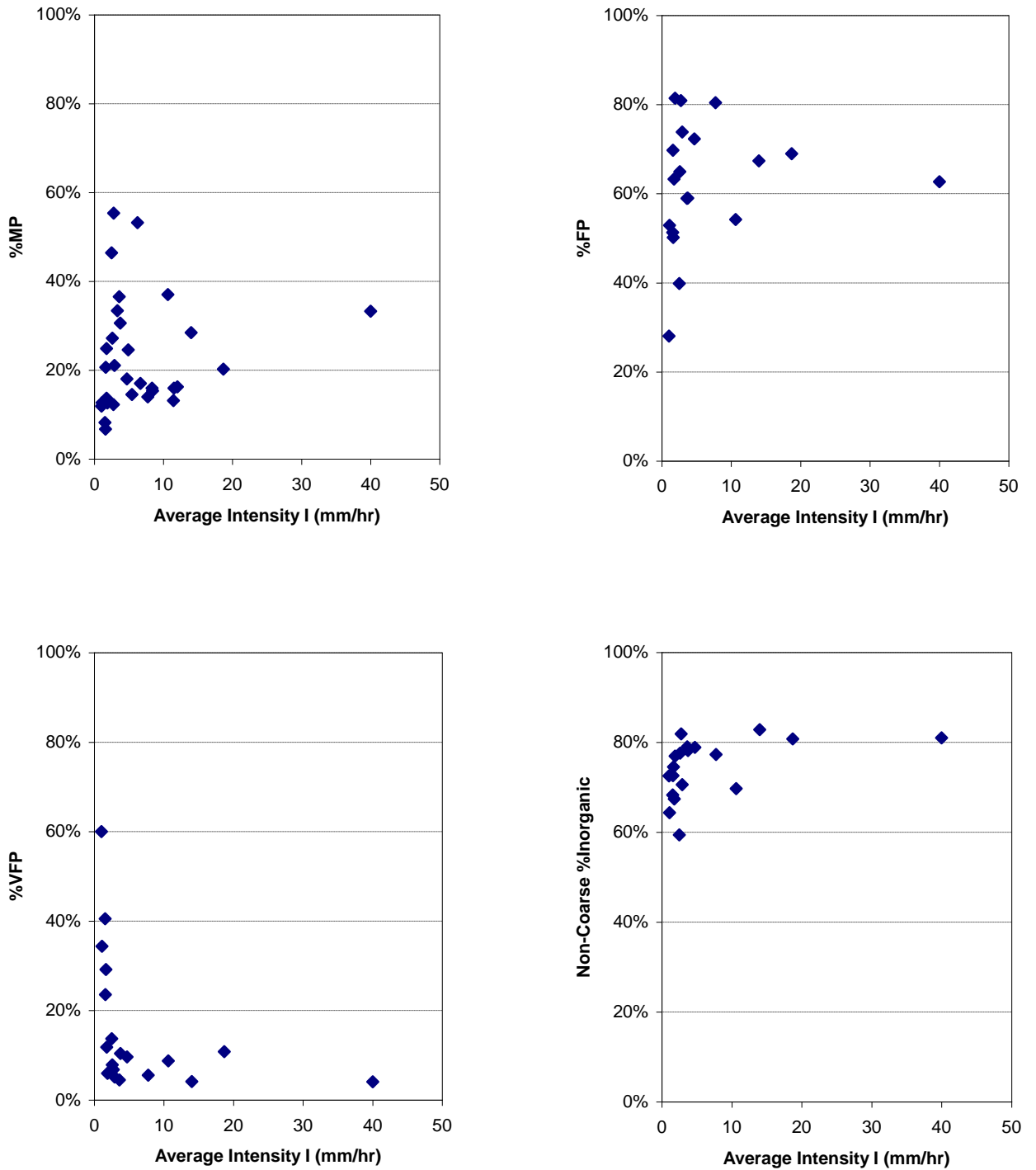
Compared to carpark runoff, road runoff as shown in **Figure 7.16** has a higher FP content generally of the order of 65%, lower MP content (approximately 30%) and similar VFP content (less than 10%). As was the case for carpark runoff, the road data shows an increase in VFP content and an inorganic content decrease for storms having low rainfall intensities. A point of difference is that these effects are accompanied by a FP reduction, rather than a lower MP content which occurred for carpark runoff.



■ **Figure 7.14 Scatter plots for roof particle compositions against average rainfall intensity for December 2004 to January 2006 runoff events**



■ **Figure 7.15 Scatter plots for carpark particle compositions against average rainfall intensity for December 2004 to January 2006 runoff events**



■ **Figure 7.16 Scatter plots for road particle compositions against average rainfall intensity for December 2004 to January 2006 runoff events**

7.5 Scatter Plots of Pervious Surface Non-Coarse Particle Load Data

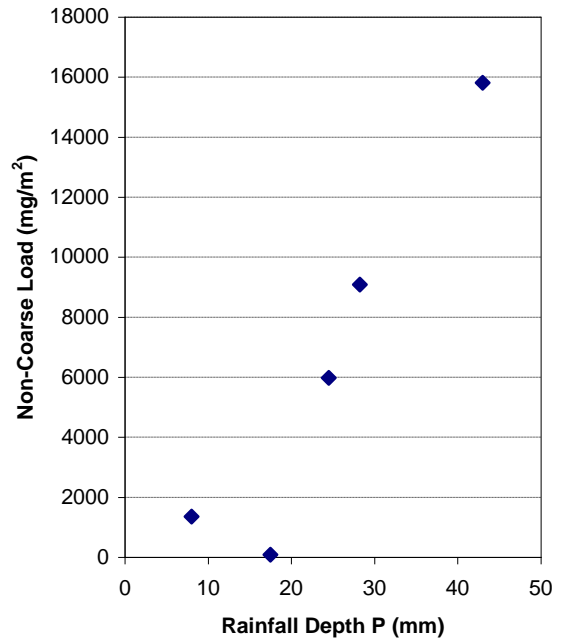
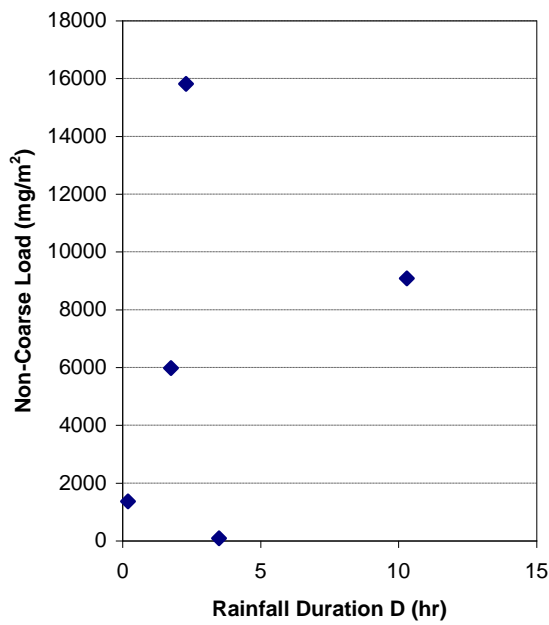
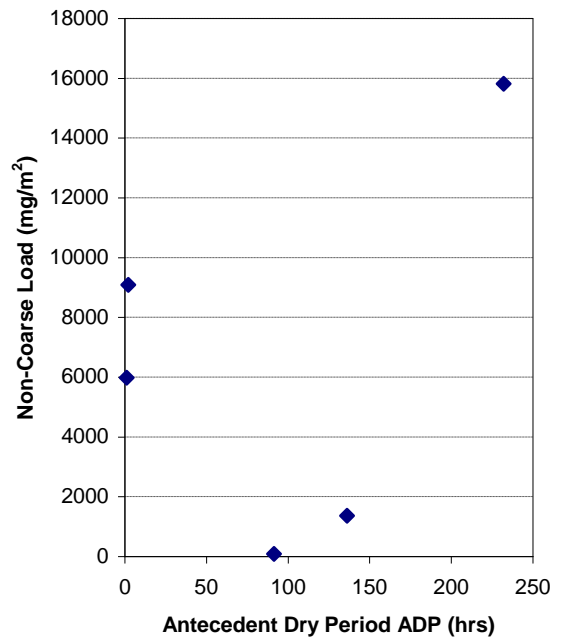
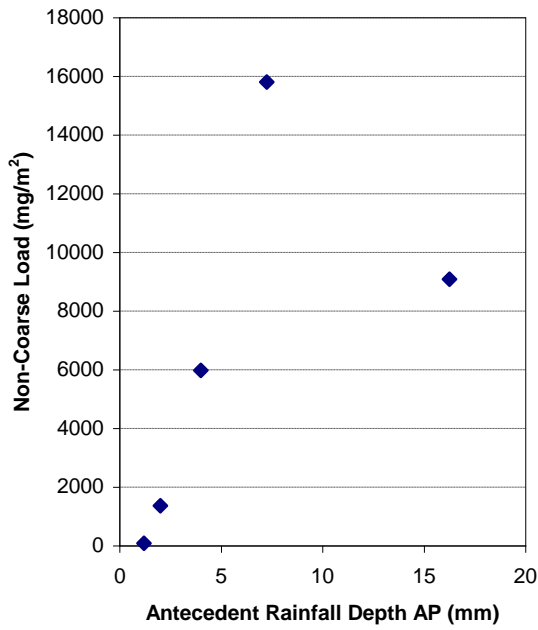
7.5.1 Bare Surface Non-Coarse Particle Loads versus Rainfall Parameters

On the same basis as the impervious surfaces, scatter plots of bare soil Non-Coarse Particle loads against the nominated rainfall parameters were prepared and are shown as **Figures 7.17** and **7.18**. Scatter plots for the grass surface are not practical due to the small number of runoff events that were sampled. A visual assessment was undertaken of potential correlations between bare soil Non-Coarse Particle loads and rainfall characteristics. The qualitative scales provided in **Table 7.6** were applied and the outcomes of the assessment are summarised in **Table 7.8**.

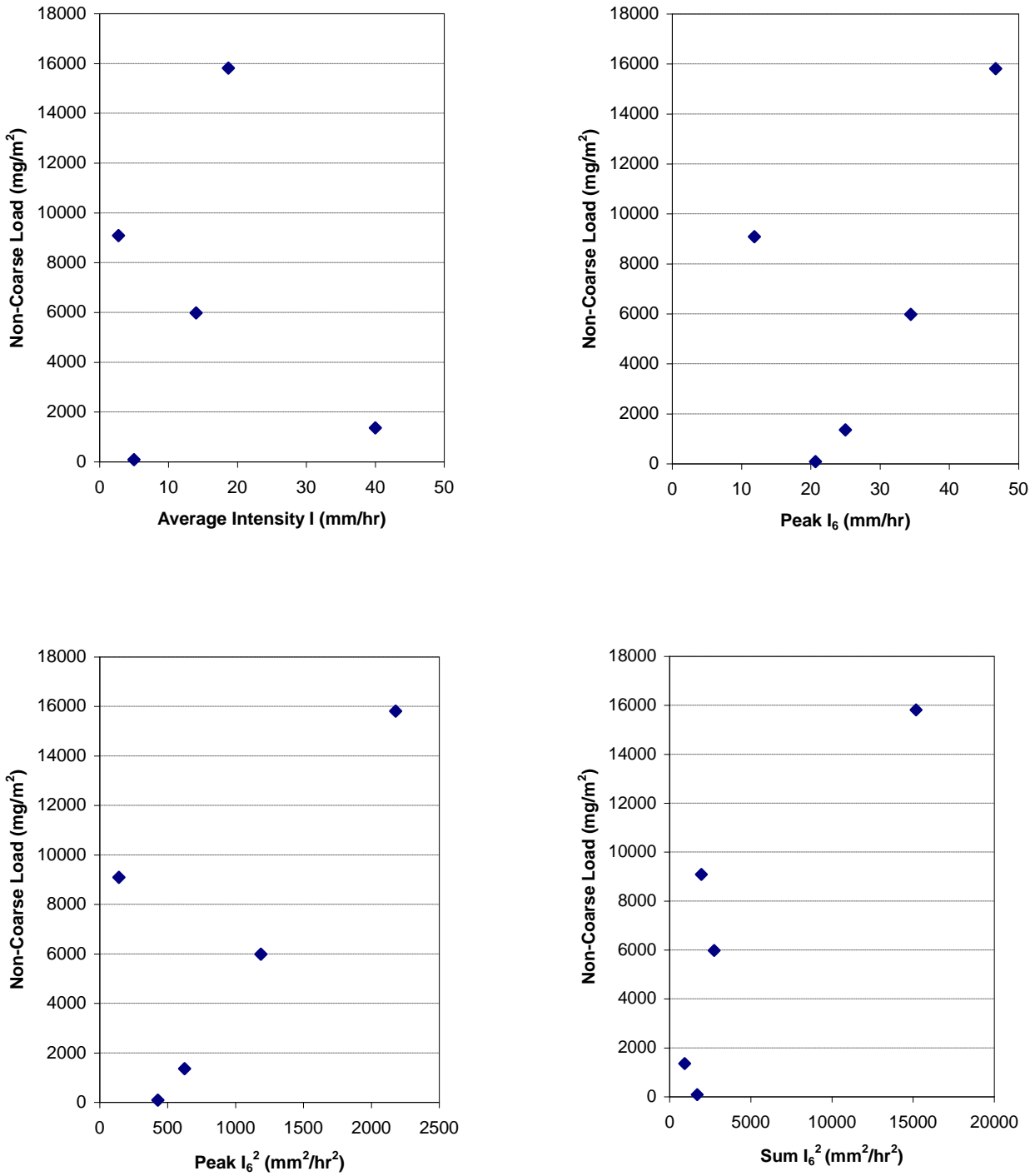
- **Table 7.8 Assessment of visual correlation between bare soil Non-Coarse Particle loads and selected rainfall parameters**

Rainfall Parameter	Bare Soil Loads
Antecedent Rainfall Depth AP	+
Antecedent Dry Period ADP	NA
Rainfall Duration D	+
Rainfall Depth P	++
Average rainfall intensity I	NA
Peak I_6	+
Peak I_6^2	+
$\sum I_6^2$	++

Although the number of runoff events is small, a positive correlation between load and rainfall depth P is clearly evident in the scatter plot. Load is a function of EMC and runoff, which in turn is dependant on rainfall depth. This interdependency of rainfall parameters and the small dataset makes it difficult to identify causative factors in generating bare soil particle loads. A potential candidate is $\sum I_6^2$, which is a measure of the total rainfall kinetic energy for the storm. This is consistent with studies of interrill soil erosion which have identified raindrop energy as a major factor in particle washoff (Gilley, Woolhiser & McWhorter 1985; van Dijk 2002). No significant trends between load and other rainfall parameters, including antecedent rainfall depth, antecedent dry period, storm duration and intensity-related parameters, are visually apparent in the scatter plots.



- Figure 7.17 Scatter plots of bare soil Non-Coarse Particle loads against rainfall parameters for December 2004 to January 2006 runoff events – Antecedent and event rainfall parameters



■ **Figure 7.18 Scatter plots of bare soil Non-Coarse Particle loads against rainfall parameters for December 2004 to January 2006 runoff events – Rainfall intensity and energy parameters**

In summary, various forms of analysis of the measured particle data are described in this Chapter. This includes an assessment of the full range of particle types including Non-Coarse Particles, Medium Particles (MPs), Fine Particles (FPs) and Very Fine Particles (VFPs) in relation to both EMC and load. Particle loads were derived by multiplying the measured EMC with the runoff volume predicted for each storm using the DRAINS model.

Box plots of particle EMCs indicate a substantial range for most surface types, with a 10 to 100-fold difference between the minimum and maximum concentrations being typical. Generally in all particle classes, the mean EMCs fell into the following order from lowest to highest concentration; roof<carpark and grassed surface<road<bare soil. Most of the particle mass was found to be inorganic, with the inorganic content of Non-Coarse Particles generally falling in the range of 55 to 85%.

Scatter plots are included in this Chapter and provide a visual guide to possible correlations between particle loads generated from individual storms and rainfall characteristics. Although not definitive, the plots for impervious surfaces demonstrate the presence of a weak negative correlation between Non-Coarse Particle load and antecedent dry period (ADP). Also the loads tend to decrease with an increase in the antecedent rainfall depth (AP). The strongest positive trends are exhibited between Non-Coarse Particle load and average rainfall intensity (I) and with peak 6-minute intensity (Peak I₆). This outcome provides a basis to investigate further the inter-relationships between Non-Coarse Particle load and rainfall characteristics, which is the subject of the next Chapter (Chapter 8).

8 Relationships between Non-Coarse Particle Loads and Rainfall Parameters for Impervious Surfaces

8.1 Approach to Identify Relationships between Non-Coarse Particle Loads and Rainfall Parameters

The scatter plot analysis in **Chapter 7** indicates potential correlations between impervious surface Non-Coarse Particle loads and various rainfall parameters. The load for individual storms appears to be positively correlated to the average rainfall intensity of the storm. This potential relationship is investigated further in this Chapter. Various composite indices, utilising different combinations of the basic rainfall parameters, were trialled as an alternative to average rainfall intensity. The aim of grouping the parameters together was to identify a composite rainfall index that would reduce the degree of scatter exhibited by the Non-Coarse Particle load data. The rainfall index may also provide an insight into the physical processes that are important in particle washoff from impervious urban surfaces.

The above approach was conducted in three stages during the stormwater monitoring period as data from approximately 10 rainfall events became available. These stages correspond to the following periods: December 2004 to February 2005 (14 storms), March 2005 to June 2005 (10 storms) and July 2005 to January 2006 (16 storms). These defined sets of data were also used in the staged development of a predictive model of particle mass balance for impervious urban surfaces, which is described in **Chapter 9**.

The identification of relationships between Non-Coarse Particle load and rainfall parameters was not undertaken for the pervious grassed and bare soil surfaces as the amount of measured data was limited to a few storms (less than 6 in number).

8.2 General Form of Particle Washoff Relationship for Impervious Surfaces

As noted by Duncan (1995), particle washoff from impervious surfaces is almost always represented by an exponential function. Adoption of an exponential washoff relationship emerged from the early work of Metcalf & Eddy Inc., *et al.* (1971)

developing the Storm Water Management Model (SWMM) and the subsequent widespread use of this model. In the first version of SWMM, it was proposed that the rate of pollutant generation, including washoff of suspended sediments, during a storm event is directly proportional to the mass of pollutant remaining on the surface:

$$\frac{dL_R}{dt} = -kL_R \quad [8.1a]$$

where L_R is the particle load on the surface available for washoff, t is the time since the beginning of the storm, and k is a decay coefficient

In SWMM, it was assumed that k is proportional to the stormwater discharge per unit area q (mm/s), which leads to Equation 8.1b.

$$\frac{dL_R}{dt} = -KqL_R \quad [8.1b]$$

where K is an empirical washoff coefficient and the stormwater discharge per unit area q is a function of time and can vary throughout the storm

Equation 8.1b can be integrated to give Equation 8.1c, as demonstrated by Millar (1999):

$$L_R = L_o e^{-KR} \quad [8.1c]$$

where L_o is the particle load on the surface available for washoff at the start of the storm and R is the cumulative runoff depth since the start of the storm ($= \int q dt$).

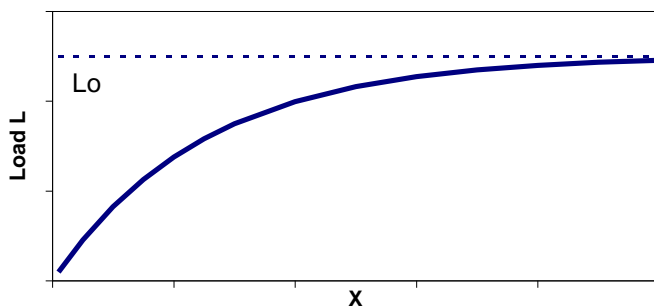
As the particle load washed from the surface (L) is the difference between L_o and L_R , this yields a generalised equation to describe particle loads washed from impervious surfaces given in Equation 8.1d:

$$L = L_o (1 - e^{-KX}) \quad [8.1d]$$

where L denotes the particle load washed from the surface and X is a rainfall or runoff parameter (and in the case of SWMM, X is the cumulative runoff depth R)

Figure 8.1 indicates graphically the general shape of the exponential-type washoff function given as Equation 8.1d. A range of rainfall or runoff parameters (X) have been used in previous studies, such as the product of rainfall intensity and time of

rainfall (Sartor *et al.* 1974). Cumulative runoff depth has been used by several researchers as X in Equation 8.1d (Grottker 1987; Hijioka *et al.* 2001; Osuch-Pajdzinska & Zawilski 1998; Sheng *et al.* 2005; Tsihintzis & Hamid 1997) as well as using a stormwater discharge or runoff rate parameter similar to SWMM in Equation 8.1b (Haster & James 1994; Haiping & Yamada 1998). Other variants include the use of a polynomial function based on rainfall intensity to derive the decay coefficient k in Equation 8.1a (Zug, *et al.* 1999). Nakamura (1984) used a polynomial function incorporating runoff rate and cumulative runoff volume instead of stormwater discharge per unit area in Equation 8.1b, whereas Ahlman & Svensson (2002) adopted rainfall intensity.



■ **Figure 8.1 Exponential type form of particle washoff relationships**

The exponential function of Equation 8.1d is typically used to predict the suspended particle load response (or loadograph) during individual storms. In this application, X is time dependant and is used to derive particle loads as an intra-event time series.

Alternatively, Equation 8.1d has been used to derive total particle loads for a range of storm events by direct substitution of an event total X value. For example, Haiping & Yamada (1996) used daily total runoff depth to determine a best-fit washoff coefficient K for an urban catchment in Kyoto, Japan. Total runoff depth was also used by Chen & Adams (2006) to develop cumulative distribution functions for various pollutants and also by Charbeneau & Barrett (1998) to predict Event Mean Concentrations (EMCs) of total suspended solids in runoff from single-land use catchments. Butcher (2003) adopted an approach similar to Charbeneau & Barrett to derive site-specific washoff parameters from observed storm EMCs for use in

modelling. The alternative application of Equation 8.1d on a total event basis was used in this thesis.

Based on the roof scatter plots (previously shown in Figures 7.8 and 7.9), the load point data do not appear to closely follow an exponential-type curve for any of the selected rainfall parameters. For some of the road load data points (Figures 7.12 and 7.13), an exponential curve function may be applicable for rainfall depth P , average rainfall intensity I and $\sum I_6^2$, and may apply to I and $\sum I_6^2$ in the case of carpark loads (Figures 7.10 and 7.11).

As a starting point, average rainfall intensity was used as the parameter X in the exponential washoff relationship. Rainfall intensity has previously been identified as a primary factor in particle washoff, most notably by the early street runoff tests performed by Sartor & Boyd (1972). More recently, Egodawatta *et al.* (2006) found by principal component analysis that average rainfall intensity is the most significant rainfall-runoff parameter associated with TSS loads generated from residential catchments. Many other researchers have highlighted the importance of rainfall intensity in particle washoff, including Yaziz *et al.* (1989) in the case of roof runoff and Vaze & Chiew (2003) who conducted rainfall simulator tests on impervious surfaces.

8.3 Particle Washoff Relationships Using December 2004 to February 2005 Data

8.3.1 Use of Average Rainfall Intensity I

Average rainfall intensity I scatter plots using data for the December 2004 to February 2005 period are shown in **Figure 8.2**. For the majority of storms, the use of I provides a reasonable consistency with an exponential-type washoff curve. There are four storms that do not fit this pattern. These outlying points are labelled on the scatter plots (and plotted as \diamond). These storms had a rainfall depth exceeding 20mm or average intensity greater than 10mm/hr.

These outlying points include the load for the 11/12/04 storm which is significantly below the expected values for both the roof and carpark sites. This storm occurred prior to the operation of the road sampler. In the case of the 26/12/04 storm, the loads are above the expected values for the roof and road sites, as is the 3/02/05 load from

the roof site. An outlying point below expected values is also evident in the carpark data for the 7/01/05 storm.

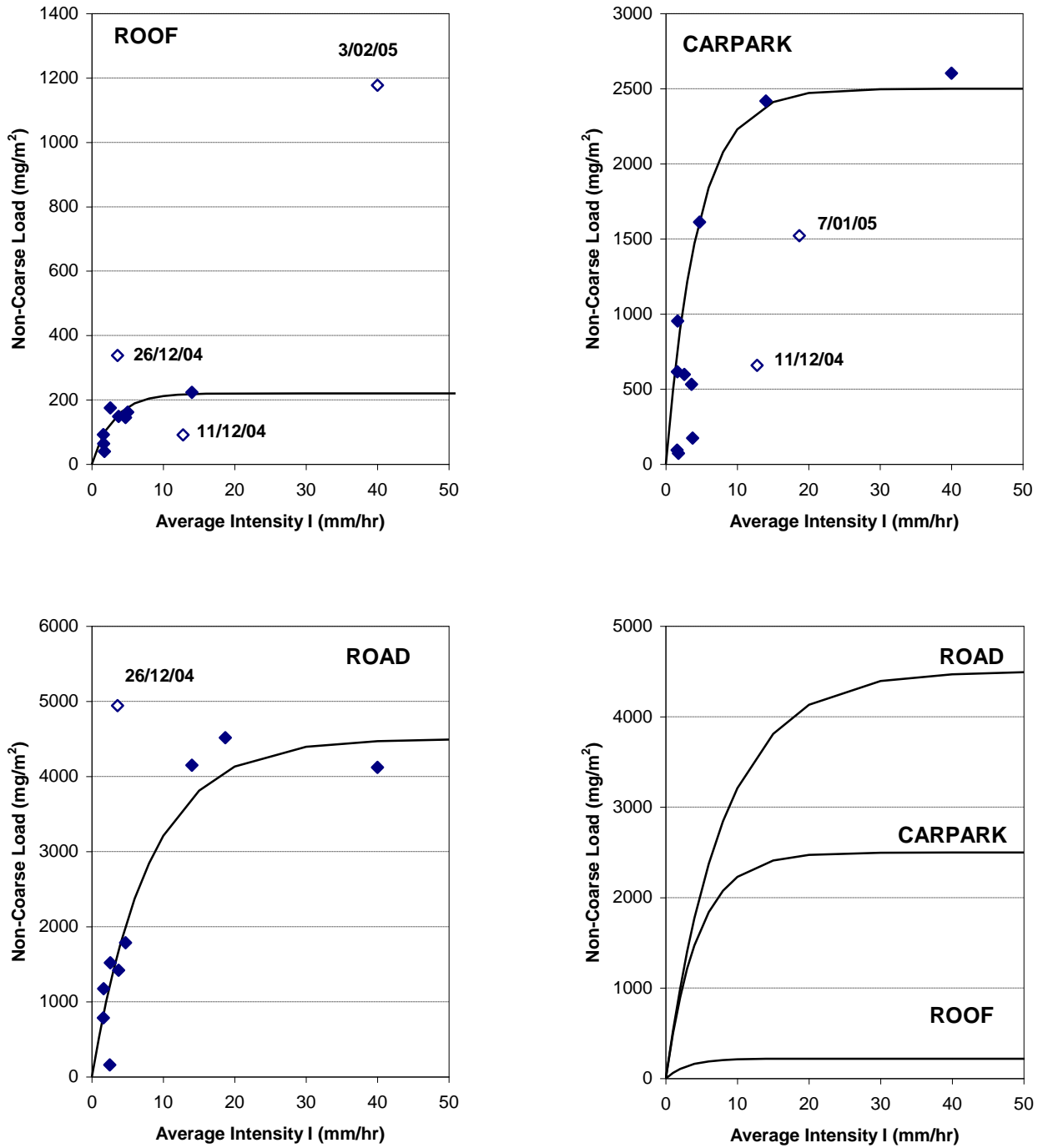
Exponential-type washoff relationships based on **Equation 8.1d** were fitted against the load data with the outliers removed. The resulting regression lines are presented on the graphs in **Figure 8.2** and coefficients are summarised in **Table 8.1**. The analysis demonstrates that the use of average rainfall intensity accounts for at least 74% of the variability within the roof and carpark load data and a very high 92% of the road variability after selected outliers are excluded from the analysis.

■ **Table 8.1 Exponential-type regression of Non-Coarse Particle loads against average rainfall intensity for December 2004 to February 2005 storm data**

Parameter	Roof	Carpark	Road
L_0 (mg/m ²)	220	2500	4500
K	0.33	0.22	0.125
R ²	0.75 (n=8)	0.74 (n=10)	0.92 (n=9)
Form of regression: Exponential based on Equation 8.1d			

The regression parameters L_0 and K fitted to the December 2004 to February 2005 Non-Coarse Particle data are consistent with known surface characteristics. The particle load available for washoff on the roof is expected to be substantially less than for the road and this is reflected by the smaller L_0 value. The main contributor to roof particles is atmospheric dust whereas the road surface is also subjected to additional traffic-related sources.

The proportionality constant K governs the shape of the rising limb of the washoff curve. A high K value indicates a more rapid rate of washoff in response to rainfall intensity compared to a lower K value and represents a surface where particles are easily washed off. As the roof is a smooth and steeply graded surface compared to the road, the K value for the roof is greater than the road K value. The carpark has washoff properties intermediate between the roof and road surfaces and this is reflected by the carpark K and L_0 values.



■ Figure 8.2 Roof, carpark and road Non-Coarse Particle loads plotted against average rainfall intensity based on December 2004 to February 2005 data. Fitted exponential curves are also shown.

8.3.2 Identification of the Rainfall Detachment Index

Rainfall indices other than average rainfall intensity were investigated to improve the degree of fit with the expected exponential trend. The indices included different combinations of the basic rainfall parameters listed previously in **Table 6.2** and **Table 7.5**.

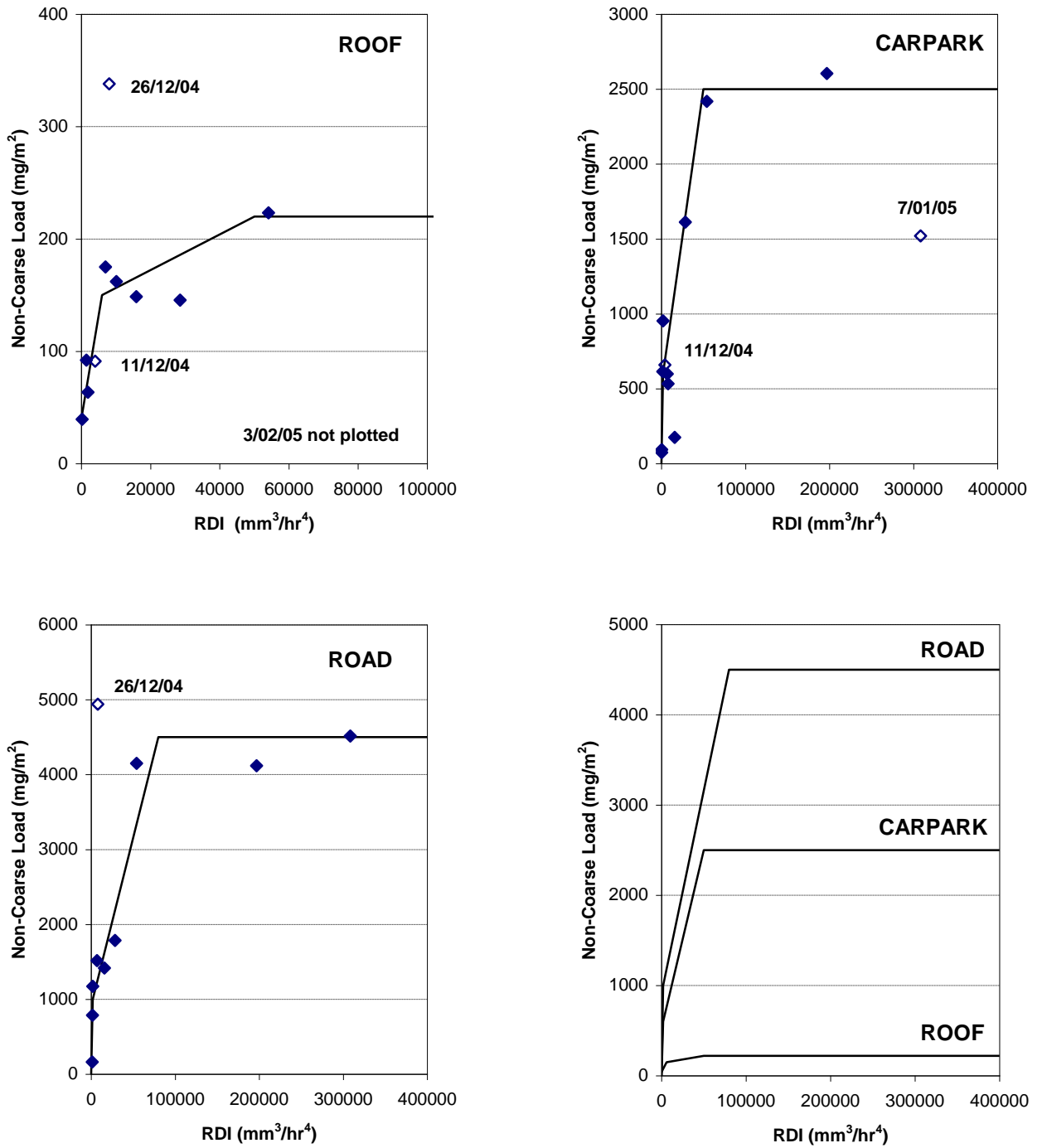
An index defined as the product of $\sum I_6^2$ and $\text{Peak}I_6$ divided by storm duration D (or $\sum I_6^2 \cdot \text{Peak}I_6/D$) was found to improve the plotting position of some outlying load points. For discussion purposes, this rainfall index $\sum I_6^2 \cdot \text{Peak}I_6/D$ is termed the Rainfall Detachment Index (or RDI). Scatter plots of Non-Coarse Particle loads against RDI are provided in **Figure 8.3**.

The location of the 11/12/04 storm data points for the carpark and roof sites are shifted closer to other points which have similar loads yet different rainfall intensities. This outcome suggests that, for this particular storm, RDI provides a better representation of rainfall-associated processes that affect particle washoff. However, other outlying points, specifically for 26/12/04, 7/01/05 and 3/02/05 (not plotted for reasons of clarity) remain inconsistent in that they do not follow the graphed RDI relationship.

The form of the RDI-load plots departs from an exponential-type curve and is closer to a piecewise linear plot. A general form of a piecewise linear relationship which incorporates three linear segments is provided as **Equation 8.2**.

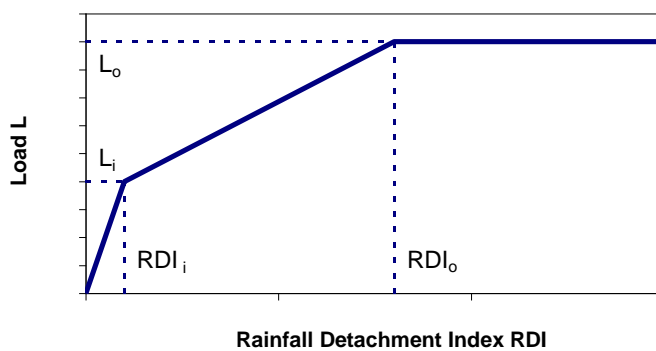
$$\begin{aligned}
 L &= L_o && : RDI \geq RDI_o && [8.2] \\
 L &= L_i + \frac{(RDI - RDI_i) \times (L_o - L_i)}{(RDI_o - RDI_i)} && : RDI_i \leq RDI < RDI_o \\
 L &= RDI \times \frac{L_i}{RDI_i} && : RDI < RDI_i
 \end{aligned}$$

where L is the particle load washed from the surface, RDI is the rainfall detachment index estimated for the storm, L_o is the particle load on surface available for washoff, RDI_o is the RDI corresponding to complete washoff of L_o , L_i is the initial particle load on the surface that is easily washed off and RDI_i is the RDI corresponding to complete washoff of L_i .



■ Figure 8.3 Roof, carpark and road Non-Coarse Particle loads plotted against RDI based on December 2004 to February 2005 data. Fitted piecewise linear curves are also shown

Figure 8.4 indicates graphically the general shape of the piecewise linear-type washoff equation. The theoretical basis of the piecewise relationship is that there is an ‘initial’ particle load (L_i) that is easily washed off the surface at low RDI values. If the RDI of the storm exceeds RDI_i , complete washoff of the initial particle load occurs. As RDI increases, washoff of particles that are not as easily mobilised as the initial load starts to occur. The higher amounts of RDI that is needed to washoff these remaining particles is reflected in the flatter slope of the line segment above L_i . Full washoff of the available particle load occurs when the storm RDI exceeds RDI_o .



■ **Figure 8.4 Piecewise linear form of particle washoff relationships**

Piecewise linear washoff relationships based on **Equation 8.2** were fitted against the load data with the outliers removed except for 11/12/04 load data. The resulting regression lines are presented on the graphs in **Figure 8.3** and coefficients of determination are summarised in **Table 8.2**.

The analysis demonstrates that the use of RDI accounts for 88% of the variability within the roof data, 86% of the carpark variability and 93% of the road variability (after selected outliers are excluded). These R^2 values are marginally higher than the regression values based on average rainfall intensity, indicating that RDI explains slightly more of the particle load responses to storm rainfall than does the simpler average rainfall intensity.

■ **Table 8.2 Piecewise linear regression of Non-Coarse Particle loads against Rainfall Detachment Index for December 2004 to February 2005 storm data**

Parameter	Roof	Carpark	Road
L_o (mg/m ²)	220 ¹	2500	4500
RDI_o (mm ³ /hr ⁴)	50 000	50 000	80 000
L_i (mg/m ²)	150	600	1000
RDI_i (mm ³ /hr ⁴)	6000	2000	2000
R^2	0.88 ($n=8$)	0.86 ($n=10$)	0.93 ($n=9$)
Form of regression: Piecewise linear based on Equation 8.2			

Note: 1. Based on one data point only

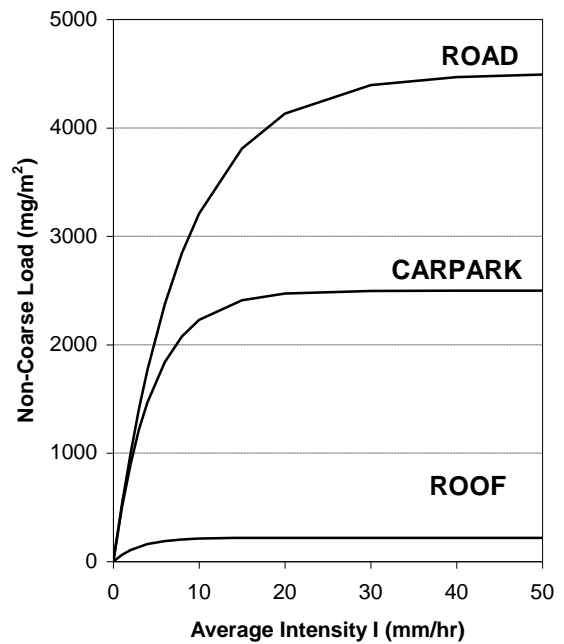
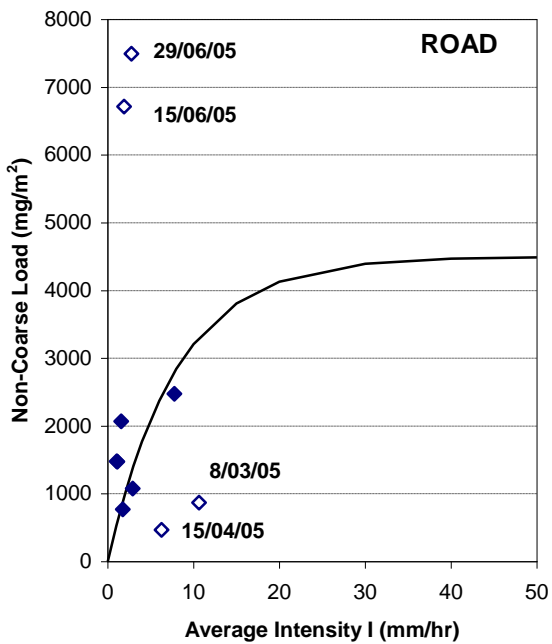
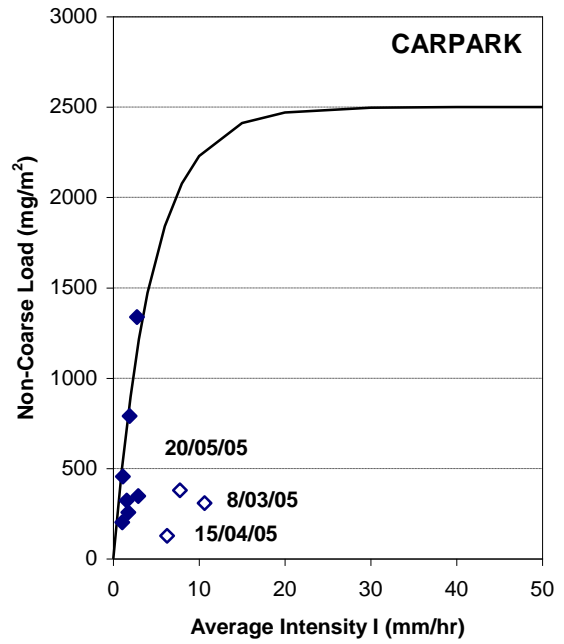
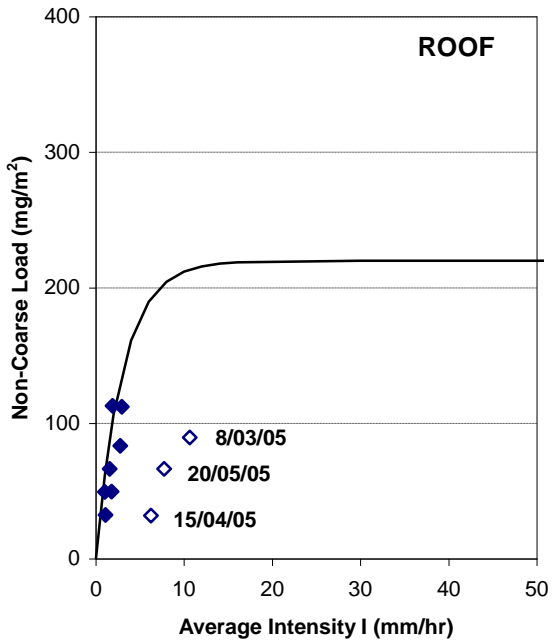
8.4 Particle Washoff Relationships Using March 2005 to June 2005

Data

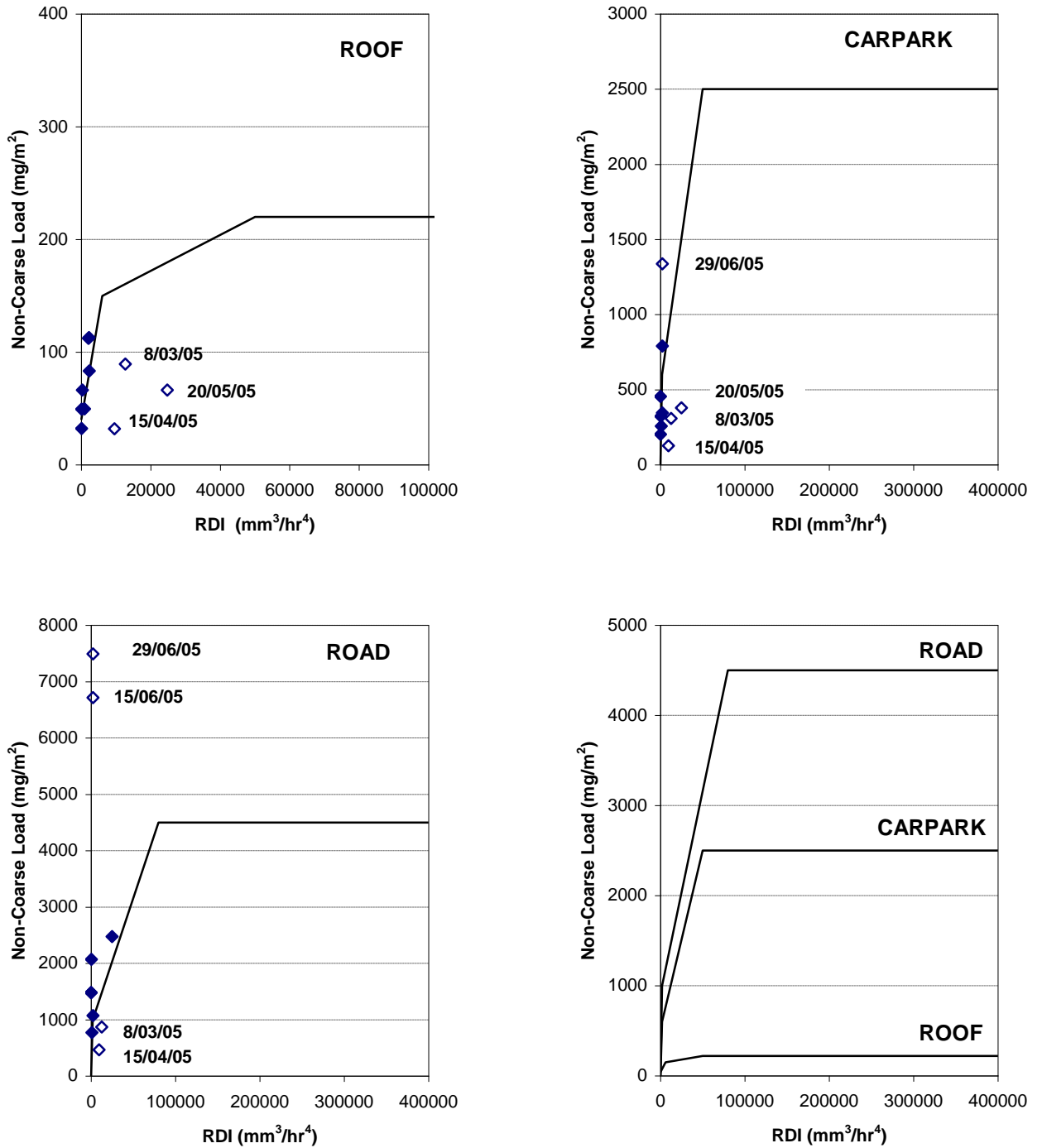
Data collected during the second phase of stormwater monitoring from March 2005 to June 2005 were applied to further evaluate the particle washoff relationships established from the initial December 2004 to February 2005 set of data.

Non-Coarse Particle loads plotted against average rainfall intensity using data for March 2004 to June 2005 are shown on **Figure 8.5**. Storms that correspond to low rainfall intensity ($I < 5$ mm/hr) tend to have generated Non-Coarse Particle loads that are consistent with the curves fitted against the initial December 2004 to February 2005 data. The plots of loads against RDI are shown in **Figure 8.6** and also indicate a good fit for the same storms (in this case, corresponding to $RDI < 5000$) with the initial regression piecewise lines.

Particle load data for some storms were inconsistent with the intensity regression curves and these outlying points are labelled on the scatter plots (and plotted as \diamond). Three storms (8/03/05, 15/04/05 and 20/05/05) are consistently below the exponential washoff curves for all impervious surfaces, except that the 20/05/05 load data for the road surface is relatively close to the washoff curve. The group of storms representing the data outliers have similar rainfall characteristics. Storm durations are short (less than 1 hour) and the rainfall depths are relatively small and fall in a range from 2.5 to 7.75mm.



■ Figure 8.5 Roof, carpark and road Non-Coarse Particle loads plotted against average rainfall intensity based on March 2005 to June 2005 data. Exponential curves fitted to December 2004 to February 2005 data are also shown

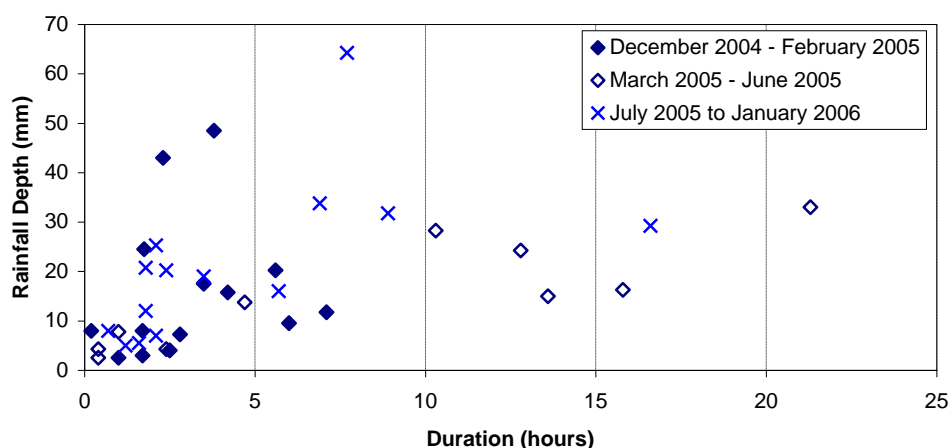


■ Figure 8.6 Roof, carpark and road Non-Coarse Particle loads plotted against RDI based on March 2005 to June 2005 data. Piecewise linear curves fitted to December 2004 to February 2005 data are also shown

The plotting positions for these three storms indicate a closer match to the RDI-regression curves for the carpark and road surfaces. This suggests that RDI provides a better measure of rainfall-associated washoff processes for these individual storms. However, no significant improvement in the relative plotting position has occurred in the roof data for these events.

Additional outliers located above the intensity regression curve are present in the case of the road surface. These points coincide with the storms of 15/06/05 and 29/06/05; both of which were long duration storms (12.8 and 10.3 hours, respectively) with moderate rainfall depths (24.25 and 28.25mm, respectively). These storms also plot above the RDI linear piecewise curve for the road surface and the 29/06/05 storm is also an outlier in the case of the carpark surface.

The scatter plots in **Figures 8.5** and **8.6** indicate that significant departures from the I and RDI regression curves are present within the March 2005 to June 2005 data set. These outlying points are associated with storm events at near-opposite ends of the rainfall spectrum. They correspond to low rainfall, short duration storms and to moderate rainfall, long duration storms. As shown in **Figure 8.7**, long duration storms in particular are a feature of the March 2005 to June 2005 data and are mainly absent from the December 2004 to February 2005 data. This reflects seasonal rainfall patterns that involve short, relatively intense storms during summer followed by longer events of overcast and low rainfall conditions during autumn and winter.



- **Figure 8.7 Storm durations and rainfall depths for December 2004 to February 2005 events compared with March 2005 to June 2005 events and July 2005 to January 2006 events**

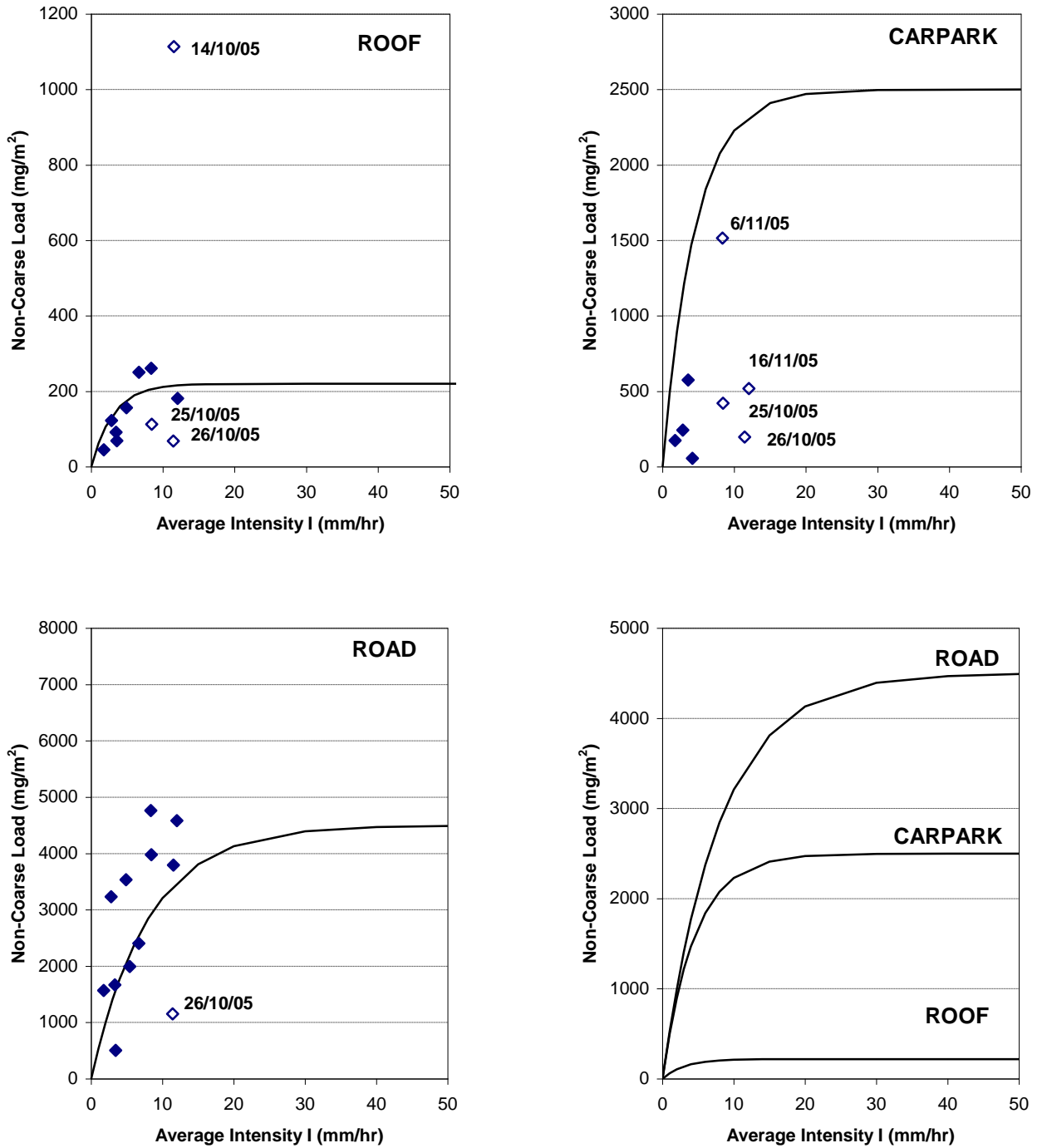
8.5 Particle Washoff Relationships Using July 2005 to January 2006 Data

The degree of fit of the third data set from July 2005 to January 2006 data was also investigated with the I and RDI regression curves. Non-Coarse Particle loads plotted against average rainfall intensity are shown in **Figure 8.8** and the corresponding scatter plots based on RDI are given in **Figure 8.9**. As can be seen from **Figure 8.7**, the storms that were monitored during July 2005 to January 2006 included several long duration events ($D > 5$ hours), similar to the preceding February 2005 to June 2005 data set.

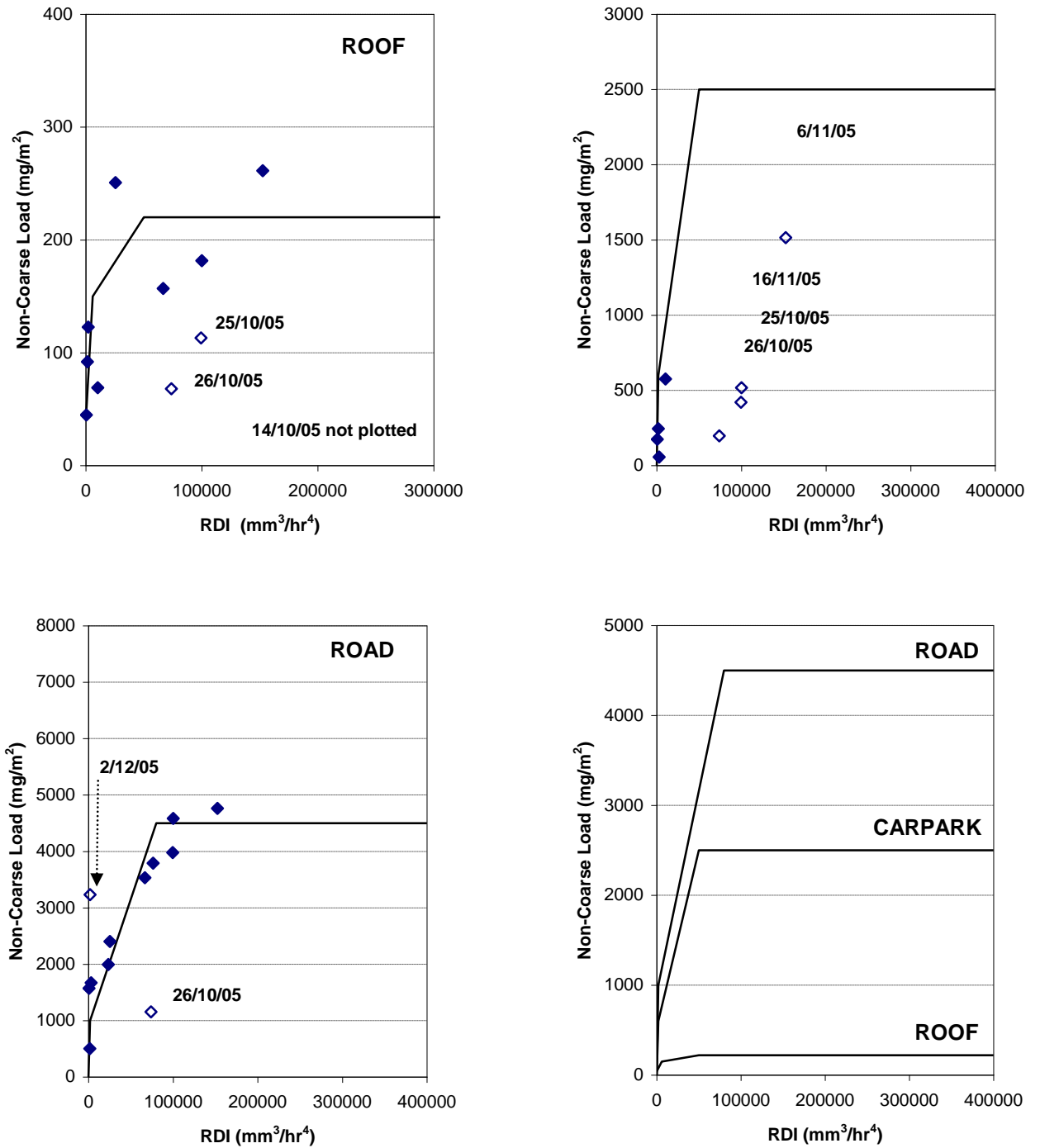
Generally, the fitting of data around both the I and RDI regression curves is not as close as for the previous datasets. A cluster of points in the road Non-Coarse Particle load that range from 3000 to 5000 mg/m² are above the I-regression curve. By comparison, the loads corresponding to these events show a better match with the RDI-regression curve presented in **Figure 8.9**, except for the 2/12/05 storm. As was the case for the other sets of data, there is commonality in the relative plotting positions of some storms. For example, loads for the 25/10/05 and 26/10/05 storms plotted substantially below both the I and RDI regression curves for the roof and carpark surfaces. The same spatial pattern is also evident for the 26/10/05 road data point.

Other outliers include the 14/10/05 roof load and the 06/10/05 carpark load. These outliers are present in both the I and RDI-load scatter plots.

The evaluation of the three sets of data indicates that, for many events, a reasonable match is present between measured loads and an exponential regression curve based on average rainfall intensity I. In some cases, the degree of fit improves if a piecewise linear curve based on RDI is applied. However, there are clusters of data that do not conform to these curves and data points for the same set (or subset) of storms often have similar plotting positions for different surfaces. This suggests that additional factors controlling particle washoff during these events are not accounted for by I or RDI and these factors may be independent of the surface type. The aspect of outliers is discussed further in Section 8.7.



■ Figure 8.8 Roof, carpark and road Non-Coarse Particle loads plotted against average rainfall intensity based on July 2005 to January 2006 data. Exponential curves fitted to December 2004 to February 2005 data are also shown



■ Figure 8.9 Roof, carpark and road Non-Coarse Particle loads plotted against RDI based on July 2005 to January 2006 data. Piecewise linear curves fitted to December 2004 to February 2005 data are also shown

8.6 Physical Basis of the Rainfall Detachment Index

8.6.1 General Form of Rainfall Detachment Index

The basic form of RDI is repeated from **Section 8.3.2** in **Equation 8.3** as follows.

$$RDI = (\sum I_6^2 / D) \times Peak I_6 \quad [8.3]$$

where RDI is the rainfall detachment index, $\sum I_6^2$ is defined in accordance to **Table 7.5**, D is the rainfall duration in hours and $Peak I_6$ is the peak 6 minute rainfall intensity during the storm in mm/hr.

Presented in this way, RDI has a very similar form to the Rainfall Erosivity Index (or EI_{30}) which is commonly used in the prediction of soil erosion from pervious surfaces. EI_{30} is used in the Universal Soil Loss Equation to estimate annual soil loss. It is a measure of the potential ability of rainfall to cause erosion and originates from the work of Wischmeier & Smith (1978) who found that while soil erosion was correlated to the kinetic energy of the rainfall, a better estimator was the product of total kinetic energy of the rainfall (E_K) and the peak 30 minute rainfall intensity ($Peak I_{30}$), as shown in **Equation 8.4**.

$$EI_{30} = 0.001 \times E_K \times Peak I_{30} \quad [8.4]$$

where EI_{30} is the rainfall erosivity index, E_K is the total kinetic energy of the rainfall (J/m^2) and $Peak I_{30}$ is the peak 30 minute rainfall intensity (mm/hr).

The similarity between RDI and EI_{30} suggests a close relationship is anticipated between $\sum I_6^2$ and E_K , as both are intended to be a measure of the total amount of rainfall energy in a storm event. This indeed is the case, as discussed further in **Section 8.6.2** of this Chapter.

Given that the term $\sum I_6^2$ is a measure of the kinetic energy E_K of the storm rainfall, it follows that the term $(\sum I_6^2 / D)$ is a measure of the kinetic energy available for particle detachment per unit area of surface averaged over the duration of the storm. This time derivative of kinetic energy is a measure of the average ‘rain power’ expressed in units W/m^2 ; a term used by Gabet & Dunne (2003) to describe detachment of interrill soil particles due to raindrop impact.

The second term of the RDI, Peak I_6 , is part of the well known Rational Equation (defined in **Chapter 9** as **Equation 9.1**) used to estimate peak runoff discharge from small urban areas. As the time of concentration of the impervious surfaces approximates 6 minutes and rainfall losses are minimal, Peak I_6 is a direct measure of peak stormwater discharge. It becomes an indicator of the hydraulic capacity of overland flows to transport particles that have been physically detached by rainfall impact to the drainage outlet.

Thus the RDI reflects the two main physical processes involved in particle washoff; namely the rain power that causes particle detachment and initial mobilisation followed by the capacity of overland flows to transport the suspended particles to the point of discharge.

8.6.2 Relationship between $\sum I_6^2$ and Rainfall Kinetic Energy E_K

Kinetic energy of rainfall is a composite parameter derived from the size distribution of raindrops and their corresponding terminal velocity. In the original development of the Universal Soil Loss Equation, measurements of drop sizes and velocities made at Washington D.C. (Laws 1941; Laws & Parsons 1943) were used to derive a logarithmic relationship between rainfall intensity I and E_K per unit rainfall depth (or e_K equal to E_K/P).

This relationship, formulated by Wischmeier & Smith (1978) is shown in **Equation 8.5**. The parameter e_K is generally referred to as the ‘kinetic energy content’ of rainfall. More recently, van Dijk *et al.* (2002) fitted an exponential equation (**Equation 8.6**) to rainfall energy data collected from 12 different locations worldwide.

Kinetic energy content based on logarithmic function (Wischmeier & Smith 1978)

$$e_K = 11.87 + 8.73 \log(I) \quad : I < 76 \text{ mm/hr} \quad [8.5]$$

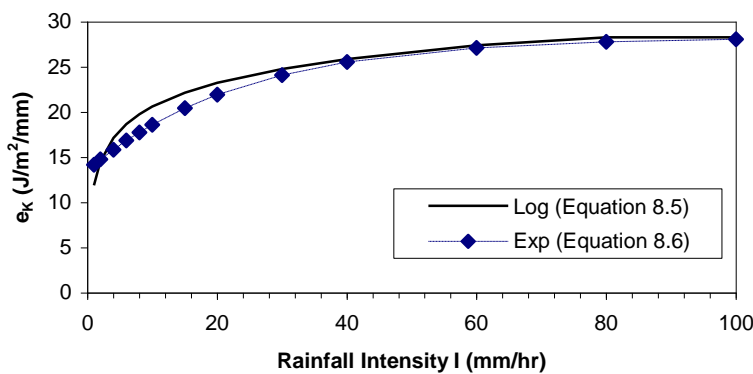
$$e_K = 28.3 \quad : I > 76 \text{ mm/hr}$$

Kinetic energy content based on exponential function (van Dijk *et al.*, 2002)

$$e_K = 28.3 \times (1 - 0.52e^{-0.042I}) \quad [8.6]$$

where e_K is the kinetic energy per unit rainfall depth ($J/m^2/mm$) and I is the rainfall intensity (mm/hr).

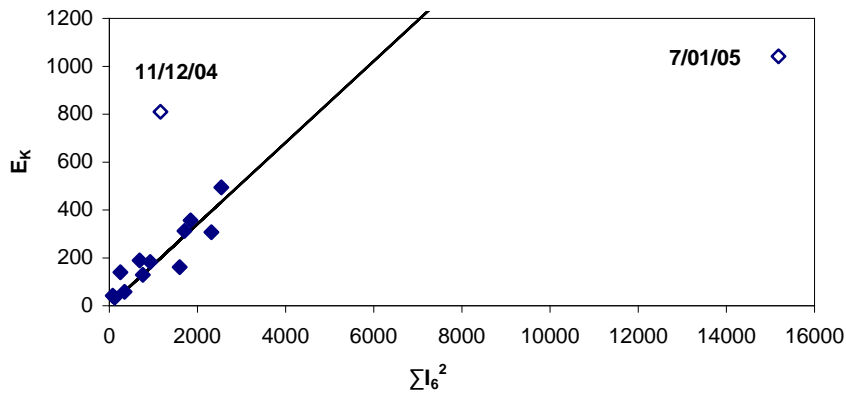
The two equations provide similar estimates of e_K as shown graphically in **Figure 8.10**. In both cases, an upper limit of $28.3 \text{ J/m}^2/\text{mm}$ applies as there is a physical limit to rain drop size and hence kinetic energy. This size limit is of the order of 6 to 8 mm due to terminal velocity and air drag effects (Laws & Parsons 1943). It should be noted that there is considerable scatter of measured data around the e_K equations (e.g. $R^2=0.52$ for the Washington D.C. data), indicating that there is a high variability in the kinetic energy of storms that have the same rainfall intensity. Differences in synoptic conditions and wind effects may be responsible for most of this variability in e_K (van Dijk *et al.* 2002).



■ **Figure 8.10 Kinetic energy contents relationships based on Equations 8.5 and 8.6**

The kinetic energy E_K for a selection of the Toowoomba monitored storms was estimated by summing the product of e_K and rainfall depth P in each 6 minute increment of the storm period (i.e. $\sum e_K \cdot P_6$). The exponential form of the e_K relationship (**Equation 8.6**) was used to derive values for kinetic energy per unit rainfall depth. The E_K values were derived for the all storms in the initial monitoring period from December 2004 to February 2005 for the purpose of confirming a potential relationship between E_K and $\sum I_6^2$.

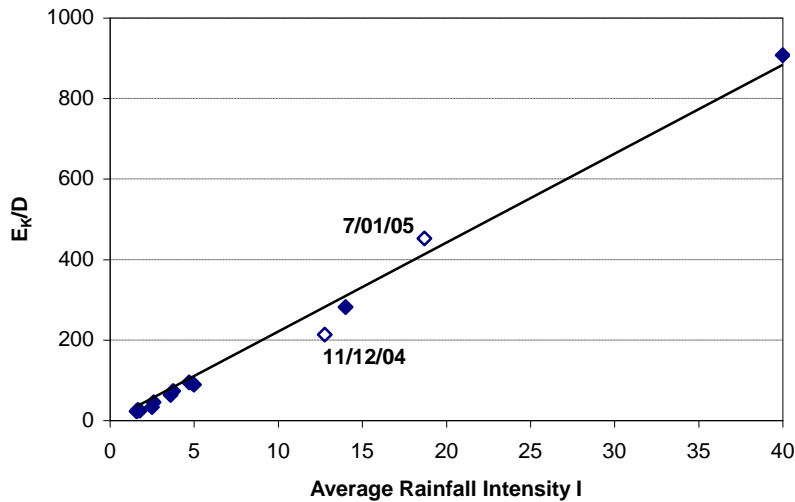
Figure 8.11 shows a plot of the derived E_K values against $\sum I_6^2$ and indicates that a strong positive linear correlation is present for E_K less than 500 J/m^2 ($E_K = 0.17 \sum I_6^2$, $R^2 = 0.81$). Most storms with average rainfall intensity less than 5 mm/hr fall into this category. The high correlation suggests that $\sum I_6^2$ is highly representative of the total kinetic energy of rainfall, particularly for low intensity events.



- **Figure 8.11** Plot of E_K against $\sum I_6^2$ for December 2004 to February 2005 storm events

It is of interest that two storms 11/12/04 and 7/01/05 are outliers from the E_K - $\sum I_6^2$ regression line and are outlying points on the Non-Coarse Particle load plots against I shown previously in **Figure 8.2**. Based on this limited evidence, it was postulated that there may be a close correlation between average rainfall intensity I and ‘rain power’ based on E_K instead of $\sum I_6^2$ (i.e. E_K/D). As shown in **Figure 8.12**, a linear relationship does exist between these two parameters ($E_K/D = 22.1I$, $R^2=0.99$) that closely incorporates the outlying storms of 11/12/04 and 7/01/05.

The above finding highlights that average rainfall intensity I provides a reasonable basis to determine Non-Coarse Particle loads, at least for low intensity storms less than 5 mm/hr. The intensity appears to provide a reasonable measure of rainfall kinetic energy, specifically the time rate of energy supplied by rainfall E_K/D or ‘rain power’. However, the kinetic energy of some larger storms can not be simply predicted by I and other measures such as $\sum I_6^2$ may constitute a better predictor. This is demonstrated by the shifting of plotting positions of load data for the storm of 11/12/04 when RDI is applied instead of I (as shown in **Figure 8.3**).



■ **Figure 8.12 Plot of E_K/D against average rainfall intensity I for December 2004 to February 2005 storm events**

The apparent poor performance of using E_K as an indicator of rainfall power for the 11/12/04 storm could be the result of the adopted kinetic energy contents relationship (**Equation 8.6**) setting a minimum e_K value for low rainfall intensities. In the case of the exponential function, the lower limit is $13.6 \text{ J/m}^2/\text{mm}$. The setting of a non-zero floor value for e_K may lead to overestimation of E_K if a storm has a period of very low intensity rainfall (less than 1 to 2 mm/hr) imbedded in the overall temporal pattern, as was the case for the 11/12/04 storm. In these circumstances, the use of $\sum I_6^2$ makes more sense as the E_K measure approaches zero as rainfall intensity diminishes.

However, using the $\sum I_6^2$ approach may lead to a measure of rain power that is overestimated as there is no numerical upper limit as is the case for E_K estimation. As shown in **Equation 8.6**, there is an asymptotic ceiling to e_K of $28.3 \text{ J/m}^2/\text{mm}$ based on the maximum raindrop size that can be attained. The e_K is close to this upper limit when rainfall intensity exceeds approximately 30 mm/hr. On this basis, the use of $\sum I_6^2$ may significantly overestimate rain power for high intensity storms. This is demonstrated in **Figure 8.11** by the rainfall energy based on $\sum I_6^2$ being substantially higher than the corresponding E_K measure for the 7/01/05 storm. During this storm, periods of intense rainfall exceeding 40 mm/hr occurred.

Although it is a simple measure, average rainfall intensity appears to provide a sound basis to estimate rainfall power during low intensity storms (<5 mm/hr). For larger events, the use of I may become less reliable especially for storms imbedded with lengthy periods of low rainfall. In these circumstances, the use of $\sum I_6^2$ (and hence RDI) maybe be a more accurate representation of rain power. However, for very intense storms (>30 mm/hr bursts) the use of $\sum I_6^2$ may substantially overestimate the rain power that is available for particle washoff.

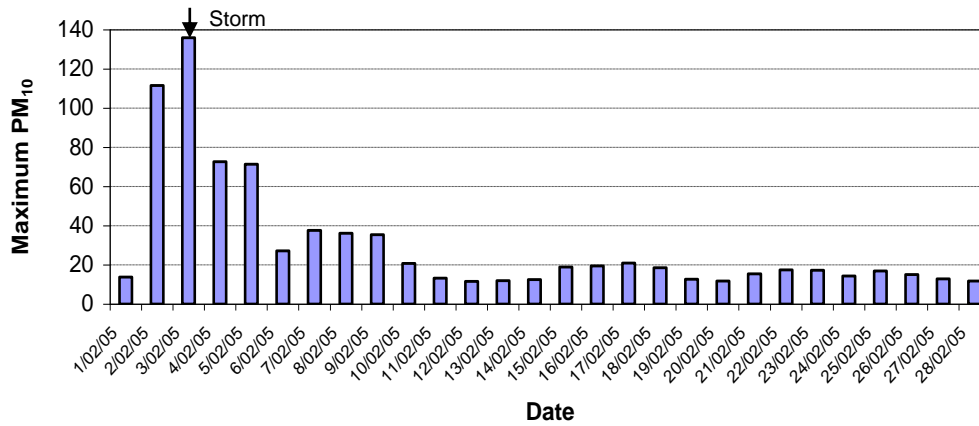
8.7 Washoff Effects Unexplained by I and RDI

Although RDI provides a better definition of the rainfall energy and transport processes than does average rainfall intensity I, some data outliers are not fully explained by either parameter. Data outliers are present in the scatter plots in this Chapter which show measured Non-Coarse Particle loads up to five times the expected value based on the fitted curves. The roof loads for the events of 3/2/05 and 14/10/05 are examples. These outlying points are specific to one type of surface. However, there are clusters of outlying points that plot in a consistent pattern (i.e. either above or below the fitted curves) for more than one type of surface. Outlying points are discussed further in this section.

8.7.1 Effect of Dustfall on Roof Non-Coarse Particle Loads

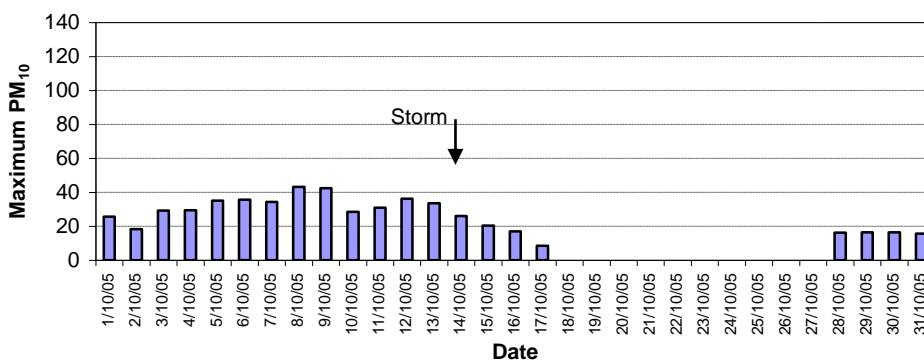
A major outlier in the data is the roof load for the 3/02/05 storm, which resulted in Non-Coarse Particle washoff of about 1200 mg/m^2 , a 5-fold increase above particle loads measured in other rainfall events. To investigate this issue, air pollution data was obtained from a monitoring station located 1.2km north of the roof site. This station continuously records the concentration of airborne particles smaller than $10 \mu\text{m}$ (PM_{10}) and maximum daily values for February 2005 are shown in **Figure 8.13**.

A major dust storm coincided with the 3/02/05 event and this is reflected by the high PM_{10} of $136 \mu\text{g/m}^3$ recorded for that day. Ambient PM_{10} values for February 2005 were generally less than $20 \mu\text{g/m}^3$. It is concluded that the very high Non-Coarse Particle load measured from the roof during 3/02/05 was mainly attributed to the occurrence of unusually high rates of dustfall during and prior to the storm.



■ **Figure 8.13 Maximum daily PM₁₀ for February 2005 recorded at Toowoomba**

Roof runoff from the storm of 14/10/05 also exhibited Non-Coarse Particle loads that were very high and in the order of 1100 mg/m^2 . The Toowoomba air monitoring station detected elevated PM₁₀ concentrations up to $43 \mu\text{g/m}^3$ over a period of at least a week prior to this event. The PM₁₀ record for October 2005 is shown as **Figure 8.14**. The period of high airborne dust concentrations also coincided with dry conditions. No rainfall was recorded during the fortnight before the storm, with only a 2.25mm rainfall registered on 30/9/2005. It is considered that the prolonged period of high dust concentrations prior to the 14/10/05 storm was a major factor in elevating the Non-Coarse Particle load for this event.



■ **Figure 8.14 Maximum daily PM₁₀ for October 2005 recorded at Toowoomba**

It is concluded that abnormal atmospheric dust levels (i.e. higher than $20 \mu\text{g/m}^3$) during the antecedent dry period or as dustfall during the storm itself, leads to a significant increase in Non-Coarse Particle load washed from the roof surface. This

causative factor to elevated particle loads is not accounted for in the rainfall-based parameters I and RDI.

8.7.2 Effect of Storm Duration and Rainfall Depth

As previously described, clusters of data outliers are present within the Non-Coarse Particle load plots against both I and RDI. In many cases, the location of these points relative to the fitted curves is similar for different surfaces. This suggests that there are particle washoff behaviours that are not fully accounted for by the use of I or RDI and these unexplained effects may be related to other rainfall characteristics.

To demonstrate these rainfall effects, the road Non-Coarse Particle loads for all the sets of available data from December 2004 to January 2006 were plotted against average rainfall intensity I. The data was initially divided into two main groupings based on rainfall depth P, namely less than 5mm and greater than 5mm. As can be seen from **Figure 8.15**, the loads corresponding to the small rainfall depths less than 5mm (plotted as x) are substantially less than the expected loads defined by the exponential curve.

Previous studies have identified relatively small particle loads in response to rainfall events less than 5mm depth. Sansalone *et al.* (1998) measured particle concentrations from a highway pavement at Cincinnati during several storms from 1995 to 1996. The events were grouped as either ‘flow-limited’, low runoff volume events associated with small particle mass loads or ‘mass-limited’, high runoff volume events. Rainfalls for the flow-limited events were less than 4mm depth and it was considered that the amount of runoff flow was not sufficient to mobilise all available particles (i.e. particle washoff as a process was flow-limited).

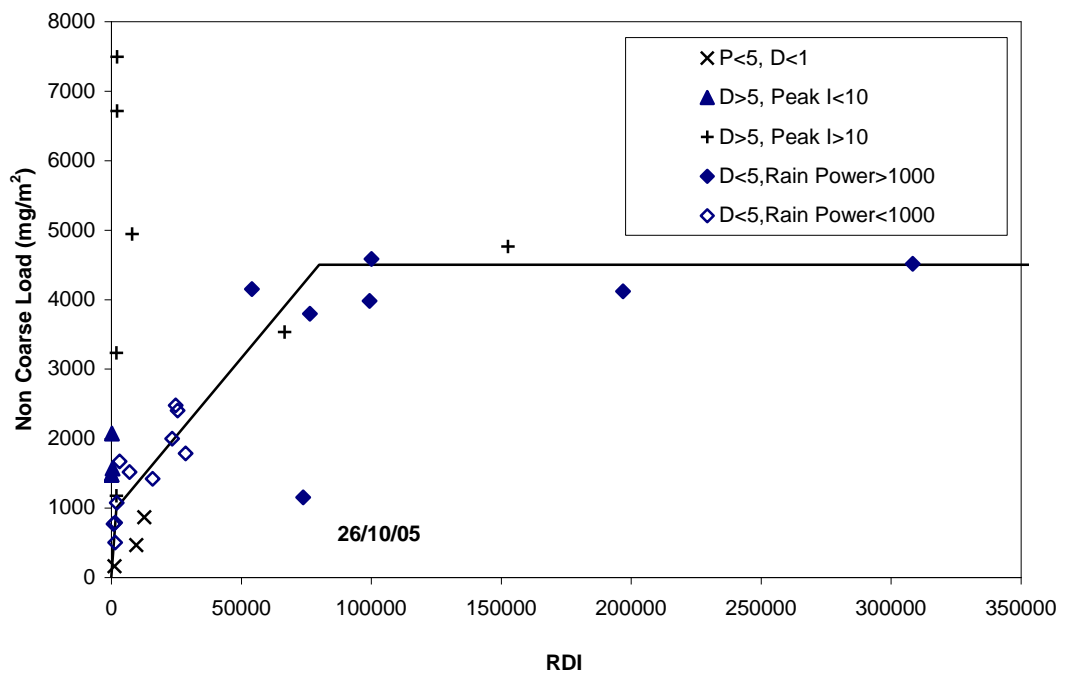
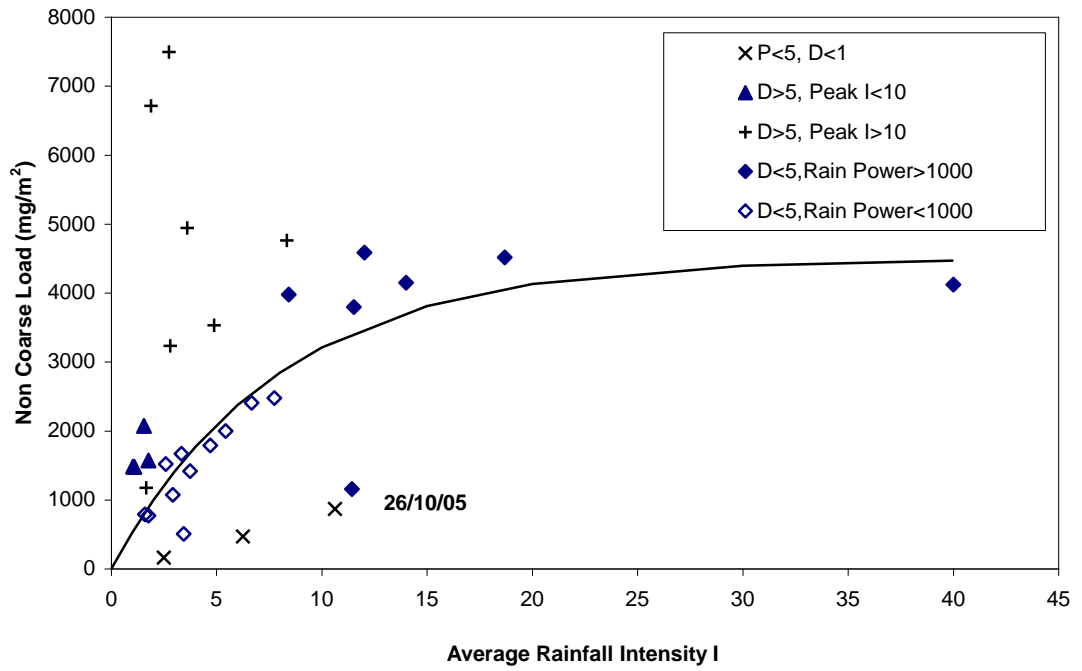
As shown in **Figure 8.15**, the loads corresponding to rainfall exceeding 5mm were further divided into two groupings based on storm duration D. It can be seen that loads for storm durations less than 5 hours plot reasonably close to the exponential curve. These events exhibit mainly single-burst rainfall patterns. Also, the loads for storms with rain power ($\sum I_6^2/D$) less than $1000 \text{ mm}^2/\text{hr}^3$ all plot along the rising limb of the exponential curve corresponding to rainfall intensity less than 10 mm/hr (shown as \diamond). Storms with rain power exceeding $1000 \text{ mm}^2/\text{hr}^3$ generally resulted in measured loads from the road surface of approximately 4000 mg/m^2 and these points

plot on the upper tail of the exponential curve (shown as \blacklozenge). One exception is the 26/10/05 event load which is significantly below the exponential curve. The data points generally indicate that rain power of at least $1000 \text{ mm}^2/\text{hr}^3$ is required for complete washoff of available particle loads from the road surface. Using terms described by Sansalone *et al.* (1998), these events are ‘mass-limited’ as minimal remaining particle mass is available for washoff by the end of the storm.

The road Non-Coarse Particle loads for storm durations longer than 5 hours consistently plot above the exponential curve. This trend is most notable for storms with high Peak I_6 ($>10 \text{ mm/hr}$ and shown as $+$) and in some cases the corresponding loads are comparatively high (approximately 8000 mg/m^2). In the majority of these events, the storm temporal patterns consist of multiple bursts of rainfall separated by periods of low to no rainfall. It is apparent that additional contributions to the particle load are occurring during these long duration storms which are absent in the shorter events (less than 5 hours). Clearly, these additional particle loads are not accounted by the fitted exponential curve.

For storms greater than 5 hours duration that have low Peak I_6 ($<10 \text{ mm/hr}$ and shown as \blacktriangle), the departure above the exponential curve is not as great. A possible explanation of this effect is that, although there may be some additional loads associated with the longer storm duration, the peak runoff discharge (which is in proportion to Peak I_6) is insufficient to fully transport all particles to the drainage outlet.

Also presented in **Figure 8.15** are the road Non-Coarse Particle loads plotted against RDI grouped according to storm duration and rainfall depth (with subgroups based on rain power and Peak I_6). The trends that have been outlined based on I are also broadly exhibited in the RDI plot, including the outstanding point corresponding to the 26/10/05 event. In general, most points are in closer proximity to the RDI regression curve compared to the fit with the exponential curve based on I . This includes some loads corresponding to storm durations longer than 5 hours. However, a strong tendency persists for loads generated from storms exceeding 5 hours to plot significantly above the regression line, as was the case for I .



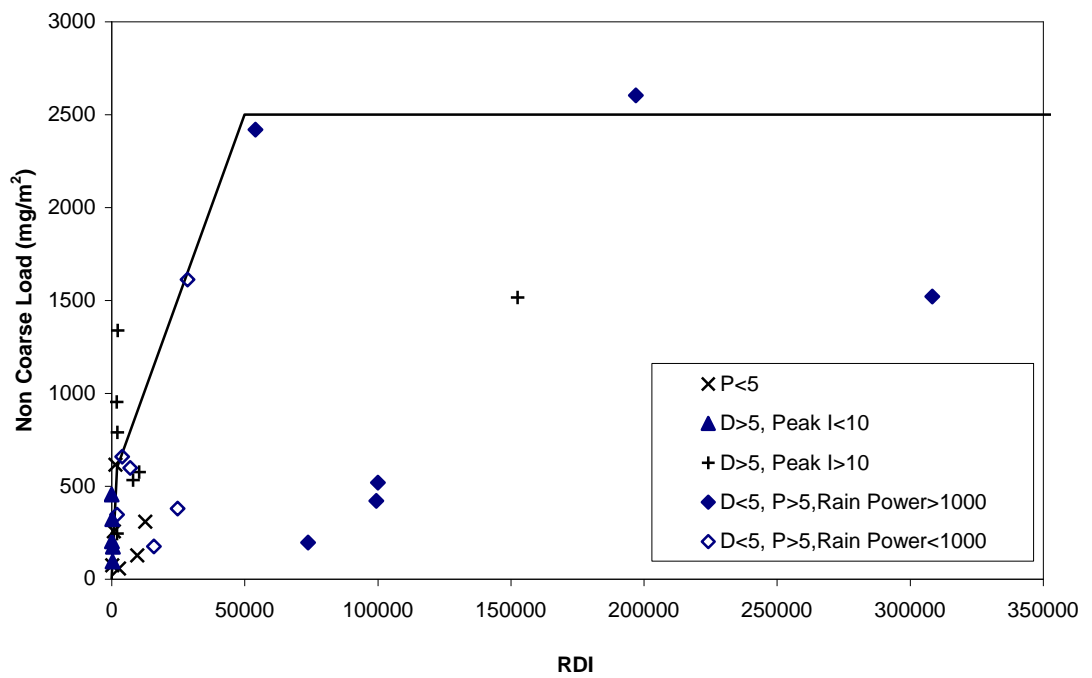
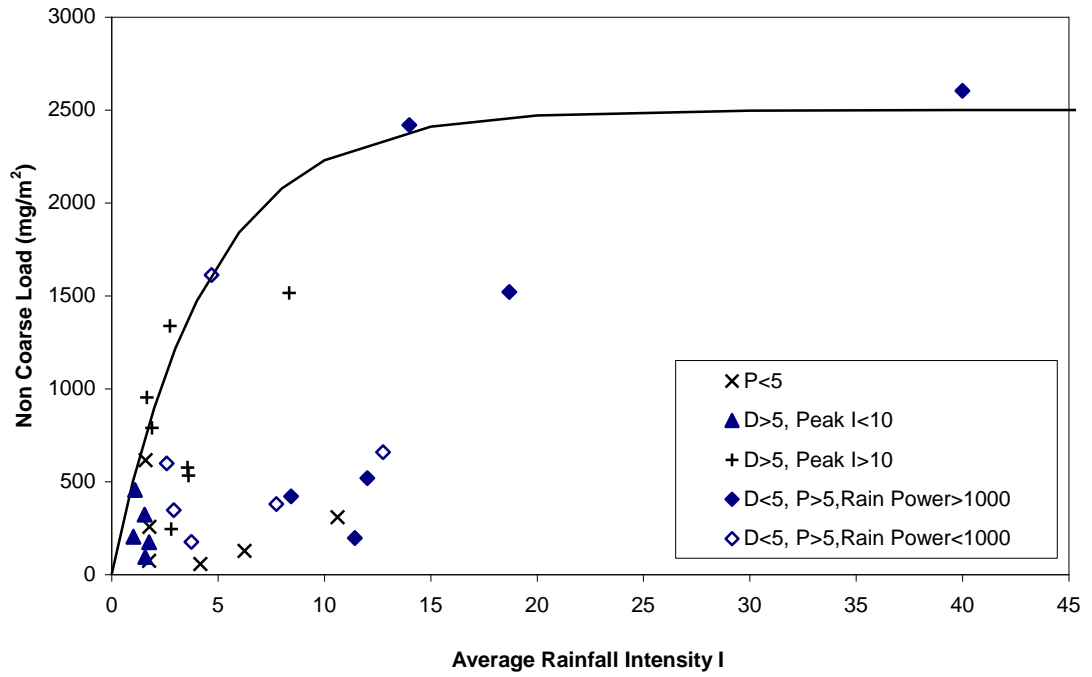
■ Figure 8.15 Road Non-Coarse Particle loads plotted against I and RDI using December 2004 to January 2006 data grouped based on rainfall characteristics

The carpark Non-Coarse Particle loads plotted against I and RDI grouped according to duration and rainfall depth are presented in **Figure 8.16**. The corresponding plots for the roof data are shown in **Figure 8.17**. Clusters of points around the exponential curve similar to the road data are also present in the carpark and roof plots, but are not as clearly defined as is the case of the road surface. This may be the result of the particle concentrations for these surfaces being inherently much lower than the road concentrations, making it more difficult to distinguish between the various groupings.

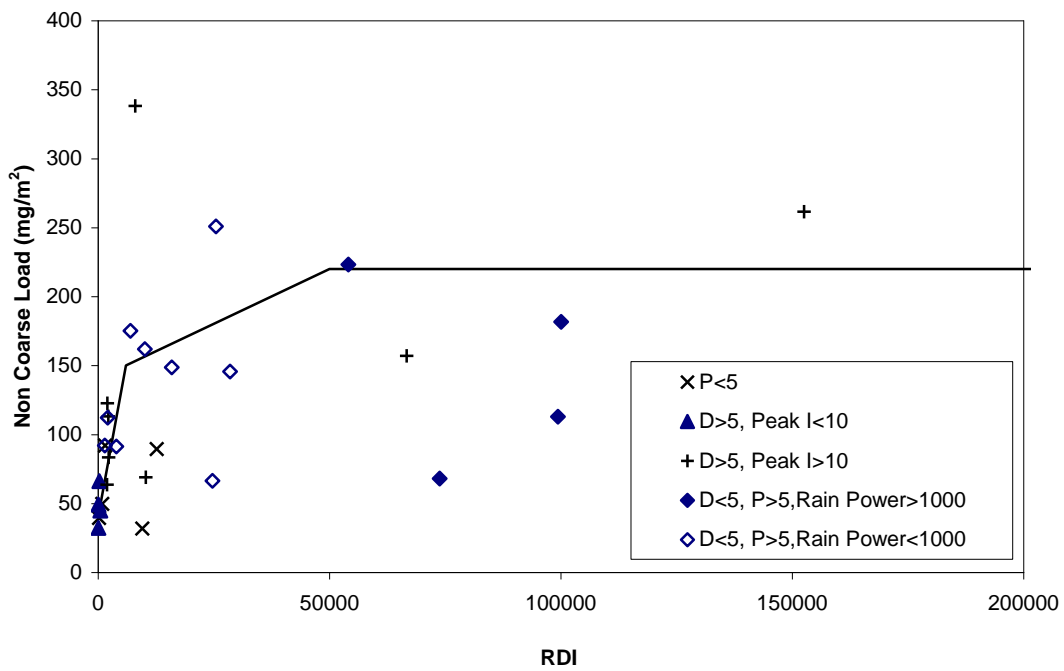
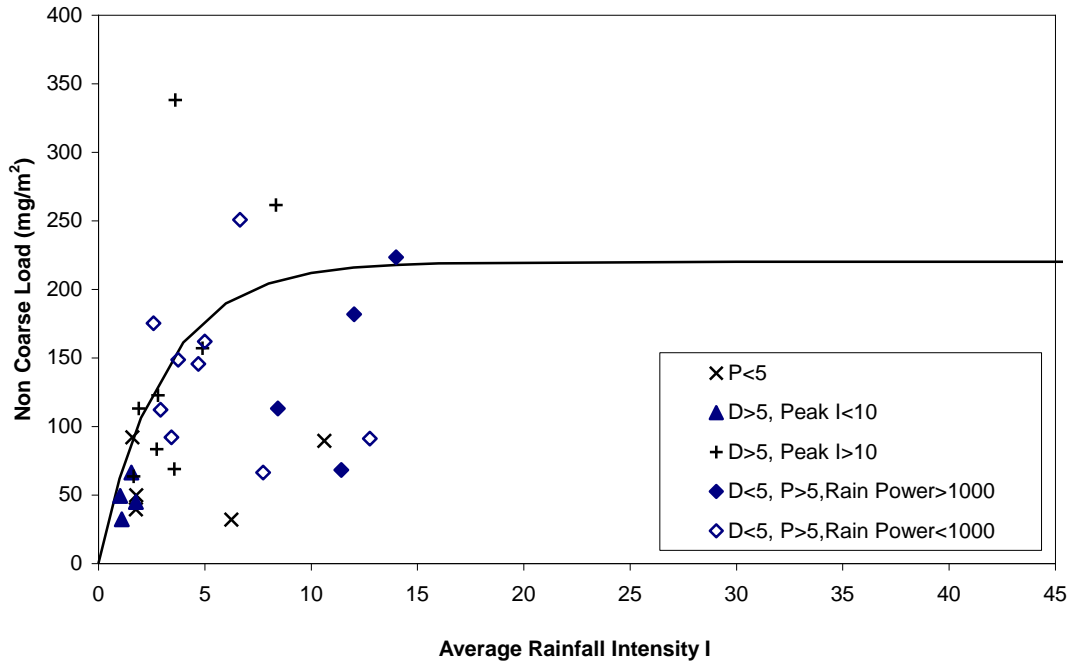
A tendency remains for some carpark and roof data points, especially for storms durations less than 5 hours, to plot below the fitted curves. This possibly suggests that, even though there is adequate rainfall energy for washoff, the amount of particle mass available for washoff delivered to the point of discharge was reduced in some way.

Data points for storms longer than 5 hours that plot above the fitted curves are considerably reduced in number for both the carpark and roof surfaces, compared to the road data. Also, these outlying points are positioned relatively closer to the curves. A process specific to the road surface appears to be acting to add to the particle mass during long duration storms. This process is largely absent from the roof and carpark surface. A possible candidate for this mass addition is vehicle traffic during the storm.

In summary, it is suggested that the regression curves based on I and RDI have the greatest application in deriving particle load estimates for single-burst storms of short to moderate duration (less than 5 hours) in excess of 5mm rainfall. The relationships would tend to overestimate the Non-Coarse Particle loads for low rainfall (less than 5mm) storms. Non-Coarse Particle loads for multi-burst storms (typical of events exceeding 5 hour duration) maybe underestimated, especially for the road surface. These observations are not as clearly defined for the roof and carpark surfaces.



■ Figure 8.16 Carpark Non-Coarse Particle loads plotted against I and RDI using December 2004 to January 2006 data grouped based on rainfall characteristics



■ Figure 8.17 Roof Non-Coarse Particle loads plotted against I and RDI using December 2004 to January 2006 data grouped based on rainfall characteristics

8.8 Particle Washoff Relationships Using Selected December 2004 to January 2006 Data

The investigation of washoff effects unexplained by I or RDI (discussed in **Section 8.7**) suggest that the regression relationships, initially fitted to the December 2004 to February 2005 data set, are mainly relevant to storms with more than 5mm rainfall and shorter than 5 hours duration. This outcome provides a basis to select data from the whole monitoring period from December 2004 to January 2006 to refit the curves with an enhanced number of data points.

The process is illustrated with reference to **Figure 8.18** which shows selected road Non-Coarse Particle load data plotted against average rainfall intensity I. The selected data is restricted to storms with P>5mm and D<5 hours, which for the period December 2004 to January 2006 corresponds to 15 data points (compared to 9 data points in the initial December 2004 to February 2005 set of data).

Two kinds of regression line were fitted and are also shown in **Figure 8.18**. The first is a piecewise linear relationship, as defined by **Equation 8.7**. This was introduced to check the viability of using a simpler relationship compared to the exponential form of **Equation 8.1**.

$$L = L_o \quad : I > I_o \quad [8.7]$$

$$L = L_o \times \frac{I}{I_o} \quad : I < I_o$$

where L is the particle load washed from the surface, L_o is the particle load on surface available for washoff and I_o is the average rainfall intensity corresponding to complete washoff of L_o

The second relationship is a modified version of the exponential curve adapted from **Equation 8.1d** and defined as **Equation 8.8**. An additional parameter I_c is incorporated as it was considered that the rising limb of the curve may be offset from the origin by a relatively small amount, referred to as the critical average rainfall intensity I_c .

$$L = L_o \{1 - e^{-K(I-I_c)}\} \quad [8.8]$$

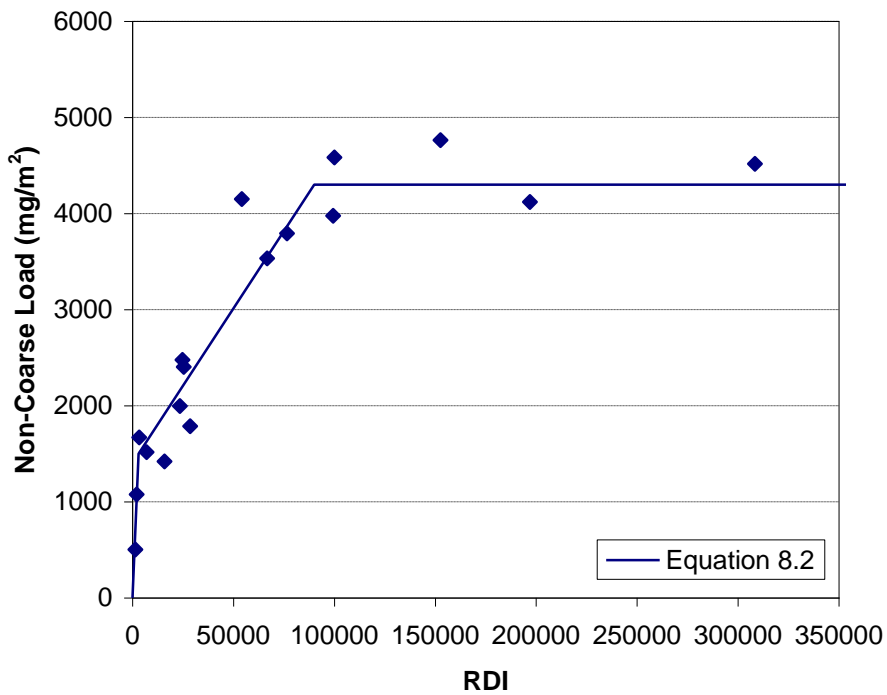
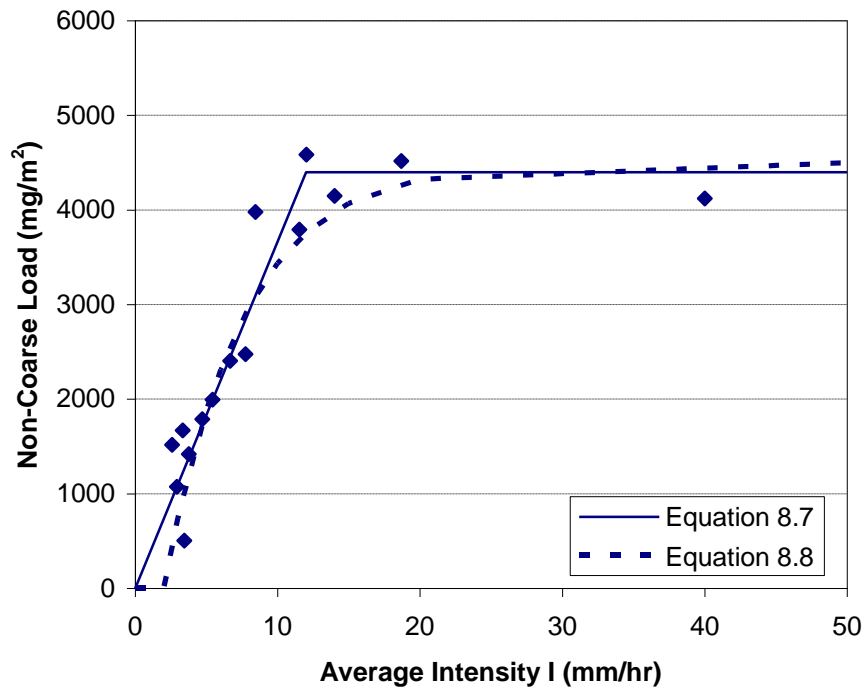
The critical rainfall intensity can be viewed as the minimum intensity that is required to initiate the mobilisation of particles from each type of surface. Murakami *et al.* (2004) introduced a similar term; the critical runoff rate for washoff R_C , to model the behaviour of particle bound polycyclic aromatic hydrocarbons from roads and roofs. They recommended R_C values of 0.5 mm/hr for roof surfaces, and 1.0 mm/hr and 2.0 mm/hr, respectively for ‘fine’ particles ($< 45\mu\text{m}$) and ‘coarse’ particles ($> 45\mu\text{m}$) from roads. Also, as average rainfall intensity I is a lumped parameter (defined by P/D), all load points will plot with at least some degree of offset from the origin.

Fitted curves using **Equations 8.7** and **8.8** against the selected Non-Coarse Particle loads for the road surface are shown in **Figure 8.18**. The load data plotted against RDI are also presented in this figure and fitted with a piecewise linear relationship using **Equation 8.2**. Similar plots are presented for the carpark and roof data as **Figure 8.19** and **Figure 8.20** respectively. The points selected for the curve fitting of carpark and roof data included storms longer than 5 hours duration to add to the population of data points. As previously discussed in **Section 8.7**, data outliers for these long duration events appear to be a feature of the road surface and are not as prominent for the roof and carpark sites. Regression parameters and coefficients are summarised in **Table 8.3**.

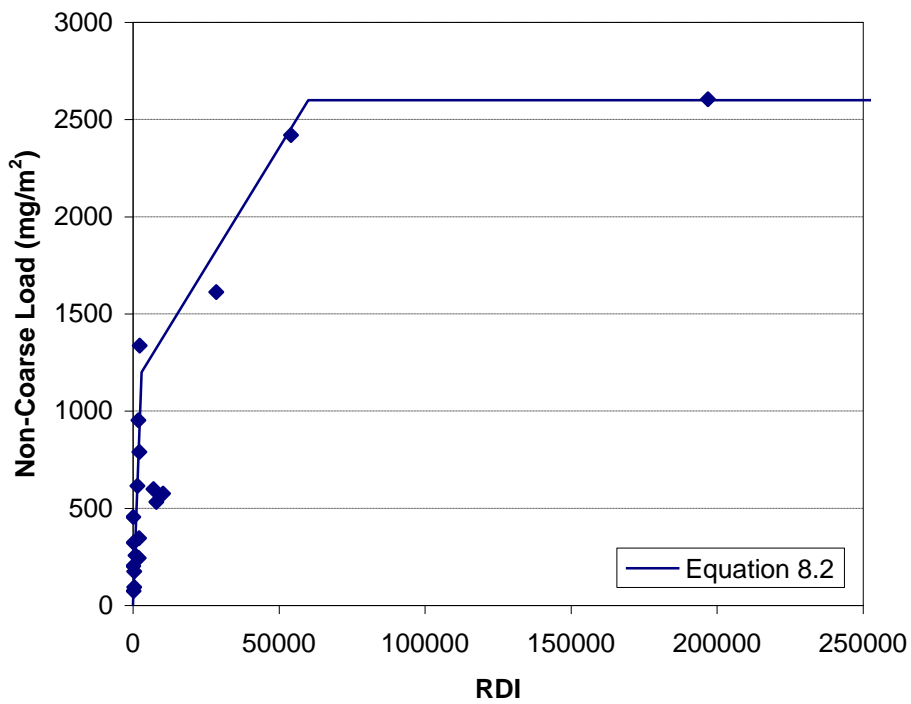
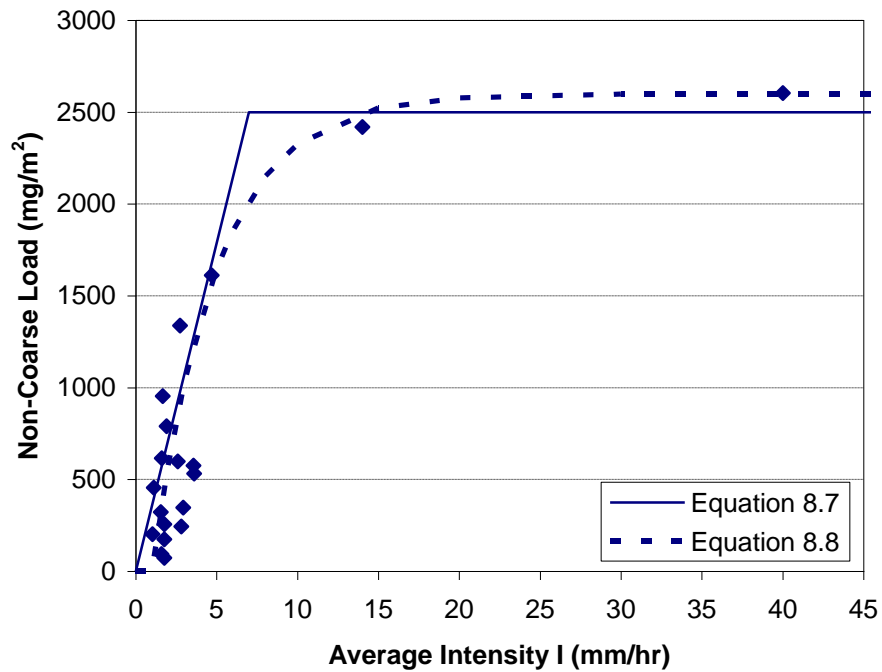
The results of the regression analysis suggests that, although it is simpler, the piecewise linear equation using average rainfall intensity I (Equation 8.7) yielded a higher coefficient of determination (R^2) than the exponential relationship (Equation 8.8) . This was the case for all surfaces. The piecewise linear equation using RDI (Equation 8.2) had slightly better R^2 values, with the exception of the roof data. The regression equations are used in the development of planning tools based on the estimation of particle loads from urban surfaces. This aspect is documented in Chapter 10 of this thesis.

- Table 8.3 Regression of Non-Coarse Particle loads against I and RDI for selected December 2004 to January 2006 storm data

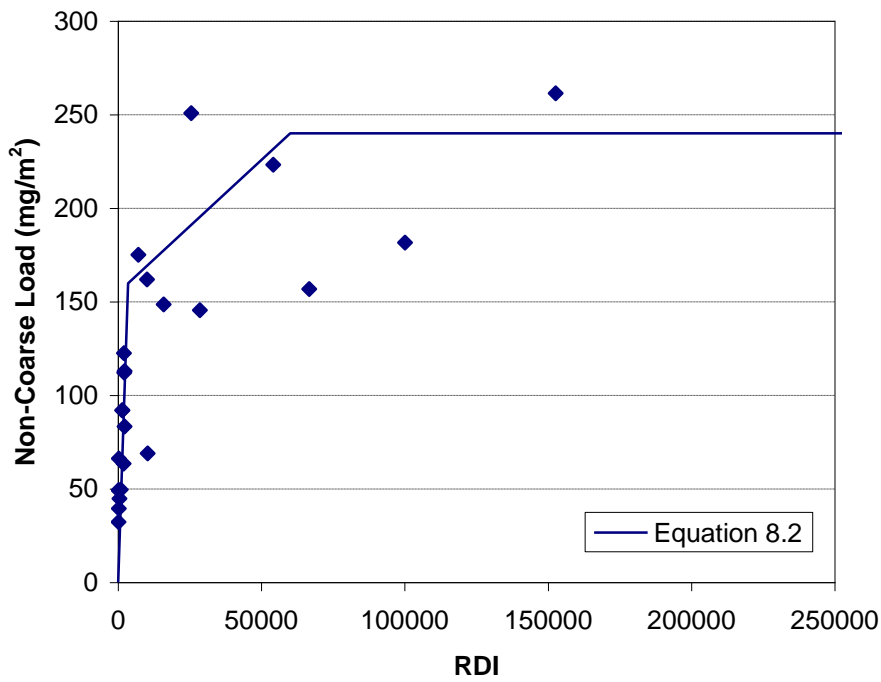
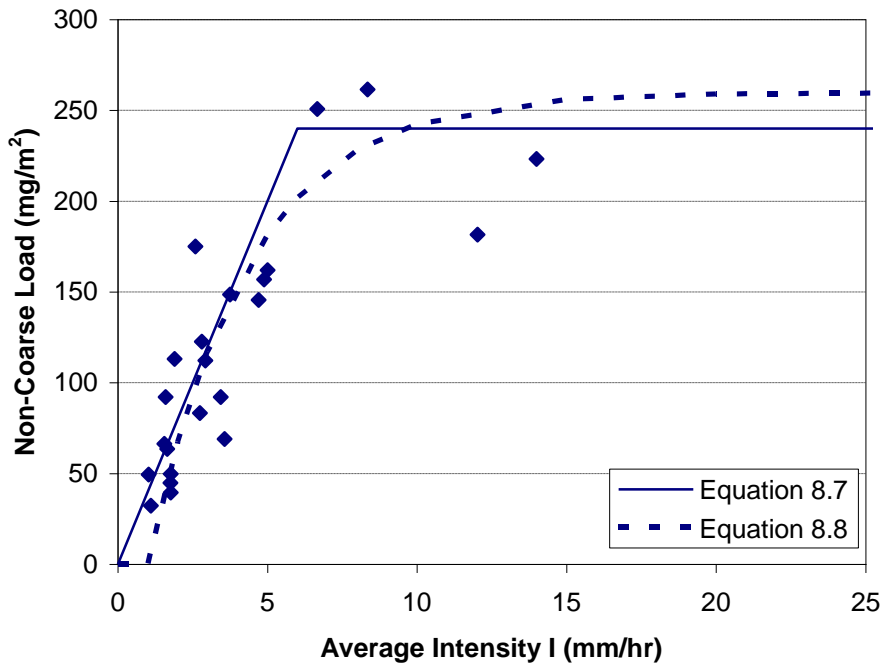
Parameter	Roof	Carpark	Road
Form of regression: Piecewise linear based on I using Equation 8.7			
I_0 (mm/hr)	6.0	7.0	12.0
L_0 (mg/m ²)	240	2500	4400
R^2	0.778 ($n=23$)	0.761 ($n=19$)	0.914 ($n=15$)
Form of regression: Exponential based on I using Equation 8.8			
L_0 (mg/m ²)	260	2600	4500
K (hr/mm)	0.3	0.25	0.18
I_c (mm/hr)	1	1	2
R^2	0.750 ($n=23$)	0.729 ($n=19$)	0.879 ($n=15$)
Form of regression: Piecewise linear based on RDI using Equation 8.2			
L_0 (mg/m ²)	240	2600	4300
RDI_0 (mm ³ /hr ⁴)	60 000	60 000	90 000
L_i (mg/m ²)	160	1200	1500
RDI_i (mm ³ /hr ⁴)	3500	3000	3000
R^2	0.747 ($n=23$)	0.772 ($n=19$)	0.933 ($n=17$)



■ Figure 8.18 Road Non-Coarse Particle loads plotted against I and RDI using selected December 2004 to January 2006 data and showing fitted regression curves



- Figure 8.19 Carpark Non-Coarse Particle loads plotted against I and RDI using selected December 2004 to January 2006 data and showing fitted regression curves



■ Figure 8.20 Roof Non-Coarse Particle loads plotted against I and RDI using selected December 2004 to January 2006 data and showing fitted regression curves

9 Non-Coarse Particle Mass Balance Model for Impervious Urban Surfaces

9.1 Approach for Development of a Particle Mass Balance Model

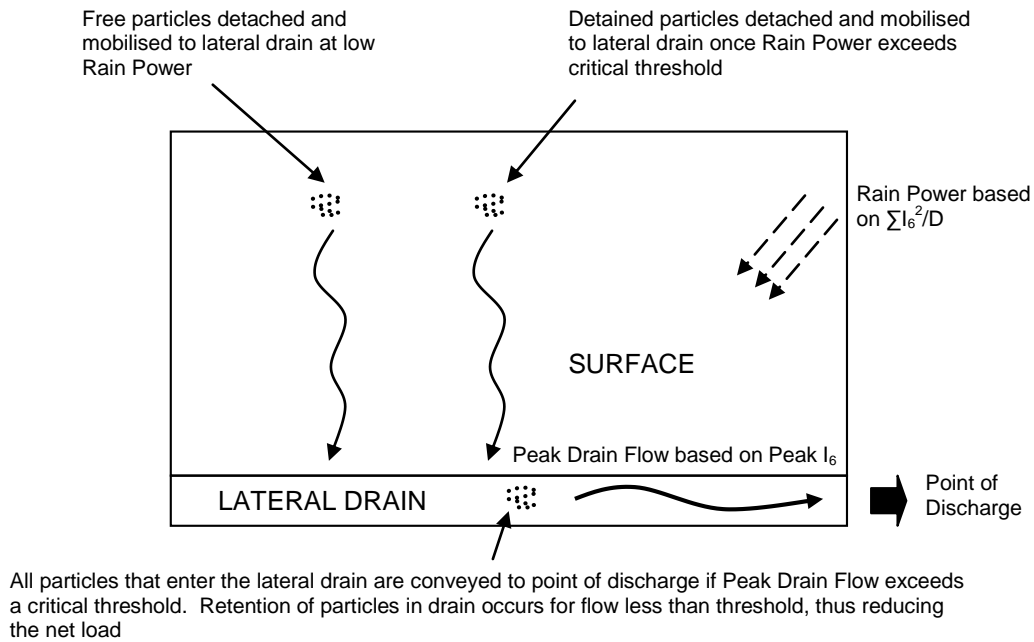
Development of a particle Mass Balance Model coincided with data collection and included three distinct phases, as stormwater data progressively became available. The first phase was **initial model conceptualisation** based on the monitoring results from the first set of 14 storm events recorded during December 2004 to February 2005. This was followed by a **model refinement phase** making use of data from the next sequence of 10 storms during the March 2005 to June 2005 period. Lastly, **model validation** was performed against measured data from 16 storms from July 2005 to January 2006.

9.2 Basic Conceptual Model of Particle Washoff Processes

A conceptual model of the washoff of Non-Coarse Particles from impervious surfaces is initially postulated from previous observations, discussions and data analysis. Reference is made to previous research in supporting the key processes that form the basis of a model to predict the particle mass in stormwater runoff from impervious surfaces. The key processes involved in particle washoff are shown schematically in **Figure 9.1** and discussed in more detail in this Section.

Chapter 8 suggests that RDI reflects the two main physical processes involved in particle washoff; namely 1) Rain power which causes particle detachment and initial mobilisation from the surface and 2) Flow capacity to transport the suspended particles along the lateral drain to the point of discharge. On this basis, the main driver for particle washoff from the surface is considered to be rain power (based on $\sum I_6^2/D$), and the subsequent transport of particles along the lateral drain is governed by peak discharge (proportional to Peak I_6).

These observations form the core of a conceptual model of washoff processes and are also consistent with analysis of suspended solids data collected from two small urban surfaces (a parking lot and a street pavement) by Deletic *et al.* (1997). Their study found that rainfall intensity, as it relates to the kinetic energy of rain drops, and overland flow rate are particularly important in washoff processes.



- **Figure 9.1 Conceptual model of basic washoff processes for urban impervious surfaces**

9.2.1 Inclusion of Surface and Drainage System

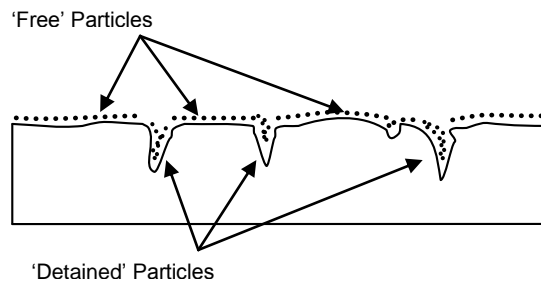
The physical components of urban surfaces include not only the surface itself but also the lateral drainage system that convey the stormwater runoff to a point of discharge. These components are introduced previously as **Figure 6.4**. The lateral drainage systems take a number of forms (e.g. roof guttering, road kerbing) and, depending on their physical characteristics, potentially have different efficiencies in transporting particles to the discharge point. Flow regimes within the drainage also tend to be deep and narrow compared to the shallow overland flows associated with surface runoff.

Both the surface and its drainage system should be adopted as the two major physical components to be modelled in order to predict the net transport of particles to the point of discharge.

9.2.2 Free and Detained Particles

Non-Coarse Particles can be notionally partitioned into two groups depending on their availability to be physically washed from the surface. This division is based on the different rain powers required for mobilisation. In this thesis, the groups will be

referred to as ‘free’ particles and ‘detained’ particles. They conceptually occupy different zones of the impervious surface as illustrated in **Figure 9.2**.



■ **Figure 9.2 Free and detained particles on impervious surfaces**

Free particles are postulated to loosely sit on the surface and are easily moved by wind action and other processes such as traffic-induced air turbulence (in the case of road surfaces). These particles are readily detached by rain and transported from the surface by runoff into the adjacent lateral drainage system. The detained particles occupy interstices within the surface such as those provided by cracking and roughness or texture. These particles are less exposed to rain impact and are harder to detach and mobilise during a storm event. It should be noted that free and detained particles occupy conceptual storages on an impervious surface and in reality it may be difficult to physically distinguish between them.

The concept of two types of particles with different propensities to being mobilised by rainfall is supported by the piecewise linear form of the Non-Coarse Particle load relationship with RDI. As described in **Section 8.3.2**, there appears to be an ‘initial’ particle load that is easily washed off the surface at low RDI values. As RDI increases in magnitude, washoff of particles not as easily mobilised starts to occur and full washoff results when the storm RDI exceeds a threshold value.

The concept of road particles able to be delineated by a threshold rainfall characteristic is consistent with research by Hogan (2000) who monitored TSS loads from a road surface located at Mascot, Sydney. The collected data was able to be separated into two groups separated by a threshold rainfall intensity of 6 mm/hr.

The two types of particles are analogous to the ‘free’ and ‘fixed’ particles delineated by Vaze & Chiew (2002) on the basis of the energy required for their physical removal from the surface when sampled in dry weather. Free particles were able to be easily collected by vacuum without any brushing. Particles collected after the surface was lightly scrubbed with a fibre brush to release fine particles were defined as fixed. These definitions were used by Vaze & Chiew (2002) to partition dry samples taken daily from centre parking bays along an inner city street in Melbourne over a period of 36 days. The fixed particles generally had a finer grain size compared to the free particles.

In their research of roof and road runoff in Japan, Murakami *et al.* (2004) also considered that road particles can be classified into highly and less mobile fractions. This distinction between particles was not based on size, as both types were classed as ‘fine’ (<45µm). It was assumed that the less mobile particles are more ‘photolysed’ while attached to the road surface than the highly mobile particles. Also, it was postulated that the less mobile particles may contain particles originating from the pavement material.

The classification of surface particles as either free or detained is considered to be important to accurately predict the net washoff of particles from impervious surfaces.

9.2.3 Particle Detachment from the Surface Based on Rain Power

Free particles are detached and mobilised by shallow overland flow to the lateral drain. These particles are easily washed off at low rain power but threshold values can be expected to vary with surface characteristics such as slope, roughness and overland flow length.

Detained particles are harder to mobilise as they are conceptually contained within surface interstices and a greater threshold of rain power is needed to be reached before significant washoff of these particles will occur. For smooth, steep surfaces such as iron roofs the amount of detained particles may be insignificant and thus washoff behaviour will be dominated by free particles. In these circumstances, the ‘store’ of detained particles can be neglected. For rough surfaces such as asphalt road pavements, the amount of detained particles may contribute more significantly to the

overall particle characteristics in stormwater runoff particularly for high energy rainfalls.

The detained particles that can be washed off the surface may be limited by factors other than the store of particles available. As noted by Gabet & Dunne (2003), particle detachment is attenuated at high rainfall intensities because raindrop impact is lessened by the presence of a surface water layer. At water depths greater than 3 drop diameters, the rain impacts are considered to be relatively non-erosive (Moss & Green 1983). Also, the rainfall energy content e_K approaches a maximum limit as rainfall intensity increases. These attenuating effects may limit particle washoff, particularly Coarse Particles.

The main driver for the physical washoff of Non-Coarse particles from impervious surfaces is rain power, as expressed by $\sum I_6^2/D$. Free particles are washed off the surface at lower values of rain power than the less mobile detained particles.

9.2.4 Particle Transport along the Lateral Drain Based on Peak Rainfall Intensity

The RDI concept suggests that another key driver for particle movement is the capacity of the lateral drain to transport particles to the point of discharge, as indicated by the measured Peak I_6 for the storm.

The lateral drainage system conveys runoff and associated particles from the contributing surface area to a point of discharge. This system component may take a number of forms including a narrow gutter or a kerb and channel. A main factor in transporting particles is considered to be the peak stormwater discharge in the drain which has a direct relationship with Peak I_6 as expressed in the well known Rational Method (**Equation 9.1**).

$$Q = \frac{CI_{tc}A}{360} \quad [9.1]$$

where Q is the peak discharge (L/s), C is the runoff coefficient, I_{tc} is the rainfall intensity (mm/hr) for the storm duration corresponding to the time of concentration of the catchment (equal to Peak I_6 given the time of concentration is of the order of 6 minutes) and A is the catchment area (ha).

It is postulated that all particles that enter the drain from the adjacent surface are completely washed through the drain to the point of discharge once a critical Peak I_6 is exceeded. The critical Peak I_6 is expected to vary depending on the physical configuration of the lateral drain. Length, longitudinal grade, geometry and surface roughness all influence the hydraulic efficiency in transporting stormwater particles.

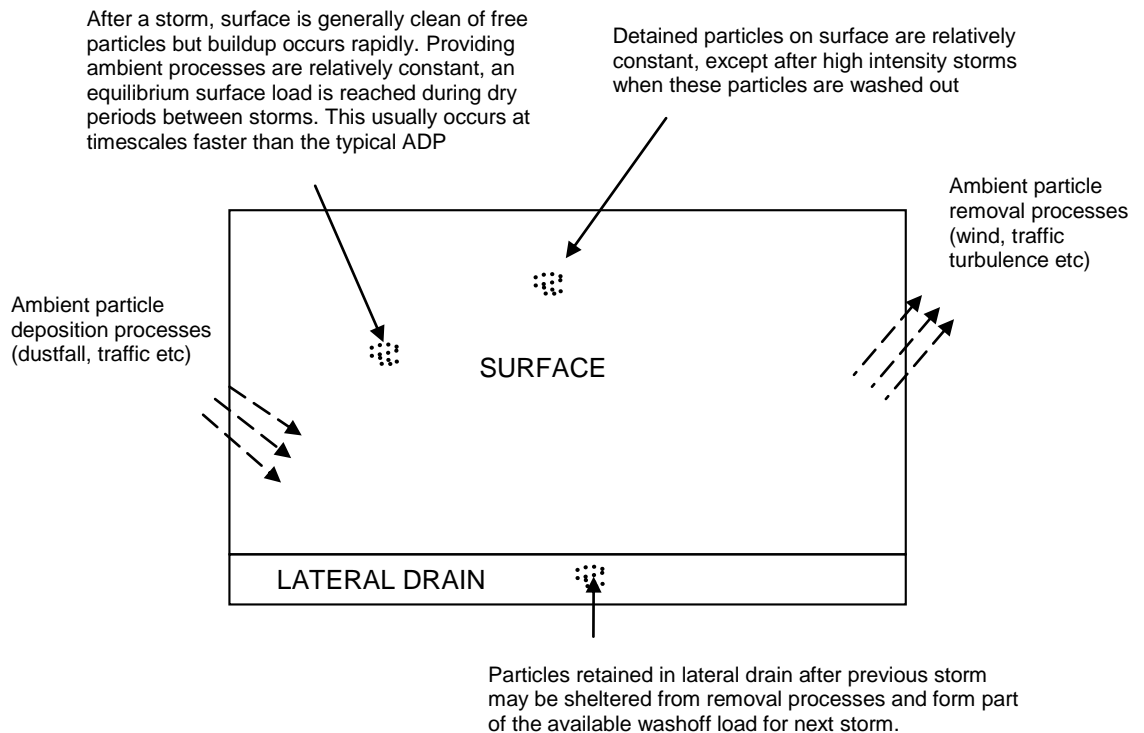
Post-storm retention of some particles within the drain will occur if the Peak I_6 is less than this critical threshold. Under very low Peak I_6 conditions, as may occur when the rainfall depth is only a few millimetres, the majority of particles could be retained within the lateral drain after the storm.

Once washed off the surface, the net transport of particles to the point of discharge is considered to be mainly governed by the hydraulic efficiency of the lateral drain.

This transport efficiency is in response to the Peak I_6 of the storm.

9.3 Basic Conceptual Model of Particle Buildup Processes

A conceptual model of the buildup of Non-Coarse Particles on impervious surfaces is now postulated. The key processes involved in particle buildup are illustrated in **Figure 9.3** and discussed in more detail in this Section.



- **Figure 9.3 Conceptual model of basic buildup processes for urban impervious surfaces**

9.3.1 Rapid Post-Storm Recovery of Free Particles

The reviewed literature includes studies that have measured net particle accumulation on impervious surfaces, mainly roads. They have included Coarse Particles much larger than what can be mobilised by stormwater runoff. Particles that can be mobilised during a storm are Non-Coarse Particles smaller than 500 μm . It is important to recognise that the particles in stormwater runoff, particularly from trafficable surfaces, may represent a small portion of the total particle mass accumulating on the surface. This is particularly true for free particles.

The mass of free particles distributed on the surface at any time represents the difference between supply and removal processes. The sources of particle supply in dry weather depend on the surface type. All surfaces are subject to atmospheric dust fall which is the dominant particle source for roofs. Roads and car parks also accumulate traffic related particles including wear products from vehicle components (tyres, engine, brakes etc), settleable exhaust products and pavement wear. Dry

weather removal processes include wind, both natural and traffic induced, and street cleaning activities.

Providing ambient conditions for the major supply and removal processes remain relatively constant, the load of free particles on the surface will return to similar equilibrium magnitudes following washoff by rainfall. The free particles are loosely detached to the surface and the store of these particles may be quickly reduced, and then rapidly replenished.

It is considered that after a high intensity storm, the surface is generally clean of free particles but replenishment of this type of particle load is a rapid process. The buildup of free particles on the surface tends to reach an equilibrium condition determined by supply and removal processes.

This view of a rapid post-storm recovery of free particles is supported by analysis of dry particle samples collected by Vaze & Chiew (2002) from centre car parking bays close to the Melbourne central business district. 'Free' loads fluctuated from 10,000 to 40,000 mg/m² in response to dry weather accumulation, street sweeping and rain events. The 'free' loads were considered available for washoff, but also contained Coarse Particles (>500µm and up to 3000µm in size) that are not readily mobilised. Interpretation of the Vaze & Chiew data suggests that Non-Coarse Particles represents between 20 to 50% of the 'free' load by weight. The 'free' loads on the Melbourne street were found to increase quickly after storms and stabilise after a few days of dry weather.

A rapid post-storm recovery of free particles suggests that a long antecedent dry period (ADP) is not necessary for the full replenishment of particles on the surface. If a long ADP is required, then a positive correlation between ADP and Non-Coarse Particle load in stormwater runoff may be expected. **Section 7.4** of this thesis indicates only a weak negative correlation is present for all impervious surfaces. This is consistent with previous studies of impervious surface runoff e.g. Deletic & Maksimovic (1998) although other studies, mainly of road and highway runoff, have found a positive correlation between ADP and particle load e.g. Ball *et al.* (1998). Other researchers who have reported a weak correlation of highway particle load with ADP include Kerri *et al.* (1985) and Harrison & Wilson (1985). However,

interpretation of these findings is confounded as they relate to the total particle load (TSS) in stormwater runoff rather than the free particle component only.

9.3.2 Relatively Constant Detained Particle Load

A key concept that is proposed in this thesis is the differentiation of particles into two types; an easily mobilised and replenished free particle load and a less mobile detained particle load. The washoff of detained particles occurs less frequently than free particles as the rainfall energy requirements are higher. It is expected that this effect will be more pronounced in rough textured surfaces such as some types of road surfaces in combination with a low intensity rainfall climate.

As detained particle washoff occurs infrequently, it is expected that a relatively constant detained particle load on the surface would be maintained on the surface.

A relatively constant detained particle load on the surface is consistent with the findings of a number of studies. Chiew *et al.* (1997a) demonstrated by modelling TSS loads from urban catchments that storms typically remove only a small proportion of the available particles. Malmquist (1978) repeatedly flushed a street pavement using a rainfall simulator at high intensity and found that many successive large events were needed to remove most of the surface particles. Reinersten (1981) and, more recently, Barry *et al.* (2004) reached a similar conclusion in their rainfall simulator experiments on road surfaces. In a Melbourne study of street particles, Vaze & Chiew (2002) measured minimal changes in the 'fixed' particle load during a 36 day monitoring event that included three rainfall events ranging from 4mm to 39.4mm. The proportion of Non-Coarse Particles (less than 500 μ m) represented approximately 75 to 85% of the 'fixed' particle mass.

9.3.3 Particle Retention within the Lateral Drain

In addition to surface accumulation of particles, a further store for particles is located within the lateral drainage system. It is postulated that, depending on the physical characteristics of the drain, any particles that are retained in the lateral drain after a storm are likely to be sheltered from removal processes. As a consequence, these remaining particles within the drain could be mobilised to the discharge point during the next storm. The particles available for washoff thus include free and detained

particles on the surface in addition to particles detained in the lateral drain from the antecedent storm.

This postulation is supported by the scatter plot analysis in **Section 7.4** which shows graphically a negative correlation between Non-Coarse Particle load and antecedent rainfall depth AP, particularly for the carpark and road surfaces. The highest measured loads are clustered in groups that have APs less than 7mm, and the majority have APs between 2 to 4mm.

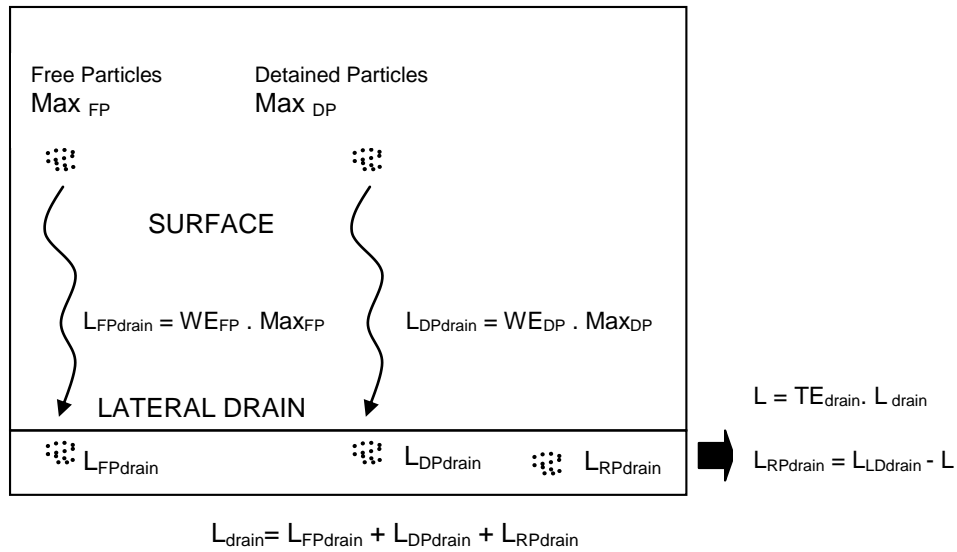
This potentially indicates that small preceding rainfalls may lead to high loads in stormwater runoff in the next storm event. This can be explained on the basis that the small rainfalls were sufficient to wash off particles from the surface, but insufficient to fully transport the particles from the drain. The particles remained in the drain after the small storm and added to the particle mass mobilised out during the next storm.

9.4 Initial Particle Mass Balance Model

9.4.1 Parameterisation of Initial Particle Mass Balance Model

A simple particle mass balance was performed for each of the impervious surfaces based on the above conceptual descriptions of buildup and washoff processes.

Parameterisation of the Mass Balance Model is presented in **Figure 9.4**.



■ **Figure 9.4 Parameterisation of initial particle Mass Balance Model for urban impervious surfaces**

A description of each parameter is provided as **Table 9.1**. The loadings of free and detained particles on the surface prior to the storm (Max_{FP} and Max_{DP}) are assumed constant as dictated by the rapid equilibrium that is reached by ambient removal and deposition processes. During the storm, washoff of free particles from the surface to the lateral drain occurs at an efficiency dependent on the rain power. All free particles are washed off when $\sum I_6^2/D$ exceeds a critical threshold (RP_{FPcr}). A similar basis is used for the washoff of detained particles, but significant mobilisation only occurs when $\sum I_6^2/D$ is above a threshold value (RP_{DPi}).

The total particle load contained in the lateral drain during the storm (L_{drain}) is the sum of the free and detained particle loads washed to the drain ($L_{FPdrain}$ and $L_{DPdrain}$) and the particles retained, if any, within the drain after the previous storm ($L_{RPdrain}$). This total load represents the particles available to be transported via the lateral drain to the point of discharge. The transport efficiency (TE_{drain}) to the point of discharge depends on the hydraulic features of the drainage system. If the peak drain flow (as measured by Peak I_6) exceeds a critical threshold (PI_{cr}), 100% of particles are assumed to be washed out. At lower flows ($Peak I_6 < PI_{cr}$), some particles are retained in the drain ($L_{RPdrain}$) and are available for washoff during the next storm. This particle retention reduces the net particle load (L) at the drainage outlet.

The transport efficiency (TE_{drain}) relationship to Peak I_6 is established for the lateral drainage system that conveys runoff generated from the surface. This relationship is expected to be influenced by several factors that affect particle transport hydraulics such as drain geometry, surface roughness and gradient. Also in the case of road kerbs, deposits of coarse particles may provide an ‘armouring’ layer that protects finer solids from being washed out (Memon & Butler, 2005). Leaf litter may also provide a sheltering effect that enhances the detention of coarse particles within the kerb. These factors are not modelled explicitly, but are incorporated into a single, representative transport efficiency curve for each lateral drainage system.

■ **Table 9.1 Description of parameters used in initial particle Mass Balance Model**

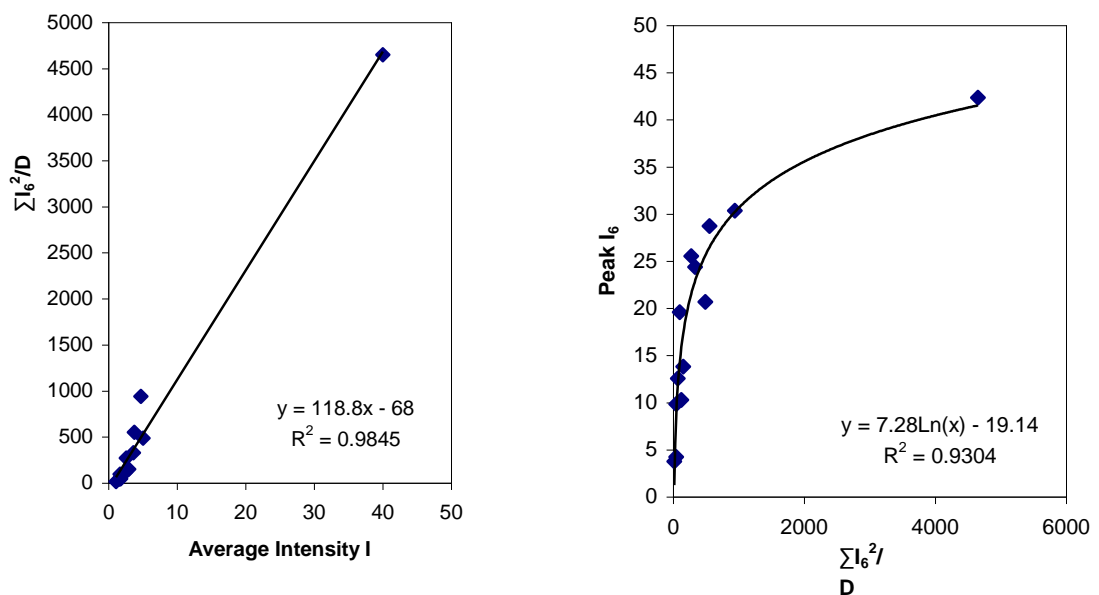
Parameter	Units	Description
Max_{FP}^1	mg/m^2	Maximum free particle load on surface prior to start of storm. Assumed to be a constant value for each surface
Max_{DP}^1	mg/m^2	Maximum detained particle load on surface prior to start of storm. Assumed to be a constant value for each surface
$L_{FP\text{drain}}$	mg/m^2	Free particle load washed to the lateral drain during storm from surface.
WE_{FP}	%	Washoff efficiency of free particles to lateral drain. Equal to 100% if rain power measure ($\sum I_6^2/D$) exceeds critical threshold = RP_{FPcr}
$L_{DP\text{drain}}$	mg/m^2	Detained particle load washed to the lateral drain during storm from surface
WE_{DP}	%	Washoff efficiency of detained particles to lateral drain. Equal to 100% if rain power measure ($\sum I_6^2/D$) exceeds critical threshold = RP_{DPcr} and starts when $\sum I_6^2/D$ exceeds an initial value = RP_{DPI}
$L_{RP\text{drain}}$	mg/m^2	Retained particle load within the lateral drain from previous storm
L_{drain}	mg/m^2	Total particle load in lateral drain available for mobilisation to point of discharge. Equal to sum of $L_{FP\text{drain}}$, $L_{DP\text{drain}}$ and $L_{RP\text{drain}}$
L	mg/m^2	Net particle load at point of discharge
TE_{drain}	%	Transport efficiency of net particles within lateral drain to point of discharge. Equal to 100% if peak drain flow measure (Peak I_6) exceeds critical threshold = PI_{cr}

Note: 1. These parameters were replaced by other parameters in refining the particle Mass Balance Model as described in **Section 9.5**.

9.4.2 Calibration of Initial Particle Mass Balance Model

An initial Non-Coarse Particle mass balance analysis was undertaken for each impervious surface monitored in this thesis study for the period December 2004 to February 2005. For some storms, short timescale rainfall data was not available due to pluviograph failure and direct determinations of $\sum I_6^2/D$ and Peak I_6 could not be made. These storm characteristics were derived from regression equations relating $\sum I_6^2/D$ to I and Peak I_6 to $\sum I_6^2/D$. The regression plots are provided in **Figure 9.5** and indicate a reasonably high correlation between these rainfall variables.

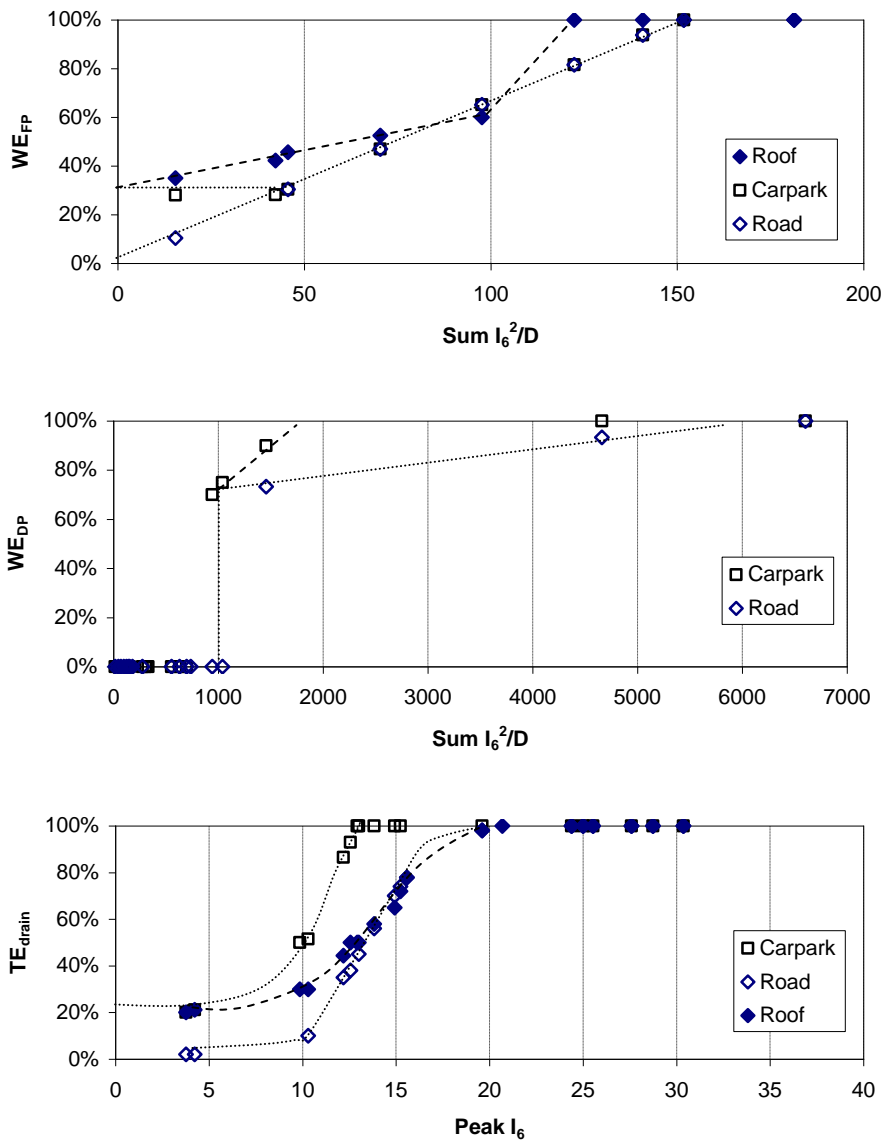
The mass balance analysis was performed using an EXCEL spreadsheet. Key parameters were adjusted by trial and error so that the predicted Non-Coarse Particle loads closely matched measured loads. The washoff and transport efficiencies (WE_{FP} , WE_{DP} and TE_{drain}) were varied from storm to storm with other parameters held constant. As the roof is steep, in good condition and smooth, no detained particle load was assumed to apply to this surface. The preliminary set of calibrated parameters is provided in **Table 9.2**.



- **Figure 9.5 Regression plots of Average rainfall intensity I , $\sum I_6^2/D$ and Peak I_6 based on December 2004 to February 2005 storm data**
- **Table 9.2 Particle mass balance parameters calibrated against December 2004 to February 2005 Non-Coarse load data**

Parameter	Roof	Carpark	Road
Max _{FP} (mg/m ²)	150	600	1500
Max _{DP} (mg/m ²)	-	1000	3000
FRP _{cr} (mm ² /hr ³)	100	150	150
DRP _{cr} (mm ² /hr ³)	-	2000	6000
DRP _i (mm ² /hr ³)	-	600	1000
PI _{cr} (mm/hr)	20	11	20

The washoff and transport efficiency curves that were derived by iterative adjustment for each storm event are shown graphically in **Figure 9.6**. As given in **Table 9.2**, complete washoff of free particles (100% WE_{FP}) is achieved at comparatively low rain power corresponding to FRP_{CR} values of the order of 100 to 150 mm^2/hr^3 . Storms did occur with $\sum I^2/D$ less than these critical thresholds and the corresponding washoff efficiency are determined to be as low as 30% for the roof and carpark, and approach zero for the roof surface.



■ **Figure 9.6 Washoff and transport efficiency curves (WE_{FP} , WE_{DP} and TE_{drain}) for roof, carpark and road surfaces used in initial Mass Balance Model**

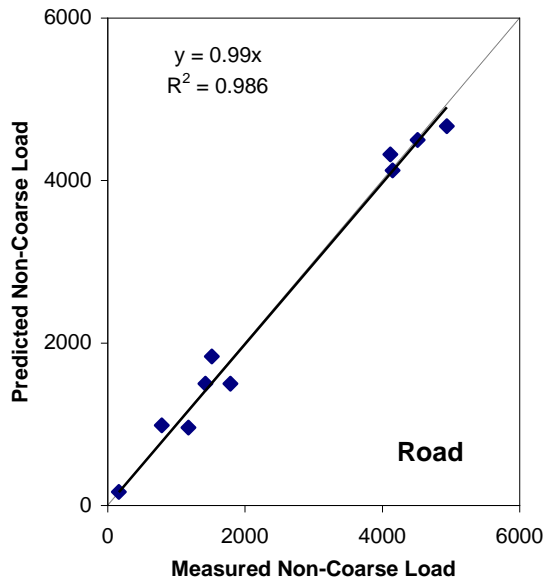
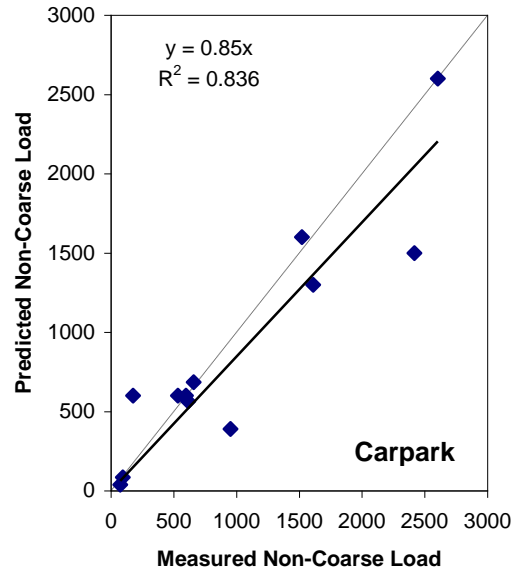
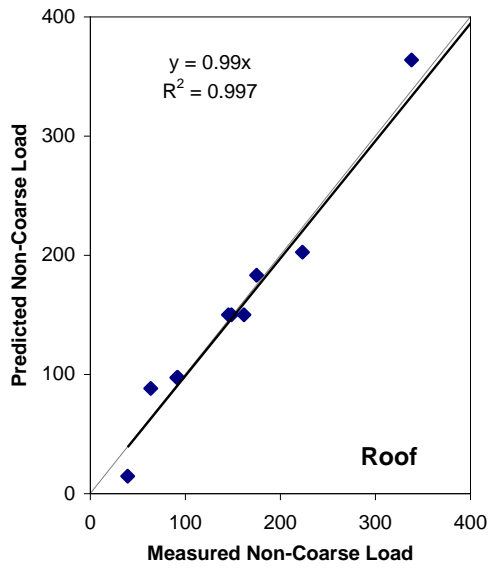
The transport efficiency (TE_{drain}) curves shown in Figure 9.6 suggest that the carpark kerb drainage has a higher efficiency in particle transport compared to the road drainage system. This outcome is consistent with the drain characteristics which, as shown previously in Table 6.1, have a similar surface grade (0.8 to 0.9%) but the carpark drainage length ($L_S=4.8\text{m}$) is substantially shorter than the road drainage length ($L_S=75\text{m}$).

Plots of predicted and measured Non-Coarse Particle loads for each surface are provided in **Figure 9.7**. As shown, the calibration process resulted in an accurate reproduction of the measured loads particularly for the roof and road surfaces ($R^2=0.99$). The correlation ($R^2=0.84$) for the carpark data is not as high and tends to overestimate the measured loads by approximately 15%. The uncertainty in the carpark results may be due to other sources of variability unaccounted for in the mass balance, including factors such as the number of cars parked during each storm, pedestrian activities such as littering and the presence of an industrial bin and a large tree close to the site.

9.5 Additional Particle Washoff and Buildup Processes

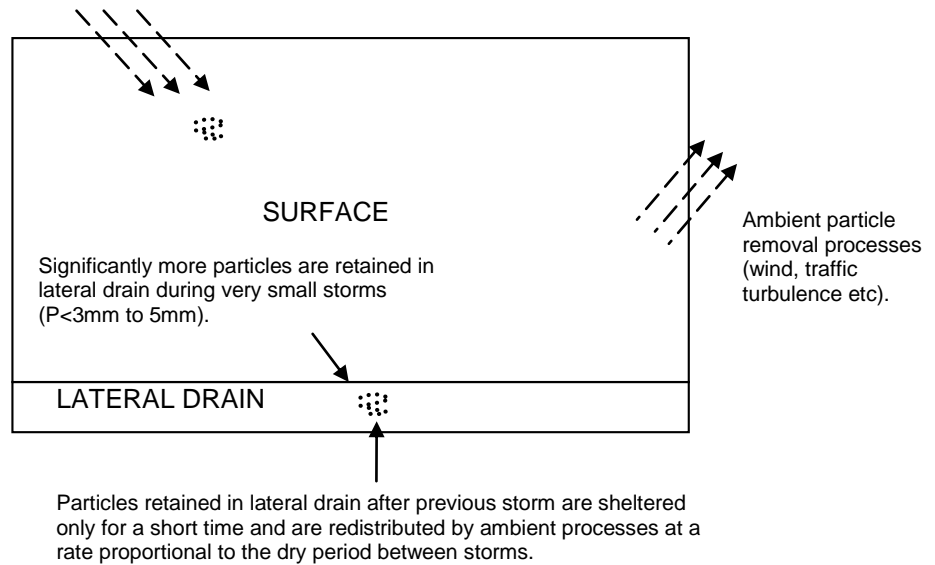
Predicted Non-Coarse Particle loads by the basic modelling approach yielded a good match with the December 2004 to February 2005 measured data. This dataset corresponds mainly to short-duration storms of less than 5 hours. As described in **Chapter 8**, RDI (and I) provides an accurate basis to predict Non-Coarse Particle loads for this type of storms. It follows that the Mass Balance Model predictions based on the principal components of the RDI (Peak I_6 and rain power $\sum I^2/D$) would also provide a good match with the December 2004 to February 2005 data.

The basic Mass Balance Model was applied to predicting Non-Coarse Particle loads for the March 2005 to June 2005 storms. For many storms, the match between predicted and measured loads was poor. This outcome is consistent with the presence of outlying data points from the RDI relationship proposed in **Chapter 8**, coinciding with storms longer than 5 hours duration (particularly for trafficable surfaces) and very small storms less than 3 to 5mm rainfall. It is clear that additional processes are needed to be introduced into the particle mass model to provide more accurate load predictions for these kinds of storms. These additional processes are illustrated in **Figure 9.8** and discussed further in this Section.



■ Figure 9.7 Plots of predicted and measured Non-Coarse loads using basic mass balance analysis of December 2004 to February 2005 storm data. Line of equal value shown as a dashed line.

Wet weather particle accumulation occurs in low rainfall periods that may be present in long duration ($D > 5$ hours), multi-burst storms. These particles add to the free particle load on surface, especially for trafficable areas. The amount of particles depends on the time period between storm peaks. A maximum particle accumulation applies. Drying of the surface should be also be taken in account.



- **Figure 9.8 Additional processes to the conceptual model of particle buildup and washoff for urban impervious surfaces**

9.5.1 Particle Retention in Lateral Drain During Very Small Storms

During the development phase of the Mass Balance Model, it was identified that small rainfalls of the order of a few millimetres were insufficient to mobilise particles out of the lateral drain. As a result, a significant proportion of the particle load would be retained within the drain until the next storm occurs. During the March 2005 to June 2005 period, monitoring of particle loads also included very minor storms and the resulting data tended to confirm this retention process.

9.5.2 Particle Loss in Drain After Storms

Another aspect of the basic modelling approach that was refined was the amount of particles retained within the lateral drain during the antecedent dry period (ADP). It was assumed in the initial model development that particles remaining in the drain after a storm would be sheltered from removal processes, and form part of the available washoff load for the next storm. This conservative assumption was appropriate for the short ADPs present in the initial December 2004 to February 2005 data used to establish the basic conceptual model.

However, the March 2005 to June 2005 data which involved longer dry periods between storms suggests that particle losses from the drain do occur. Over timescales of days to weeks, particles are expected to be redistributed out of the lateral drain by ambient processes including wind and traffic induced turbulence.

A more specific justification of this loss effect in the drain is the findings of Deletic & Orr (2005) who routinely sampled sediments from a road surface in Aberdeen, Scotland for a period of 17 months. Sediments collected within 1m^2 sites on the road pavement were collected, weighed and sieved to determine particle size distributions. The most mobile particles were regarded to be the smallest size range from 2 to $63\mu\text{m}$. A weak negative correlation was found between the 2 to $63\mu\text{m}$ particle mass at the road curb and ADP suggesting a loss of particles during longer periods of dry weather. This loss was attributed by the researchers to particle resuspension by wind and vehicles.

9.5.3 Wet Weather Particle Accumulation in Long Duration Storms

From the **Chapter 8** scatter plots (**Figures 8.15 to 8.17**), it is clear that for some long duration storms, the loads were atypically higher than other monitored events. This was evident for the road surface, less so for the carpark surface and was nearly absent in the roof load data. Based on this pattern, it was suggested that wet weather particle accumulation is occurring during long duration storms. For the road and carpark surfaces, this buildup is thought to be attributed mainly to vehicular traffic. Due to this differentiation, wet weather particle accumulation for the roof surface was considered on a separate basis to the trafficable carpark and road surfaces.

A major particle source for the roof is atmospheric dust fall which is a continuous process as dust particles settle onto the roof surface. If this accumulative contribution of particles is not accounted for in long duration events then predicted estimates of roof loads may be underestimated. To counter this effect, particle accumulation was assumed in the roof surface model to occur at a constant rate (expressed as $\text{mg}/\text{m}^2/\text{hr}$) until a maximum limit is reached.

An additional wet weather source is contributing to the particle load on trafficable surfaces and it becomes pronounced during long duration storm events. The magnitude of this within-storm particle accumulation appears to differ between

surfaces and is highest for the road surface. Apart from limited manoeuvring of vehicles within the car park, the road surface is the only monitored surface that is subjected to significant traffic and this may account for the greater particle accumulation. A possible mechanism is the pumping action of tyres in contact with the wet surface breaking down and mobilising particles detained in the road pavement. This may effectively transfer particles from a detained state within interstices to the free particle store on the surface. Particles brought in from external areas on tyres and other vehicle components and subsequently dislodged by water spray may also be a contributing process.

Traffic induced particle loads during prolonged wet weather have previously been identified as a significant factor in the runoff of road solids by a number of researchers. For example, traffic sources adding to the washoff load during a storm were allowed for in road runoff modelling by Kim (2002). In this case, a concentration coefficient dependant on the total runoff volume was introduced to allow for additional pollutant contributions during rainfall.

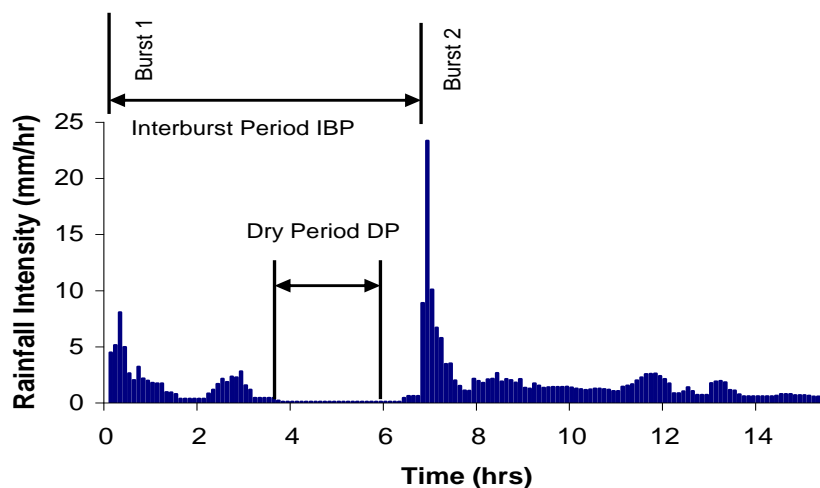
A measure that has been introduced by other researchers to predict the solids loadings from highways is the number of vehicles during the storm (VDS in counts/event). A correlation between VDS and contaminant loading in highway runoff has been reported in the literature (Asplund *et al.* 1982; Chui *et al.* 1982; Horner & Mar 1983). Enhanced mobilisation of particles has been attributed to energy being applied by tires and undercarriage winds to the wet surface. Exhaust particles may also be wet-deposited from the air during rainfall, adding particles to the runoff that otherwise may have drifted from the highway (Gupta *et al.* 1981).

The vehicle intensity during the storm (VIDS in counts per unit time or unit discharge) has also been suggested as an index for the estimation of particle loads from highways (Irish *et al.* 1995). Sansalone *et al.* (1998) considered that the number of vehicles per runoff volume (in counts/L) had an influence on the TSS load generated from a high traffic roadway in Cincinnati, USA.

The lack of traffic monitoring data for the Toowoomba road site curtailed the use of measures such as VDS and VIDS being used in refining the particle Mass Balance Model. Instead, it was assumed that the period of time between rainfall bursts

provides a reasonable measure of traffic-related particle supply within the storm. This time period, referred to as the interburst period (IBP in hours), is defined in **Figure 9.9** using the 15/06/2005 storm as an example. It is postulated that the first rainfall burst results in the removal of most free particles from the road surface, but the free particles are progressively replenished due to traffic acting on the wet pavement during the IBP. The second rainfall burst, in turn, washes off some or the entire replenished store of free particles that accumulated on the wet road. This cycle of particle removal and replenishment is repeated throughout the storm, depending on the number of burst and interburst sequences that occur.

As shown in **Figure 9.9**, the interburst period for this example storm ends with a period of no rainfall. If this dry period (DP) is sufficiently long and causes drying of the surface then ‘dry weather’ particle removal processes such as wind and traffic-induced air currents will begin to act. These processes will tend to equilibrate the mass of free particles on the surface towards ambient dry weather levels. It was found from further analysis of the March 2005 to January 2006 road data that the return to dry weather equilibrium loads occurs when the DP exceeds approximately six hours. This offers a more definitive approach to differentiate a rainfall temporal pattern into a sequence of rainfall bursts or as separated storm events, in which case the ADP corresponds to the dry period DP.



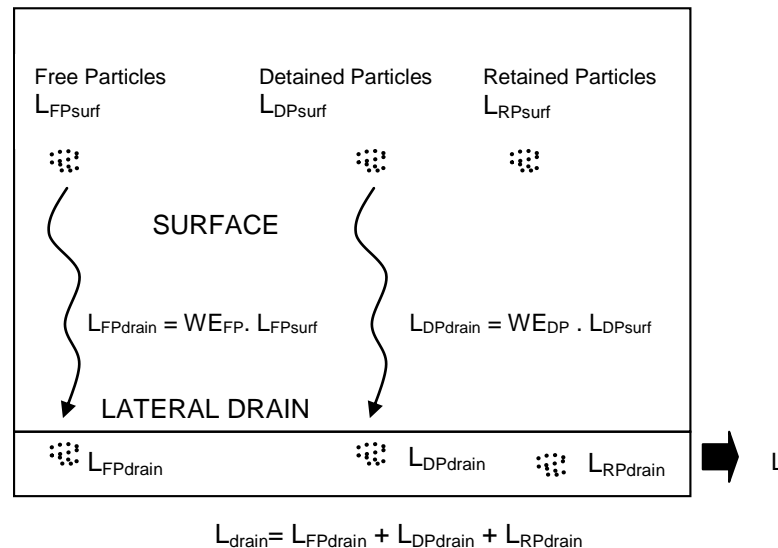
- **Figure 9.9 Definition of rainfall bursts and interburst period (IBP) and dry period (DP) using the 15/06/05 storm temporal pattern as an example**

9.6 Refinement of Initial Particle Mass Balance Model

9.6.1 Parameterisation of Refined Particle Mass Balance Model

To refine the particle Mass Balance Model, a number of adjustments were made to the basic set of parameters and new parameters were introduced. The key parameters associated with the refined model are shown in **Figure 9.10**.

A major refinement to the model is the use of terms L_{FPsurf} and L_{DPsurf} to represent the loads of free particles and detained particles, respectively that are available for washoff during the storm. The magnitude of these terms varies from storm to storm and replaces the constant Max_{FP} and Max_{DP} parameters used in the simpler basic model. They were introduced to allow for the effect of wet weather particle accumulation on loads.



■ Figure 9.10 Parameterisation of refined particle Mass Balance Model

The calculation of L_{FPsurf} is based on the free particle load at the start of the storm and the addition of any wet weather accumulation of particles during the storm, up to a maximum value. This calculation uses **Equation 9.2**.

$$L_{FPsurf} = \text{Min}(Max_{FPwet}, L_{FPi} + L_{FPwet}) \quad [9.2]$$

where Max_{FPwet} is the maximum free particle load on the surface in wet weather, L_{FPi} is the free particle load on the surface at the start of the storm based on **Equation 9.3** and L_{FPwet} is

the wet weather buildup of free particles on the surface during the storm based on **Equation 9.5**. All units are in mg/m^2 .

$$L_{FPi} = \text{Min}(\text{Max}_{FPdry}, L_{RPsurf} + T_{dry} \times AR_{FPdry}) \quad [9.3]$$

where Max_{FPdry} is the maximum free particle load on the surface in dry weather (mg/m^2), L_{RPsurf} is the free particle load not washed off during the previous storm and retained on the surface (mg/m^2) using **Equation 9.4**, T_{dry} is the dry weather accumulation period for free particles (hours) and assumed to be equal to antecedent dry period ADP; and AR_{FPdry} is the dry weather buildup rate of free particles on the surface ($\text{mg}/\text{m}^2/\text{hr}$).

$$L_{RPsurf} = L_{FPsurfi} - L_{FPdraini} \quad [9.4]$$

where $L_{FPsurfi}$ is the free particle load on the surface available for washoff in the previous storm and $L_{FPdraini}$ is the free particle load washed to the lateral drain during the previous storm. All units are in mg/m^2 .

The wet weather buildup of free particles on the surface during the storm L_{FPwet} is based on **Equation 9.5**.

$$L_{FPwet} = \text{Min}(\text{Max}_{FPwet}, T_{wet} \times AR_{FPwet}) \quad [9.5]$$

where Max_{FPwet} is the maximum free particle load on the surface during wet weather (mg/m^2), T_{wet} is the wet weather accumulation period for free particles (hours) and assumed to be equal to the storm duration D for the roof and the interburst period IBP for the road and carpark; and AR_{FPwet} is the wet weather buildup rate of free particles on the surface ($\text{mg}/\text{m}^2/\text{hr}$).

During some storms, no rainfall fell at the end of the interburst period leading to the potential for drying out of the road and carpark surfaces. This condition is expected to initiate removal of particles from the surface due to wind and traffic-induced turbulence. To allow for this effect, Max_{FPdry} was used in place of the Max_{FPwet} term in **Equation 9.5** if the period of no rainfall (DP) exceeded 6 hours.

The calculation of L_{DPsurf} is based on the detained particle load on the surface at the end of the previous storm not washed into the lateral drain and the addition of any dry weather accumulation of particles during the ADP, up to a maximum value. This calculation uses **Equation 9.6**.

$$L_{DPsurf} = \text{Min}(\text{Max}_{DPdry}, L_{DPsurfi} - L_{DPdraini} + T_{dry} \times AR_{DPdry}) \quad [9.6]$$

where Max_{DPdry} is the maximum detained particle load on the surface in dry weather (mg/m^2), $L_{DPsurfi}$ is the detained particle load on the surface available for washoff in the previous storm (mg/m^2), $L_{DPdraini}$ is the detained particle load washed to the lateral drain during the previous storm (mg/m^2), T_{dry} is the dry weather accumulation period for detained particles (hours) assumed to be equal to antecedent dry period ADP and AR_{DPdry} is the dry weather buildup rate of detained particles on the surface ($mg/m^2/hr$).

For the purpose of model refinement, it was assumed that particle loss from the lateral drain is a linear function dependent on the dry period between storms as presented in **Equation 9.7**.

$$L_{RPdrain} = Max\{0, L_{RPdraini}(1 - T_{dry} \times LR_{RPdrain})\} \quad [9.7]$$

where $L_{RPdrain}$ is the particle load retained in the lateral drain at the start of the storm (mg/m^2), $L_{RPdraini}$ is the particle load retained in the lateral drain at the end of the previous storm (mg/m^2), T_{dry} is the dry weather loss period for detained particles in the drain (hours) assumed to be equal to antecedent dry period ADP and $LR_{RPdrain}$ is the rate of dry weather loss from the drain ($\%/hr$)

The relationship given in **Equation 9.8** was also incorporated in the refined Mass Balance Model to allow for increased particle retention in the lateral drain during very small events and the subsequent reduction in net particle load at the point of discharge L.

$$L = C_p \times TE_{drain} \times L_{drain} \quad [9.8]$$

where C_p is an adjustment factor for small rainfall events (less than 3 to 5mm depending on the surface), TE_{drain} is the transport efficiency of net particles to point of discharge (%) and L_{drain} is the total particle load in lateral drain available for mobilisation to point of discharge (mg/m^2), equal to sum of $L_{FPdrain}$, $L_{DPdrain}$ and $L_{RPdrain}$

A summary of the parameters used in the refined particle mass model is provided in **Table 9.3**.

■ **Table 9.3 Description of parameters used in refined particle Mass Balance Model**

Parameter	Units	Description
Max _{FPdry}	mg/m ²	Maximum free particle load on surface prior to start of storm. Assumed to be a constant limit for each surface
Max _{FPwet}	mg/m ²	Maximum free particle load on surface during the storm. Assumed to be a constant limit for each surface
Max _{DPdry}	mg/m ²	Maximum detained particle load on surface prior to start of storm. Assumed to be a constant limit for each surface
L _{FPsurf}	mg/m ²	Free particle load available for washoff on the surface during the storm
L _{DPsurf}	mg/m ²	Detained particle load available for washoff on the surface during the storm
L _{RPsurf}	mg/m ²	Free particle load retained on the surface at the end of the storm
L _{FPdrain}	mg/m ²	Free particle load washed to the lateral drain during storm from surface.
L _{DPdrain}	mg/m ²	Detained particle load washed to the lateral drain during storm from surface
L _{RPdrain}	mg/m ²	Retained particle load within the lateral drain at the end of the storm
L _{drain}	mg/m ²	Total particle load in lateral drain available for mobilisation to point of discharge. Equal to sum of L _{FPdrain} , L _{DPdrain} and L _{RPdrain}
L	mg/m ²	Net particle load at point of discharge
WE _{FP}	%	Washoff efficiency of free particles to lateral drain. Equal to 100% if rain power measure ($\sum I_6^2/D$) exceeds critical threshold = RP _{FPcr}
WE _{DP}	%	Washoff efficiency of detained particles to lateral drain. Equal to 100% if rain power measure ($\sum I_6^2/D$) exceeds critical threshold = RP _{DPcr}
TE _{drain}	%	Transport efficiency of net particles within lateral drain to point of discharge. Equal to 100% if peak drain flow measure (Peak I ₆) exceeds critical threshold = PI _{cr}
AR _{FPdry}	mg/m ² /hr	Dry weather accumulation rate of free particles on the surface before the storm. Assumed to be a constant value for each surface
AR _{FPwet}	mg/m ² /hr	Wet weather accumulation rate of free particles on the surface during the storm. Assumed to be a constant value for each surface
AR _{DPdry}	mg/m ² /hr	Dry weather accumulation rate of detained particles on the surface before the storm. Assumed to be a constant value for each surface
LR _{RPdrain}	%/hr	Dry weather loss rate of retained particles in the drain before the storm. Assumed to be a constant value for each surface
C _P	%	Adjustment factor to L _{drain} for very small rainfalls less than 3 to 5mm

9.6.2 Calibration of Refined Particle Mass Balance Model

The March 2005 to June 2005 data were used to determine appropriate parameters for the refined Mass Balance Model. The rainfall temporal patterns for storms longer than 5 hours duration were viewed and divided into two to three subperiods covering the predominant rainfall bursts. Rainfall characteristics including Peak I₆, rain power $\sum I_6^2/D$ and interburst period IBP were derived for each rainfall subperiod and these formed the basis of the particle washoff and buildup calculation during the storm. Storms shorter than 5 hours duration were modelled as a single event.

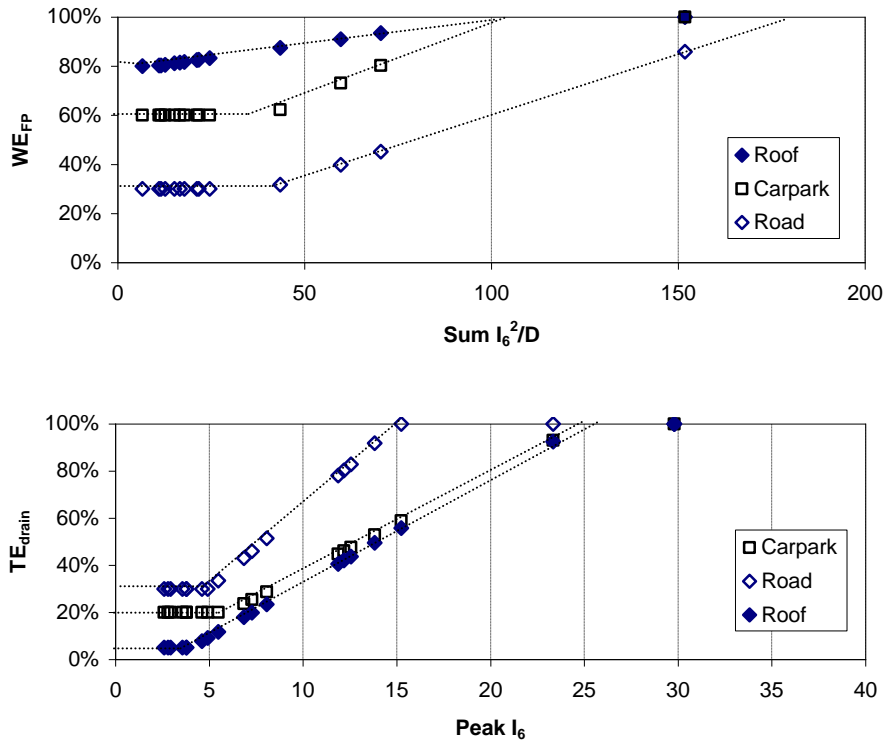
As particle load estimates are partly governed by preceding events, the mass balance analysis also included the December 2004 to February 2005 storms as starting conditions. To ensure consistency in the modelling approach, storms in this dataset longer than 5 hours were also divided into discrete subperiods and their rainfall characteristics were determined. This was done for the storms of 26/12/2004 and 25/01/2005.

Key parameters within the refined model were found by fitting the predicted Non-Coarse Particle loads to the March 2005 to June 2005 data. This exercise was essentially a repeat of the calibration process undertaken during the basic model development, but incorporating the modifications described in **Equations 9.2 to 9.8**. The fitted parameters are listed in **Table 9.4**.

The washoff and transport efficiencies (WE_{FP} and TE_{drain}) were iteratively adjusted for each storm and are shown graphically in **Figure 9.11**. The curves are simpler than the initial S-shaped curves used in the basic model and consist of piecewise line segments. For detained particle washoff from the surface, a step function is used representing no washoff unless rain power exceeds the critical threshold RP_{DPcr} and, under these conditions, full washoff is assumed to occur. The adopted values of RP_{DPcr} are provided in **Table 9.4**.

■ **Table 9.4 Refined particle mass balance parameters calibrated against March 2005 to June 2005 Non-Coarse load data**

Parameter	Roof	Carpark	Road
Max_{FPdry} (mg/m^2)	160	500	1600
Max_{FPwet} (mg/m^2)	250	500	6000
Max_{DPdry} (mg/m^2)	-	1000	2600
AR_{FPdry} ($mg/m^2/hr$)	5	300	1000
AR_{FPwet} ($mg/m^2/hr$)	3	300	2000
AR_{DPdry} ($mg/m^2/hr$)	-	5	30
$LR_{RPdrain}$ ($\%/hr$)	0.5	0.5	0.4
C_P (%)	30% for $P < 5mm$	30% for $P < 3mm$	25% for $P < 3mm$
RP_{FPcr} (mm^2/hr^3)	100	100	180
RP_{DPcr} (mm^2/hr^3)	-	940	1300
PI_{cr} (mm/hr)	25	25	15



- **Figure 9.11 Washoff and transport efficiency curves (WE_{FP} and TE_{drain}) for roof, carpark and road surfaces used for in refined Non-Coarse Particle Mass Balance Model**

9.6.3 Validation of Refined Particle Mass Balance Model

The mass balance analysis was extended to incorporate the June 2005 to January 2006 data to validate the fitted model parameters. This dataset included several storms with durations exceeding 5 hours and these events were divided and included in the analysis as rainfall subperiods. The inclusion of this dataset meant that the full sequence of monitored storms from December 2004 to January 2006 were included in the analysis.

As discussed in **Section 8.7.1**, two storms had occurred which coincided with abnormal airborne dust conditions. The dust fall for these events, 3/2/2005 and 14/10/2005, resulted in very high particle loads from the roof surface in particular. A dust fall contribution of 1000 mg/m^2 was added to the particle mass on the roof surface for both events. This additional loading gave a good match with measured particle loads in both cases and also improved the data fit for the carpark surface. However, the addition of the dust fall contribution in the analysis of the road surface did not yield an improved match with the measured loads. This may be due to road

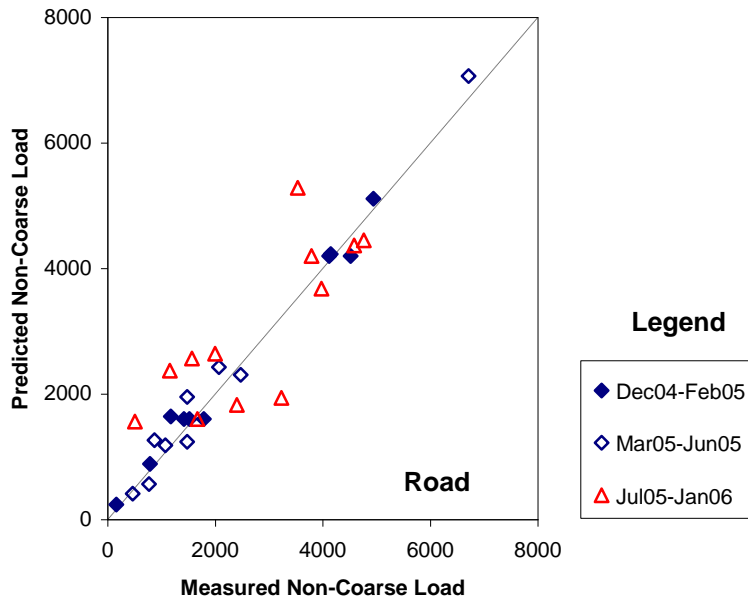
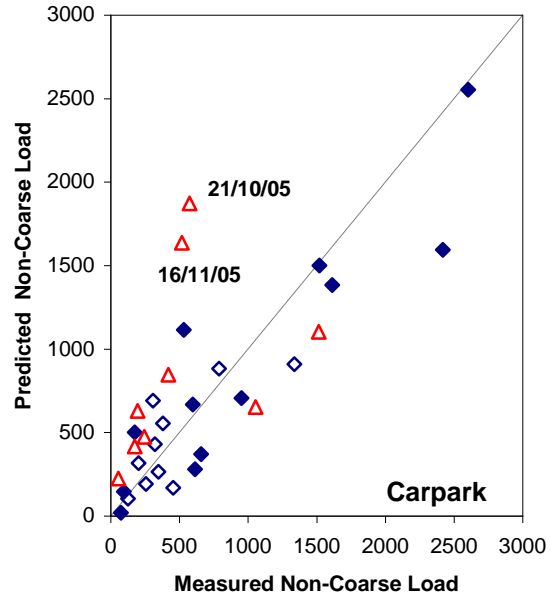
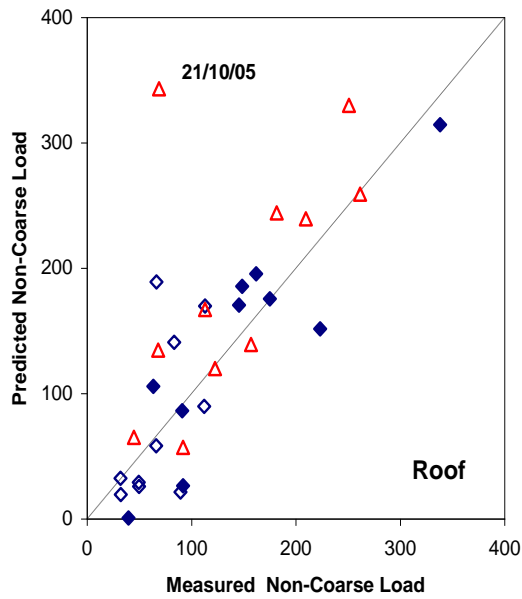
traffic remobilising the dust during the dry period shortly prior to rainfall and thus cancelling the effect of the dust fall. This remobilisation by vehicles is expected not to be significant in the low traffic carpark area and absent in the case of the roof.

Plots of predicted and measured Non-Coarse loads for each surface are provided in **Figure 9.12**. These plots correspond to the application of the refined Mass Balance Model to storm data from March 2005 to June 2005. For completeness, the initial December 2004 to February 2005 data is also plotted in addition to the June 2005 to January 2006 data.

In the case of the roof surface, the plot of predicted loads against measured loads has been scaled to exclude the abnormal events associated with high dust fall (3/2/2005 and 14/10/2005 storms) to improve clarity. The Non-Coarse Particle load is significantly overestimated for the 21/10/05 storm and it is unclear why this has occurred.

A possible explanation is that as the roof water sample had very low particle concentrations (approximately 2 mg/L) and close to the level of precision of the laboratory methods. This may have introduced an error in the determination of the measured load for this event. A reasonable consistency exists between the predicted roof loads with the remaining measured data ($R^2=0.974$ if abnormal events 3/2/2005 and 14/10/2005 also excluded).

The 21/10/2005 data point is also an outlier on the carpark load plot, as is the predicted load for the 16/11/05 storm. During these storms, the rain power exceeded the threshold RP_{DPer} and consequently the detained particle load was assumed to be washed off the carpark surface by the refined model. As peak storm conditions coincided with business hours, it is highly likely that the carpark area was occupied with vehicles. The physical presence of the cars may have sheltered the carpark surface from the high energy of the rainfall and significantly reduced the potential for detained particle washoff. This scenario would explain most of the over prediction of Non-Coarse Particle load for these two events. A moderate correlation ($R^2=0.741$) is present between the predicted loads and the remaining measured carpark loads.



■ Figure 9.12 Plots of predicted and measured Non-Coarse particle loads (mg/m^2) using refined mass balance analysis of December 2004 to June 2005 storm data. Line of equal value shown as a dashed line.

Of the range of monitored impervious surfaces, the load predictions for the road surface show the highest level of consistency against measured data ($R^2=0.905$). The match for the March 2005 to June 2005 data is close; given this was the data set that

formed the basis of selecting model parameters. During the validation period of July 2005 to January 2006, there is some departure of predicted loads from corresponding measured values but this scatter is considered to be within acceptable limits. Overall, the refined modelling approach provides a reasonable basis for estimation of Non-Coarse Particle loads for the road surface. The model accounts for wet weather contributions due to traffic based on a simple interburst period (IBT) and if substituted with a traffic variable (such as VDS or VIDS) the model may provide more accurate load predictions.

The spreadsheet calculations for the roof, carpark and road surfaces over the full monitoring period from December 2004 to January 2006 are tabulated in **Appendix B**.

9.6.4 Discussion on Parameter Selection for Refined Particle Mass Balance Model

The refinements to the particle Mass Balance Model have introduced several parameters to account for wet weather accumulation effects and particle loss in the lateral drain during dry weather. In predictive modelling, there is a risk of developing a model that is over parameterised. This may lead to greater uncertainty in the selection of appropriate parameter values and hence introduce significant errors when the model is applied outside of its calibration range. Thus, model complexity needs to be balanced and ‘parsimonious’ models (i.e. having the least number of model parameters to describe key processes based on available data) are considered to be desirable (Willems 2005). It is considered that the refined model structure is broadly consistent with a ‘parsimonious’ conceptual model of particle accumulation and washoff processes.

The calibrated parameters are consistent with the known characteristics of each surface. For example, the maximum free and detained particles loads (Max_{FP} and Max_{DP}) for the road is expected to be higher than the carpark loads due to the rough texture, poorer condition and flatter grade of the road surface. For the same reasons, the rain power required to mobilise the detained particles (RP_{DPcr}) is also expected to be higher for the road surface.

The washoff efficiency curves for free particles (WE_{FP}) are also consistent with surface characteristics. High washoff efficiencies (>80%) have been assigned to the steep, smooth roof surface and lower efficiencies (30% minimum) apply to the rough textured road surface. Conversely, the transport efficiency curves (TE_{drain}) of the roof gutter reflects a higher rate of particle retention compared to the road kerb. This is due to the flatly graded nature of the roof gutter and a high potential for water ponding during low intensity rainfalls.

The free particle accumulation rates (AR_{FPdry} and AR_{FPwet}) for the trafficable carpark and road surfaces indicate a quick recovery after washoff to maximum loads within a few hours. The accumulation rate for the roof is based on atmospheric dust fall which, except for abnormal conditions, is a slower, more ambient process. The accumulation rates for detained particles (AR_{DPdry}) appear to be lower than anticipated. The road values were based on a single sequence of a high intensity storm closely followed by another storm with sufficient rain power to mobilise detained particles. For the majority of storms, the adopted accumulation rate resulted in the full recovery of the detained particle load prior to the event.

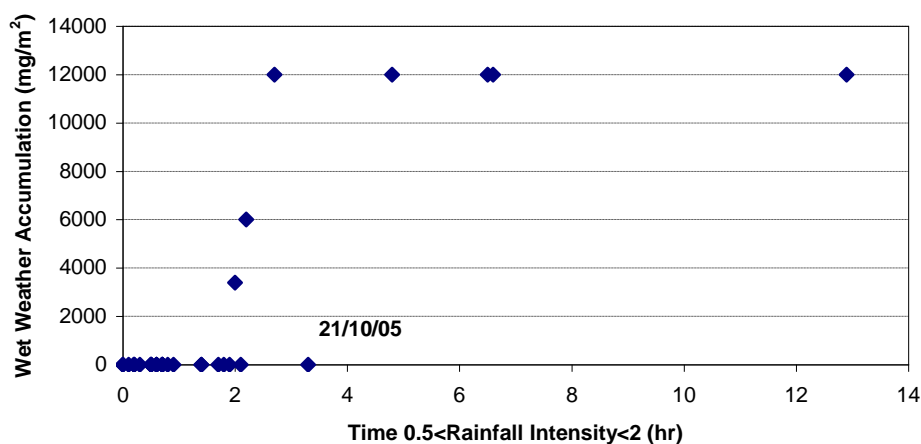
A key modelling assumption is that no significant wet weather accumulation of free particles occurs on the trafficable surfaces during storms shorter than 5 hours duration. This assumption is graphically shown in the **Chapter 8** scatter plots (**Figures 8.15 to 8.17**) which indicate that the loads for storms longer than 5 hours were atypically higher than other monitored events. As a result of this observed trend in the measured data, an allowance for wet weather accumulation was made for storms longer than 5 hours only.

This aspect was further investigated with all storms during the full monitoring period from December 2004 to January 2006. A determination was made of the time period that minor rainfall, or drizzle, occurred throughout each storm. A drizzle period is arbitrarily defined as corresponding to rainfall intensities that fall in the range of 0.5 to 2mm/hr and is assumed to provide conditions conducive to particle accumulation on the surface, particularly for the road.

For storms shorter than 5 hours duration, the drizzle period was found to be consistently less than 2 hours long. For storms exceeding 5 hours, the drizzle period

exceeded 2 hours. These outcomes are illustrated in **Figure 9.13** which shows the wet weather particle load used in the refined model analysis and the corresponding drizzle time based on the measured rainfall pattern.

It is clear that a two hour drizzle time marks a threshold above which wet weather accumulation is rapidly initiated. An exception is the 21/10/2005 storm as no wet weather buildup was assumed in the analysis as the dry period (DP) for this event exceeded 6 hours. The physical basis of this interpretation of results is not clear and warrants further research.



- **Figure 9.13** Plot of wet weather fine particle load (mg/m^2) on road surface used in refined mass balance analysis against the duration that rainfall intensity is within the range of 0.5 to 2mm/hr for December 2004 to January 2006 storm data

In summary, a 'parsimonious' model of Non-Coarse Particle loads in stormwater runoff from impervious surfaces has been developed in this Chapter. The model started with rainfall energy principles identified from the Rainfall Detachment Index (RDI) and was progressively refined to allow for surface particle accumulation during wet weather and also the effect of very small storm events. An assessment of the accuracy of the refined Mass Balance Model compared with the regression based methods developed in Chapter 8 is described in Chapter 10.

10 Development of Planning Tools Based on Urban Surfaces

10.1 Planning to Achieve Water Quality Outcomes

Past management of urban stormwater has mainly focussed on the control of drainage and flooding impacts due to increased runoff. More recently, attention has been given to the issue of stormwater quality as part of the planning of new development within urban areas. Although point-sources of pollution such as wastewater discharges have been largely eliminated, it is recognised that non-point sources including urban runoff may also need to be reduced in order to meet desired water quality outcomes. In response, regulatory authorities have introduced requirements to reduce stormwater pollution discharged from new urban developments. Selected examples of these planning approaches taken from US and Australian practice are described in **Table 10.1**.

A common theme of the selected planning approaches is the estimation of concentrations or loads which then form the basis of setting requirements for stormwater treatment or reduction. This Chapter will explore various predictive methods that could be used as planning tools to assess the management of urban stormwater quality.

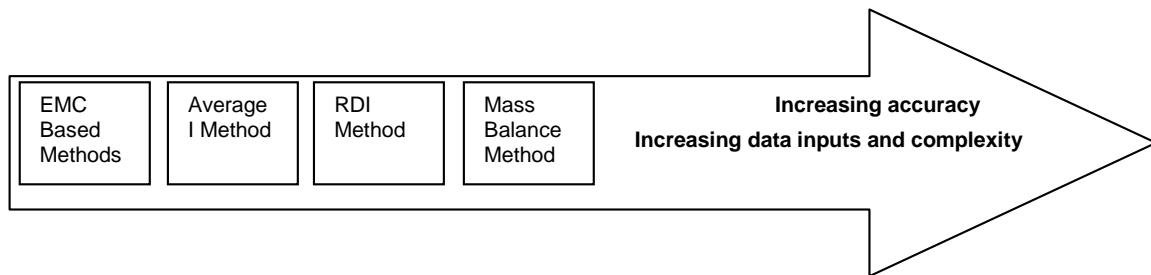
10.2 Stormwater Particle Load Estimation Methods for Impervious Surfaces

The relationships between Non-Coarse Particle load and various rainfall characteristics including average rainfall intensity and RDI provide methods to estimate stormwater particle loads for impervious surfaces. The mass balance approach based on the concept model of particle buildup and washoff processes also gives a predictive method. The three methods, referred to as the Average I, RDI and Mass Balance Methods are indicated on **Figure 10.1** in terms of increasing levels of data requirements, complexity and subsequent accuracy of results.

■ **Table 10.1 Selected examples of planning approaches to manage stormwater pollutant loads**

Description
<p>US EPA Total Maximum Daily Loads (TMDL)</p> <p>Under the framework of the National Pollutant Discharge Elimination System (NPDES), if US waterbodies are deemed to be impaired due to an increase in certain pollutants then a TMDL order can be placed to prevent further water quality degradation. The TMDL is specific to each critical pollutant type and is based on determination of the 'loading capacity' of the waterbody to receive pollution without violating water quality standards. The TMDL process accounts for existing sources and applies a margin of safety in identifying limits to future loads. Description of the TMDL process and tools for analysis are provided by the US EPA (Shoemaker <i>et al.</i> 1997)</p>
<p>Maine Department of Environmental Protection</p> <p>To control TSS pollution of downstream waterways, the Maine DEP has proposed that new urban developments be subject to meeting a sliding scale of requirements for stormwater treatment. Treatment requirements, expressed as a percentage removal of the annual TSS load, vary from Level A (60-70% removal) to Level C (85-100% removal). The treatment level is assigned to the development depending on the type and state of the downstream waterbody. (DEP 2003)</p>
<p>Australian Runoff Quality Guidelines</p> <p>The draft Australian guidelines for stormwater management (IEAust 2003) recommends that a 'sustainable average annual export load' (SAAEL) for a waterbody be used as a basis to control pollutant impacts. The SAAEL matches the water quality 'trigger level' that is referenced to a desired condition or water use. The trigger level may be based on a pollutant concentration, generally a median value. It is suggested that long-term daily timestep modelling be used to statistically derive an appropriate SAAEL.</p>
<p>Water Sensitive Planning for the Sydney Region</p> <p>Planning guidelines for new development in Sydney have set performance standards for stormwater treatment (Planning Plus 2003a). These targets may be established locally by Councils and, if absent, a minimum reduction in the expected annual pollutant load is required. Requirements are specific to the pollutant type and range from 70% reduction in litter to a 45% nutrient reduction. The targets have been benchmarked at what is considered to be a cost-effective level of treatment.</p>

Simpler methods that utilise measured EMC values to estimate loads (referred to as EMC Based Methods) will also be considered. These simple approaches include the Arithmetic Mean EMC, Logarithmic Mean EMC and Stochastic EMC Methods that are currently widely used in engineering practice. Two additional EMC based methods (Rainfall Depth Adjusted EMC and Rainfall Intensity Adjusted EMC Methods) are proposed in this Chapter.



- **Figure 10.1 Relative position of stormwater pollutant estimation methods on a scale of increasing accuracy, data inputs and complexity**

The data requirements for the eight methods are compiled in **Table 10.2**. The various methods were used to derive Non-Coarse Particle concentrations and loads for storms during the full monitoring period from December 2004 to January 2006 and the predictions were compared with measured data. As the intent was to compare the accuracy of each method, the analysis was performed for a single urban surface and the Toowoomba road surface was selected for this purpose.

- **Table 10.2 Data requirements of Non-Coarse Particle load estimation methods**

Method	Input Data ¹
Arithmetic Mean EMC ²	Selected mean EMC
Logarithmic Mean EMC ²	Selected mean EMC
Stochastic Mean EMC ²	Selected mean EMC and standard deviation
Rainfall Depth Adjusted EMC	Selected mean EMC values across expected rainfall range, Rainfall depth P
Rainfall Intensity Adjusted EMC	Rainfall depth P, Storm duration D, Average rainfall intensity I
Average I	Rainfall depth P, Storm duration D, Average rainfall intensity I
RDI	Rainfall depth P, Peak I ₆ , Storm duration D, Rain power $\sum I_6^2/D$
Mass Balance	Refer Section 9.5.4 for details

Notes:

1. All methods require catchment area A and runoff depth R to estimate loads
2. These methods are currently in common use

10.3 Current EMC Based Methods for Particle Load Estimation

10.3.1 Arithmetic and Logarithmic Mean EMC Methods

EMC provides a basis to estimate particle loads and several different approaches can be taken in the estimation process. The Mean EMC Method is the simplest method used in current engineering practice (e.g. used as an optional method in MUSIC) and determines load as the product of EMC and the volume of stormwater runoff for each storm. A constant EMC that is specific to an urban land use or surface type is often used and a mean or median EMC based on data pooled from several or more storms is often directly applied. As a constant EMC value is used, the approach assumes there is no variability in EMC between storms.

An arithmetic mean value or, alternatively, a mean based on the logarithmic EMC is generally used in the analysis. The means based on monitoring data for the Toowoomba surfaces are provided in **Table 10.3** and show that the arithmetic means are significantly higher than the logarithmic means. The mean of log-EMC values may be a better measure of central tendency as previous studies have found that TSS concentrations often follow a log-normal distribution (as discussed in Section 2.3.1). Use of both types of means was evaluated in the error analysis for comparative reasons.

Application of all of the EMC based methods involves multiplying the selected EMC by the runoff stormwater volume to determine the particle load. Stormwater runoff volume can be derived based on catchment area *A*, runoff coefficient *C* and rainfall depth *P*.

- **Table 10.3 Mean Non-Coarse Particle EMCs for December 2004 to January 2006 runoff events. Standard deviations are also provided**

Surface	Arithmetic Mean EMC (mg/L)	Mean Logarithmic EMC (mg/L)
Roof ¹	10.8±7.7	8.1±3.5
Carpark	64±75	39±15
Road	229±150	190±101
Bare	736±486	555±207
Grass	40	-

Note:

1. Roof EMC for 3/2/2005 and 14/10/2005 storms were excluded from statistics due to abnormally high dustfall

10.3.2 Stochastic EMC Method

The stochastic generation of EMC is employed in engineering practice to estimate particle loads. It is an optional feature of stormwater models such as AQUALM and MUSIC. The method has its basis on TSS concentrations for urban surfaces following a log-normal distribution. Given a mean and standard deviation of a known log-EMC dataset as provided in **Table 10.3**, a stochastic set of EMC values can be generated using standard statistical methods. A common technique is to randomly select a log-EMC value within the range of ± 1 standard deviation from the mean. An EMC is calculated from the random selection and used to derive the particle load for an individual storm. The process is repeated for each storm in the sequence of events under analysis.

The stochastic approach aims to replicate the statistical variability that is present in the measured concentration data used to derive the adopted mean and standard deviation. It ignores any trends that may be present in the measured data, such as a decrease in EMC as rainfall increases. Despite this limitation, the Stochastic EMC Method is widely used to estimate stormwater pollutant loads.

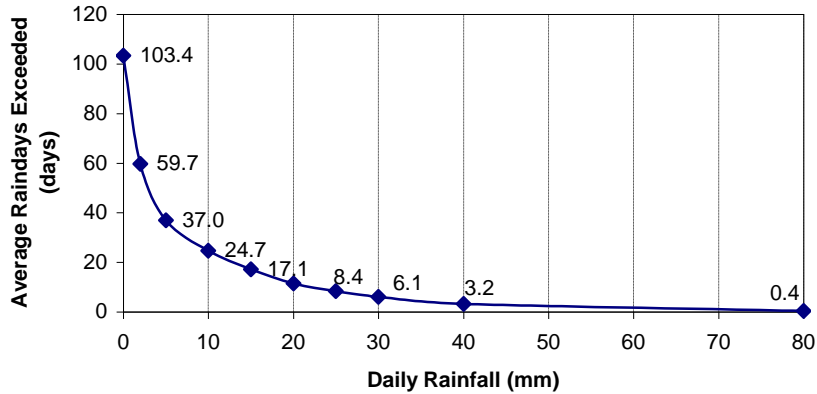
10.4 Proposed Methods for Particle Load Estimation

10.4.1 Rainfall Depth Adjusted EMC Method

The Rainfall Depth Adjusted EMC Method is proposed in this thesis as a variation to the commonly used Mean EMC Methods. The basis of the method is to account for an apparent negative correlation between EMC and rainfall depth for the impervious roof, carpark and road surfaces. This trend is briefly discussed in **Chapter 6** and is attributed to dilution of the washoff load at high rainfalls.

To facilitate adjusting EMC to rainfall, a rainfall exceedence curve was produced for Toowoomba based on daily data recorded for the period 1980 to 2004 at the local airport weather station. This station is located 3 km west of the stormwater monitoring sites. The exceedence curve is presented in **Figure 10.2**.

The exceedence curve indicates that, on average, rain occurs over a total of 103 days throughout the calendar year with only a few occasions (~3 days) when rainfall exceeds 40mm. Rainfall is greater than 10mm on approximately 25% of raindays.



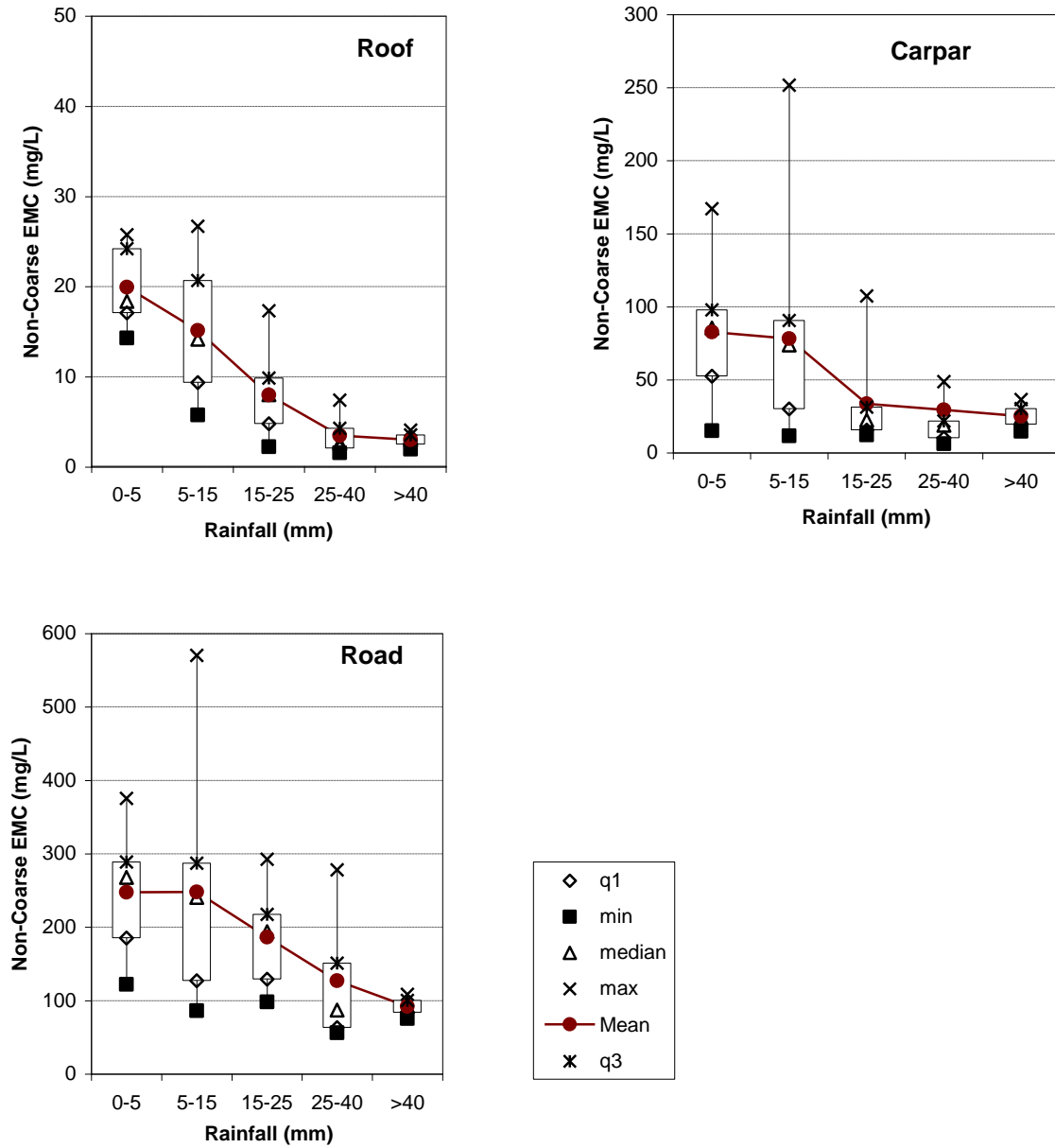
- **Figure 10.2 Daily rainfall frequency curve for Toowoomba based on 1980 to 2004 data**

Based on the shape of the rainfall exceedence curve, daily rainfall was divided into a small number of discrete ranges and an EMC value was assigned to each individual range. The ranges incorporated 0-5mm, 5-15mm, 15-25mm, 25-40mm and >40mm total daily rainfalls. These ranges were selected on the basis that the cumulative sum of the rainfall within each range (i.e., the area under the exceedence curve for each range segment) is approximately equal.

EMC box plots, similar to those presented in **Section 7.3**, were generated for each rainfall range based on measured concentration data for December 2004 to June 2005 storms. The box plots were produced for the impervious roof, carpark and road surfaces and are presented as **Figure 10.3**.

A distinct trend of decreasing EMC with increasing daily rainfall is evident for all three impervious surfaces. The deviation of data around the mean is large, especially for small to moderate storms (less than 15 to 20mm rainfall). The number of measured events within each rainfall range varies from 2 to 10 storms.

The arithmetic mean EMCs for each land use and rainfall range were extracted from the box plots and are compiled in **Table 10.4**. The Rainfall Depth Adjusted EMC Method is simply based on determining the appropriate rainfall range for a particular storm and assigning the corresponding mean EMC value to that event. In this way, the EMC is adjusted to account for rainfall depth and provides a more realistic basis compared to applying a constant EMC across all storm events.



■ Figure 10.3 Box plots of Non-Coarse Particle EMCs in various rainfall ranges for impervious surfaces for December 2004 to June 2005 runoff events. Note q1=first quartile value (25%), min = minimum value, max = maximum value and q3 = third quartile value (75%).

- **Table 10.4 Arithmetic Mean Non-Coarse Particle EMCs for impervious surfaces based on discrete rainfall ranges for December 2004 to January 2006 runoff events. Standard deviations are also provided.**

Rainfall Range	Roof EMC (mg/L) ¹	Carpark EMC (mg/L)	Road EMC (mg/L)
0-5mm	20±4.9	83±53	248±92
5-15mm	15.2±7.1	78±69	248±147
15-25mm	8.0±4.6	34±33	186±66
25-40mm	3.5±2.2	29±17	127±103
>40mm	3.0±1.5	25±11	92±23

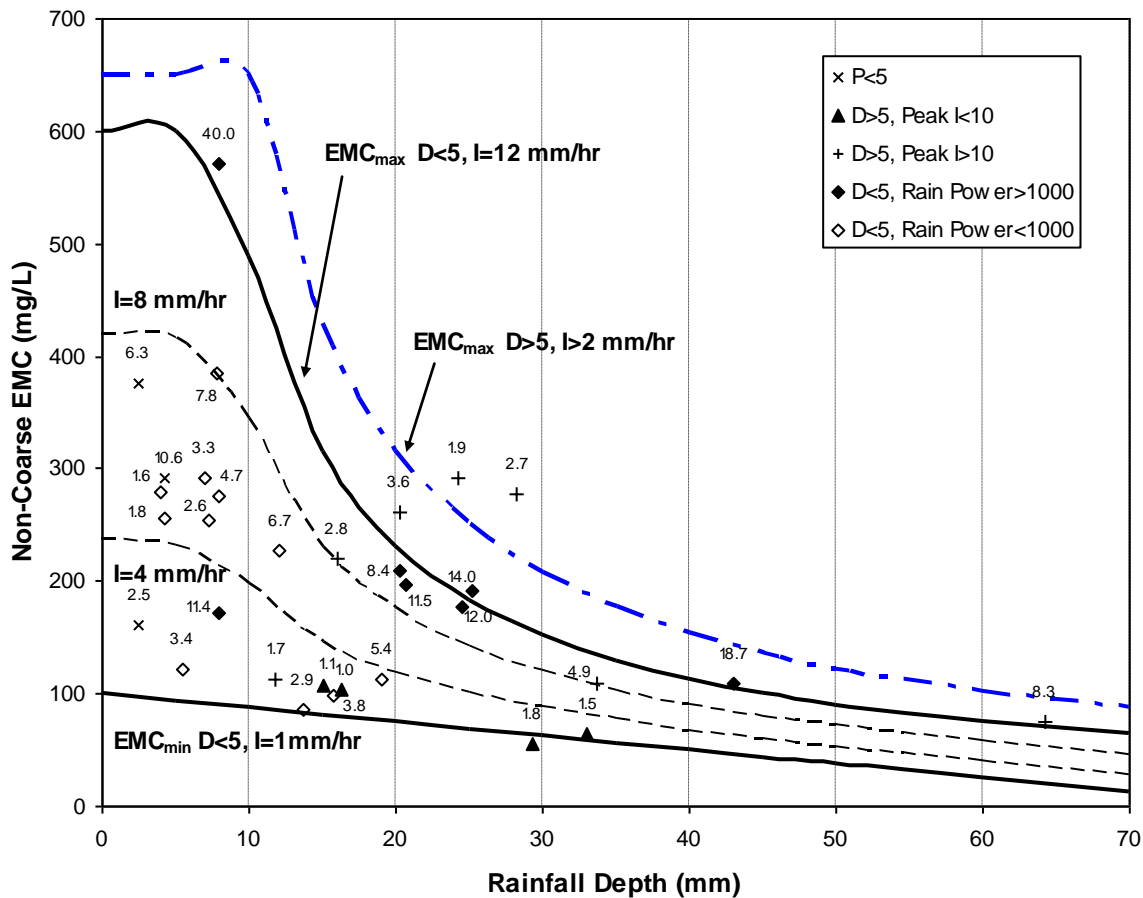
Note: 1. Roof EMC for 3/2/2005 and 14/10/2005 storms were excluded from statistics due to abnormally high dustfall

10.4.2 Rainfall Intensity Adjusted EMC Method

As evident in the scatter plots shown in **Figure 6.11**, increased rainfall generally moderates EMC but this dilution effect only partly explains the variance in EMC. The EMC variation around the mean is relatively large, particularly within the 5 to 15mm rainfall range. Rain power and peak rainfall intensity are major factors that influence particle washoff and hence EMC variability between storms. The Rainfall Intensity Adjusted EMC Method is proposed to accommodate these factors related to rainfall intensity in the EMC estimation.

The basis of the method is shown on the rainfall depth-EMC plot for the road surface in **Figure 10.4**. Data points for individual storms during the full monitoring period from December 2004 to January 2006 are plotted. The wide variation in EMC is clearly shown; especially for rainfalls less than 20mm. The average rainfall intensity I for each event is labelled.

The data points are also presented in groups depending on storm duration and rainfall intensity characteristics, as reproduced from the scatter plots presented in **Figure 8.15**. The method is founded on EMC contours that fit, as far as practical, to the graphical spread of data. The contours are based on average rainfall intensity and take into account the washoff characteristics of the road surface.



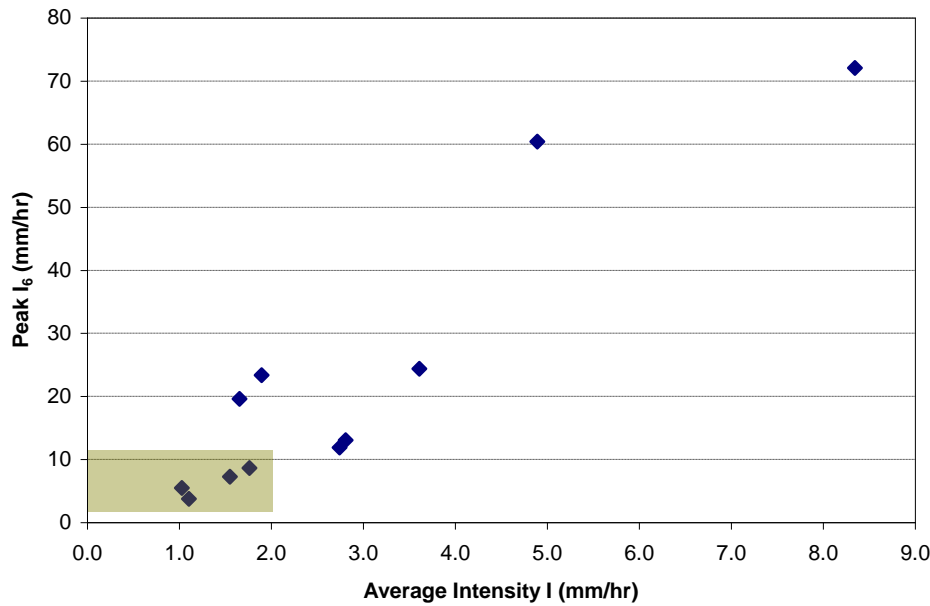
- Figure 10.4 Plot of road Non-Coarse EMCs against Rainfall Depth with interpolated contours based on average rainfall intensity. Measured average rainfall intensities are labelled on the data points

A maximum EMC contour for moderate duration storms (less than 5 hours) is shown labelled 'EMC_{max} D<5, I=12 mm/hr'. This contour corresponds to the washoff of the maximum available washoff load (or L_0 equal to 4400 mg/m^2) and as indicated previously in **Figure 8.18**, this complete washoff occurs for storm intensities that exceed 12 mm/hr. The maximum EMC contour was derived by dividing the load L_0 by the runoff depth. The runoff depth was calculated by deducting an initial loss equal to 1mm from the total rainfall, consistent with the DRAINS analysis of the road surface (as discussed in **Section 7.2**). This contour line corresponds to storm durations less than 5 hours, during which traffic-related wet weather accumulation of particles on the road is not significant.

The minimum EMC contour labelled ‘ $EMC_{\min} D < 5, I = 1 \text{ mm/hr}$ ’ corresponds to the low concentration band measured for the road surface which is of the order of 100 mg/L. The EMC minima values that were measured appear to be inversely related to rainfall depth. This trend was accounted for by sloping the EMC contour line so it passes through the measured data points. An intensity of 1 mm/hr was assigned to this contour as it corresponds to the minimum rainfall intensity that was recorded. The ‘ $EMC_{\max} D < 5, I = 12 \text{ mm/hr}$ ’ and ‘ $EMC_{\min} I = 1 \text{ mm/hr}$ ’ contours represent the upper and lower boundaries of measured EMCs for storm durations less than 5 hours. Intermediate contours corresponding to average rainfall intensities of 4 and 8 mm/hr were generated by linear interpolation between the upper and lower limits.

The derived contours provide a reasonable representation of the measured EMCs for storms less than 5 hours duration. High rain power events (corresponding to $\sum I_6^2/D$ greater than $1000 \text{ mm}^2/\text{hr}^3$) leading to full particle washoff are plotted as \blacklozenge and closely follow the maximum EMC contour. Events with less intensity (plotted as \blacklozenge) are distributed between the maximum and minimum limits and although there are discrepancies, there is some consistency between the measured data and the intermediate contours.

Wet weather particle accumulation during storms longer than 5 hours is also accounted for in the proposed Rainfall Intensity Adjusted EMC Method. Storms with low peak I_6 less than 10 mm/hr have EMC values close to the minimum EMC contour (plotted as \blacktriangle). As can be seen from **Figure 10.5**, a positive correlation is evident between Peak I_6 and average rainfall intensity I (Peak $I_6 = 9.8I - 5.1$, $R^2 = 0.856$). Storm data points with Peak I_6 less than 10 mm/hr are shaded and correspond to average rainfall intensities of less than approximately 2 mm/hr. It is postulated that even though wet weather particle accumulation occurred during these events, the low Peak I_6 resulted in high particle retention within the drain, leading to low EMCs. This effect is consistent with the transport efficiency curve determined for the road drain shown previously in **Figure 9.11**. Based on this outcome, no correction was made for storms longer than 5 hours with average rainfall intensity less than 2 mm/hr (i.e. the contours for the duration less than 5 hours are applicable to these events).



- **Figure 10.5 Plot of Peak I₆ against Average Intensity I for December 2004 to January 2006 storms longer than 5 hours duration. Storms with Peak I₆ less than 10mm/hr are shaded**

Storms with Peak I₆ exceeding 10 mm/hr are not limited by low transport efficiencies within the drain and yield higher EMCs compared to low Peak I₆ storms. As shown in **Figure 10.5**, the majority of these storms have an average rainfall intensity above 2mm/hr. Considerable scatter in these points (plotted as + in **Figure 10.4**) is present, including a cluster of points located above the maximum EMC contour derived for the shorter duration storms less than 5 hours. To account for this type of event (Duration D>5 hours, I>2 mm/hr), it was decided to fit by trial and error an EMC contour through the data cluster and this is referred to as the ‘EMC_{max} D>5, I>2mm/hr’ line in **Figure 10.4**. This resulting contour line corresponds to a constant load of 6000 mg/m³. It is apparent that this approach is very simplistic and accounts for the elevated EMC measured for only a proportion of recorded events of this type.

In overall terms, the nominated EMC contours provide the basis of the Rainfall Intensity Adjusted EMC Method. Providing rainfall depth P, storm duration D and average rainfall intensity I are known, the contours can be used to interpolate an EMC estimate for an individual storm event.

10.4.3 Average I Method

The proposed Average I Method is based on regression analysis and uses the linear piecewise equation (**Equation 8.7**) to predict particle load directly from the average rainfall intensity I of each storm. This form of equation was selected as it produced the highest coefficient of determination (R^2) against the measured Toowoomba data. As is the case for the Mean EMC Method, this approach requires the rainfall depth P but the storm duration D is also needed to determine I . The Average I Method differs to the previously discussed methods in that the load is estimated, rather than EMC.

A particle load correction for storms longer than 5 hours was made in a fashion similar to that used in the Rainfall Intensity Adjusted EMC Method. A load equal to 6000 mg/m^2 was selected if the rainfall intensity exceeded 2 mm/hr ; otherwise the predicted load from the piecewise linear equation was used. For storms with very low rainfall (less than 3 mm), the particle load was factored by 25%. This is consistent with the correction parameter C_P used in the refined Mass Balance Model discussed in **Section 9.6.1**.

10.4.4 RDI Method

The proposed RDI Method is also based on regression and utilises the linear piecewise relationship between rainfall detachment index and particle load (**Equation 8.2**). Determination of the RDI for individual storms requires rainfall intensity data at short time increments and thus a pluviograph is necessary. Data requirements are thus more temporally detailed compared to the rainfall depth measurement used in the Average I and Mean EMC Methods. The particle load corrections for storms longer than 5 hours duration and for very low rainfalls used in the Average I Method were also applied.

10.4.5 Mass Balance Method

The most complex of the proposed methods is the Mass Balance Method which is directly based on the refined model of particle washoff and buildup processes detailed in **Section 9.5.4**. As was the case for the RDI Method, to utilise this approach requires rainfall data at short time intervals to estimate rain power and identify the peak rainfall intensity. Details on surface and lateral drainage characteristics are also required.

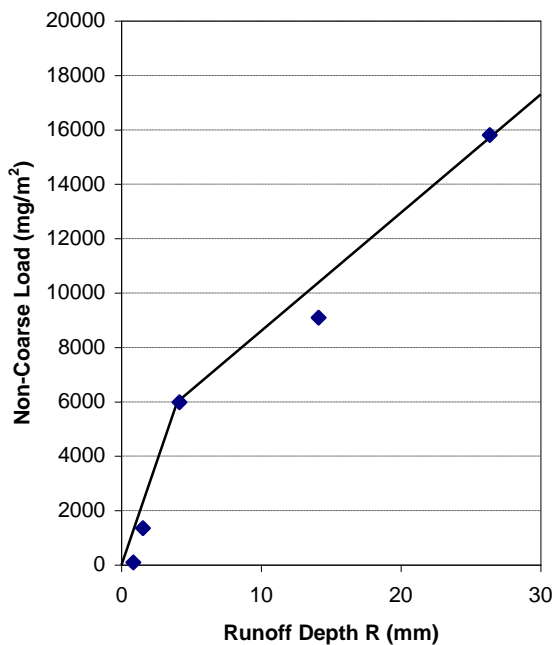
10.4.6 Particle Load Estimation Methods for Pervious Surfaces

The small available dataset of measured loads makes it difficult to identify causative factors in particle washoff from the pervious bare soil and grassed surfaces. In particular, the number of measured events for the grass surface is limited to two storms only. Given these circumstances, very simple estimation methods are applicable, such as the Mean EMC Method previously described in **Section 10.3.1**. Using this approach gives **Equation 10.1** as a basis to estimate Non-Coarse Particle loads from grassed surfaces.

$$L_{GRASS} = 40R \quad [10.1]$$

where L_{GRASS} is the Non-Coarse Particle load from the grassed surface (mg/m^2) and R is the runoff depth (mm).

Measured loads from the bare soil surface are available for five storms and as indicated in **Figure 10.6** these loads have a positive correlation to runoff depth. A regression of load based on runoff depth R thus provides a predictive basis to estimate loads and a piecewise linear regression is also presented on **Figure 10.6**.



■ **Figure 10.6 Regression line of bare soil Non-Coarse Particle load against runoff depth for December 2004 to January 2006 runoff events**

The regression relationship for bare soil load ($R^2=0.993$) is provided in **Equation 10.2**.

$$L_{BARE} = 1500R \quad : R < 4\text{mm} \quad [10.2]$$

$$L_{BARE} = 6000 + 435(R - 4) \quad : R \geq 4\text{mm}$$

where L_{BARE} is the Non-Coarse Particle load from the bare soil surface (mg/m^2) and R is the runoff depth (mm).

10.5 Error Analysis of Stormwater Particle Load Estimation Methods for Impervious Surfaces

An error analysis was conducted to compare the performance of each predictive method to estimate stormwater particle loads. Each method was applied to derive Non-Coarse Particle loads in response to storms measured during the period from December 2004 to January 2006 for the Toowoomba road surface. A total of eight different methods were included in the comparative analysis. Five methods based on particle concentration were applied, namely the Arithmetic Mean EMC, the Logarithmic Mean EMC, the Stochastic EMC, the Rainfall Depth Adjusted EMC and the Rainfall Intensity Adjusted EMC techniques. The remaining three methods (Average I, RDI and Mass Balance) are based on the direct determination of particle loads.

To graphically compare the estimation procedures on an equal basis, scatter plots of predicted EMCs against measured EMCs were prepared. The plots for the five different Mean EMC methods are presented in **Figure 10.7** and the results for the load-based Average I, RDI and Mass Balance approaches are included as **Figure 10.8**. Concentration values for the load-based methods were determined by dividing the predicted load by the runoff volume for each storm. The plots show that as the complexity and data requirements of the modelling approach increases, this generally translates into a better agreement between measured and predicted EMC values, in line with the progressive scale shown in **Figure 10.1**.

The gross simplification of assuming a constant EMC, either an arithmetic or logarithmic mean, independent of rainfall depth clearly results in a poor ability to

predict EMCs for individual storms. A random spread of data points within an upper and lower bound is apparent in the Stochastic EMC scatter plot, consistent with the principal assumptions that underlie this method. The grouping of data into the four rainfall ranges adopted in the Rainfall Depth Adjusted EMC Method is also clearly seen in the scatter plot for this approach. However, any visual improvement in providing a better fit to measured data by the use of the Stochastic EMC and Rainfall Depth Adjusted EMC Methods appears to be marginal.

By comparison, the Rainfall Intensity Adjusted Method signifies a substantial gain in better matching, at least visually, the measured EMC values. The Average I, RDI and Mass Balance Methods demonstrate similar degrees of scatter.

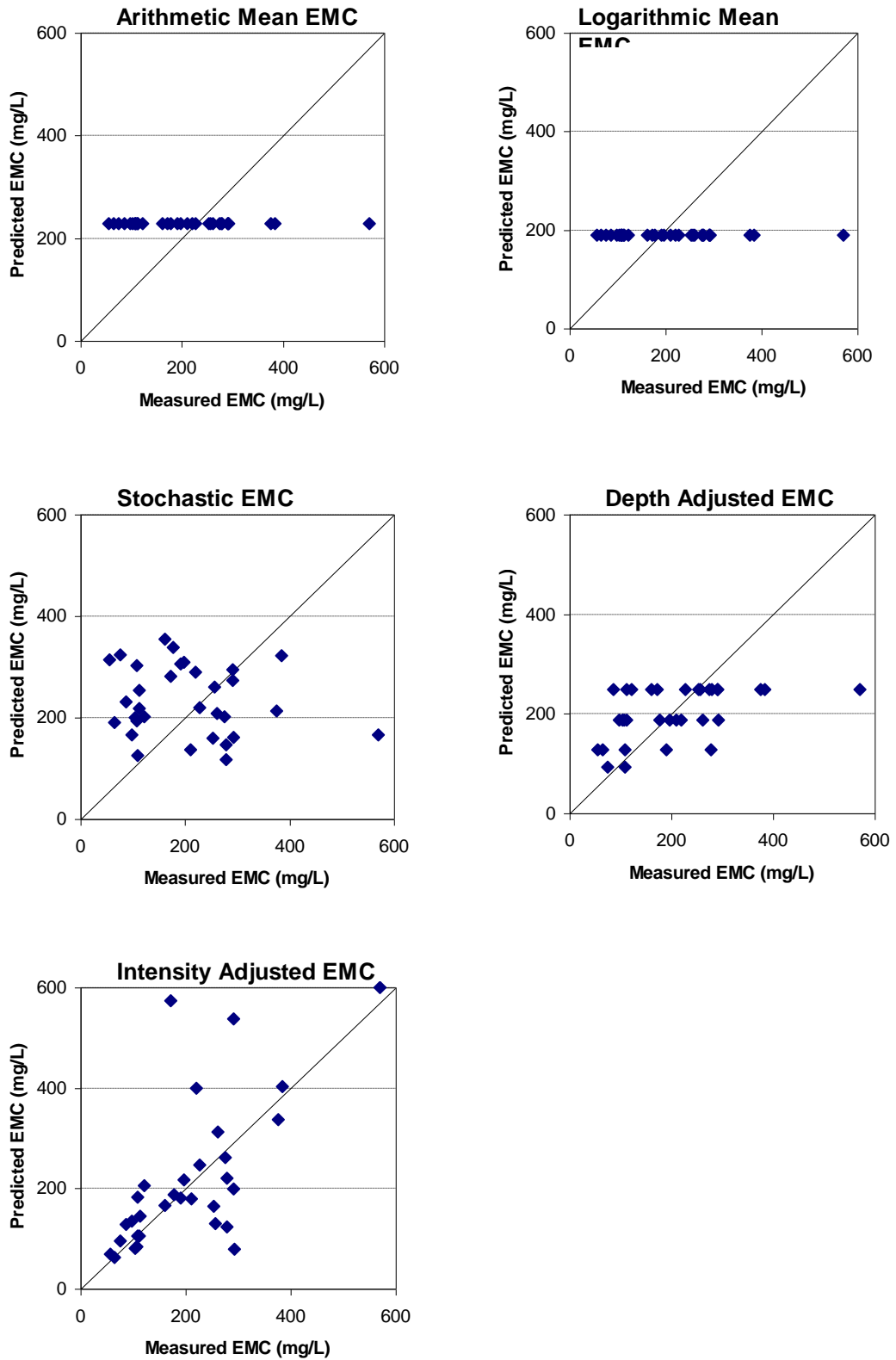
The EMC scatter plots in **Figures 10.7** and **10.8** provide only a visual guide to predictive accuracy and a further comparison between methods was done by statistical analysis. Predicted results were compared with measured loads and key error statistics were generated, including the cumulative load error and maximum load error.

The error statistics are defined in **Equations 10.3** and **10.4** and provide a basis to identify overall model performance in reproducing the total load over the full monitoring period and the measured load for individual storms, respectively

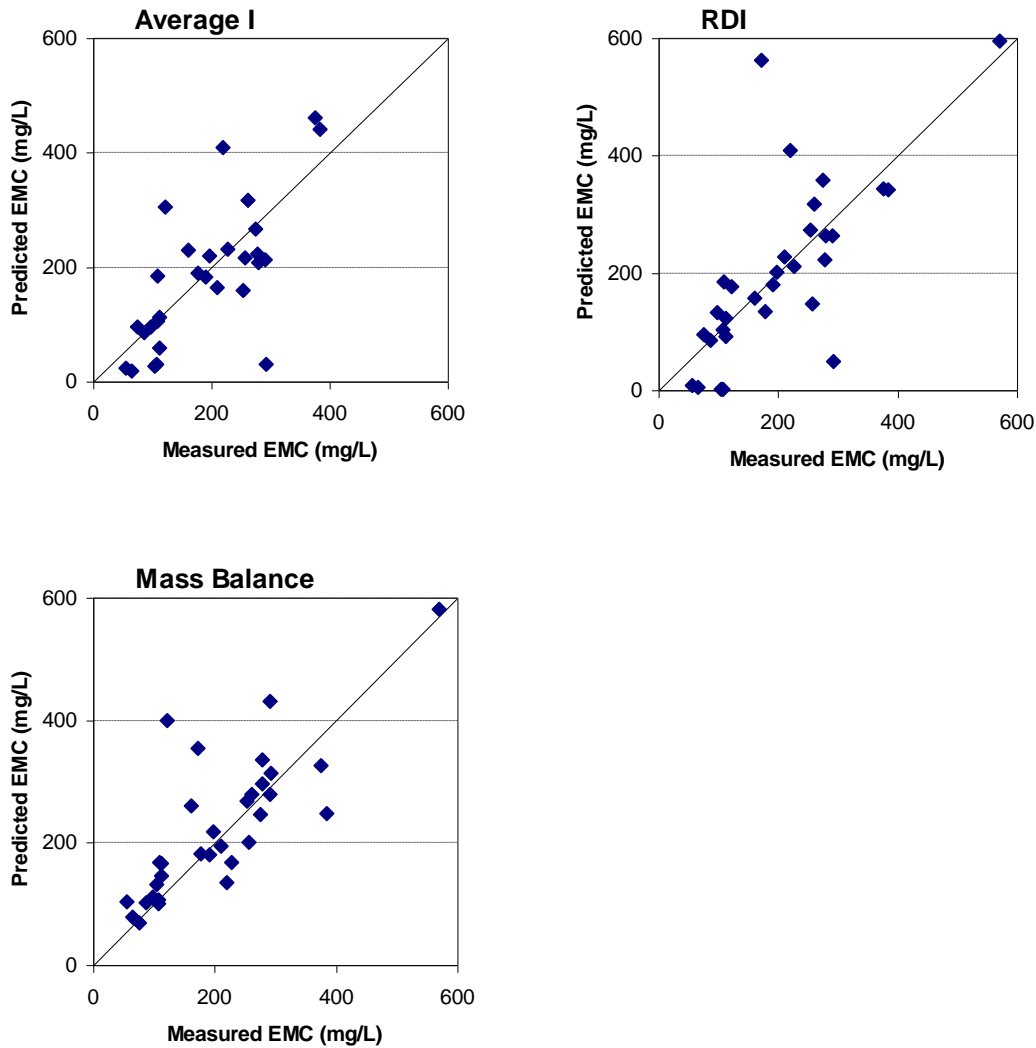
$$CLE = \frac{\sum L_P - \sum L_M}{\sum L_M} \quad [10.3]$$

$$MLE = \sqrt{\text{Max}\left(\frac{L_P - L_M}{L_M}\right)^2} \quad [10.4]$$

where *CLE* is the cumulative load error, *MLE* is the maximum load error, L_P is the predicted load and L_M is the measured load.

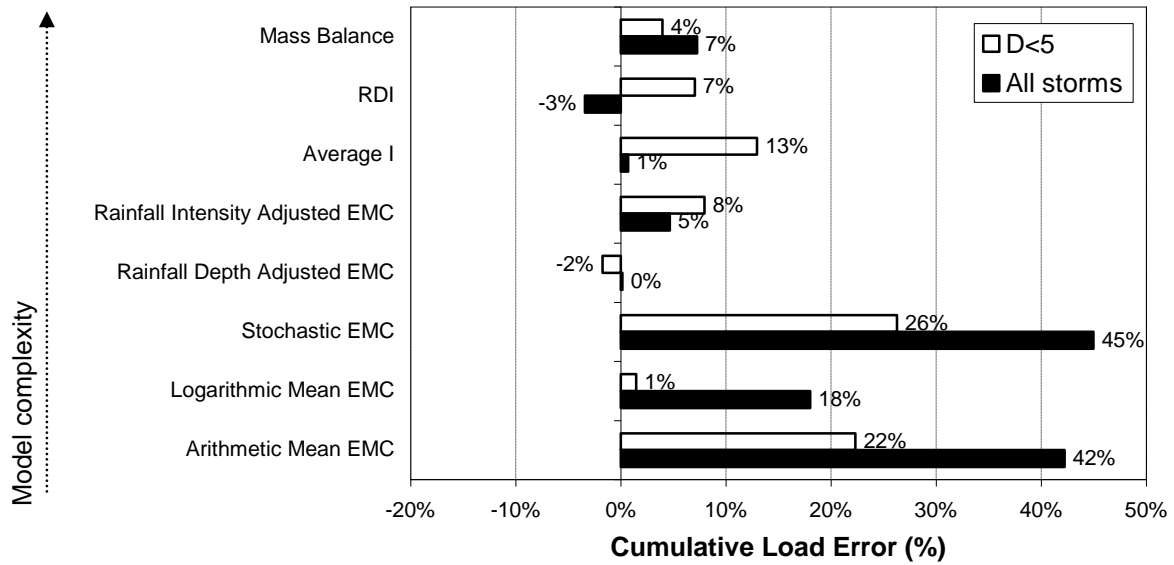


■ Figure 10.7 Plots of predicted EMC using EMC based methods and measured EMC for road surface and December 2004 to January 2006 runoff events



- **Figure 10.8 Plots of predicted EMC using Average I, RDI and Particle Mass Balance methods and measured EMC for road surface and December 2004 to January 2006 runoff events**

The cumulative load error (CLE) statistics are shown graphically as **Figure 10.9**. This plot presents the results using all storms within the December 2004 to January 2006 monitoring period and also the subset of storms that are of moderate duration ($D < 5$ hrs). Broadly, it reflects the expected trend of higher levels of accuracy being produced as the method used becomes more complex. A notable exception is the unexpected high accuracy of the Rainfall Depth Adjusted EMC Method in estimating cumulative load, even though this method is relatively simple. This good result is attributed to assigning a comparatively low concentration to runoff for large rainfall events ($>40\text{mm}$) that make significant contributions to the cumulative total.



- Figure 10.9 Cumulative Load Error (CLE) using each estimation method for road surface and December 2004 to January 2006 runoff events. CLE values are labelled as %**

The more sophisticated load-based approaches (Average I, RDI and Mass Balance) produced cumulative loads that are generally within 10% of the measured total. An exception is the 13% overestimate by the Average I Method for the cumulative load from storms with duration less than 5 hours. This is countered by the high accuracy (within 1%) of this method to predict the cumulative load of all storm events.

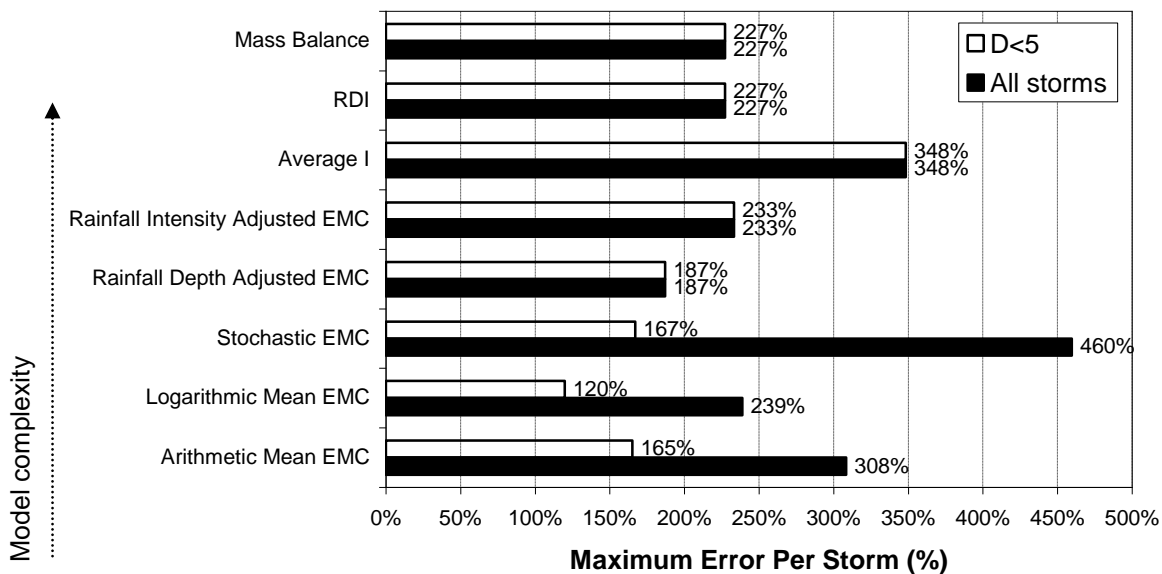
The error associated with the simpler EMC-based methods (Arithmetic Mean, Logarithmic Mean and Stochastic) in estimating the cumulative load for all storms is relatively high (in the range of 18 to 45%). These methods overestimate the total load as the trend of EMC being inversely related to rainfall is unaccounted for by these approaches. The adoption of an average EMC would tend to overestimate the runoff EMC for large storms which, depending on the number of these events in the storm sequence, can make significant contributions to the cumulative load.

On this basis, the performance of these methods is sensitive to the distribution of rainfall magnitude across the storms under analysis. The results are also very sensitive to the average EMC value as demonstrated by the difference in error between the Arithmetic and Logarithmic Mean EMC methods. The Logarithmic

Mean EMC Method uses a constant EMC that is 17% less than the Arithmetic Mean EMC value but the resulting error is reduced by up to 93%.

The predicted cumulative load from the Stochastic EMC Method poorly matched the measured load. A problem with this method is that, as it is based on a random selection of event EMCs within a statistical range, the predictions are not reproducible when the method is repeated. This lack of repeatability also applies to the error statistics. The results presented in **Figure 10.9** for this method are thus unique to the specific analysis run that was completed and a rerun of the analysis will yield very different error statistics.

The maximum load error (MLE) statistics are shown graphically as **Figure 10.10**. This plot presents the results using all storms within the December 2004 to January 2006 monitoring period and also the subset of storms that are of moderate duration (D<5 hrs).



- **Figure 10.10 Maximum Load Error (MLE) for each estimation method for road surface and December 2004 to January 2006 runoff events. MLE values are labelled as %**

The MLE is specific to an individual storm event that had the highest error relative to the measured load. As such, all method results included some storm events that were unable to be accurately predicted, with corresponding errors ranging from 120 to 460%. The event corresponding to the MLE generally varied with the method used,

although the MLE storm for both the Logarithmic Mean EMC and Arithmetic Mean EMC Methods was the same event (17/10/2005). This was also the case for the Rainfall Intensity Adjusted EMC and RDI Methods (26/10/2005).

The MLE storm associated with the more sophisticated load-based models (Average I, RDI and Mass Balance) were minor rainfall events less than 8mm. By comparison, the MLE storms for the simple EMC-based methods (Arithmetic Mean, Logarithmic Mean and Stochastic) were of higher rainfalls in the range of 30 to 65mm.

The MLE chart in **Figure 10.10** uses the maximum error produced for a single storm to make a comparison between the different methods. A more comprehensive approach is to determine the percentage of storms events that each method predicts within a specific error (e.g. within 25%). This proportion of events was determined for a range of specific errors from 10% to 100% and the resulting error curve for each method is graphically presented as **Figure 10.11**. Broadly, the error curves mirrors the expected trend of higher levels of accuracy being produced as the method used becomes more complex

The Mass Balance Method is the most accurate method as its error curve is closest to the ideal 100 % 'Proportion of Storms within Error' asymptote. Approximately 38% of the Mass Balance load estimates were within 10% error and 63% were within 25% error. The error curve for the RDI Method was slightly less accurate than the Mass Balance Method and this is consistent with the relative complexity of these approaches. On the same basis, the Average I Method error curve is slightly less accurate than the RDI Method curve. Of interest is the error curve for the Rainfall Intensity Adjusted EMC Method which has errors close to the Mass Balance Method, even though it is a much simpler approach.

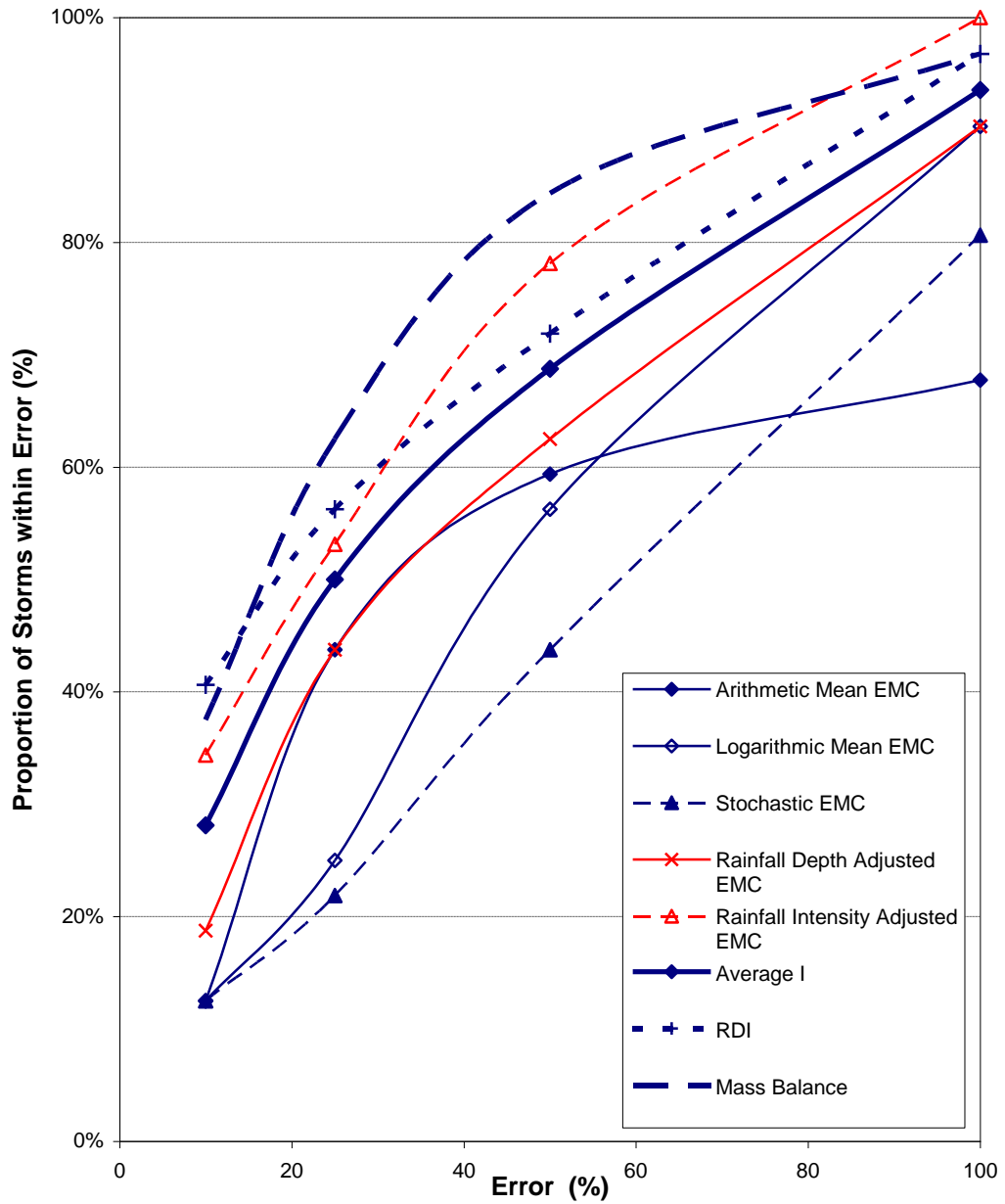
The error curves associated with the simple approaches that are currently used in practice (Arithmetic Mean, Logarithmic Mean and Stochastic Mean) demonstrate a much lower level of accuracy compared to the other methods. The Rainfall Depth Adjusted EMC Method has an intermediate level of accuracy given the midway position of its error curve relative to the other curves.

In summary, the comparative error analysis of the eight different techniques indicates a general trend of higher accuracy with increased complexity within the

methodology used. The Mass Balance Method error curve demonstrates the greatest accuracy but has the highest level of data input requirements. A much simpler approach, the Rainfall Intensity Adjusted EMC Method, gives results of comparable accuracy. This method may be preferred if available data is limiting.

The error curves also highlight the poor performance of simple approaches that are presently in common usage. These methods include the Arithmetic Mean, Logarithmic Mean and Stochastic EMC Methods. The ability of these methods to produce consistently reliable load estimates is questionable.

*In situations that require an estimate of cumulative load (e.g. an annual load), the more sophisticated models are expected to outperform the simpler EMC-based methods in terms of accuracy. As demonstrated by the CLE results presented in **Figure 10.9**, this is generally confirmed by the comparative analysis. However, the relatively simplistic Rainfall Depth Adjusted EMC Method gave a highly accurate estimate of cumulative load which suggests that this approach may be a useful tool in annual load estimation. The Arithmetic Mean, Logarithmic Mean and Stochastic EMC Methods are very sensitive to the constant EMC values that are adopted in analysis. This introduces a high level of uncertainty if these approaches are used in the prediction of cumulative loads.*



■ Figure 10.11 Error curves for each EMC and load estimation method for road surface and December 2004 to January 2006 runoff events

11 Application of Planning Tools

11.1 Approach to Application of Planning Tools

Analytical methods to predict particle concentrations and loads in runoff generated from urban surfaces are compared in **Chapter 10**. The predictive methods vary in complexity from simple Mean EMC Methods to the Mass Balance Method that uses the modelling approach detailed in **Chapter 9**. All of these methods are potentially useful tools in stormwater planning and some applications are demonstrated in this Chapter.

A number of examples and case studies are provided including 1) an assessment of the relative contribution that different urban surfaces make to the particle load in runoff; 2) an investigation into how surface-specific data can be directly transferred to represent a large-scale urban catchment located in a different climate; 3) a comparative analysis of the particle loads generated from Residential and Commercial land uses; 4) an assessment of the effect of exposed areas of bare soil on the particle loads from a Residential catchment; 5) an evaluation of the effect that widespread adoption of rainwater tanks may have on particle concentration in Residential urban runoff and 6) an assessment of the particle load reductions by the use of a grass swale to treat road runoff.

The various analyses provided in this Chapter give a comprehensive illustration of the use of surface-related data and modelling tools in stormwater management, particularly in the context of WSUD.

11.2 Relative Contribution of Urban Surfaces

An understanding of the relative amounts of Non-Coarse Particles that various types of urban surfaces contribute during storms is an important aspect of stormwater management. The identification of dominant pollutant sources within urban areas would assist in the more effective targeting of source control strategies.

Median loads provide a simplistic indication of the relative amounts of Non-Coarse Particles washed off the various surfaces. Median values and ranges are provided in **Table 11.1** for each Toowoomba surface based on December 2004 to January 2006 data. As demonstrated by the large ranges, the load generated by each surface varies

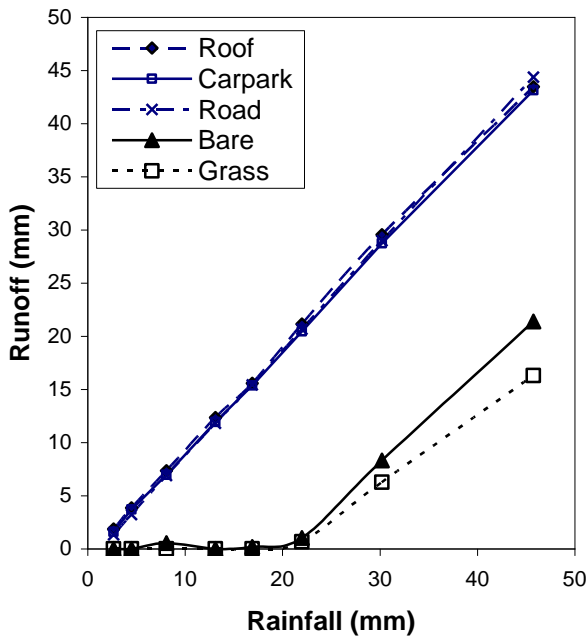
significantly for different storms. The median Non-Coarse Particle load for the carpark and grass surface is approximately five times the magnitude of the roof surface load. Road and bare surface median loads are at least an order of magnitude higher (approximately 20 times and 60 times the roof load, respectively).

- **Table 11.1 Non-Coarse Particle load statistics (mg/m²/storm) for monitored surfaces based on December 2004 to January 2006 runoff events**

Site	Measured Events	Median Load (mg/m ²)	Load Range (mg/m ²)
Roof	34	113	32-1180
Road	34	2030	160-7570
Carpark	32	490	56-2600
Grass	2	500	74-910
Bare Soil	5	5980	90-15800

Particle loads vary from storm to storm depending on a number of factors. Storm characteristics, such as rainfall depth, intensity and duration, all influence the amount of particles washed off. The absence of runoff from pervious surfaces in minor storms should also be taken into account.

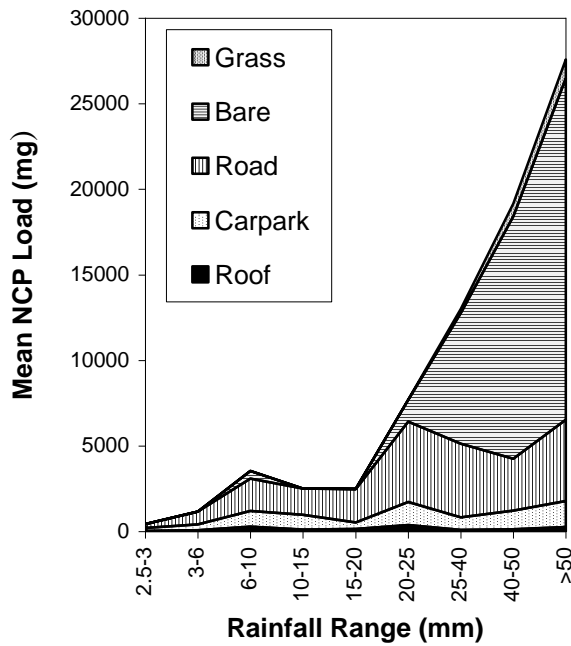
This aspect is demonstrated in **Figure 11.1** which shows the mean runoff produced by each surface for various rainfall ranges. Runoff was generated from the impervious surfaces when rainfall exceeded only 1mm depth. As infiltration is negligible, most of the rainfall on these surfaces (typically more than 95%) was converted to runoff. **Figure 11.1** also shows that about 20mm of rainfall infiltrated into the ground before runoff occurred from the grass and bare soil plots (an exception being the bare soil plot yielding minor runoff during an 8mm storm having a very high intensity of 40 mm/hr). Pervious runoff occurred during less than 20% of storms within the monitoring period.



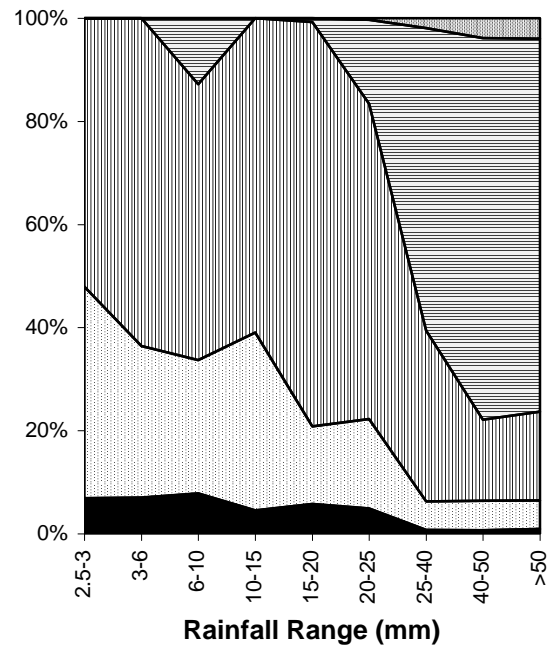
■ **Figure 11.1 Mean runoff in response to rainfall for each surface based on December 2004 to January 2006 runoff events**

Any comparison between Non-Coarse Particle loads generated from different surfaces should be made over a number of storm events. Such a comparison was made for the five surface types for a sequence of 36 storms monitored from December 2004 to January 2006. Measured Non-Coarse Particle loads were grouped according to various rainfall ranges and averaged. Missing data for impervious surfaces was filled in using the Mass Balance Model results described in **Chapter 9**. Missing data for the grass and bare soil surfaces were derived by use of **Equations 10.1** and **10.2**. The mean values are plotted as a stacked graph in **Figure 11.2** against the nominated rainfall ranges and represent the load that 1m^2 of each surface type generates, on average, for the storms that occurred during the monitoring period.

It is clear from **Figure 11.2** that, on a per square metre basis, the Non-Coarse Particle load contributed by the roof is negligible. Carpark loads are moderate and less significant compared to the road loads. The bare soil produced a high load for rainfalls exceeding 15 to 20mm and, with the road surface, was the dominant contributor to Non-Coarse Particle loadings. The grass surface contributed relatively small loads when rainfalls exceeded 25mm.



■ Figure 11.2 Mean Non-Coarse Particle load in mg against rainfall ranges. This is based on 1m² of each surface, giving 5m² area in total



■ Figure 11.3 Mean Non-Coarse Particle load as percentage of the total of the five surface loads against rainfall ranges

The relative contribution that each surface makes to overall Non-Coarse Particle load can be seen in **Figure 11.3**. In this plot, the loads are expressed as a percentage of the load totalled for all five surfaces. It demonstrates that the road surface contributes 50 to 70% of the total Non-Coarse Particle load for storms less than 15 to 20mm. This proportion diminishes in larger storms due to increasing bare soil loads.

It should be noted that the comparison is based on equal areas (in this case 1m²) of each surface type. In reality, an urban catchment would consist of unequal proportions of each surface which would change the results and this aspect is discussed further in **Section 11.3**.

As generally is the case, minor rainfalls occur in Toowoomba on a more frequent basis than larger storms. For example as previously shown in **Figure 10.2**, daily rainfalls in excess of 40mm occur on only 3 raindays, on average, throughout the year compared with 37 raindays for rainfalls less than 5mm. Due to their more

frequent occurrence, the loads associated with small storms, when totalled, may represent a sizable portion of the load generated during a year or a season. The cumulative load defined as the sum of loads for a number of storm events thus provides a useful basis to compare the various surfaces.

On this basis, the cumulative loads from each surface were calculated for the 36 storms that occurred during the monitoring period. To provide a relative context, the cumulative load for each surface is presented as a ratio of the roof load. This analysis was also done for the runoff volumes and the results are compiled as **Table 11.2**.

- **Table 11.2 Cumulative Non-Coarse Particle loads and runoff volumes from each surface for December 2004 to January 2006 storms, expressed as a ratio of the roof estimates**

Site	Cumulative Runoff	Cumulative Load
Roof ¹	1.0	1.0
Road	0.97	14.5
Carpark	0.97	4.4
Grass	0.16	0.7
Bare soil	0.22	16.1

Note:

1. For reference, cumulative runoff = 626mm and cumulative load=6300 mg/m² for the roof. Cumulative rainfall =659mm

All of the impervious surfaces produced similar runoff quantities, but the cumulative Non-Coarse Particle load from the road was approximately 14.5 times the roof load and significantly greater than the carpark load (4.4 times). The cumulative load from the bare soil (16.1 times) was similar in magnitude to the road load but was associated with significantly less runoff. The grass load was relatively minor (0.7 times). All of these loads are on a per m² basis.

Although the monitored surfaces are typical examples found in urban areas, it is anticipated that particle loads would vary within surfaces of the same general type. For example, Sartor & Boyd (1972) found that TSS load from road pavements was dependent on surface texture and condition. The surface grade of the bare soil plot is relatively flat (1%) and previous studies indicate that sediment mobilization increases significantly with slope (Musgrave 1947; Zingg 1940). On this basis, the

relative Non-Coarse Particle load contributions given in **Table 11.2** are indicative only.

It is becoming recognized that urban runoff from the more frequent storms (generally less than 15 to 20mm) is potentially a major cause of environmental impact to downstream waterways. Urban development leads to a substantial increase in the frequency of these ‘small-to-moderate’ runoff events, which in undeveloped catchments may be absent due to infiltration. The flows and pollution associated with these events can lead to a wide range of impacts, including channel erosion, reduced biodiversity, more variable water temperatures and poor water quality (Walsh *et al.* 2004).

On this basis, the Non-Coarse Particle loads generated from urban surfaces in small-to-moderate storms are of particular interest. On a per m² basis, the road surface generated the highest particle load in events less than 20mm rainfall and is thus likely to be an important contributor to adverse environmental effects. Road drainage is also generally efficient in conveying stormwater directly to waterways which increases the impact potential.

11.3 Representation of Urban Land Use Based on Surface Composition

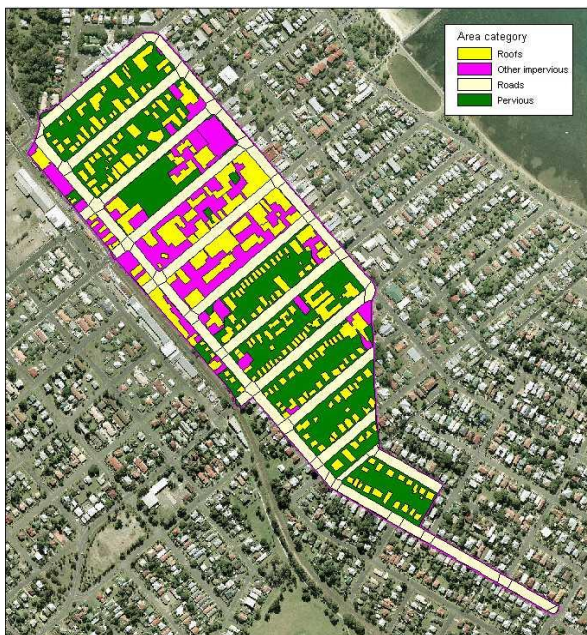
An important aspect of stormwater planning is the prediction of pollutant loads from urban land. Urban areas can encompass a wide mixture of uses including Residential, Commercial and Industrial. In terms of accuracy, the Mass Balance Model demonstrated a high performance in predicting particle loads from individual surfaces. This model was selected to analyse how component surfaces can be applied to represent various types of urban land use. As a first step, the effectiveness of the modelling approach in reproducing an independent set of measured particle loads, specifically TSS loads from an urban catchment located in Brisbane, was evaluated.

The selected urban catchment is situated in Wynnum, a bay suburb of Brisbane. Climatic conditions at Brisbane can be described as subtropical and differ significantly to the Toowoomba climate. Mean annual rainfall is 1280mm distributed, on average, over 177 raindays and high intensity storms can occur during summer months.

11.3.1 Description of Wynnum Stormwater Monitoring

Brisbane City Council has been monitoring stormwater quality from several catchments of various land use since 1994. Measurements of stormwater discharge, TSS, total nitrogen and total phosphorus have been conducted in catchments ranging in size from 10 ha to 2192 ha and incorporating a broad range of land use type including Residential, Commercial, Industrial, Rural and Bushland areas (BCC 2004). Automatic sampling methods are used in the stormwater monitoring.

A data review by Ahlman & Fletcher (2003) indicates that measurements from the Wynnum monitoring station are the most suitable of the available catchment data sets for pollutant model verification. The Wynnum data was applied to validate the stormwater load module of the process-based SEWSYS model (Ahlman & Svensson 2002) and this work included mapping the urban surfaces, as reproduced in **Figure 11.4**.



■ **Figure 11.4 Distribution of roofs, roads, other impervious and pervious surfaces in Wynnum catchment from Ahlman & Fletcher (2003)**

Land use within the 35ha Wynnum catchment has been defined by BCC (2004) as 63% Residential, 24% Commercial, 7% Industrial and 6% Recreation and Parks. Based on the surface mapping, this land use mix can be alternatively defined as consisting of 30.5% (10.67ha) road, 23.9% (8.38ha) roof, 13.4% (4.69ha) carpark and 32.2% (11.26ha) pervious, the latter assumed to be grassed. Approximately half

(51.5%) of the total roof area is galvanised iron, a third (33%) is painted roofing and the remaining area is either tile or fibro roofing.

Monitoring data is available for storms occurring during the period February 1999 to April 2003. A review of the available data indicated several limitations as listed below:

- The dataset includes conventional TSS concentrations for sampled stormwater runoff. As discussed in **Chapter 2**, many researchers have questioned the reliability of TSS in providing a measure of suspended particle concentrations in stormwater, particularly if automatic samplers are used. On this basis, direct comparisons between TSS and Non-Coarse Particle data are approximate only.
- No rainfall gauges are located within the Wynnum catchment itself and the nearest pluviometer, which closed in 2001, is located 900m from the monitoring site. The rainfall record at the pluviometer may not be fully representative of the Wynnum catchment, especially during short duration summer storms. Six-minute rainfall intensities have been recorded but have been rounded off to the nearest 10 mm/hr. This results in a relatively imprecise definition of storm characteristics, especially in the estimation of rain power based on $\sum I_6^2/D$.
- In some storm events, a limited number of samples were obtained (often as low as 1 or 2 samples). Sampling did not always cover the full runoff duration, leading to unrepresentative estimates of event mean concentration.

All of the limitations add uncertainty to the measured TSS loads and affect the comparison between Non-Coarse Particle loads predicted by the Mass Balance Model.

The mass balance analysis using the Wynnum data was conducted in two parts. Initially, runoff flow volumes for the majority of 1999 to 2003 storms were estimated and compared against measured volumes. Non-Coarse Particle loads for runoff events occurring during 1999 were estimated using the Mass Balance Model and used to predict EMCs, which were compared with the measured TSS EMC data.

11.3.2 Analysis of Stormwater Runoff Volumes for Wynnum

Stormwater discharge is measured by a submerged velocity sensor installed at the Wynnum monitoring site. Discounting storm events that were subject to equipment failure or missing data, a total of 55 events during the period 1999 to 2003 were considered suitable for analysis.

An EXCEL spreadsheet analysis was performed to predict runoff volume based on the recorded event rainfalls. In accordance to the mapped distribution of urban surfaces, the Wynnum catchment was represented as consisting of 10.67ha road, 8.38ha roof, 4.69ha carpark and 11.26ha grassed area. The runoff volume for each surface was predicted using **Equations 11.1** and **11.2** which are simple linear approximations to the mean runoff responses provided in **Figure 11.1**.

$$R = F_{IC} \times (P - 1) \text{ for impervious surfaces} \quad [11.1]$$

$$R = \text{Max}(0, 0.62 \times P - 12.3) \text{ for grassed surfaces} \quad [11.2]$$

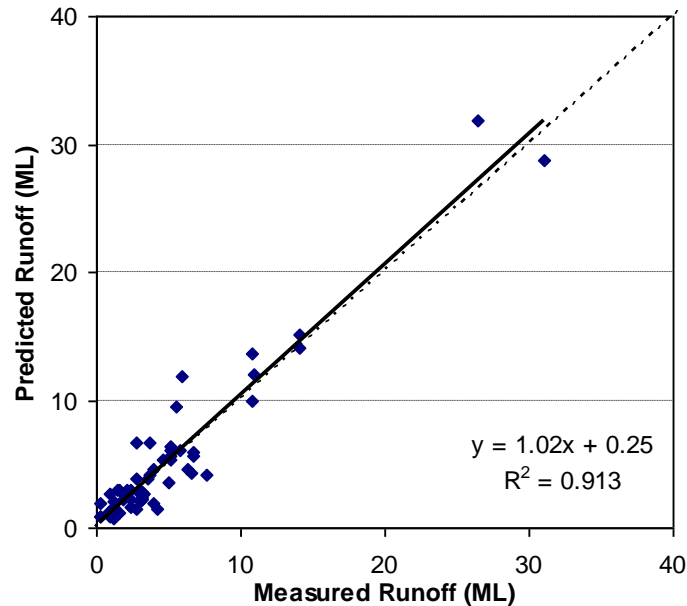
where R is the runoff depth (mm), P is the rainfall depth (mm) and F_{IC} is an adjustment factor to allow for indirectly connected impervious areas (range 0-1).

The adjustment factor F_{IC} was introduced to account for impervious areas that are not connected to the formal stormwater drainage system. As Wynnum is situated in a long established part of Brisbane, a significant proportion of residential houses have roof downpipes that are unconnected to street drainage. On this basis, a F_{IC} value equal to 0.4 was applied to the roof surface area in order to match the recorded runoff. Carpark and road surface areas were assumed to be fully connected ($F_{IC} = 1$).

Apart from the roof adjustment, the runoff characteristics determined from the Toowoomba monitoring was directly applied to the Wynnum catchment. The Wynnum soil landscape is described (BCC 2004) as predominately red earths derived from sandstones or red clay soils derived from basalt (krasnozems), which is of similar classification to the Toowoomba surface soil. Infiltration properties of the Wynnum pervious areas are expected to be similar to the Toowoomba soil conditions.

Runoff for each surface type was estimated and aggregated to predict the total runoff at the Wynnum monitoring site. This calculation was made for each of the 55

selected storms. The predicted and measured runoff depths for individual storms are plotted as **Figure 11.5**. Given the uncertainty in measured data, the simple runoff estimation methods provide a very good match ($R^2=0.913$) with recorded runoff volumes.



- **Figure 11.5 Plot of predicted and measured runoff volume at Wynnum monitoring site for 1999 to 2003 storms. Line of equal value shown as a dashed line.**

11.3.3 Analysis of Non-Coarse Particle Loads for Wynnum

An EXCEL spreadsheet analysis was conducted to predict Non-Coarse Particle loads for the Wynnum catchment for storms monitored during 1999. Sampling was not conducted, or was limited, in many runoff events and this provided a reduced dataset of 15 events for use in the analysis. For each storm, rainfall characteristics required as part of the Mass Balance Model including antecedent rainfall, antecedent dry period, storm duration, Peak I_6 and $\sum I_6^2$ were derived from pluviometer records. A number of sampled events were associated with wet weather periods in which several, intermittent storms occurred. In these cases, the individual storms were modelled separately and aggregated particle load estimates were compared with the measured TSS load. In total, 27 individual storms were incorporated in the mass balance analysis which is comparable with the dataset used in model development.

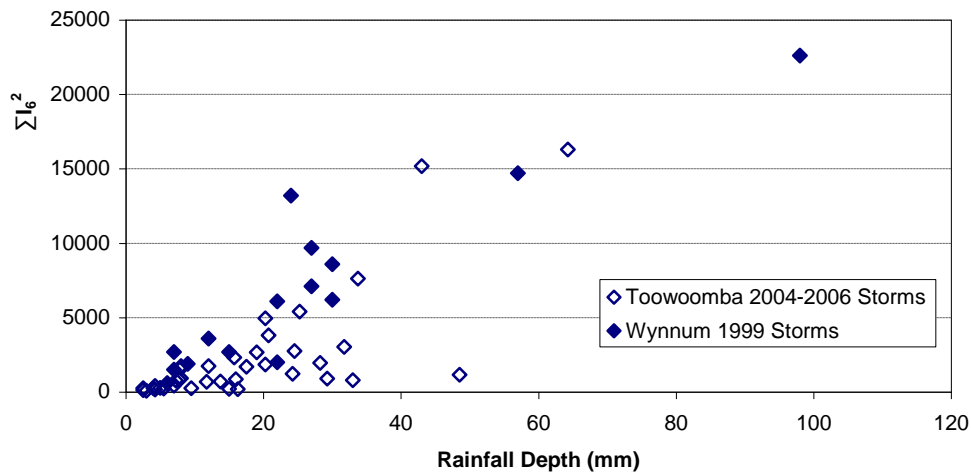
A statistical summary of rainfall characteristics of the monitored 1999 storms is provided in **Table 11.3**. Rainfall depths are similar to the Toowoomba storms that were monitored (refer **Table 6.3**) but intensity characteristics, specifically average rainfall intensity I and Peak I_6 , are significant higher.

- **Table 11.3 Statistics of rainfall characteristics of selected Wynnum storms ($n=27$) during 1999**

Statistic	P (mm)	D (hr)	I (mm/hr)	Peak I_6 (mm/hr)	ADP (hrs)	AP (mm)
Maximum	59	11.3	40.0	80	452	41.0
Minimum	2	0.1	1.4	10	0	1.0
Median	13	2.5	6.5	30	12	8.0
Mean \pm S.D	16.1 \pm 13.8	3.5 \pm 3.25	10.0 \pm 9.4	36 \pm 19	65 \pm 120	12.8 \pm 12.3
Coeff. Of Variation	0.9	0.9	10.9	0.5	1.8	1.0

S.D = Standard Deviation

Due to the higher intensities, the rainfall energy of the majority of the selected Wynnum storms was generally higher than the energy contained in the Toowoomba storms. This is demonstrated by the comparison of $\sum I_6^2$ estimates plotted in **Figure 11.6**.

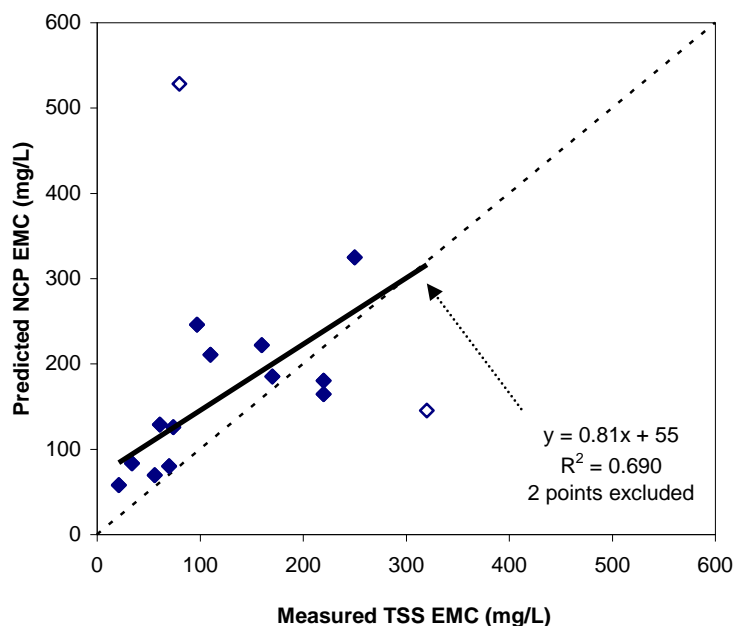


- **Figure 11.6 Plot of $\sum I_6^2$ against rainfall depth for Wynnum 1999 storms and Toowoomba December 2004 to June 2005 storms**

Calibrated Mass Balance Model parameters for the Toowoomba roof, carpark and road surfaces previously reported in **Table 9.4** were directly applied in the analysis.

This includes surface properties such as maximum free and detained particle loads, washoff efficiency curves and dry weather loss rates. **Equation 10.1** was applied to estimate Non-Coarse Particle loads from the Wynnum grassed areas. On this basis, the analysis represents the direct transfer of parameters derived from Toowoomba surface data to the Wynnum catchment analysis. This provides a significant test of the potential to use surface data to represent a mix of land uses at a larger catchment scale (of the order 30 to 40ha) under a climatically different set of storm conditions.

Non-Coarse Particle loads were estimated from each surface component of the Wynnum catchment for each storm and summed to estimate the total load and EMC at the monitoring site. Washoff of detained particles from the Wynnum road surface was predicted to occur during 67% of storms compared to only 23% of the lower-energy Toowoomba storms. No treatment measures are present in the Wynnum stormwater drainage system so no adjustment was made to the load estimates to reflect potential reductions. A plot of the measured TSS EMC and predicted Non-Coarse Particle EMC data is provided as **Figure 11.7**.



- **Figure 11.7 Plot of predicted Non-Coarse Particle EMC and measured TSS EMC at Wynnum monitoring site for 1999 storms. Line of equal value shown as dashed line.**

Although significant data limitations are present, a reasonable consistency is present when comparing the predicted Non Coarse Particle EMCs with the measured TSS concentration data. With the exception of two storms (plotted as \diamond), a simple linear expression shown in **Equation 11.3** provides a moderate correlation ($R^2=0.689$) between Non-Coarse Particle and TSS concentrations. The outlier storm events correspond to minor rainfalls less than 7mm in total. The graphed data suggests that the predicted Non-Coarse Particle EMCs are typically greater than the TSS EMCs for the majority of storms under analysis.

$$NCP_{EMC} = 0.81 \times TSS_{EMC} + 55 \quad [11.3]$$

In terms of the cumulative particle load resulting from the 15 storms, the total predicted Non-Coarse Particle load is 10420 kg, approximately 48% more than the total measured TSS load of 7030 kg. It should be noted that most of this discrepancy may be due to the different laboratory techniques used in TSS and Non-Coarse Particle analysis. Gray *et al.* (2000) identified that the SSC method, on which the Non-Coarse Particle determination is based, yields concentrations that are typically 25 to 34% higher than corresponding TSS values.

The higher Non-Coarse Particle EMCs may also be due to particle retention processes which may be occurring in the larger-scale Wynnum catchment that were not present in the small-scale surfaces monitored in Toowoomba. Furthermore, the higher Non-Coarse Particle EMCs may be simply associated with the direct use of Toowoomba derived surface parameters and recalibration of these parameters is required to better fit the specific properties of the Wynnum surfaces.

The uncertainty in the Wynnum data precludes a more detailed assessment of the differences in TSS and Non-Coarse Particle EMCs. However, this initial analysis highlights that a very significant potential exists to transfer surface-specific data to represent a large-scale urban catchment located in a different climactic condition. More collection of Non-Coarse Particle loads generated from urban catchments is required to validate and refine this potential.

11.4 Case Study Assessment of Stormwater Management Issues

The application of the Mass Balance Model to a range of stormwater management issues is further demonstrated in this Section. The following are provided as a series of case studies:

- A comparative analysis between Non-Coarse Particle loads generated from urban areas with Residential and Commercial land uses
- An assessment of the effect that exposed areas of bare soil may have in increasing Non-Coarse Particle loads from a Residential catchment
- An assessment of the effect that widespread adoption of rainwater tanks may have on Non-Coarse Particle loads from a Residential catchment
- An assessment of the Non-Coarse Particle load reductions associated with using grass swales to treat stormwater runoff from a road surface.

The spreadsheet calculations and results for each of the case studies are tabulated in **Appendix C**.

11.4.1 Effect of Urban Land Use Type on Non-Coarse Particle Loads

It is common practice to characterise stormwater runoff in terms of the land use within a catchment. In the USA, the EPA conducted the Nationwide Urban Runoff Program (NURP) from 1978 to 1983 to compile data for 2300 storms from 81 catchments (US EPA 1983). Most of the data were obtained from Residential areas, but it incorporated other land use categories. More recently, the US EPA are in the process of collating stormwater data collected as a requirement of the National Pollutant Discharge Elimination System (NPDES) into a database, referred to as the National Stormwater Quality Database (NSQD). As at the end of 2003, data from 3770 separate storm events from 66 authorities had been entered into the NSQD (Pitt *et al.* 2004). Again, the currently preferred basis is to present and analysis the data according to land use type.

Data such as NSQD obtained for regulatory purposes is expected to encompass a range of experimental designs, sampling procedures and analytical techniques. These factors and site specific properties such as climate and catchment size introduce

considerable uncertainty in the ability to make direct data comparisons. More importantly, land use represents only a generic label and there is significant variation within the definition of any particular land use type. For example, the impervious cover in the NSQD catchments grouped as 'Residential' varies from less than 10% to greater than 80% (Maestre & Pitt 2005). Mitchell *et al.* (2005) noted key factors such as housing density are changing with a trend, at least in Australia, towards smaller allotments (range 460 to 550 m²) compared to what has traditionally been the case (minimum 700 m²).

Given that a specific land use can encompass a broad range of catchment characteristics, any comparative analysis to identify the effect of land use on stormwater particle loads can only be performed at an indicative level. This kind of broad analysis has been statistically conducted using TSS data from the NURP and NSQD studies for Residential, Commercial and Industrial land uses, in addition to a review of overseas data by Duncan (1999). The various statistical measures are reproduced in **Table 11.4**.

■ **Table 11.4 TSS EMC statistics for Residential, Commercial and Industrial land uses from various stormwater monitoring studies**

Study/Statistic	Residential	Commercial	Industrial
Brisbane City Council monitoring 2002/2003 of representative catchments (BCC 2004)			
Number of samples, <i>n</i>	209	120	71
Mean (log transformed)	151	144	83
Mean±S.D (log transformed)	62-370	60-347	30-230
% Effective impervious	37-38	61-71	72-91
Review of world-wide data (Duncan 1999)			
Number of samples, <i>n</i>	109	25	12
Mean (log transformed)	141	133	150
Mean±S.D (log transformed)	51-393	51-350	45-494
US National Stormwater Quality Database NSQD (Pitt <i>et al.</i> 2004)			
Number of samples, <i>n</i>	1075	503	524
NSQD Median (untransformed)	48	43	77
NURP Median (untransformed)	101	69	-
Median %Impervious	37	83	75

S.D = Standard Deviation

The EMC statistics from Duncan (1999) suggest that median or mean EMCs are similar across all land use types. This outcome is partly supported by the stormwater monitoring conducted by Brisbane City Council (BCC 2004) which presented similar TSS EMCs for Residential and Commercial land uses, but a lower mean EMC for the Industrial land use. This was also the case for the NSQD medians, except contrary to the Brisbane data; the Industrial median was higher relative to the other land uses.

The magnitude of the Brisbane TSS EMCs is consistent with the overseas statistics reported by Duncan (1999), but appears significantly higher than the USA values. In broad terms, the statistical analysis of the USA and overseas data suggests that the TSS concentrations, on average, for stormwater runoff from Residential and Commercial areas are similar in magnitude. This EMC similarity is present even though the impervious cover in Commercial areas (typically of the order of 80%) is substantially greater than Residential areas (typically of the order of 40%). TSS concentrations from Industrial areas may differ in response to the type, intensity and controls placed on the industrial activities that occur within the catchment.

The consistency in mean or median TSS concentrations of runoff from Residential and Commercial areas can be demonstrated by use of the surface-specific load data. Non-Coarse Particle loads, on a per hectare basis, from both land use types were determined for the Toowoomba sequence of 36 storms from December 2004 to January 2006. The relative proportions of roof, grass, carpark (represented mainly by off street vehicle driveways and parking areas) and road surfaces were selected to reflect typical conditions found in each land use and are summarised in **Table 11.5**. It was assumed that each land use was well established with no bare soil areas.

■ **Table 11.5 Adopted surface composition (%) for hypothetical Residential and Commercial land uses**

Surface	Residential	Commercial
Roof	20	30
Carpark	10	20
Road	12	20
Grass	58	30
Total impervious	42%	70%
Total pervious	58%	30%

The Residential area is a hypothetical example of ‘Traditional Suburban’ areas within many Australian cities and includes 700m² lots with occupancy of 2.6 persons/household and a gross density of 10 houses/ha. (Mitchell *et al.* 2005). The impervious surfaces within the Traditional Suburban land use equates to 42%, marginally higher than the average values reported in **Table 11.4**. By comparison, the impervious surfaces represent 70% coverage of the hypothetical Commercial area. It is assumed that the impervious surfaces are fully directly connected to the stormwater drainage system.

The adopted surface compositions were modelled as hypothetical 1ha areas by the Mass Balance Method and analysed for the Toowoomba storm sequence. Loads and stormwater volumes from the individual surfaces were derived for each storm and summed to provide the total land use loading. Non-Coarse Particle EMCs were then derived from the load and volume predictions. Results compiled for the Residential and Commercial areas are summarised in **Table 11.6**.

- **Table 11.6 Results of Non-Coarse Particle load analysis for hypothetical Residential and Commercial land uses based on Toowoomba December 2004 to January storms, on a per hectare basis**

Statistic	Residential	Commercial
Total runoff volume for 36 storms ¹ (kL/ha)	3180	4625 (+45% ²)
% Contribution of each surface to total runoff (Roof -Carpark-Road-Grass)	39%-19%-23%-18%	41%-26%-26%-7%
Total NCP load for 36 storms (kg)	174	268 (+54% ²)
% Contribution of each surface to total NCP load (Roof -Carpark-Road-Grass)	7%-16%-63%-14%	7%-20%-68%-5%
Mean EMC (log transformed)	60	62
EMC Range	15-317	16-327

Note:

1. Total rainfall = 659mm
2. Percentage change from Residential value

The statistics indicate that the predicted mean EMCs for both land uses are very similar, as was the case for the review of TSS data summarised in **Table 11.4**. Total runoff volume for the Commercial area is 45% more than the Residential area, and this is accompanied by a 55% increase in Non-Coarse Particle load. As both runoff volumes and loads have increased in approximately the same proportion, the net change in mean EMC is minimal. In both cases, the roof surface is a dominant source

of runoff volume but makes only a minor contribution to the particle load.

Consistent with the relative contribution analysis (discussed in **Section 11.2**), the road surface generates approximately 60 to 70% of the overall Non-Coarse Particle load.

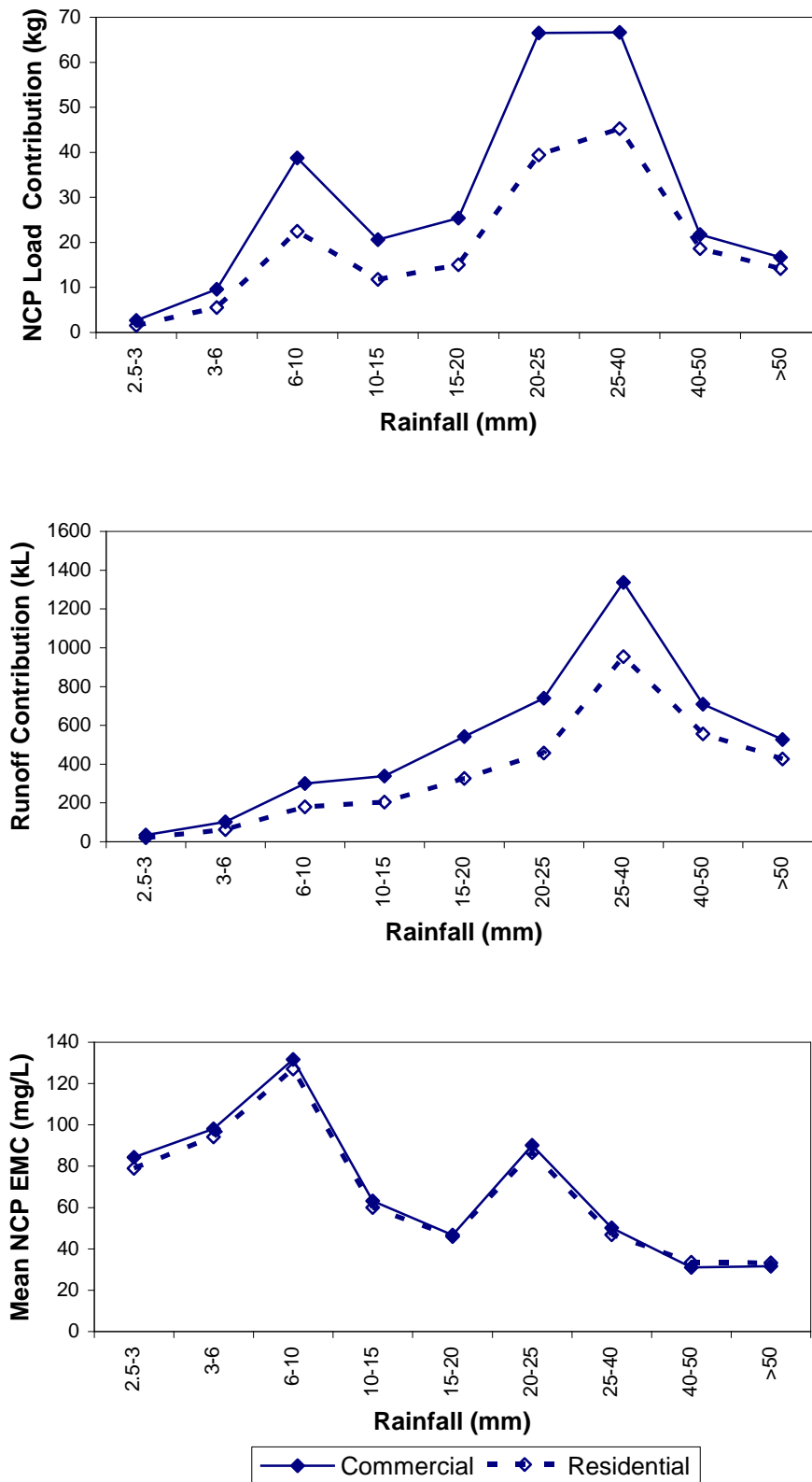
To further elucidate the differences between the hypothetical Residential and Commercial areas, the total Non-Coarse Particle load (kg) and runoff volume (kL) generated by the subsets of storms within different rainfall ranges were computed. These calculations provide a measure of the contribution that is made by rainfall events of varying magnitude within the sequence of storms. The results are plotted as **Figure 11.8**.

The Commercial area is predicted to generate substantially greater runoff volumes for storm rainfalls more than 6mm. This effect is not as marked in larger rainfalls greater than 40mm. This produces a significant increase in particle loads for storms within the 6 to 40mm range. A graph of the mean EMC associated with each rainfall range is also provided, which clearly shows the negligible difference between Residential and Commercial Non-Coarse Particle concentration across all storms.

11.4.2 Effect of Bare Soil Areas on Non-Coarse Particle Loads

The previous assessment of Residential land use assumes that all pervious surfaces are grassed. This may be the case in long established and well maintained urban development, but in newly constructed or poorly maintained areas, the proportion of the surface exposed as bare soil may be significant. As previously noted in **Section 11.2**, the Non-Coarse Particle load generated from bare soil during rainfall exceeding 20mm is relatively high. To check the significance of this aspect, the mass balance analysis of the typical Residential area was repeated with a portion of the pervious area assumed to be bare soil. Specifically, the 58% pervious area in the Residential land use was assumed to consist of 48% grassed and 10% bare soil, expressed as percentages of the total area.

Results of the bare soil analysis are compiled in **Table 11.7** and the percentage differences between the Residential land use with no bare soil component are also provided.



■ Figure 11.8 Plots of Non-Coarse Particle load contribution, runoff contribution and mean Non-Coarse Particle EMC for various rainfall ranges for hypothetical 1 ha Residential and Commercial areas and December 2004 to January 2006 storms

- Table 11.7 Results of Non-Coarse Particle load analysis for hypothetical Residential land use with 10% bare soil based on Toowoomba December 2004 to January 2006 storms, on a per hectare basis**

Statistic	Residential + 10% Bare Soil
Total runoff volume for 36 storms ¹ (kL/ha)	3220 (+1%) ²
% Contribution of each surface to total runoff (Roof -Carpark-Road-Grass-Bare)	39%-19%-23%-15%-4%
Total NCP load for 36 storms (kg)	273 (+57%) ²
% Contribution of each surface to total NCP load (Roof -Carpark-Road-Grass-Bare)	5%-10%-40%-7%-38%
Mean EMC (log transformed)	75 (+25%) ²
EMC Range	15-344

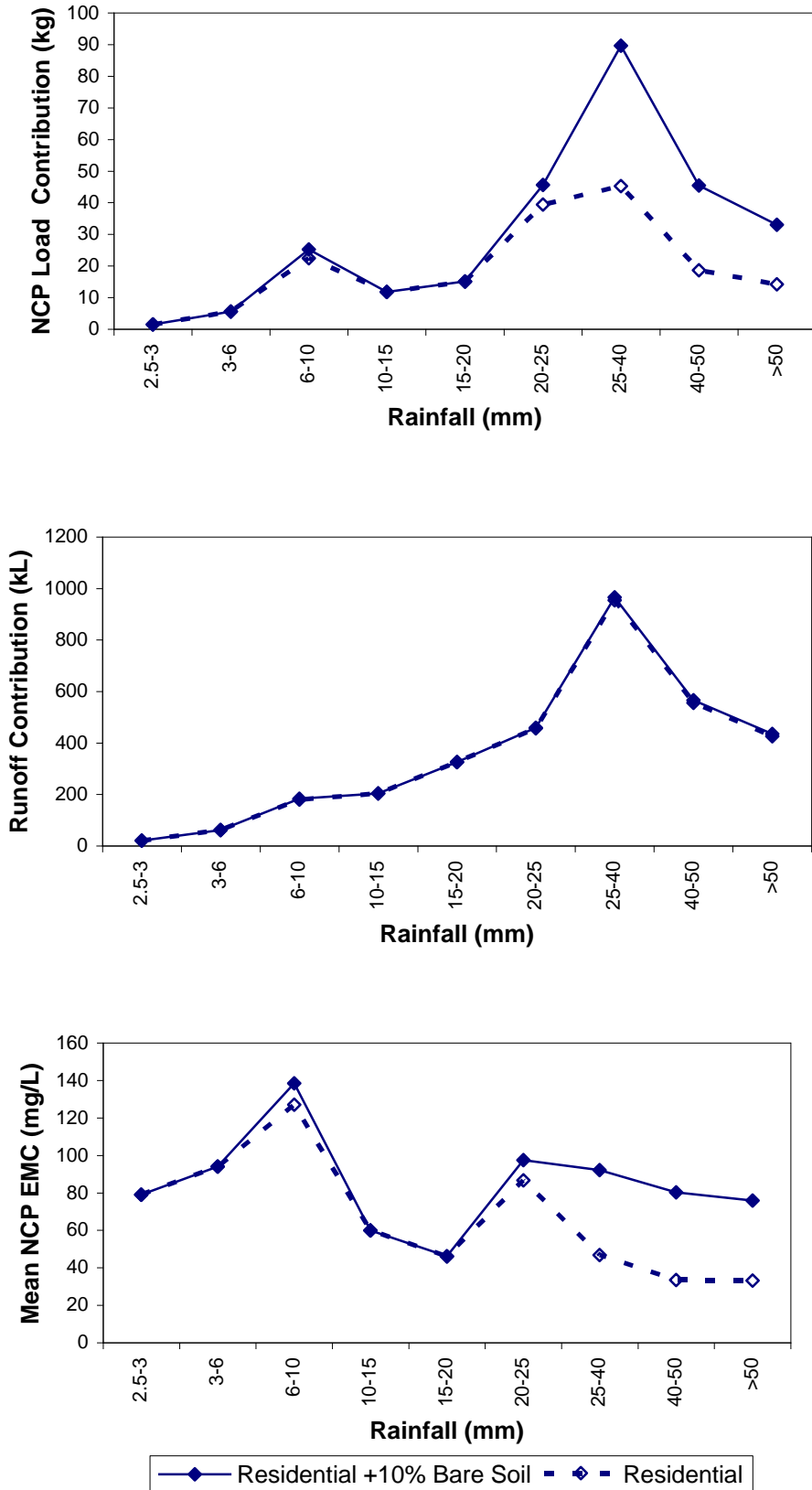
Note:

- Total rainfall = 659mm
- Percentage change from Residential value

As the runoff characteristics of bare and grassed surfaces are very similar, the total runoff volume has marginally increased. The runoff from bare soil areas is highly concentrated and consequently the total particle load has increased dramatically by 57%. The increase in mean EMC is not as high but is of the order of 25%. Plots of the Non-Coarse Particle load and runoff volume contributions for each rainfall range are provided in **Figure 11.9**, together with the variation in mean EMC with rainfall. As presented, the change in runoff due to the introduction of the bare soil is minimal, but significant increases in EMC and hence load is evident for storms greater than 20mm rainfall. As bare soil runoff is initiated only when rainfall exceeds soil infiltration capacity, the effect of bare soil in small-to-moderate storms is largely absent.

11.4.3 Effect of Rainwater Tanks on Non-Coarse Particle Loads from Residential Areas

A considerable amount of Australian research has been undertaken on the water supply benefits of installing rainwater tanks. Reductions in mains water use up to 85% can be achieved with tank sizes between 5 to 15 kL, provided that dual water supply is incorporated and the roof water is used for indoor purposes (Coombes *et al.* 2002a; Mitchell *et al.* 2002) As a specific example, the installation of two 2.2kL rainwater tanks with mains water trickle top up at a small cottage in Newcastle was found to have resulted in a 45% reduction in



■ Figure 11.9 Plots of Non-Coarse Particle load contribution, runoff contribution and mean Non-Coarse Particle EMC for various rainfall ranges for hypothetical 1 ha Residential and Residential +10% Bare Soil areas and December 2004 to January 2006 storms

mains water use during a drought (Coombes *et al.* 2004). When full, the tanks were able to supply total household demand for about 11 days.

The capture of roof water for domestic use reduces the amount of runoff discharging from a housing allotment. An 80% reduction in the one year ARI peak stormwater discharge was predicted if 10 kL rainwater tanks were adopted in the Parramatta region of New South Wales (Coombes *et al.* 2002b). As a consequence, the use of rainwater tanks is a common WSUD feature. However, minimal research has been conducted on the potential quality effects of removing roof water as a component of urban runoff generated from residential catchments. Roof runoff water has a low particle concentration but volumetrically is a major component of urban stormwater. As demonstrated by the analysis of a hypothetical Residential area, roof runoff constitutes approximately 39% of the stormwater volume but only 7% of the Non-Coarse Particle load. The extraction of roof water from the stormwater flow may result in less dilution of the more highly concentrated particle sources, especially roads, causing a net increase of Non-Coarse Particle concentration.

To check this aspect, the mass balance analysis of the hypothetical Residential area was repeated with allowance for storage and use of roof runoff. The analysis was performed on a per hectare basis and a number of assumptions were made, consistent with an assessment of roof water storage requirements for various Australian cities by Mitchell *et al.* (2005):

- Household use of roof water was assumed to be 1.3 kL/ha/day based on a constant demand of 50 L/person/day, an average household of 2.6 persons/household and a development density of 10 houses/ha. The household demand is based on toilet flushing and some additional component of non-potable indoor use.
- The tank storage was set at 100 kL/ha, equivalent to 10 kL/household.
- The roof water contribution to urban stormwater is the overflow from the tank storage. The tank overflow volume was computed for each storm event and the overflow Non-Coarse Particle concentration was assumed to be equivalent to the roof runoff concentration. This is a conservative assumption as particle settling is expected to occur within the tank storage.

A simple mass balance approach was used to estimate the tank overflow volume for each storm. A calculation is made of the roof water storage volume S_O that provides a measure of the tank status at the end of the storm (i.e. whether the tank has overflowed or is partly full). **Equation 11.4** is used in the S_O determination.

$$S_O = S_i + R_{roof} \quad [11.4]$$

where S_i is the tank storage volume at the start of the storm (kL) and R_{roof} is the roof runoff (kL)

S_i is derived based on the tank storage volume at the end of the previous storm S_a , U which is the household demand (kL/ha/day) and ADP which is the antecedent dry period (hr) in accordance to **Equation 11.5**.

$$S_i = \text{Max}(0, S_a - U \times ADP/24) \quad [11.5]$$

After S_O is calculated, it is used to determine the tank storage overflow $R_{overflow}$ and S_a (to determine S_i for the next storm) based on the tank storage capacity S_C in accordance to the rules provided as **Equation 11.6**.

$$\text{If } S_O > S_C, \text{ then tank has overflowed and } R_{overflow} = S_O - S_C \text{ and } S_a = S_C \quad [11.6]$$

$$\text{If } S_O < S_C \text{ then tank is partly full and } R_{overflow} = 0 \text{ and } S_a = S_O$$

The tank storage and overflow algorithm was included in the mass balance spreadsheet for the hypothetical Residential area and the December 2004 to January 2006 storm sequence was reanalysed. Roof surface was assumed to represent 20% (or 2000 m²) of the 1ha Residential catchment. The simulation results are provided in **Table 11.8**. Capture and use of the roof water reduced the total stormwater volume generated by the urban land area by 10%. For the sequence of storms analysed, approximately 75% of the roof water overflowed the tank storage and the remaining 25% was available for household use.

- Table 11.8 Results of Non-Coarse Particle load analysis for hypothetical Residential land use with rainwater tank strategy based on Toowoomba December 2004 to January 2006 storms, on a per hectare basis**

Statistic	Residential + Rainwater Tanks
Total runoff volume for 36 storms ¹ (kL/ha)	2860 (-10%) ²
% Contribution of each surface to total runoff (Roof -Carpark-Road-Grass)	33%-21%-26%-20%
Total NCP load for 36 storms (kg)	169 (-3%) ²
% Contribution of each surface to total NCP load (Roof -Carpark-Road-Grass)	5%-16%-65%-14%
Mean EMC (log transformed)	74 (+23%) ²
EMC Range	23-367

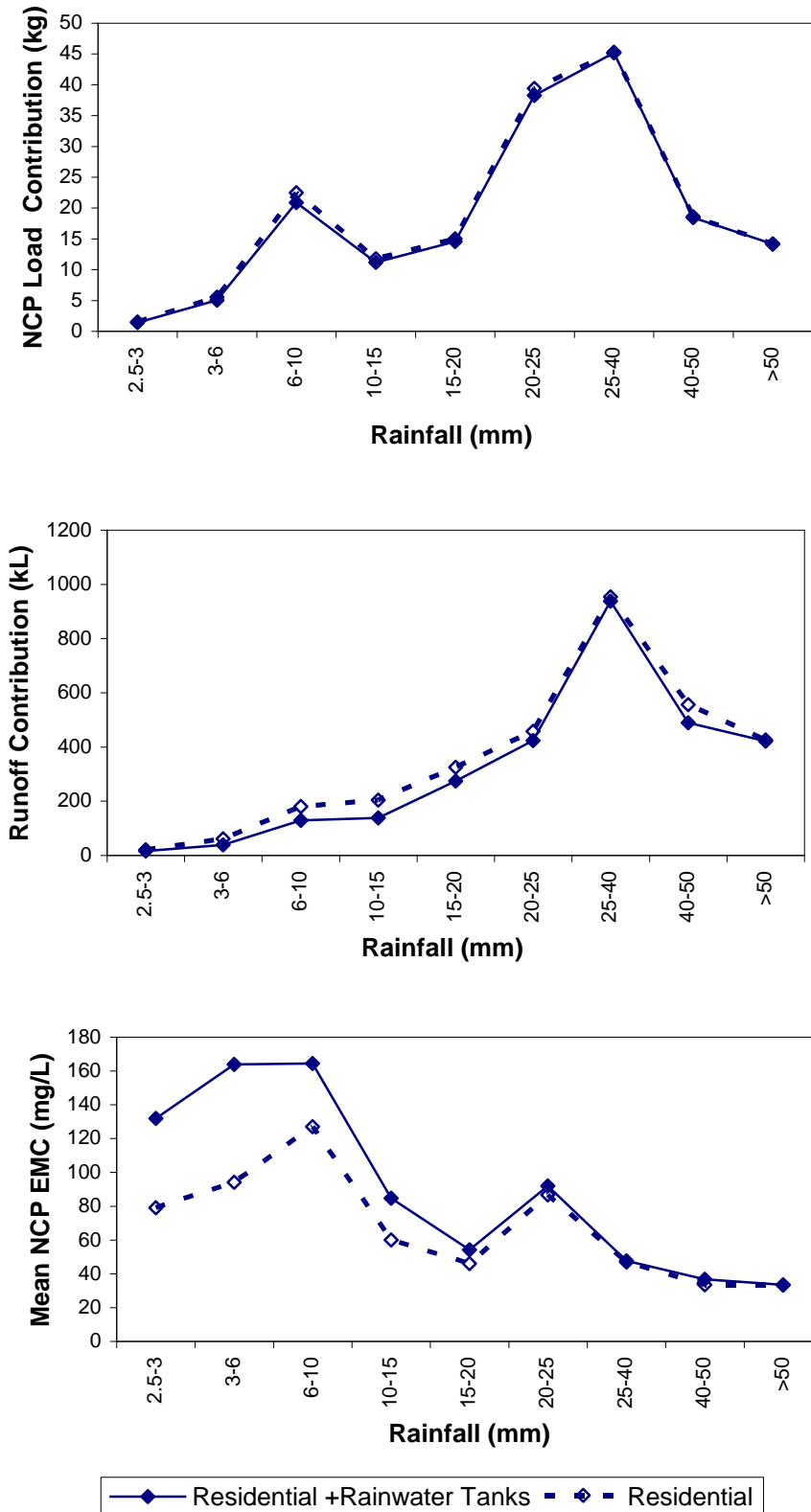
Note:

- Total rainfall = 659mm
- Percentage change from Residential value

As the roof runoff has low Non-Coarse Particle concentrations, the reduction in the total particle load for the Residential area is minor. A 23% increase in the mean EMC for Non-Coarse Particles is predicted and as indicated in **Figure 11.10**, this outcome is due to higher runoff concentrations for small to moderate storms less than 20mm. During these storms, the tank storage captures a more significant proportion of the roof water and the particle load from the other surfaces is thus less diluted than otherwise would be the case for the no rainwater tank scenario. A concentration increase of particles and associated pollutants for these minor, frequent events may adversely impact on some types of aquatic habitats.

11.4.4 Effect of Grass Swales on Non-Coarse Particle Loads from Road Surfaces

Grass swales and vegetated drains are recognised measures to control stormwater pollutants generated from roads and highways (Barrett *et al.* 1998b; Wong *et al.* 2000) and are also becoming more popular as an important WSUD element within urban developments. Swales are typically constructed trapezoidal drains that are turfed or planted with tufted grasses to remove sediments from adjacent paved areas. Longitudinal grades of the swale are generally low (less than 4%) to promote sediment deposition and to limit the potential for high flow velocities that may cause erosion of the swale bed.



■ Figure 11.10 Plots of Non-Coarse Particle load contribution, runoff contribution and mean Non-Coarse Particle EMC for various rainfall ranges for hypothetical 1 ha Residential and Residential + Rainwater Tanks areas and December 2004 to January 2006 storms

Numerous studies have been conducted that have evaluated the sediment removal performance of grass swales. Fletcher (2002) reviewed 18 studies of swales used for both urban and rural stormwater control and derived a mean swale performance of $72\pm 19\%$ for TSS removal. On this basis, grass swales are considered relatively effective in sediment removal particularly for coarse material.

A laboratory investigation of sediment deposition within a grassed channel was conducted by Deletic (1999). The experiments were based on steady state flow conditions within a 12.5m long by 0.3m wide channel surfaced with astro-turf. Sediment mixtures of the order of 600 to 2700 mg/L TSS were pumped into the channel and samples were extracted at various points along the channel length. No grass bending or bed infiltration effects were included in the laboratory setup.

The ability of the grass surface to trap sediments, or trapping efficiency, was determined to be a function of the particle fall number $N_{f,s}$, as given in **Equations 11.7** and **11.8** (Deletic 2001):

$$N_{f,s} = \frac{lV_s}{hV} \quad [11.7]$$

where $N_{f,s}$ is the particle fall number for a given particle size fraction or d_s , l is the grass channel length (m), V_s is the Stokes' settling velocity of the particle d_s (m/s), h is the flow depth (m) and V is the average mean velocity between grass blades (m/s), and;

$$T = \frac{N_{f,s}^{0.69}}{N_{f,s}^{0.69} + 4.95} \quad [11.8]$$

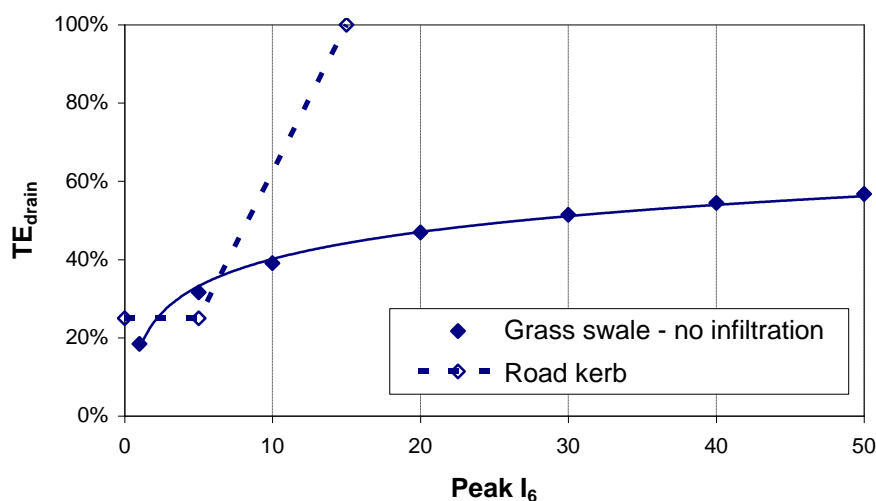
where T is the trapping efficiency for particle d_s (range 0 to 1)

To demonstrate the potential effectiveness of grass swales, the scenario of theoretically substituting the existing kerb characteristics of the Toowoomba road monitoring site with a grassed swale was analysed in the Mass Balance Model. The grass swale was assumed to be nominally 1m wide and set at 0.9% grade along the full 75m length of the roadway. Peak discharge from the roadway was estimated for a range of Peak I_6 values up to 50 mm/hr by use of the Rational Method (**Equation 9.1**). The flow depth h was then derived using Mannings equation based on

roughness coefficients that ranged from 0.05 to 0.4, depending on grass submergence (Barling & Moore 1993).

Sediment trapping efficiencies were derived using **Equations 11.7** and **11.8** for each Non-Coarse Particle size class (VFP, FP and MP). Assumed representative particle sizes were set at 200 μm , 20 μm and 2 μm respectively for each class to derive the settling velocities for use in **Equation 11.7**.

The above analysis indicated that most of the MPs would be retained in the grass swale (Trapping efficiency $T=0.89-0.99$). Depending on the magnitude of the discharge, the trapping of FPs varied from less than 0.2 to 0.5. Only a small proportion of VFPs were predicted to be trapped within the grass swale ($T=<0.01-0.1$) for the range of discharges. Particle composition in road runoff discharging into the grass swale was assumed to be 30% MP, 60% FP and 10% VFP by mass, based on the measured particle size composition (refer **Chapter 6**). The trapping efficiency for each particle range was then used to derive an overall TE_{drain} curve for the hypothetical grass swale and this is plotted in **Figure 11.11**. For comparison, the transport efficiency curve determined for the existing road kerb (and adopted in the refined Mass Balance Model) is also shown.



- **Figure 11.11** Transport efficiency (TE_{drain}) curve for hypothetical grass swale based on Particle Fall Number ($N_{f,s}$) assuming no infiltration compared with curve for road kerb, extracted from Figure 9.11

The estimation of road Non-Coarse Particle loads using the Mass Balance Model was repeated with the scenario of the roadside drainage system replaced with the 1m-wide grassed swale. Loads were determined for storms during the full monitoring period from December 2004 to January 2006. The TE_{drain} curve for the road kerb was substituted with the grass swale curve shown in **Figure 11.11**. Based on regression ($R^2=0.995$), the grass swale curve follows **Equation 11.9**.

$$TE_{\text{drain}} = 10\text{Log}(PeakI_6) + 17.1 \quad [11.9]$$

In addition to substituting the TE_{drain} curve used in the mass balance analysis, it was assumed that particles retained in the swale after a storm would be effectively trapped within the grass surface and unavailable for mobilisation during the next storm.

The net Non-Coarse Particle load at the point of discharge L from the swale was estimated for each storm using the revised model parameters. Individual L values were summed to determine the cumulative load discharged from the swale. By comparison with the cumulative load for the roadway with kerb, the reduction in Non-Coarse Particle load due to the swale is estimated to be 68%. A summary of the analysis results is provided as **Table 11.9**.

- **Table 11.9 Results of Non-Coarse Particle load analysis for 450m² Toowoomba road surface with existing kerb and hypothetical grass swale based on December 2004 to January storms**

Statistic	Road with Existing Kerb	Road with Grass Swale
Total runoff volume for 36 storms ¹ (kL)	232	232 (0% ²)
Total NCP load for 36 storms (kg)	47	15 (-68% ²)
Mean EMC (log transformed)	182	60
EMC Range	19-582	18-194

Note:

1. Total rainfall = 659mm
2. Percentage change from Road with Existing Kerb value

The predicted swale performance in reducing particle loads is consistent with the measured swale results (approximately 70% TSS reduction) compiled by Fletcher (2002). As noted in **Table 11.9**, the total runoff volume for the grass swale and existing kerb scenarios are identical as the effect of infiltration into the swale has not been taken into account. At the beginning and end of a rain event, a grass swale may

infiltrate all runoff leading to complete deposition of sediment particles. In low intensity storms, complete infiltration of runoff may occur. On this basis, the particle reductions are conservative estimates and are expected to be higher than the predicted values. Complex models such as TRAVA that account for runoff generation, infiltration dynamics and sediment transport (Deletic 2001) are expected to provide a more accurate assessment of swale performance.

12 Conclusions and Recommendations

12.1 Summary and Conclusions

Suspended solids concentrations provide a measure of potential water quality impact associated with urban runoff. Surrogate measures of pollution, such as **Total Suspended Solids** are used to determine the likely effects of urban development on the quality of downstream waters. It is common practice to use relationships between TSS load and land use type to predict the amount of suspended solids exported from an urban catchment. Targets for pollution control are often expressed in terms of percent reduction in TSS load or compliance within an acceptable TSS concentration range.

The main theme of this thesis is to demonstrate that the identification and analysis of pollutant load from urban surfaces can provide a viable, if not better, alternative to the current approach based on land use type. Any type of use (e.g. Residential, Commercial and Industrial) can be fundamentally defined by its component surfaces, which include roads, roofs, carparks and grassed or landscaped areas.

The dissertation demonstrates the effectiveness of a surface-based approach and achieves its objectives in several phases that:

- Establishes a particle classification system and associated laboratory procedures suitable for the determination of suspended solids concentrations in urban runoff.
- Develops a robust and cost effective sampling technique that can be used to measure stormwater particle loads generated from urban surfaces.
- Monitors runoff from typical urban surfaces and characterises the amount and concentration of generated stormwater particles.
- Develops predictive models that estimate the stormwater particle loads produced from urban surfaces.
- Demonstrates approaches based on urban surfaces that can be applied to stormwater infrastructure planning in urban areas, in order to more effectively deliver improvements in water quality.

12.1.1 Particle Classification and Laboratory Analysis

This thesis, as have previous investigations (de Ridder *et al.* 2002), questions the use of TSS as an accurate determinant of suspended solids in urban stormwater. The TSS method was originally developed for the analysis of solids in wastewater samples after initial settling. TSS procedures to obtain subsamples by pouring or pipetting are inadequate for the analysis of samples containing particles larger than 62 μm , as is the case for urban stormwater (Gray *et al.* 2000).

In response to this concern, this thesis develops new laboratory procedures to measure the concentration of various particle size classes found in stormwater runoff. Particle washoff behaviour, contaminant associations such as heavy metal adsorption and stormwater treatment processes are closely allied with particle size. It is considered that a breakdown of suspended particles into size fractions is a critical prerequisite in defining particle characteristics.

The proposed laboratory method is a variant of the **Suspended Sediment Concentration** (SSC) analysis that determines the concentration of **Non-Coarse Particles** (NCP) less than 500 μm in size. NCP is further divided by screening and filtering techniques into Very Fine Particles (VFP, less than 8 μm), Fine Particles (FP, 8-63 μm) and Medium Particles (MP, 63-500 μm). Analysis was performed to determine the organic and inorganic fractions of each particle class.

12.1.2 Design and Testing of Passive Sampling Devices

Passive samplers include a wide range of devices that are installed insitu within the stormwater flowpath and collect a proportion of the runoff volume during a storm. They offer a simple and cost effective method to collect samples from urban surfaces, but are prone to some technical limitations. For example, some samplers may rapidly fill and preclude a representative sample over the full rainfall event from being obtained.

Passive samplers can be classified by the main hydraulic principle applied in design, including gravity flow, siphon flow, rotational flow, flow splitting and direct sieving. A literature review of sampler designs concluded that flow splitters had the most relevant attributes in collecting a flow-proportional runoff sample, necessary in deriving the **Event Mean Concentration** (EMC) of stormwater particles. Available

flow splitter designs have limitations including being a relatively large size, having an exposed surface that may collect airborne dust and a hydraulic requirement to be installed at a steep incline.

An alternative and compact flow splitter design was produced that overcame these technical limitations. A prototype flow splitter was tested in a hydraulic laboratory and found to be capable of collecting a fixed proportion of water discharges operating in the range of 1 to 5 L/s to within $\pm 2\%$ accuracy. A relatively constant Sample Flow Volume Ratio (SVFR) of this accuracy is a key requirement in obtaining a representative EMC sample. Based on the hydraulic test results, the flow splitter is more accurate compared to similar devices reported in the literature (Hwang *et al.* 1997).

The efficacy of the prototype flow splitter in capturing unbiased particle concentrations was also evaluated. A sediment testing rig was established and was operated at a constant flow of 3 L/s. A pre-prepared sediment slurry mixture was added to the water flow. As the particle composition of the slurry was measured, theoretical estimates of the particle concentrations in the water flow (in terms of VFP, FP and MP) were able to be made. The ratio of the theoretical and sampled concentration provided a measure of sampler performance.

Based on the outcomes of three sediment test runs, it was concluded that the flow splitter was able to provide a representative EMC sample that is comparable to, if not more consistent than, very frequent (1 minute) grab sampling. On average, the Non-Coarse Particle concentrations of the flow splitter samples were 9% less than theoretical values. Concentration discrepancies were mainly introduced by poor sampling capture of MP sized particles.

Hydraulic and sediment testing were also conducted on another passive sampler design referred to as the orifice-weir device. This was initially proposed as an alternative to the flow splitter, but demonstrated under testing to have a lower performance. The flow splitter was selected as the preferred device for the monitoring of urban surfaces.

12.1.3 Collection and Analysis of Stormwater Particle Data from Urban Surfaces

A network of five stormwater monitoring sites was established within inner city Toowoomba, Queensland. The monitoring sites have small catchments (50 to 450m² area) representative of a selection of urban impervious areas (galvanized iron roof, concrete carpark and bitumen road pavement) and pervious areas (grassed and exposed bare soil). Flow-weighted composite samples were taken by flow splitter devices installed at each site and analysed to determine the EMC of Non-Coarse Particles, associated particle classes (VFP, FP and MP) and organic contents. Overall, a total of 40 storms with rainfalls from 2.5mm to 64.3mm were sampled during the 13-month monitoring period from December 2004 to January 2006.

A tipping bucket pluviometer was installed to measure the temporal pattern of rainfall. A manually read rain gauge was also used to check recorded rainfall totals. All five sites are situated within a close radius of 70m to reduce runoff variability that may be introduced due to spatial differences in rainfall.

Particle EMC tended to decrease with increasing rainfall depth for impervious surfaces, indicative of a dilution effect. Generally in all particle classes, the roof EMCs were the lowest, followed by the carpark and road in that order. The bare soil surface yielded the highest EMCs with the grass data being of the same order as the carpark EMCs. An exception to this pattern is the grass VFP EMCs which are of similar magnitude to the road data.

In terms of particle size distribution, FPs tended to comprise the greatest mass in road and roof runoff with percentages generally in the 50 to 70% range. Bare soil runoff had similar proportions of FPs and MPs with median percentages of approximately 40%. The MP percentage by mass were generally less than 30% for roof, road and grass runoff and slightly higher than 30% for carpark runoff. The proportion of VFPs tended to be relatively small for all surfaces at typically less than 20%.

For all surfaces and particle classes, most of the particle mass was inorganic matter. Overall, the inorganic content of Non-Coarse Particles ranged from 55% to 85%.

Estimates of runoff volume for each storm event were made using the DRAINS urban hydrology model (O'Loughlin & Stack 2003). As the flow splitters had a relatively constant sample flow volume ratio (SVFR), the sample volume collected after each storm provides a proportional measure of runoff volume. By comparing the estimated and sample-based runoff volumes, it was concluded that the installed samplers captured a reasonable proportion of the runoff hydrograph generated during the monitored storms.

The measured EMCs and runoff volume estimates from DRAINS analysis were combined to derive particle loads (in $\text{mg}/\text{m}^2/\text{storm}$).

12.1.4 Predictive Models to Estimate Particle Loads

Effective predictive models of Non-Coarse Particle (NCP) load generation were developed in stages. Scatter plots using impervious surface data were first prepared for NCP load against a range of rainfall-related parameters. The selected parameters include antecedent rainfall depth (AP), antecedent dry period (ADP), rainfall duration (D), rainfall depth (P), average rainfall intensity (I), peak six-minute rainfall intensity (Peak I_6), the square of the peak six-minute rainfall intensity (Peak I_6^2) and the sum of six-minute rainfall intensities during the storm ($\sum I_6^2$).

A qualitative analysis of the correlation between NCP load and each parameter was performed based on a visual assessment of the scatter plots. For all impervious surfaces, a weak negative correlation is present between ADP and the NCP load that is generated. The load tends to decrease with an increase in AP although this trend is weaker for the road surface. A relationship between load and rainfall depth is not evident, except for a weak positive correlation for the road surface. The strongest positive trends are exhibited between loads and average rainfall intensity (I) and peak 6-minute intensity (Peak I_6).

Correlation analysis of data from the pervious surfaces was restricted by the small number of runoff events that were measured. Most rainfalls less than approximately 20mm depth were infiltrated into the soil and no surface runoff was produced. Based on a scatter plot dataset of five values, positive correlations between the bare soil NCP load and rainfall depth and $\sum I_6^2$ were perceived. A piecewise linear regression

based on runoff depth was used as a basis to predict bare soil NCP loads (**Equation 10.2**).

In the case of the impervious roof, carpark and road surfaces, a reasonable match is identified between measured NCP load and an exponential regression curve (**Equation 8.1**) based on average rainfall intensity ($R^2 = 0.74$ to 0.92 depending on surface type). Single burst storms of short to moderate duration (less than 5 hours) tended to more closely fit the exponential relationship than other types of storm events.

For some individual storms, the degree of fit improves if a composite index of rainfall parameters is used instead of average rainfall intensity. The index, referred to as the Rainfall Detachment Index (RDI), is defined as the product of $\sum I_6^2$ and $\text{Peak}I_6$ divided by storm duration D . The ratio $\sum I_6^2/D$ in RDI is a measure of the kinetic energy of rain drops (E_K) available for particle detachment per unit area of the surface averaged over the duration of the storm. As a time derivative of kinetic energy, $\sum I_6^2/D$ is thus a measure of ‘rain power’, a term used by Gabet & Dunne (2003) in their study of interill soil detachment. The remaining component of RDI, $\text{Peak}I_6$, is part of the well known Rational Equation (**Equation 9.1**) used to estimate the peak runoff discharge from small urban areas.

The $\sum I_6^2/D$ and $\text{Peak}I_6$ terms that are represented in RDI reflect the two main physical processes involved in particle washoff; the rain power that causes particle detachment and initial mobilisation from the surface followed by the flow capacity to transport the suspended particles to a point of discharge.

Piecewise linear relationships (**Equation 8.2**) using RDI were fitted to NCP load data for selected storms less than 5 hours duration. Piecewise linear relationships based on average rainfall intensity I (**Equation 8.7**) were also fitted by regression. A modified exponential relationship (**Equation 8.8**) that incorporates an additional term (the critical average intensity I_C at which particle mobilisation is initiated) was also applied. The derived relationships for each surface were used in simple methods to estimate NCP loads in response to rainfall.

The insight gained from the RDI analysis led to the development of a particle Mass Balance Model for impervious surfaces. Key features of the Mass Balance Model follow:

- Both the surface and its lateral drainage system are incorporated as the major physical components modelled to predict the net particle transport to the point of discharge.
- Surface particles are partitioned into highly mobile ‘free’ particles and less mobile ‘detained’ particles. The washoff of the two particle types are defined for each surface by use of characteristic efficiency curves based on rain power ($\sum I_6^2/D$).
- Following washoff from the surface, the amount of particles transported to the point of discharge is dependant on the hydraulic efficiency of the lateral drain. This transport capacity is defined by a characteristic efficiency curve based on Peak I_6 . Significantly more particles are retained in the lateral drain during very small storms (less than 3 to 5mm rainfall).
- After each storm event, the buildup of free particles on the surface reaches a maximum equilibrium condition, as determined by a balance between supply and removal processes.
- Depending on the peak storm intensity, some particles may be retained within the lateral drain. These retained particles may be removed from the drain by dry weather processes such as wind. If the dry period between storms is short, then the remaining retained particles form part of the load available for washoff during the next storm.
- Allowance is made for wet weather accumulation due to atmospheric dust fall on roof surfaces. This was made by using a constant particle accumulation rate (as $\text{mg/m}^2/\text{hr}$).
- Allowance is also made for an additional wet weather source contributing to particle load on trafficable surfaces. The amount of particle mass added was assumed to be dependent on the time period between storm peaks, or interburst period (IBT). A maximum particle accumulation applies and drying of the surface, which may initiate removal processes, is also taken into account.

Mass Balance Models for the roof, carpark and road surfaces were calibrated and validated against measured NCP loads collected during the December 2004 to January 2006 monitoring period.

The Mass Balance Model approach and the average rainfall intensity and RDI regression relationships form part of a suite of eight methods established to estimate NCP loads from impervious surfaces. The methods are listed and briefly described in **Table 12.1**. Three of the methods (Arithmetic Mean EMC, Logarithmic Mean EMC and Stochastic Mean EMC) are currently in common use. The remaining five methods were devised as part of this study.

■ **Table 12.1 Brief descriptions of NCP load estimation methods for impervious surfaces**

Method	Description
Arithmetic Mean EMC	Uses a constant EMC to estimate load based on the arithmetic mean of measured data
Logarithmic Mean EMC	Uses a constant EMC to estimate load based on the logarithmic mean of measured data
Stochastic Mean EMC	Uses a randomly selected EMC to estimate load. The selection is within the range of \pm standard deviation of the logarithmic mean of measured data
Rainfall Depth Adjusted EMC	Assigns an EMC value to estimate load based on the rainfall depth. The value is based on the mean of measured data within discrete rainfall ranges.
Rainfall Intensity Adjusted EMC	Uses an EMC value obtained from an EMC-rainfall depth graph. The value is selected based on the duration and average rainfall intensity of the storm.
Average I	Uses the linear piecewise regression of NCP load against average rainfall intensity (Equation 8.7)
RDI	Uses the linear piecewise regression of NCP load against RDI (Equation 8.2)
Mass Balance	Uses the Mass Balance Model

The methods in **Table 12.1** are listed in order of increasing data requirements and complexity. An error analysis of the methods was conducted by comparing predicted and measured NCP loads for the Toowoomba road surface. Generally, a trend was present with greater accuracy accompanying increased complexity within the method used.

The Mass Balance Method yielded the most accurate results for predicting loads for individual storms, but a simpler approach, the Rainfall Intensity Adjusted EMC Method gave results of comparable accuracy. This method may be preferred if

available data is limiting. The relatively simplistic Rainfall Depth Adjusted EMC Method provided a very accurate estimate of cumulative NCP load which suggests that this approach may be a useful tool in annual load estimation.

It was also concluded from the error analysis that the ability of the three simple methods in common usage (Arithmetic Mean EMC, Logarithmic Mean EMC and Stochastic Mean EMC) to produce consistently reliable load estimates is questionable. The estimates of cumulative load are also sensitive to the magnitude of the EMC value that is selected to form the basis of the analysis.

12.1.5 Demonstration of Application of Stormwater Planning Tools

The NCP load estimation methods listed in **Table 12.1** provide a suite of useful tools that can be applied in the planning of stormwater infrastructure and control measures. A number of examples and case studies are provided in this thesis to demonstrate the application of surface-related data and modelling tools, particularly in the context of Water Sensitive Urban Design (WSUD).

The various example applications are summarised in **Table 12.2**. A total of six applications are provided.

The research hypothesis posed in this dissertation is that urban stormwater management can be better planned on the basis of identification and analysis of pollutant load from component surfaces, compared to a more generic land use based approach. This is clearly the case when WSUD measures such as grass swales and rainwater tanks are employed which necessitate the prediction of pollutant loads from individual surface types such as roads and roofs. These WSUD approaches are provided as specific case studies in this thesis (Case Studies 5 and 6).

In addition to being directly applicable to small scale and distributed measures, a surface-based approach is a physically realistic way to model an urban catchment as a whole. This is proven by the comparative analysis of particle loads generated from Residential and Commercial land uses (Case Study 3) and the comparison of predicted and measured particle loads from a large-scale, mixed land use catchment in Brisbane (Case Study 2).

It is impractical to isolate the dominant pollutant sources within an urban area based on land use, but this can be done if a surface based approach is used. This is demonstrated by the analysis of the effect of bare soil areas (Case Study 4) and the assessment of the relative contribution of urban surfaces (Case Study 1).

- **Table 12.2 Brief descriptions of examples and case studies to demonstrate application of stormwater planning tools**

Case Study 1: Relative Contribution of Urban Surfaces

Identification of dominant pollutant sources within urban areas is important to more effectively target source control strategies. In response to this issue, a comparison was made of measured NCP loads generated from the five different surfaces during the December 2004 to January 2006 monitoring period. In terms of cumulative load on a per m² basis, the main contributors were the road and bare soil surface. These surface loads were a factor of 14.5 and 16, respectively, larger than the roof load. The grass surface NCP load was relatively low (0.7 roof load) compared to the moderate contribution made by the carpark surface (4.4 roof load).

Pervious surfaces generated runoff in the less frequent storms when rainfall exceeded 15 to 20mm. For storms less than this magnitude, the road surface contributed between 50 to 70% of the NCP load on an equal area basis. This is important as urban runoff from these small-to-moderate events can lead to a wide range of environmental impacts including channel erosion, reduced biodiversity and poor water quality (Walsh *et al.*, 2004).

Case Study 2: Representation of Urban Land Use Based on Surface Composition

An analysis was conducted to investigate the use of surface-specific data to represent a large-scale urban catchment. TSS monitoring data was made available by Brisbane City Council for a 35ha mixed land use urban catchment located at Wynnum, Brisbane. The coverage of various types of surfaces was known and this information was used to establish a Mass Balance Model of the catchment. Model parameters derived from the Toowoomba monitoring were directly applied. Although significant limitations were present in the monitored dataset and NCP and TSS are not directly comparable, the Mass Balance Model was able to provide reasonable predictions against the measured TSS EMCs ($R^2=0.6895$, 2 points excluded). The modelling exercise highlighted the significant potential of surface-based models to represent urban catchments.

Case Study 3: Effect of Urban Land Use Type on Non-Coarse Particle Loads

A Mass Balance Model analysis was performed on two hypothetical urban catchments, each 1ha in area. The surface composition in terms of percentage coverage of roof, carpark, road and grass was set at expected values representative of Residential and Commercial land uses. A NCP load analysis was then performed based on the sequence of 36 storms monitored at Toowoomba. Compared to Residential land use, the predicted results indicated that the greater coverage of impervious surfaces associated with Commercial land use led to a 45% increase in total runoff and a 54% increase in total NCP load. As both runoff volumes and loads increased in approximately the same proportion, the mean EMCs for the two land use types are almost identical. This is consistent with TSS EMC statistics that have been compiled from a number of stormwater monitoring studies (Duncan 1999, BCC 2004). For both land uses, roof areas is a dominant source of runoff (~40%) but makes a minor contribution to particle load (7%). Roads were predicted to generate approximately 60 to 70% of the overall NCP load.

Case Study 4: Effect of Bare Soil Areas on Non-Coarse Particle Loads

As noted previously, bare soil areas can generate significant NCP loads primarily in storms in excess of 15 to 20mm rainfall. The sensitivity of introducing a bare soil area within the hypothetical 1ha Residential catchment was tested using the Mass Balance Model. It was assumed that the bare soil area constituted 10% of the total area, with an attendant reduction in the grassed area (from 58% to 48%). Compared with the Residential land use with no bare soil, a marginal 1% increase in total runoff volume was predicted. The change in total NCP load was substantial with a 57% increase predicted due to the introduction of bare soil. The analysis highlights the importance of minimising the extent of exposed bare soil areas within urban areas.

Case Study 5: Effect of Rainwater Tanks on Non-Coarse Particle Concentrations from Residential Areas

This case study was introduced to demonstrate how the Mass Balance Model can be applied to evaluate the adoption of rainwater tanks within a Residential catchment. The extraction of roof water from the stormwater flow may result in less dilution of the more concentrated particle sources, particularly road runoff. This effect may lead to an increase in NCP concentration during small-to-moderate storms. A tank storage and overflow algorithm was added to the Mass Balance Model of the hypothetical 1ha Residential catchment. A typical tank scenario involving storage of 10kL/household and a household roofwater use of 1.3 kL/ha/day was tested. Total runoff volume from the Toowoomba storm sequence was predicted to reduce by 10% due to capture of roof water. As roof water has a low NCP concentration, the net reduction in total NCP load is minor (3%). However, the mean EMC increased by 23% with the greatest elevations in NCP concentration associated with rainfalls less than 15 to 20mm. The analysis confirms that water quality impacts due to rainwater tanks warrants further investigation.

Case Study 6: Effect of Grass Swales on Non-Coarse Particle Loads from Road Surfaces

This case study was performed to illustrate how the Mass Balance Model can be adapted to simulate the stormwater treatment performance of a WSUD technique. In this case, the effect of a grass swale in reducing NCP loads from the Toowoomba road surface was modeled. The transport efficiency curve for the existing road kerb was modified to reflect the particle trapping capabilities of a grass swale. These modifications were based on research by Deletic (1999, 2001). The results of the analysis indicate that the NCP load from the road surface would be reduced by 68%, which is consistent with the mean measured swale performance compiled from 18 studies by Fletcher (2002).

12.2 Recommendations for Further Research

This project has covered a broad range of work and many individual aspects of stormwater quality prediction have been considered. Not all issues could be resolved within the scope of this dissertation. Specific recommendations for further research based on the outcomes of this study are:

- A standardised method to determine the particle concentration across a range of particle size gradations within urban stormwater samples needs to be widely adopted. A common methodology is necessary to make viable comparisons between different urban runoff studies. The laboratory method used in this thesis is considered to be a candidate for a suitable standard.
- All sampling methods evaluated in the sediment testing, including very frequent grab sampling, underestimated the proportion of Medium Particles (MP, 63-500 μ m) in the test flow. Further investigations should be made to improve the sampling capture of MPs by the flow splitter device.
- Traffic-induced particle contributions on road surfaces are potentially significant during storms, particularly for events longer than 5 hours. More research is required, including the collection of traffic data contiguous with stormwater runoff monitoring. Traffic parameters, such as vehicles during storm (VDS) and vehicle intensity during storm (VIDS) may provide a more accurate representation of this particle contribution compared to the simpler interburst period used in the Mass Balance Model. Rainfall drizzle time (time period during the storm with minor intensities in the range of 0.5 to 2 mm/hr)

may also be a factor that influences the traffic-induced particle contribution that occurs during long storms.

- The comparison of results from the Mass Balance Model against measured TSS data for a 35ha mixed land use catchment in Brisbane demonstrates a significant potential for surface based models to predict particle loads generated from large-scale urban areas. Further validation and refinement of this potential is needed by the collection of Non-Coarse Particle data from urban catchments.
- This study has focused on particle loads in runoff from urban surfaces. The methodologies that were developed in this thesis should be repeated to collect data for other pollutants such as nutrients and heavy metals. These efforts would greatly add to the knowledge base relating to stormwater pollutants generated from urban areas.
- Analysis using the Mass Balance Model highlighted a potential for the widespread adoption of rainwater tanks to cause an increase in Non-Coarse Particle concentration during small-to-moderate storms. The environmental implications of this effect warrant further investigation. Stormwater monitoring of urban areas with rainwater tanks should also be conducted to validate the predicted effects, which are based on a hypothetical Residential catchment.

13 References

- Abbot, J 1977, *Guidelines for the Calibration and Application of STORM*, Hydrologic Engineering Centre, Davis, California.
- Ahlman, S & Svensson, G 2002, 'Modelling Substance Flows in Urban Sewer Systems Using MATLAB/Simulink', Proceedings 9th International Conference on Urban Drainage, Portland, Oregon USA, 8-13 September 2002.
- Ahlman, S & Fletcher, T 2003, *Verification of a Process-based Stormwater Pollution Model for Brisbane Conditions: Interim Findings*, Chalmers University of Technology and Monash University, prepared for Brisbane City Council.
- APHA 1998, *Standard Methods for the Examination of Water and Wastewater*, 20th Edn, American Public Health Association, American Water Works Association, Water Pollution Control Federation, Washington D.C.
- Artina, S, Bolognesi, A, Liserra, T & Maglionico, M 2005, 'Comparision Between Simulation Tools on a Small Urban Storm Sewer Network', paper presented to 10th International Conference on Urban Drainage, Copenhagen, Denmark, 21-26 August 2005.
- Asplund, R, Ferguson, JF & Mar, BW 1982, 'Total Suspended Solids in Highway Runoff in Washington State', *Journal Environmental Engineering*, vol. 108, pp. 391-404.
- ASTM 2002, *Standard Test Method for Determining Sediment Concentration in Water Samples*, ASTM Designation D 3977-97 (Reapproved 2002), American Society for Testing and Materials.
- Athayde, DN, Shelley, PE, Driscoll, ED, Gaboury, D & Boyd, D 1983, *Results of the National Urban Runoff Program*, PB84-185537, United States EPA, Washington D.C.

- Ball, JE & Abustan, I 1995, 'An Investigation of Particle Size Distribution During Storm Events From an Urban Catchment', paper presented to 2nd International Symposium on Urban Stormwater Management, Melbourne, Australia, 11-13 July 1995.
- Ball, JE, Jenks, R & Aubourg, D 1996, 'Dry Weather Build-up of Constituents on Road Surfaces', Proceedings 7th International Conference on Urban Storm Drainage, Hanover, Germany.
- Ball, JE, Jenks, R & Aubourg, D 1998, 'Assessment of the Availability of Pollutant Constituents on Road Surfaces', *Science of the Total Environment*, vol. 209, no. 2-3, pp. 243-54.
- Ball, JE, Hogan, PM, Bately, GE & Brockbank, C 1994, 'Assessing the Quantity and Quality of Stormwater Runoff from Road Surfaces', Proceedings of Water Down Under '94, IEAustralia National Conference, Adelaide, Australia, 21-25 November 1994.
- Ball, JE, 2000, 'Modelling Contamination in Stormwater Runoff', Proceedings of Hydro 2000, 3rd International Hydrology and Water Resources Symposium, IEAustralia, Perth, Australia, 20-23 November 2000.
- Bannerman, RT, Owens, DW, Dodds, RB & Hornewer, NJ 1993, 'Sources of Pollutants in Wisconsin Stormwater', *Water Science and Technology, Proceedings of the IAWQ 1st International Conference on Diffuse (Nonpoint) Pollution: Sources, Prevention, Impact, Abatement*, vol. 28, no. 3-5, pp. 241-59.
- Barling, RD & Moore, ID 1993, 'The Role of Buffer Strips in the Management of Waterway Pollution', in J Woodfull, B Finlayson & TA McMahon (Eds.), *The Role of Buffer Strips in the Management of Waterway Pollution From Diffuse Urban and Rural Sources*, Canberra.
- Barrett, ME, Irish, LB, Malina, JF & Charbeneau, RJ 1998a, 'Characterisation of Highway Runoff in Austin, Texas Area', *Journal Environmental Engineering*, vol. 124, no. 131.

- Barrett, ME, Walsh, PM, Malina, JF & Charbeneau, RJ 1998b, 'Performance of Vegetative Control for Treating Highway Runoff', *Journal Environmental Engineering*, vol. 124, no. 11, pp. 1121-8.
- Barry, ME, McAlister, AB, Weber, TR, Abal, E & Scott, N 2004, 'Impacts of Stormwater Runoff From Roads in South East Queensland', paper presented to WSUD 2004 Cities as Catchments Conference, Adelaide, South Australia, 21-24 November 2004.
- Barten, JM & Jahnke, E 1997, *Suburban Lawn Runoff Water Quality in the Twin Cities Metropolitan Area, 1996 and 1997*, Suburban Hennepin Regional Park District.
- BCC 2003, *Guidelines for Pollutant Export Modelling in Brisbane, Version 7*, Brisbane City Council.
- 2004, *Brisbane City Council Stormwater Quality Monitoring Program 2002/2003*. Brisbane City Council.
- Beach, D 2003, *Coastal Sprawl: The Effect of Urban Design on Aquatic Ecosystems in the United States*, Pew Oceans Commission, Arlington, Virginia.
- Bent, GC, Gray, JR, Smith, KP & Glysson, GD 2001, *A Synopsis of Technical Issues for Monitoring Sediment in Highway and Urban Runoff*, USGS OFR 00-497, U.S. Geological Survey.
- Birch, GF & Scollen, A 2003, 'Heavy Metals in Road Dust, Gully Pots and Parkland Soils in a Highly Urbanised Sub-catchment of Port Jackson, Australia', *Australian Journal of Soil Research*, vol. 41, pp. 1329-42.
- Bonta, JV 2001, 'Modification and Performance of the Coshocton Wheel with the Modified Drop-box Weir', *Journal of Soil and Water Conservation*, vol. 57, no. 6.

- Brezonik, PL & Stadelmann, TH 2002, 'Analysis and Predictive Models of Stormwater Runoff Volumes, Loads and Pollutant Concentrations from Watersheds in the Twin Cities Metropolitan Area, Minnesota, USA', *Water Research*, vol. 36, no. 7.
- Butcher, JB, 2006, 'Buildup, Washoff, and Event Mean Concentrations', *Journal of the American Water Resources Association*, vol. 39, no. 6, pp. 1521-1528.
- Caltrans 2000, *Caltrans Guidance Manual: Stormwater Monitoring Protocols*, CTSW-RT-00-005, July 2000. California Department of Transportation.
- Characklis, GW & Wiesner, MR 1997, 'Particles, Metals and Water Quality in Runoff from Large Urban Watershed', *Journal Environmental Engineering*, vol. 123, no. 8, pp. 753-9.
- Charbeneau, RJ & Barrett, ME 1998, 'Evaluation of Methods for Estimating Stormwater Pollutant Loads', *Water Environment Research*, vol. 70, no. 7, pp. 1295-302.
- Chebbo, G & Bachoc, A 1992, 'Characterization of Suspended Solids in Urban Wet Weather Discharges', *Water Science and Technology*, vol. 25, no. 8, pp. 171-9.
- Chen, J & Adams BJ 2006, 'Analytical Urban Storm Water Quality Models Based on Pollutant Buildup and Washoff Processes', *Journal of Environmental Engineering*, ASCE, vol. 132, no. 10, pp. 1314-1330.
- Chiew, FHS, Duncan, H & Smith, W 1997a, 'Modelling Pollutant Buildup and Washoff - Keep it Simple', Proceedings Wai-Whenua 1997, 24th Hydrology and Water Resources Symposium, Auckland, NZ, 24-28 November 1997, pp. 131-136.
- Chiew, FHS, Mudgway, LB, Duncan, HP & McMahon, TA 1997b, *Urban Stormwater Pollution Industry Report*, CRC for Catchment Hydrology, Australia.

- Chui, TW, Mar, BW & Horner, RR 1982, 'Pollutant Loading Model for Highway Runoff', *Journal Environmental Engineering*, vol. 108, no. EE6, pp. 1193-210.
- City Design 2000, *Guidelines for Pollutant Export Modelling in Brisbane*, Waterways Program, Brisbane City Council.
- Clarke, DL, Asplund, R, Ferguson, J & Mar, BW 1981, 'Composite Sampling of Highway Runoff', *Journal Environmental Engineering*, vol. 107, pp. 1067-81.
- Coombes, PJ, Kuczera, G & Kalma, JD 2002a, 'Economic, Water Quantity and Quality Results From a House With a Rainwater Tank in the Inner City', Proceedings 27th Hydrology and Water Resources Conference, Melbourne, Australia.
- Coombes, PJ, Frost, A, Kuczera, G, O'Loughlin, GG & Lees, S 2002b, 'Rainwater Tank Options for Stormwater Management in the Upper Parramatta River Catchment', Proceedings 27th Hydrology and Water Resources Conference, Melbourne, Australia.
- Coombes, PJ, Spinks, A, Evans, C & Dunstan, H 2004, 'Performance of Rainwater Tanks at an Inner City House in Carrington NSW During a Drought', paper presented to WSUD 2004 Cities as Catchments Conference, Adelaide, South Australia, 21-24 November 2004.
- Crabtree, B, Moy, F & Whitehead, M 2005, 'Pollutants in Highway Runoff', paper presented to 10th International Conference on Urban Drainage, Copenhagen, Denmark, 21-26 August 2005.
- Davies-Colley, RJ & Smith, DG 2001, 'Dialogue on Water Issues - Turbidity, Suspended Sediment and Water Clarity: A Review', *Journal of the American Water Resources Association*, vol. 37, no. 5, pp. 1085-101.
- DeGroot, AJ 1995, 'Metals and Sediment: a Global Perspective', in AE Herbert (ed.), *Metal Contaminated Aquatic Sediment*, Ann Arbor Press, pp. 1-20.

- de Ridder, SA, Darcy, SI, Calvert, PP & Lenhart, JH 2002, 'Influence of Analytical Method, Data Summarization Method and Particle Size on Total Suspended Solids Removal Efficiency', Proceedings 9th International Conference on Urban Drainage, Portland, Oregon USA, 8-13 September 2002.
- Deletic, AB 1999, 'Sediment Behaviour in Grass Filter Strips', *Water Science and Technology*, vol. 39, no. 9, pp. 129-36.
- 2001, 'Modelling of Water and Sediment Transport Over Grassed Areas', *Journal of Hydrology*, vol. 248, pp. 168-82.
- Deletic, AB & Maksimovic, CT 1998, 'Evaluation of Water Quality Factors in Storm Runoff From Paved Areas', *Journal Environmental Engineering*, vol. 124, no. 9, pp. 869-79.
- Deletic, AB & Orr, DW 2005, 'Pollution Buildup on Road Surfaces', *Journal Environmental Engineering*, vol. 131, no. 1, pp. 49-59.
- Deletic, AB, Maksimovic, C & Ivetic, M 1997, 'Modelling of Storm Washoff of Suspended Solids From Impervious Surfaces', *Journal of Hydraulic Research*, vol. 35, no. 1, pp. 99-118.
- DEP, M 2003, *Runoff Quality: A Simpler Alternative to the TSS Standards*, viewed 17/6/05 <<http://mainegov-images.informe.org/dep/blwq/docstand/stormwater/group/qualdiscstand.pdf>>.
- Desbordes, M & Servat, E 1987, 'Transport Model over Urban Catchment Surfaces Regarding TSS, BOD5 and COD', Proceedings 4th International Conference on Urban Storm Drainage, Lausanne, Switzerland, pp 75-76.
- DNR 1992, *Queensland Urban Drainage Manual*. Queensland Department of Natural Resources with Brisbane City Council and IMEAQ, Volumes 1 & 2, September 1992.

- Drapper, D 1998, *Road Runoff Water Quality in South-east Queensland*, Department of Main Roads, Queensland (unpublished).
- Drapper, D, Tomlinson, RB & Williams, PR 1999, 'An Investigation of the Quality of Stormwater Runoff from Road Pavements: A South-East Queensland Case Study', Proceedings 8th International Conference on Urban Stormwater Drainage, Sydney, Australia, 30 August- 3 September 1999.
- Driscoll, ED 1986, *Lognormality of Point and Nonpoint Source Pollutant Concentrations*, EPA-600/9-86-023, United States EPA, Orlando, Florida.
- Driscoll, ED, Shelley, PE & Strecker, EW 1990, *Pollutant Loadings and Impacts from Highway Stormwater Runoff, Volumes I-IV*, FHWA/RD-88-006-9, Federal Highway Administration, Woodward-Clyde Consultants, Oakland, CA.
- Dudley, LA 1995, 'Low Cost Automatic Stormwater Sampler', in HC Torno (ed.), *Stormwater NPDES Related Monitoring Needs*, ASCE, Crested Butte, Colorado, pp. 599-608.
- Duncan, H 1995, *A Review of Urban Storm Water Quality Processes*, Report 95/9, CRC for Catchment Hydrology.
- Duncan, HP 1999, *Urban Stormwater Quality: A Statistical Overview*, Report 99/3, CRC for Catchment Hydrology.
- Egodawatta, P, Goonetilleke, A, Ayoko GA, Thomas, E 2006, Understanding the Interrelationships Between Stormwater Quality and Rainfall and Runoff Factors in Residential Catchments', Proceedings 7th International Conference on Urban Drainage Modelling and 4th International Conference on Water Sensitive Urban Design, Melbourne, Australia, 2-7 April, 2006
- Ekern, PC 1954, 'Raindrop Impact as a Measure of Storm Erosivity', *Soil Science Soc. Am. Proc.*, vol. 18, pp. 212-6.

- Ellis, JB & Harrop, DO 1984, 'Variations in Solids Loadings to Roadside Gully Pots', *The Science of the Total Environment*, vol. 33, pp. 203-11.
- EPA 2001, *Method 1684 Total, Fixed and Volatile Solids in Water, Solids and Biosolids*, United States EPA Report 821/R-01-015, Washington D.C.
- Fletcher, T 2002, 'Vegetated Swales: Simple but are They Effective?' paper presented to 2nd National Conference on Water Sensitive Urban Design, Brisbane, 2-4 September 2004.
- Francey, M, Duncan, H, Deletic, AB & Fletcher, T 2004, 'An Advance in Modelling Pollutant Loads in Urban Runoff', paper presented to 6th International Conference on Urban Drainage Modelling, Dresden, Germany, 2004.
- Francey, M, Duncan, H, Deletic, AB & Fletcher, TD 2005, 'Using a Simple Model to Predict the Behaviour of Pollutant Loads', paper presented to 10th International Conference on Urban Drainage, Copenhagen, Denmark, 21-26 August 2005.
- Furumai, H, Hijika, Y & Nakajima, F 2001, 'Modeling and Field Survey of Washoff Behaviour of Suspended Particles from Roofs and Roads', Urban Drainage Modelling, Proceedings Speciality Symposium of World Water and Envir. Resources Congress, Orlando, Florida, 20-24 May 2001.
- Gabet, EJ & Dunne, T 2003, 'Sediment Detachment by Rain Power', *Water Resources Research*, vol. 39, no. 1, pp. 1-12.
- Gilley, J, Woolhiser, D & McWhorter, D 1985, 'Interill Soil Erosion - Part II: Testing and Use of Model Equations', *Transactions ASAE*, vol. 28, no. 1, pp. 154-9.
- Gippel, CJ 1989, *The Use of Turbidity Instruments to Measure Stream Water Suspended Sediment Concentration*, Department of Geography and Oceanography, University College, Australian Defence Force Academy, Canberra ACT.

- 1995, 'Potential of Turbidity Monitoring for Measuring the Transport of Suspended Solids in Streams', *Hydrological Processes*, vol. 9, pp. 83-97.
- Gnecco, I, Berretta, LG, Lanza, LG & La Barbera, P 2005, 'Quality of Stormwater Runoff From Paved Surfaces of Two Production Sites', paper presented to 10th International Conference on Urban Drainage, Copenhagen, Denmark, 21-26 August 2005.
- Goyen, AG & O'Loughlin, GG 1999, 'Examining the Basic Building Blocks of Urban Runoff', 8th International Urban Storm Drainage Proceedings, Sydney, Australia, 30 August - 3 September 1999.
- Gray, JR & Fisk, GG 1992, 'Monitoring radionuclide and suspended-sediment transport in the Little Colorado River Basin, Arizona and New Mexico, USA', Erosion and Sediment Transport Monitoring Programs in River Basins. Proceedings of the International Symposium, Oslo, Norway, August 24-28, 1992.
- Gray, JR, Glysson, GD, Turcious, LM & Schwarz, GE 2000, *Comparability of Suspended-Sediment Concentration and Total Suspended Solids Data*, US Geological Survey WRIR 00-4191.
- Greb, SR & Bannerman, RT 1997, 'Influence of Particle Size on Wet Pond Effectiveness', *Water Environ. Research*, vol. 69, no. 6, pp. 1134 - 8.
- Gromaire-Mertz, MC, Garnaud, S, Gonzalez, A & Chebbo, G 1999, 'Characterisation of Urban Runoff Pollution in Paris', *Water Science and Technology*, vol. 39, no. 2, pp. 1-8.
- Grottker, W 1987, 'Runoff Quality From a Street With Medium Traffic Loading', *The Science of the Total Environment*, vol. 59, pp. 457-66.
- Guo, J & Urbonas, B 1996, 'Maximised Detention Volume Determined by Runoff Capture Probabilistic Models 1. Runoff Volumes', *Water Resources Research*, vol. 34, no. 12, pp. 3421-31.

- Gupta, MK, Agnew, RW & Kobriger, NP 1981, *Constituents of Highway Runoff, Vo. I: State-of-the-Art Report*, FHWA/RD-81/042, Federal Highway Administration.
- Haiping, Z & Yamada, K 1998, 'Simulation of Nonpoint Source Pollutant Loadings From Urban Area During Rainfall: An Application of a Physically Based Distributed Model', *Water Science and Technology*, vol. 38, no. 10, pp. 199-206.
- Harper, HH 1998, *Stormwater Chemistry and Water Quality*, Report 045PL, Environmental Research and Design, downloaded 8/3/2005
<http://www.stormwaterauthority.org/Library/045PLChemistry.pdf>
- Harrison, RM & Wilson, SJW 1985, 'The Chemical Composition of Highway Drainage Waters II: Major Ions and Selected Trace Metals', *The Science of the Total Environment*, vol. 43, pp. 63-77.
- Haster, TW & James, WP 1994, 'Predicting Sediment Yield in Storm Water Runoff From Urban Areas', *Journal of Water Resources Planning and Management*, vol. 120, no. 5, pp. 630-50.
- Hijioka, Y, Nakajima, F & Furumai, H 2001, 'Modified Models of Wash-Off from Roofs and Roads for Non-Point Pollution Analysis during First Flush Phenomena' Urban Drainage Modelling. Proceedings Speciality Symposium of World Water and Envir. Resources Congress, Orlando, Florida, 20-24 May 2001.
- Hogan, PM 2000, 'Stormwater Quantity and Quality From Road Surfaces'. PhD Dissertation, School of Civil and Environmental Engineering, University of New South Wales, Sydney, Australia.
- Horner, RR & Mar, BW 1983, 'Guide for Water Quality Impact Assessment of Highway Operations and Maintenance', *Transportation Research Record*, vol. 948, pp. 31-40.

- Horowitz, AJ, Smith, JJ & Elrick, KA 2001, *Selected Laboratory Evaluations of the Whole-Water Sample-Splitting Capabilities of a Prototype Fourteen-Liter Teflon Churn Splitter*, US Geological Survey Open File Report 01-386.
- Horton, RE 1933, 'The Role of Infiltration in the Hydrologic Cycle', *Trans. Am. Geophys. Union*, vol. 145, pp. 446-60.
- Huber, WC 1993, 'Contaminant Transport in Surface Water', in DR Maidment (ed.), *Handbook of Hydrology*, McGraw-Hill, New York, N.Y.
- Huber, WC & Dickinson, RE 1988, *Storm Water Management Model Users Manual, Version 4*, United States EPA/600/3-88/001a, Athens, Georgia.
- Hwang, RB, Pasha, VM & Racin, JA 1997, 'Flume Calibration Process for Continuous Composite Sampling of Non-Point Runoff', Proceedings of the 35th Heat Transfer and Fluid Mechanics Institute, Sacramento, California, May 29-30 1997.
- IDF 1999, *Passive Flow Proportional Sampler*. Technical Brief IRF Case 99-009, downloaded 3/4/2004 www.irf.uro.uidaho.edu, Idaho Research Foundation.
- IEAust 2003, *Australian Runoff Quality*, Institute of Engineers, Australia National Committee on Water Engineering, Draft Report.
- Irish, LB & Barrett, ME 1998, 'Use of Regression Models for Analysing Highway Stormwater Loads', *Journal of Environmental Engineering*, vol. 124, no. 10, pp. 987-93.
- Irish, LB, Lesso, WG, Barrett, ME, Malina, JF, Charbeneau, RJ & Ward, GH 1995, *An Evaluation of the Factors Affecting the Quality of Highway Runoff in the Austin, Texas Area*, Centre for Research in Water Resources Report CRWR 264, September 1995.

- James, RB 2003, *Measurement and BMP Removal of Suspended Material in Storm Water Runoff*, downloaded 5/6/2004 www.stormwater-resources.com
- Johanson, RC, Imhoff, JC, Kittle, JL & Donigan, S 1984, *Hydrological Simulation Program - Fortran (HSPF): User Manual for Release 8*, United States EPA-600/3/84-066, Athens, Georgia.
- Kerri, KD, Racin, JA & Howell, RB 1985, 'Forecasting Pollutant Loads From Highway Runoff', *Transportation Research Record*, vol. 1017, pp. 39-46.
- Kim, L 2002, 'Monitoring and Modeling of Pollutant Mass in Urban Runoff: Washoff, Buildup and Litter', PhD dissertation, University of California.
- Kim, L, Kim, KB, Lim, KB & Ko, SO 2005, 'Characteristics of Washed-off Pollutants and Dynamic EMCs in a Parking Lot and a Bridge During Storms', paper presented to 10th International Conference on Urban Drainage, Copenhagen, Denmark, 21-26 August 2005.
- Kuo, JT, Yan, YL & Li, KC 1993, 'A Simplified Computer Model For Nonpoint Source Pollution in a Small Urban Area', *Water Science and Technology*, vol. 28, pp. 701-6.
- Ladson, T, Walsh, C, Fletcher, T & Cornish, S 2003, 'Beyond the 10% Rule, Improving Streams by Retrofitting in Suburbs to Decrease the Connections Between Impervious Surfaces and Waterways', *Catchword. Newsletter of the CRC for Catchment Hydrology*, vol. 123, pp. 9-10.
- Lawler, DM & Brown, RM 1992, 'A Simple and Inexpensive Turbidity Meter for the Estimation of Suspended Sediment Concentrations', *Hydrological Processes*, vol. 6, pp. 159-68.
- Laws, JO 1941, 'Measurements of Fall-Velocity of Water Drops and Raindrops', *Transactions of the American Geophysical Union*, vol. 22, p. 709.

- Laws, JO & Parsons, DA 1943, 'The Relation of Raindrop Size to Intensity', *Transactions of the American Geophysical Union*, vol. 24, p. 452.
- Le Boutillier, DW, Kells, JA & Putz, GJ 2000, 'Prediction of Pollutant Load in Stormwater Runoff From An Urban Residential Area', *Canadian Water Resources Journal*, vol. 25, no. 4.
- Lee, JG & Heaney, JP 2003, 'Estimation of Urban Imperviousness and its Impacts on Storm Water Systems', *Journal of Water Resources and Planning*, vol. 129, no. 5.
- Leecaster, MK, Schiff, K & Tiefenthaler, LL 2002, 'Assessment of Efficient Sampling Designs for Urban Stormwater Monitoring', *Water Research*, vol. 36, no. 6.
- Lewis, J 1996, 'Turbidity-Controlled Suspended Sediment Sampling for Runoff-Event Load Estimation', *Water Resources Research*, vol. 32, no. 7, pp. 2299-310.
- Lloyd, SD 2001, *Water Sensitive Urban Design in the Australian Context*, Technical Report 01/7, CRC for Catchment Hydrology.
- Lloyd, SD & Wong, THF 1999, 'Particulates, Associated Pollutants and Urban Stormwater Treatment', 8th International Urban Storm Drainage Proceedings, Sydney, Australia, 30 August - 3 September 1999.
- Ma, J, Khan, S, Li, Y, Ha, H, Lau, S, Kayhanian, M & Strenstrom, MK 2002, 'Implication of Oil and Grease Measurement in Stormwater Management Systems', paper presented to StormCon 2002, North American Surface Water Quality Conference, Florida, USA, August 12-15, 2002.
- Madge, B 2004, *Analysis of Particulate-Bound Nutrients in Urban Stormwater*. United States EPA National Risk Management Research Laboratory, downloaded 31/8/2004
http://www.epa.gov/ORD/NRMRL/scienceforum/madge_b.htm

- Maestre, A & Pitt, RE 2005, *Identification of Significant Factors Affecting Stormwater Quality Using the NSQD*, University of Alabama.
- Malmquist, P 1978, 'Atmospheric Fallout and Street Cleaning- Effects of Urban Stormwater and Snow', *Prog. Wat. Tech.*, vol. 10, pp. 495-505.
- Marsalek, J, Watt, WE, Anderson, BC & Jaskot, C 1997, 'Physical and Chemical Characteristics of Sediments From a Stormwater Management Pond', *Water Quality Research Journal Canada*, vol. 32, no. 1, pp. 89-100.
- McCann, K & Michael, J 1999, *Nutrient Content and Release Rate in Water of Oak Leaves*, City of Orlando Stormwater Utility Bureau.
- McCool, DK, Brown, LC, Foster, GR, Mutchler, CK & Meyer, LD 1987, 'Revised Slope Steepness Factor for the Universal Soil Loss Equation', *Transactions ASAE*, vol. 30, no. 1387-1396.
- MDID 2001, *Urban Stormwater Management Manual for Malaysia*. Malaysian Department of Irrigation and Drainage, downloaded 24/8/2004
<http://agrolink.moa.my/did/river/stormwater/>
- Memon, FA & Butler, D 2005, 'Characteristics of Pollutants Washed Off From Road Surfaces During Wet Weather', *Urban Water Journal*, vol. 2, no. 3, pp. 171-182.
- Metcalf & Eddy Inc., University of Florida and Water Resources Engineers Inc., 1971, *Storm Water Management Model, Volume 1: Final Report*. EPA Report 11024 DOC 07-71, US Environmental Protection Agency, Washington D.C., USA.
- Meyer, LD 1981, 'How Rain Intensity Affects Interill Erosion', *Transactions ASSE*, vol. 24, pp. 1472-5.

- Meyer, LD & Wischmeier, WH 1969, 'Mathematical Simulation of the Process of Soil Erosion by Water', *Transactions of the American Society of Agricultural Engineers*, vol. 12, no. 6, pp. 754-62.
- Millar, RG 1999, 'Analytical Determination of Pollutant Wash-off Parameters', *Journal of Environmental Engineering*, vol. 125, no. 10, pp. 989-992.
- Mitchell, G, McCarthy, D, Deletic, AB & Fletcher, T 2005, *Development of Novel Integrated Stormwater Treatment and Re-Use Systems: Assessing Storage Capacity Requirements*, Institute for Sustainable Water Resources, Monash University.
- Mitchell, VG, Mein, RG & McMahon, TA 2002, 'Evaluating the Resource Potential of Stormwater and Wastewater; An Australian Perspective', *Water Resources*, vol. 2, no. 1, pp. 19-22.
- Moss, AJ & Green, P 1983, 'Movement of Solids in Air and Water by Raindrop Impact: Effect of Drop-size and Water-Depth Variations', *Australian Journal of Soil Research*, vol. 21, pp. 257-69.
- Murakami, M, Nakajima, F & Furumai, H 2004, 'Modelling of Runoff Behaviour of Particle-bound Polycyclic Aromatic Hydrocarbons (PAHs) from Roads and Roofs', *Water Research*, vol. 38, pp. 4475-83.
- Musgrave, GW 1947, 'Quantitative Evaluation of Factors in Water Erosion - A First Approximation', *Journal of Soil and Water Conservation*, vol. 2, no. 133-138.
- Muthukaruppan, M, Chiew, FHS & Wong, THF 2002, 'Characterisation of Urban Street Surface Solids', paper presented to Hydrology and Water Resources Symposium 2002, Melbourne, Australia.
- Nakamura, E 1984, 'Factors Affecting Stormwater Quality Decay Coefficient', *Proceedings of the 3rd International Conference on Urban Storm Drainage*, Goteberg, Sweden, vol. 3, pp. 979-988.

- Nearing, MA, Foster, GR, Lane, LJ & Finkner, SC 1989, 'A Process-based Soil Erosion Model for USDA-Water Erosion Prediction Project Technology', *Transactions ASAE*, vol. 32, no. 5, pp. 1587-93.
- Neary, VS, Neel, TC & Dewey, JB 2002, 'Pollutant Washoff and Loading from Parking Lots in Cookeville, Tennessee', *Global Solutions for Urban Drainage. Proceedings of the 9th International Conference on Urban Drainage, Portland Oregon, 8-13 September 2002.*
- Newham, LTH, Croke, BFW & Jakeman, AJ 2001, 'Design of Water Quality Monitoring Programs and Automatic Sampling Techniques', paper presented to 3rd Australian Streams Management Conference, Brisbane, 27-29 August 2001.
- O'Loughlin, GG 1993, *The ILSAX Program for Urban Stormwater Drainage Design and Analysis (Users Manual for Microcomputer Version V2.13)*, University of Technology, Sydney.
- O'Loughlin, GG & Stack, B 2003, *DRAINS User Manual*, Watercom Pty Ltd.
- Osuch-Pajdzinska, E & Zawilski, M 1998, 'Model of Storm Sewer Discharge. I: Description', *Journal Environmental Engineering*, vol. 124, no. 7, pp. 593-9.
- Phillips, BC & Thompson, G 2002, 'Virtual Stormwater Management Planning in the 21st Century', *Proceedings of the 9th International Journal on Urban Drainage, Portland, Oregon.*
- Pisano, MA 1976, 'Nonpoint Sources of Pollution - A Federal Perspective', *Journal Environmental Engineering, Proceedings ASCE*, vol. 102, no. EE1.
- Pitt, RE 1979, *Demonstration of Nonpoint Pollution Abatement Through Improved Street Cleaning Practices*, United States EPA-600/2-79-161, Cincinnati.

- Pitt, RE & McLean, J 1986, *Toronto Area Watershed Management Strategy Study. Humber River Pilot Watershed Project*, Ontario Ministry of the Environment, Toronto, Canada.
- Pitt, RE & Voorhees, J 2000, *The Source Loading and Management Model (SLAMM): A Water Quality Management Planning Model for Urban Storm Water Runoff*, University of Alabama.
- Pitt, RE, Maestre, A & Morquecho, R 2004, *Findings from the National Stormwater Quality Database (NSQD)*, United States EPA Centre for Watershed Protection.
- Pitt, RE, Field, R, Lalor, M & Brown, M 1995, 'Urban Stormwater Toxic Pollutants: Assessment, Sources and Treatability', *Water Environment Research*, vol. 67, no. 33, pp. 260-75.
- Planning Plus 2003a, *Water Sensitive Planning Guide for the Sydney Region*, Sydney Coastal Councils, WSROC and UPRCT, Sydney.
- 2003b, *Water Smart Model Planning Provisions for the Lower Hunter and Central Coast region*, LHCC REMS.
- Pratt, CJ & Adams, JRW 1981, 'Sediment Washoff Into Roadside Gullies' Urban Stormwater Quality, Management and Planning. Proceedings of the 2nd International Conference on Urban Stormwater Drainage, Urbana, Illinois, USA, June 14-19.
- Proffitt, APB & Rose, CW 1991, 'Soil Erosion Processes. I. The Relative Importance of Rainfall Detachment and Runoff Entrainment', *Australian Journal of Soil Research*, vol. 29, pp. 671-683.
- Rabanal, FI & Grizzard, TJ 1995, 'Concentrations of Selected Constituents in Runoff from Impervious Surfaces in Four Urban Catchments of Different Landuse', paper presented to 4th Biennial Stormwater Research Conference, Florida.

- Randall, W, Ellis, K, Grizzard, TJ & Knocke, WR 1982, 'Urban Runoff Pollutant Removal by Sedimentation', in W DeGroot (ed.), *Stormwater Retention Facilities - Planning, Designing, Operation and Maintenance*, ASCE, New Hampshire, pp. 291-300.
- Regenmorter, LC, Kayhanian, M, Chappell, RW, Burgessor, T & Tsay, K 2002, 'Particles and the Associated Pollutant Concentrations in Highway Runoff in Lake Tahoe, California', paper presented to StormCon 2003, North American Surface Water Quality Conference, Florida, USA, 12-15 August 2002.
- Reinertsen, TR 1981, 'Quality of Stormwater Runoff From Streets', Proceedings of the 2nd International Conference on Urban Stormwater Drainage, Urbana, Illinois, USA, June 14-19.
- Rose, CW 1960, 'Soil Detachment Caused by Rainfall', *Soil Science*, vol. 89, pp. 28-35.
- Rushton, B 2001, 'Low-Impact Parking Lot Design Reduces Runoff and Pollutant Loads', *Journal of Water Resources Planning and Management*, vol. 127, no. 3, pp. 172-79.
- Sansalone, JJ & Buchberger, SG 1997, 'Partitioning and First Flush of Metals in Urban Roadway Storm Water', *Journal Environmental Engineering*, vol. 123, no. 2, pp.134-43.
- Sansalone, JJ & Tittlebaum, ME 2001, 'Storm Water Transport of Particulate Matter From Elevated Urban Transportation Corridors into Waterways of Louisiana - The Role of Partitioning and Implications for Treatment', in *Louisiana Water Resources Research Institute Annual Technical Report*.
- Sansalone, JJ, Koran, JM, Smithson, JA & Buchberger, SG 1998, 'Physical Characteristics of Urban Roadway Solids Transported During Rain Events', *Journal Environmental Engineering*, vol. 124, no. 5, pp. 427-40.

- Sartor, JD & Boyd, GB 1972, *Water Pollution Aspects of Street Surface Contaminants*, United States EPA-R2-72-081, USEPA Office of Research and Monitoring, Washington D.C.
- Sartor, JD, Boyd, GB & Agardy, FJ 1974, 'Water Pollution Aspects of Street Surface Contaminants', *Journal Water Pollution Control Federation*, vol. 46, no. 3, pp. 458-67.
- Schueler, TR 1987, *Controlling Urban Runoff: A Practical Manual for Planning and Designing Urban BMPs*, Metropolitan Washington Council of Governments, Washington D.C., USA.
- 1992, 'Mitigation of the Impacts of Urbanisation', in WJ Snodgrass & JC P'Ng (eds), *Implementation of Water Pollution Control Measures in Ontario*, University of Toronto Press, Ontario, Canada.
- Sharpin, MG 1995, 'Suspended Sediment Characteristics in the Canberra Region', paper presented to 2nd International Symposium on Urban Stormwater Management, Melbourne, Australia, 11-13 July 1995.
- Sheng, Y, Sansalone, JJ & Calomino, F 2005, 'Estimation of Solids Loadings to Rainfall-runoff Unit Operations Using a Pollutant Hydrograph Concept for Source Area Watersheds', paper presented to 10th International Conference on Urban Drainage, Copenhagen, Denmark, 21-26 August 2005.
- Shoemaker, LM, Lahlou, M, Bryer, D, Kummar, D & Kratt, K 1997, *Compendium of Tools for Watershed Assessment and TMDL Development*, United States EPA 841-B-97-006, Washington D.C.
- Smith, KP 2000, *The Effectiveness of Common Best Management Practices in Reducing Total Suspended Solid Concentrations in Highway Runoff Along The Southeast Expressway, Boston, Massachusetts*. US Geological Survey.
- Spanberg, A & Niemczynowicz, J 1992, 'High Resolution Measurements of Pollution Washoff From An Asphalt Surface', *Nordic Hydrology*, vol. 23, no. 4, pp. 245-56.

- Stein, SM, Graziano, FR & Young, GK 1998, 'Sheetflow Water Quality Monitoring Device', paper presented to The 25th Annual Conference on Water Resources Planning and Management, Chicago, Illinois, June 7-10, 1998.
- Strynchuk, J, Royal, J & England, G 1999, *Grass and Leaf Decomposition and Nutrient Release Study Under Wet Conditions*, Brevard County Florida Stormwater Utility.
- Svensson, G 1987, 'Modelling of Solids and Metal Transport From Small Urban Watersheds', PhD Dissertation, Department of Sanitary Engineering, Chalmers University.
- Tan, S-K, 1989, 'Rainfall and Soil Detachment', *Journal of Hydraulic Research*, vol. 27, no. 5, pp. 699-715.
- Terstriep, ML & Stall, JB 1974, *The Illinois Urban Drainage Area Simulator ILLUDAS*, Illinois State Water Survey Bulletin 58, Urbana.
- Thomson, NR, McBean, EA, Snodgrass, W & Monstrenko, IB 1997, 'Highway Stormwater Runoff Quality: Development of Surrogate Parameter Relationships', *Water, Air and Soil Pollution*, vol. 94, no. 3-4.
- Tomanovic, A & Maksimovic, C 1996, 'Improved Modelling of Suspended Solids Discharge From Asphalt Surface During Storm Event', Proceedings of the 1995 2nd IAWQ International Specialized Conference and Symposia on Diffuse Pollution, Aug 13-18 1995, Prague, Czech Republic.
- Trimble, SW 1997, 'Contribution of Stream Channel Erosion to Sediment Yield From An Urbanising Watershed', *Science*, vol. 278, pp. 1442-4.
- Tsihintzis, VA & Hamid, R 1997, 'Urban Stormwater Quantity/Quality Modeling Using the SCS Method and Empirical Equations', *Journal of the American Water Resources Association*, vol. 33, no. 1, pp. 163-76.

- Turner, AK, McMahon, TA & Srikanthan, R 1985, 'Rainfall Intensity and Overland Flow in Relation to Soil Erosion Studies for Tropical Lands', in *Soil Erosion Management*, ACIAR Proceedings Series, pp. 24-31.
- Urbonas, B 1991, 'Summary of Stormwater Management Practices', paper presented to Water Resources Planning and Management and Urban Water Management, 18th Annual Conference and Symposium, New Orleans.
- US EPA 1999, *Measurement of TSS in Runoff*. US Environmental Protection Agency Issue Paper, prepared by URS Greiner Woodward Clyde, November 1999.
- US ACE 1995, *Engineering and Design - Sedimentation Investigations of Rivers and Reservoirs*, EM 1110-2-4000, US Army Corps of Engineers, October 1995.
- US DA 1979, *Field Manual for Research in Agricultural Hydrology*, US Department of Agriculture, Office of Research and Development, Washington DC.
- US EPA 1983, *Results of the National Urban Runoff Program*, US Environmental Protection Agency Report 84-185552, Washington D.C.
- USGS 2000a, *USGS Policy. Collection and Use of Total Suspended Solids Data*, US Geological Survey, Offices of Water Quality and Surface Water, Technical Memorandum November 27, 2000.
- 2000b, *Comparison of Water-Quality Samples Collected by Siphon Samplers and Automatic Samplers in Wisconsin*, US Geological Survey Fact Sheet FS-067-00, May 2000.
- van Dijk, AIJM 2002, 'Water and Sediment Dynamics in Bench-terraced Agricultural Steeplands in West Java, Indonesia', PhD dissertation, Vrije Universiteit.
- van Dijk, AIJM, Bruijnzeel, LA & Rosewell, CJ 2002, 'Rainfall Intensity - Kinetic Energy Relationships: A Critical Appraisal', *Journal of Hydrology*, vol. 261, pp. 1-23.

- Vaze, J & Chiew, FHS 2002, 'Experimental Study of Pollutant Accumulation on an Urban Road Surface', *Urban Water*, vol. 4, no. 4.
- 2003, 'Study of Pollutant Washoff From Small Impervious Experimental Plots', *Water Resources Research*, vol. 39, no. 6.
- Virginia DEQ 2003, *Preliminary Report of the Low Impact Development Assessment Task Force*, Department of Environmental Quality, Commonwealth of Virginia, November 2003.
- Walsh, CJ, Leonard, AW, Ladson, AR & Fletcher, TD 2004, *Urban Stormwater and the Ecology of Streams*, CRC for Freshwater Ecology & CRC for Catchment Hydrology, Canberra.
- Waschbusch, RJ, Seibig, WR & Bannerman, RT 1999, *Sources of Phosphorus in Stormwater and Street Dirt From Two Urban Residential Basins in Madison, Wisconsin, 1994-95*, Water Resources Investigations Report 99-4021, US Geological Survey.
- Westerlund, C, Viklander, M & Hernebring, C 2005, 'Modelling of Snowmelt and Rainfall Runoff - Dynamics of Road Runoff and Suspended Solid Transport', paper presented to 10th International Conference on Urban Drainage, Copenhagen, Denmark, 21-26 August 2005.
- White, MJ 1989, 'Modelling of Urban Stormwater Pollution, Jamison Park, Sydney', paper presented to Proc. of the Int. Hydrology and Water Resources Symposium, Christchurch, NZ.
- Willems, P 2005, 'Random Number Generator or Sewer Water Quality Model?' paper presented to 10th International Conference on Urban Drainage, Copenhagen, Denmark, 21-26 August 2005.
- Wischmeier, WH & Smith, DD 1978, *Predicting Rainfall Erosion Losses*, US Department of Agriculture, Handbook 537.

- Wong, THF, Breen, P & Lloyd, SD 2000, *Water Sensitive Road Design - Design Options for Improving Stormwater Quality of Road Runoff*, Technical Report 00/1, CRC for Catchment Hydrology.
- WSDE 2002, *Guidance for Evaluating Emerging Stormwater Treatment Technologies*, Washington State Department of Ecology Water Quality Program, Technology Assessment Protocol – Ecology, October 2002.
- Yaziz, MI, Gunting, H, Sapari, N & Ghazali, AW 1989, 'Variations in Rainwater Quality From Roof Catchments', *Water Research*, vol. 23, pp. 761-5.
- Zingg, AW 1940, 'Degree and Length of Land Slope as it Affects Soil Loss in Run-off', *Agricultural Engineering*, vol. 21.
- Zug, M, Phan, L, Bellefleur, D & Scrivener, O 1999, 'Pollution Wash-off Modelling on Impervious Surfaces: Calibration, Validation, Transposition', *Water Science and Technology*, vol. 39, no. 2, pp. 17-24.

Appendix A Stormwater Monitoring Data

- Table A.1 Rainfall parameter data for December 2004 to January 2006 monitoring period

Storm	AP (mm)	ADP (hrs)	D (hrs)	P (mm)	I (mm/hr)	Peak I ₆ (mm/hr)	Peak I ₆ ² (mm ² /hr ²)	∑ I ₆ ² (mm ² /hr ²)
7/12/2004	1.2	91.4	3.5	17.5	5.00	20.7	427.7	1711
9/12/2004	17.5	4.6	6.0	9.5	1.58	9.8	97.0	254
11/12/2004	9.5	2.8	3.8	48.5	12.76	12.9	167.3	1166
26/12/2004	3.5	66.9	5.6	20.25	3.61	24.4	594.3	1849
28/12/2004	20.25	37.9	2.8	7.25	2.59	25.5	553.8	766
7/1/2005	7.25	232.1	2.3	43	18.70	46.7	2179.5	15188
17/1/2005	43	256.6	2.5	4	1.60	14.5	211.6	256
18/1/2005	4	1.3	1.8	24.5	14.00	34.4	1186.7	2749
22/1/2005	24.5	76.3	4.2	15.75	3.75	28.7	825.9	2323
25/1/2005	1	15.4	7.1	11.75	1.65	19.6	384.6	693
3/2/2005	2	136.1	0.2	8	40.00	42.4	167.3	930
9/2/2005	8	176.7	1.7	8	4.71	30.4	921.7	1599
10/2/2005	8	7.2	1.7	3	1.76	4.2	17.9	78
25/2/2005	1.25	26.0	1.0	2.5	2.50	10.3	106.1	122
8/3/2005	2.5	261.3	0.4	4.25	10.63	12.2	148.6	416
18/3/2005	4.25	226.0	4.7	13.75	2.93	13.8	191.3	713
15/4/2005	1	128.3	0.4	2.5	6.25	15.2	232.4	252
28/4/2005	2.5	282.3	2.4	4.25	1.77	12.6	157.7	169
13/5/2005	4.25	363.5	13.6	15	1.10	3.8	14.2	211
20/5/2005	15	175.3	1.0	7.75	7.75	29.8	167.3	831
15/6/2005	1.5	55.4	12.8	24.25	1.89	23.3	544.8	1218
21/6/2005	24.25	91.2	21.3	33	1.55	7.3	53.0	799
28/6/2005	33	198.2	15.8	16.25	1.03	5.5	30.1	189
29/6/2005	16.25	2.2	10.3	28.25	2.74	11.9	141.0	1957
4/8/2005				10.5				

Table A.1 continued.

Storm	AP (mm)	ADP (hrs)	D (hrs)	P (mm)	I (mm/hr)	Peak I ₆ (mm/hr)	Peak I ₆ ² (mm ² /hr ²)	∑ I ₆ ² (mm ² /hr ²)
16/9/2005				13				
14/10/2005	2.25	313.4	1.8	20.75	11.53	36.1	1305.0	3810
17/10/2005	20.75	34.7	16.6	29.25	1.76	8.7	74.8	911
21/10/2005	29.25	69.5	8.9	31.75	3.57	30.2	914.4	3033
25/10/2005	31.75	69.3	2.4	20.25	8.44	48.2	2325.1	4947
26/10/2005	20.25	26.0	0.7	8	11.43	29.8	886.0	1736
27/10/2005	8	15.8	1.2	5	4.17	11.9	140.9	278
6/11/2005	1.5	84.6	7.7	64.25	8.34	72.1	5197.1	16297
16/11/2005	6	100.1	2.1	25.25	12.02	38.9	1513.0	5402
2/12/2005	1.5	119.3	5.7	16	2.81	13.1	170.7	870
17/12/2005	2.8	60.4	1.8	12	6.67	26.3	693.3	1742
4/1/2006	0.8	135.4	2.1	7	3.33	15.7	247.2	436
5/1/2006	7	5.5	6.9	33.75	4.89	60.4	3648.7	7617
6/1/2006	33.75	17.3	1.6	5.5	3.44	9.6	91.2	244
9/1/2006	5.5	9.1	3.5	19	5.43	30.7	943.3	2674

12.9 denotes computed estimate.

■ **Table A.2 Measured Particle Concentrations (mg/L) for Roof Surface for December 2004 to January 2006 monitoring period**

Storm	MP EMC	MIP EMC	MOP EMC	FP EMC	FIP EMC	FOP EMC	VFP EMC	VFIP EMC	VFOP EMC	NCP EMC
7/12/2004	3.38	1.32	2.07	6.30	4.42	1.57	1.36	0.22	0.72	11.04
11/12/2004	0.57	0.51	0.05	0.94	0.61	0.34	0.47	0.25	0.23	1.98
26/12/2004	5.99	4.95	1.04	8.53	5.63	2.90	2.82	1.64	1.18	17.34
28/12/2004	9.38	5.28	4.1	13.72	10.09	3.63	3.58	2.15	1.43	26.68
17/1/2005	4.62	2.65	1.97	15.46	9.86	5.60	4.14	2.87	1.27	24.22
18/1/2005	1.33	0.75	0.58	6.42	4.61	1.81	1.84	1.34	0.50	9.59
22/1/2005	2.29	1.43	0.86	5.30	3.13	2.17	2.28	1.54	0.74	9.87
25/1/2005	1.15	0.68	0.47	3.49	2.42	1.07	1.14	0.59	0.56	5.78
3/2/2005	18.89	13.5	5.39	98.35	82.05	16.30	37.65	31.08	6.58	154.89
9/2/2005	1.87	0.93	0.95	14.53	11.33	3.20	4.54	3.45	1.09	20.94
10/2/2005	0.7	0.56	0.14							17.08
8/3/2005	2.73	1.37	1.35	19.12	13.30	5.82	3.89	2.20	1.68	25.74
18/3/2005	1.54	1	0.54	5.17	3.56	1.61	1.96	0.80	1.17	8.67
15/4/2005	2.1	0.59	1.51	13.08	9.87	3.22	3.20	1.58	1.63	18.38
28/4/2005	3.07	2.21	0.85							14.30
13/5/2005	0.38	0.29	0.1	1.32	0.57	0.74	0.56	0.29	0.28	2.26
20/5/2005	1.49	0.83	0.66	6.36	4.30	2.06	1.71	1.14	0.57	9.56
15/6/2005	0.9	0.13	0.77	2.96	2.22	0.74	0.94	0.53	0.41	4.80
21/6/2005	0.51	0.19	0.31	1.09	0.67	0.42	0.45	0.11	0.33	2.05
28/6/2005	0.64	0.33	0.31	1.69	0.93	0.76	0.99	0.47	0.52	3.32
29/6/2005	1.11	0.79	0.42	1.20	0.59	0.61	0.71	0.29	0.42	3.02
4/8/2005	2.62	1.51	1.460	7.32	4.27	3.04	1.46	0.66	0.80	11.40

Table A.2 continued.

Storm	MP EMC	MIP EMC	MOP EMC	FP EMC	FIP EMC	FOP EMC	VFP EMC	VFIP EMC	VFOP EMC	NCP EMC
16/9/2005	4.7									16.97
14/10/2005	3.91									56.03
17/10/2005	0.46									1.57
21/10/2005	0.75									2.22
25/10/2005	1.93									5.80
26/10/2005	2.86									9.29
6/11/2005	0.87									4.09
16/11/2005	2.16									7.41
2/12/2005	1.24									8.04
17/12/2005	5.48									22.40
5/1/2006	1.34									4.74
6/1/2006	4.39									19.87

■ **Table A.3 Measured Particle Concentrations (mg/L) for Carpark Surface for December 2004 to January 2006 monitoring period**

Storm	MP EMC	MIP EMC	MOP EMC	FP EMC	FIP EMC	FOP EMC	VFP EMC	VFIP EMC	VFOP EMC	NCP EMC
9/12/2004	0.95			4.92			5.69			11.56
11/12/2004	8.01	5	3.01	6.28			0.47			14.76
26/12/2004	10.1	6.36	3.74	14.17	8.60	5.57	3.98	1.58	2.40	28.25
28/12/2004	45.31	22.47	22.84	36.38	25.03	11.36	8.06	4.63	3.43	89.75
7/1/2005	15.57	8.75	6.82	15.22	7.49	7.73	5.74	3.22	2.52	36.53
17/1/2005	96.22	66.2	30.02	59.71	39.32	20.39	11.20	7.48	3.72	167.13
18/1/2005	68.38	52.4	15.98	29.61	23.53	6.08	9.33	4.99	4.34	107.32
22/1/2005	7.31	3.54	3.77							12.16
25/1/2005	55.31	35.15	20.16	27.17	19.55	7.62	8.35	4.87	3.48	90.83
3/2/2005	197.28	147.39	49.89	139.13	109.41	29.72	17.40	11.94	5.46	353.81
9/2/2005	161.6	126.6	35	82.43	61.41	21.02	7.66	4.94	2.72	251.69
10/2/2005	5.67	3.59	2.07	23.52	14.56	8.96	12.30	7.52	4.78	41.49
25/2/2005										
8/3/2005	20.1	10.19	9.9	69.29	45.95	23.33	12.52	7.43	5.10	101.91
18/3/2005	7.76	4.3	3.47	16.93	10.27	6.67	3.15	1.39	1.77	27.84
15/4/2005	31.73	20.53	11.2							85.87
28/4/2005	33.48	15.19	18.3							84.98
13/5/2005	5.37	2.38	2.98	19.00	9.35	9.65	8.81	1.95	6.86	33.18
20/5/2005	30.62	14.53	16.09	22.04	12.75	9.29	6.67	1.89	4.79	59.32
15/6/2005	8.42	3.63	4.79	20.20	12.25	7.95	5.80	2.05	3.75	34.42
21/6/2005	0.71			5.95	1.95	4.00	3.53	0.88	2.65	10.19

Table A.3 continued.

Storm	MP EMC	MIP EMC	MOP EMC	FP EMC	FIP EMC	FOP EMC	VFP EMC	VFIP EMC	VFOP EMC	NCP EMC
28/6/2005	1.59	0.81	0.78	7.35	3.50	3.85	5.30	2.10	3.20	14.24
29/6/2005	12.05	7.11	5.06	33.09	23.91	9.18	3.66	2.61	1.05	48.80
4/8/2005	30.67	14.86	19.71	51.52	24.48	27.05	18.86	3.52	15.33	101.05
16/9/2005	35.42									88.27
17/10/2005	1.01									6.24
21/10/2005	2.91									18.91
25/10/2005	6.01									22.34
26/10/2005	10.07									29.14
27/10/2005	3.55									15.05
6/11/2005	5.76									24.06
16/11/2005	7.78									21.73
2/12/2005	3.1									16.75

■ **Table A.4 Measured Particle Concentrations (mg/L) for Road Surface for December 2004 to January 2006 monitoring period**

Storm	MP EMC	MIP EMC	MOP EMC	FP EMC	FIP EMC	FOP EMC	VFP EMC	VFIP EMC	VFOP EMC	NCP EMC
26/12/2004	95.32	75.61	19.71	153.95	122.25	31.70	11.75	8.35	3.40	261.02
28/12/2004	69.14	51.71	17.43	164.90	134.50	30.40	19.90	10.80	9.10	253.94
7/1/2005	21.90	16.56	5.34	74.74	62.15	12.59	11.74	8.84	2.90	108.39
17/1/2005	18.75	8.87	9.88	194.70	143.30	51.40	65.80	50.60	15.20	279.25
18/1/2005	50.57	39.80	10.77	119.83	102.77	17.05	7.40	4.73	2.67	177.80
22/1/2005	30.06	23.10	6.96	57.95	46.28	11.68	10.20	7.41	2.79	98.21
25/1/2005	23.12	17.69	5.43	56.20	42.00	14.20	32.68	23.75	8.93	112.00
3/2/2005	189.69	145.98	43.72	357.50	298.30	59.20	23.20	17.65	5.55	570.39
9/2/2005	49.70	36.07	13.63	199.15	161.40	37.75	26.50	19.75	6.75	275.35
25/2/2005	74.92	48.31	26.62	64.31	36.31	28.00	22.15	11.23	10.92	161.38
8/3/2005	108.05	73.15	34.90	158.24	115.07	43.17	25.51	15.16	10.34	291.79
18/3/2005	18.19	11.95	6.24	63.77	46.71	17.06	4.43	2.31	2.12	86.39
15/4/2005	200.00	148.55	51.45							375.64
28/4/2005	63.92	38.83	25.08	162.42	114.25	48.17	30.33	20.00	10.33	256.67
13/5/2005	13.63	10.59	3.04	56.74	35.11	21.63	36.89	23.33	13.56	107.26
20/5/2005	53.83	33.08	20.75	309.15	248.08	61.08	21.28	15.88	5.40	384.26
15/6/2005	36.93	22.27	14.66	238.13	189.98	48.15	17.40	12.80	4.60	292.46
21/6/2005	5.36	2.47	2.89	33.49	23.27	10.21	26.45	18.85	7.60	65.30
28/6/2005	12.37	9.75	2.62	29.14	18.95	10.19	62.29	46.57	15.71	103.80
29/6/2005	34.11	22.01	12.18	225.15	190.00	35.13	18.95	15.75	3.20	278.21
4/8/2005	70.34	49.57	21.35	543.34	444.33	99.01	27.44	20.45	6.99	641.12

Table A.4 continued.

Storm	MP EMC	MIP EMC	MOP EMC	FP EMC	FIP EMC	FOP EMC	VFP EMC	VFIP EMC	VFOP EMC	NCP EMC
16/9/2005	163.45									632.70
14/10/2005	31.45									197.12
17/10/2005	7.67									56.06
25/10/2005	32.36									210.35
26/10/2005	22.64									172.06
6/11/2005	12.05									75.47
16/11/2005	31.08									190.98
2/12/2005	121.76									220.00
17/12/2005	38.64									227.29
4/1/2006	97.19									291.08
5/1/2006	26.74									108.89
6/1/2006										122.00
9/1/2006	16.41									112.96

■ **Table A.5 Measured Particle Concentrations (mg/L) for Bare Soil Surface for December 2004 to January 2006 monitoring period**

Storm	MP EMC	MIP EMC	MOP EMC	FP EMC	FIP EMC	FOP EMC	VFP EMC	VFIP EMC	VFOP EMC	NCP EMC
7/12/2004	64.34	40	24.34	32.95	21.83	7.73	9.36	2.24	4.68	106.65
7/1/2005	272.31	199.01	73.3	195.11	153.02	42.09	132.39	107.91	24.48	599.81
18/1/2005	460.33	367.26	93.08	781.99	635.37	146.62	198.94	159.47	39.46	1441.26
3/2/2005	129.6	84.8	44.8							888.80
29/6/2005	213.8	175.8	41.7	285.50	228.00	57.50	144.50	116.75	27.75	643.80

■ **Table A.6 Measured Particle Concentrations (mg/L) for Grass Surface for December 2004 to January 2006 monitoring period**

Storm	MP EMC	MIP EMC	MOP EMC	FP EMC	FIP EMC	FOP EMC	VFP EMC	VFIP EMC	VFOP EMC	NCP EMC
7/1/2005	15.48	11.94	3.55	21.00	12.59	7.86	13.57	6.34	7.23	50.05
18/1/2005										29.93

Appendix B Mass Balance Model Calculations

■ **Table B.1 NCP load calculations for Roof for December 2004 to January 2006 monitoring period using refined model**

<i>Input Data</i>							
Area (m ²)	51.8	Max - FPdry	160	AR - FPdry	5.0	LR-RPdrain	0.5
SVFR	40.5	Max - FPwet	250	AR - FPwet	3.0	Cp	30%
		Max - DPdry	0.0	AR - DPdry	0.0		

<i>Storm Rainfall Data</i>						<i>Calculations</i>															<i>Measured</i>	
Storm	ADP hrs	D hrs	P mm	Peak I mm/hr	$\sum I_6^2/D$	TE drain %	WE FP %	Twet hrs	L FPwet mg/m ²	Tdry hrs	L DPdrain mg/m ²	Dust fall mg/m ²	L FPi mg/m ²	L FPsurf mg/m ²	L RPdrain mg/m ²	L FPdrain mg/m ²	L drain mg/m ²	L mg/m ²	Sum L mg/m ²	L RPdraini mg/m ²	L RPsurf mg/m ²	Sum L mg/m ²
7/12/2004	91.4	3.5	17.5	20.7	489	80	10	18.6	56	91.4	0	0	160	216	27	216	243	195	195	47	0	162
9/12/2004	4.6	6.0	9.5	9.8	42	31	9	19	57	4.6	0	0	23	80	46	70	116	36	36	80	10	
11/12/2004	2.8	3.8	48.5	12.9	307	45	10	29	87	2.8	0	0	24	111	78	111	190	86	86	104	0	91
23/12/2004	41.7	2.6	3.8	4.5	34	7	9	2.6	8	41.7	0	0	160	168	82	143	225	5	5	220	25	
26/12/2004A	66.9	1.5	8.0	24.4	737	97	10	1.5	5	66.9	0	0	160	165	147	165	311	302		9	0	
26/12/2004B	0.0	4.1	12.2	15.6	181	57	10	4.1	12	0.0	0	0	0	12	9	12	21	12	314	9	0	338
28/12/2004	37.9	2.8	7.3	25.5	274	100	10	2.8	8	37.9	0	0	160	168	7	168	176	176	176	0	0	175
7/1/2005	232.1	2.3	43.0	46.7	6604	100	10	6.8	20	232.1	0	0	160	180	0	180	180	180	180	0	0	
17/1/2005	256.6	2.5	4.0	14.5	102	53	10	2.5	8	256.6	0	0	160	168	0	168	168	26	26	141	0	92
18/1/2005	1.3	1.8	24.5	34.4	1571	100	10	1.75	5	1.3	0	0	6	12	140	12	152	152	152	0	0	223
22/1/2005	76.3	4.2	15.8	28.7	553	100	10	8.5	26	76.3	0	0	160	186	0	186	186	186	186	0	0	149
25/01/05A	15.4	2.4	4.0	10.1	62	33	9	13.3	40	15.4	0	0	77	117	0	107	107	10		96	10	
25/01/05B	0.0	4.7	7.8	19.6	116	76	10	6.5	20	0.0	0	0	10	29	96	29	126	95	106	31	0	64
3/2/2005	136.1	0.2	8.0	42.4	4649	100	10	16.4	49	136.1	0	1000	160	209	10	209	1219	1219	1219	0	0	1177
9/2/2005	176.7	1.7	8.0	30.4	941	100	10	3.5	11	176.7	0	0	160	171	0	171	171	171	171	0	0	146
10/2/2005	7.2	1.7	3.0	4.2	46	6	9	1.7	5	7.2	0	0	36	41	0	36	36	1	1	35	5	40
25/2/2005	26.0	1.0	2.5	10.3	122	34	10	2.3	7	26.0	0	0	135	142	31	142	173	17	17	155	0	

Appendix B Mass Balance Model Calculations

Table B.1 continued.

8/3/2005	261.3	0.4	4.3	12.2	1040	42	10	3.1	9	261.3	0	0	160	169	0	169	169	21	21	148	0	89
18/3/2005	226.0	4.7	13.8	13.8	152	49	10	7.2	22	226.0	0	0	160	182	0	182	182	90	90	92	0	112
15/4/2005	128.3	0.4	2.5	15.2	629	56	10	0.4	1	128.3	0	0	160	161	33	161	194	33	33	162	0	32
28/4/2005	282.3	2.4	4.3	12.6	70	44	9	17.5	53	282.3	0	0	160	213	0	199	199	26	26	172	14	50
13/05/2005A	363.5	9.5	9.3	2.9	12	5	8	16.7	50	363.5	0	0	160	210	0	169	169	8		160	41	
13/05/2005B	0.0	4.1	5.7	3.8	25	5	8	10.5	32	0.0	0	0	41	73	160	61	221	11	19	210	12	32
20/5/2005	175.3	1.0	7.8	29.8	831	100	10	1	3	175.3	0	0	160	163	26	163	189	189	189	0	0	66
15/06/2005A	55.4	3.6	6.8	8.1	60	23	9	3.6	11	55.4	0	0	160	171	0	156	156	36		119	15	
15/06/2005B	0.0	2.8	9.7	23.3	317	92	10	2.8	8	0.0	0	0	15	24	119	24	143	132		11	0	
15/06/2005C	0.0	6.4	7.8	2.6	18	5	8	6.4	19	0.0	0	0	0	19	11	16	26	1	170	25	4	113
21/06/2005A	91.2	12.9	21.2	7.3	43	20	9	12.9	39	91.2	0	0	160	199	14	174	187	37		150	25	
21/06/2005B	0.0	3.8	4.8	6.9	13	18	8	9.1	27	0.0	0	0	25	52	150	42	192	10		182	10	
21/06/2005C	0.0	4.6	7.0	3.8	15	5	8	10.5	32	0.0	0	0	10	42	182	34	216	11	58	205	8	66
28/6/2005A	198.2	2.5	3.5	4.6	17	8	8	24.4	73	198.2	0	0	160	233	2	190	192	4		187	43	
28/6/2005B	0.0	11.6	9.1	3.6	7	5	8	25.3	76	0.0	0	0	43	119	187	95	283	14		268	24	
28/6/2005C	0.0	3.3	3.4	5.5	22	12	8	6	18	0.0	0	0	24	42	268	35	303	11	29	292	7	49
29/6/2005A	2.0	2.6	3.1	4.9	21	9	8	2.8	8	2.0	0	0	17	26	289	21	311	9		302	4	
29/6/2005B	0.0	3.6	21.3	11.9	517	41	10	3.8	11	0.0	0	0	4	16	302	16	318	129		189	0	
29/6/2005C	0.0	3.4	3.4	2.8	11	5	8	8.2	25	0.0	0	0	0	25	189	20	209	3	141	205	5	83
11/9/2005	207.3	1.2	3.8	7.2	98	19	10	8.9	27	207.3	0	0	160	187	0	186	186	11	11	175	1	
16/9/2005	117.9	2.5	9.3	45.1	894	100	10	2.5	8	117.9	0	0	160	168	72	168	239	239	239	0	0	210
27/9/2005	245.3	0.6	2.3	4.7	74	8	9	17.1	51	245.3	0	0	160	211	0	199	199	5	5	194	12	
30/9/2005	65.2	1.0	2.3	10.7	134	35	10	3.7	11	65.2	0	0	160	171	131	171	302	32	32	270	0	
14/10/2005	313.4	1.8	20.8	36.1	2117	100	10	7.7	23	313.4	0	1000	160	183	0	183	1183	1183	1183	0	0	1114
17/10/2005A	34.8	5.3	9.4	5.9	40	14	9	0	0	34.8	0	0	160	160	0	139	139	19		119	21	
17/10/2005B	0.0	7.4	14.6	8.7	75	26	9	0	0	0.0	0	0	21	21	119	20	140	36		103	1	
17/10/2005C	0.0	3.3	5.3	5.0	36	9	9	0	0	0.0	0	0	1	1	103	1	104	10	65	95	0	45
21/10/2005A	79.1	7.0	16.0	8.0	73	23	9	17	51	79.1	0	0	160	211	57	198	255	59		196	13	

Appendix B Mass Balance Model Calculations

Table B.1 continued.

21/10/2005B	0.0	1.9	15.8	30.2	1328	100	10	25	75	0.0	0	0	13	88	196	88	284	284	343	0	0	69
25/10/2005	69.3	2.4	20.3	48.2	2061	100	10	2.4	7	69.3	0	0	160	167	0	167	167	167	167	0	0	113
26/10/2005	25.8	0.7	8.0	29.8	2479	100	10	1.9	6	25.8	0	0	129	135	0	135	135	135	135	0	0	68
27/10/2005	3.9	1.2	5.0	11.9	232	41	10	2.4	7	3.9	0	0	20	27	0	27	27	11	11	16	0	
6/11/2005	84.6	7.7	64.3	72.1	2116	100	10	84.9	250	84.6	0	0	160	250	9	250	259	259	259	0	0	261
11/11/2005	98.1	2.1	6.3	11.2	114	38	10	10	30	98.1	0	0	160	190	0	190	190	72	72	118	0	
16/11/2005	100.0	2.1	25.3	38.9	2572	100	10	8.3	25	100.0	0	0	160	185	59	185	244	244	244	0	0	182
2/12/2005A	119.3	3.5	7.5	5.1	63	10	9	3.6	11	119.3	0	0	160	171	0	157	157	15		141	14	
2/12/2005B	0.0	2.2	8.5	13.1	295	46	10	23.9	72	0.0	0	0	14	86	141	86	227	105	120	123	0	123
17/12/2005	60.4	1.8	12.0	26.3	968	100	10	28.1	84	60.4	0	0	160	244	86	244	330	330	330	0	0	251
4/1/2006	135.4	2.1	7.0	15.7	208	58	10	16	48	135.4	0	0	160	208	0	208	208	121	121	87	0	
5/1/2006	5.5	6.9	33.8	60.4	1104	100	10	8.9	27	5.5	0	0	28	54	85	54	139	139	139	0	0	157
6/1/2006	17.3	1.6	5.5	9.6	153	30	10	34.3	103	17.3	0	0	87	190	0	190	190	57	57	132	0	92
9/1/2006	9.1	3.5	19.0	30.7	764	100	10	21.5	65	9.1	0	0	46	110	126	110	236	236	236	0	0	

■ **Table B.2 NCP load calculations for Carpark for December 2004 to January 2006 monitoring period using refined model**

<i>Input Data</i>							
Area (m ²)	56.2	Max - FPdry	500	AR - FPdry	300	LR-RPdrain	0.5
SVFR	40.5	Max - FPwet	500	AR - FPwet	300	Cp	30%
		Max - DPdry	1000	AR - DPdry	5		

<i>Storm Rainfall Data</i>						<i>Calculations</i>															<i>Measured</i>	
Storm	ADP hrs	D hrs	P mm	Peak I mm/hr	∑ I ₆ ² /D	TE drain %	WE FP %	Twet hrs	L FPwet mg/m ²	Tdry hrs	L DPdrain mg/m ²	Dust fall mg/m ²	L FPI mg/m ²	L FPsurf mg/m ²	L RPdrain mg/m ²	L FPdrain mg/m ²	L drain mg/m ²	L mg/m ²	Sum L mg/m ²	L RPdraini mg/m ²	L RPsurf mg/m ²	Sum L mg/m ²
7/12/2004	91.4	3.5	17.5	20.7	489	82	100	0	0	91.4	0	0	500	500	27	500	527	431	431	96	0	
9/12/2004	4.6	6.0	9.5	9.8	42	36	62	0	0	4.6	0	0	500	500	94	308	401	145	145	256	192	95
11/12/2004	2.8	3.8	48.5	12.9	307	49	100	0	0	2.8	0	0	500	500	252	500	752	370	370	382	0	659
23/12/2004	41.7	2.6	3.8	4.5	34	20	60	0	0	41.7	0	0	500	500	303	300	603	121	121	482	200	
26/12/2004A	66.9	1.5	8.0	24.4	737	97	100	0	0	66.9	0	0	500	500	321	500	821	799		21	0	
26/12/2004B	0.0	4.1	12.2	15.6	181	60	100	1.7	500	0.0	0	0	0	500	21	500	521	315	1114	207	0	533
28/12/2004	37.9	2.8	7.3	25.5	274	100	100	0	0	37.9	0	0	500	500	168	500	668	668	668	0	0	599
7/1/2005	232.1	2.3	43.0	46.7	6604	100	100	0	0	232.1	1000	0	500	500	0	500	1500	1500	1500	0	0	1521
17/1/2005	256.6	2.5	4.0	14.5	102	56	100	0	0	256.6	0	0	500	500	0	500	500	280	280	220	0	615
18/1/2005	1.3	1.8	24.5	34.4	1571	100	100	0	0	1.3	1000	0	375	375	219	375	1594	1594	1594	0	0	2419
22/1/2005	76.3	4.2	15.8	28.7	553	100	100	0	0	76.3	0	0	500	500	0	500	500	500	500	0	0	175
25/01/05A	15.4	2.4	4.0	10.1	62	37	74	0	0	15.4	0	0	500	500	0	372	372	138		234	128	
25/01/05B	0.0	4.7	7.8	19.6	116	77	100	0	0	6.0	0	0	500	500	234	500	734	567	705	167	0	954
3/2/2005	136.1	0.2	8.0	42.4	4649	100	100	0	0	136.1	1000	1000	500	500	53	500	2553	2553	2553	0	0	2604
9/2/2005	176.7	1.7	8.0	30.4	941	100	100	0	0	176.7	884	0	500	500	0	500	1384	1384	1384	0	0	1612
10/2/2005	7.2	1.7	3.0	4.2	46	20	64	0	0	7.2	0	0	500	500	0	319	319	19	19	300	181	74
25/2/2005	26.0	1.0	2.5	10.3	122	38	100	0	0	26.0	0	0	500	500	261	500	761	87	87	674	0	
8/3/2005	261.3	0.4	4.3	12.2	1040	46	100	0	0	261.3	1000	0	500	500	0	500	1500	691	691	809	0	308

Appendix B Mass Balance Model Calculations

Table B.2 continued.

18/3/2005	226.0	4.7	13.8	13.8	152	53	100	0	0	226.0	0	0	500	500	0	500	500	265	265	235	0	347
15/4/2005	128.3	0.4	2.5	15.2	629	59	100	0	0	128.3	0	0	500	500	84	500	584	103	103	481	0	127
28/4/2005	282.3	2.4	4.3	12.6	70	48	80	0	0	282.3	0	0	500	500	0	401	401	191	191	210	99	257
13/05/2005A	363.5	9.5	9.3	2.9	12	20	60	12.5	500	363.5	0	0	500	500	0	300	300	60		240	200	
13/05/2005B	0.0	4.1	5.7	3.8	25	20	60	12.4	500	0.0	0	0	200	500	240	300	540	108	168	432	200	455
20/5/2005	175.3	1.0	7.8	29.8	831	100	100	0	0	175.3	0	0	500	500	53	500	553	553	553	0	0	380
15/06/2005A	55.4	3.6	6.8	8.1	60	29	73	0	0	55.4	0	0	500	500	0	366	366	105		261	134	
15/06/2005B	0.0	2.8	9.7	23.3	317	93	100	6.6	500	0.0	0	0	134	500	261	500	761	707		53	0	
15/06/2005C	0.0	6.4	7.8	2.6	18	20	60	5	500	0.0	0	0	0	500	53	300	353	71	883	283	200	790
21/06/2005A	91.2	12.9	21.2	7.3	43	25	62	0	0	91.2	0	0	500	500	154	311	465	118		347	189	
21/06/2005B	0.0	3.8	4.8	6.9	13	24	60	19.8	500	0.0	0	0	189	500	347	300	647	153		494	200	
21/06/2005C	0.0	4.6	7.0	3.8	15	20	60	7.8	500	0.0	0	0	200	500	494	300	794	159	430	635	200	323
28/6/2005A	198.2	2.5	3.5	4.6	17	20	60	0	0	198.2	0	0	500	500	6	300	306	61		245	200	
28/6/2005B	0.0	11.6	9.1	3.6	7	20	60	26.4	500	0.0	0	0	200	500	245	300	545	109		436	200	
28/6/2005C	0.0	3.3	3.4	5.5	22	20	60	14.8	500	0.0	0	0	200	500	436	300	736	147	317	589	200	203
29/6/2005A	2.0	2.6	3.1	4.9	21	20	60	0	0	2.0	0	0	500	500	583	300	883	177		706	200	
29/6/2005B	0.0	3.6	21.3	11.9	517	45	100	4	500	0.0	0	0	200	500	706	500	1206	539		667	0	
29/6/2005C	0.0	3.4	3.4	2.8	11	20	60	7.9	500	0.0	0	0	0	500	667	300	967	193	909	773	200	1337
11/9/2005	207.3	1.2	3.8	7.2	98	25	99	0	0	207.3	0	0	500	500	0	494	494	123	123	371	6	
16/9/2005	117.9	2.5	9.3	45.1	894	100	100	0	0	117.9	0	0	500	500	152	500	652	652	652	0	0	1056
27/9/2005	245.3	0.6	2.3	4.7	74	20	82	0	0	245.3	0	0	500	500	0	412	412	25	25	387	88	
30/9/2005	65.2	1.0	2.3	10.7	134	40	100	0	0	65.2	0	0	500	500	261	500	761	90	90	670	0	
14/10/2005	313.4	1.8	20.8	36.1	2117	100	100	0	0	313.4	1000	1000	500	500	0	500	2500	2500	2500	0	0	
17/10/2005A	34.8	5.3	9.4	5.9	40	20	60	0	0	34.8	0	0	500	500	0	300	300	60		240	200	
17/10/2005B	0.0	7.4	14.6	8.7	75	31	83	14.7	500	0.0	0	0	200	500	240	417	657	205		453	83	
17/10/2005C	0.0	3.3	5.3	5.0	36	20	60	8.8	500	0.0	0	0	83	500	453	300	753	151	415	602	200	174
21/10/2005A	79.1	7.0	16.0	8.0	73	29	82	0	0	79.1	0	0	500	500	364	409	773	221		553	91	
21/10/2005B	0.0	1.9	15.8	30.2	1328	100	100	0	0	6.0	600	0	500	500	553	500	1652	1652	1873	0	0	575

Appendix B Mass Balance Model Calculations

Table B.2 continued.

25/10/2005	69.3	2.4	20.3	48.2	2061	100	100	0	0	69.3	347	0	500	500	0	500	847	847	847	0	0	421
26/10/2005	25.8	0.7	8.0	29.8	2479	100	100	0	0	25.8	129	0	500	500	0	500	629	629	629	0	0	197
27/10/2005	3.9	1.2	5.0	11.9	232	45	100	0	0	3.9	0	0	500	500	0	500	500	224	224	276	0	56
6/11/2005	84.6	7.7	64.3	72.1	2116	100	100	0	0	84.6	443	0	500	500	159	500	1102	1102	1102	0	0	1516
11/11/2005	98.1	2.1	6.3	11.2	114	42	100		0	98.1	0	0	500	500	0	500	500	210	210	290	0	
16/11/2005	100.0	2.1	25.3	38.9	2572	100	100		0	100.0	991	0	500	500	145	500	1635	1635	1635	0	0	518
2/12/2005A	119.3	3.5	7.5	5.1	63	20	75		0	119.3	0	0	500	500	0	377	377	75		302	123	
2/12/2005B	0.0	2.2	8.5	13.1	295	50	100	0	0	6.0	0	0	500	500	302	500	802	399	474	403	0	244
17/12/2005	60.4	1.8	12.0	26.3	968	100	100		0	60.4	929	0	500	500	281	500	1710	1710	1710	0	0	
4/1/2006	135.4	2.1	7.0	15.7	208	61	100		0	135.4	0	0	500	500	0	500	500	305	305	195	0	
5/1/2006	5.5	6.9	33.8	60.4	1104	100	100		0	5.5	705	0	500	500	190	500	1394	1394	1394	0	0	
6/1/2006	17.3	1.6	5.5	9.6	153	35	100		0	17.3	0	0	500	500	0	500	500	175	175	325	0	
9/1/2006	9.1	3.5	19.0	30.7	764	100	100		0	9.1	0	0	500	500	310	500	810	810	810	0	0	

■ **B.3 NCP load calculations for Road for December 2004 to January 2006 monitoring period using refined model**

<i>Input Data</i>							
Area (m ²)	450	Max - FPdry	1600	AR -FPdry	2000	LR-RPdrain	0.4
SVFR	185	Max - FPwet	6000	AR - FPwet	1000	Cp	25%
		Max - DPdry	2600	AR - DPdry	30		

<i>Storm Rainfall Data</i>					<i>Calculations</i>																<i>Measured</i>	
Storm	ADP hrs	D hrs	P mm	Peak I mm/hr	$\sum I_6^2/D$	TE drain %	WE FP %	Twet hrs	L FPwet mg/m ²	Tdry hrs	L DPdrain mg/m ²	Dust fall mg/m ²	L FPi mg/m ²	L FPsurf mg/m ²	L RPdrain mg/m ²	L FPdrain mg/m ²	L drain mg/m ²	L mg/m ²	Sum L mg/m ²	L RPdraini mg/m ²	L RPsurf mg/m ²	Sum L mg/m ²
7/12/2004	91.4	3.5	17.5	20.7	489	100	100	0	0	91.4	0	0	1600	1600	32	1600	1632	1632	1632	0	0	
9/12/2004	4.6	6.0	9.5	9.8	42	61	31	0	0	4.6	0	0	1600	1600	0	496	496	304	304	192	1104	
11/12/2004	2.8	3.8	48.5	12.9	307	84	100	0	0	2.8	0	0	1600	1600	190	1600	1790	1512	1512	278	0	
23/12/2004	41.7	2.6	3.8	4.5	34	25	30	0	0	41.7	0	0	1600	1600	231	480	711	178	178	534	1120	
26/12/2004A	66.9	1.5	8.0	24.4	737	100	100	0	0	66.9	0	0	1600	1600	391	1600	1991	1991		0	0	
26/12/2004B	0.0	4.1	12.2	15.6	181	100	92	1.7	3400	0.0	0	0	0	3400	0	3123	3123	3123	5114	0	277	4942
28/12/2004	37.9	2.8	7.3	25.5	274	100	100	0	0	37.9	0	0	1600	1600	0	1600	1600	1600	1600	0	0	1518
7/1/2005	232.1	2.3	43.0	46.7	6604	100	100	0	0	232.1	2600	0	1600	1600	0	1600	4200	4200	4200	0	0	4516
17/1/2005	256.6	2.5	4.0	14.5	102	97	57	0	0	256.6	0	0	1600	1600	0	917	917	886	886	31	683	788
18/1/2005	1.3	1.8	24.5	34.4	1571	100	100	0	0	1.3	2600	0	1600	1600	31	1600	4231	4231	4231	0	0	4149
22/1/2005	76.3	4.2	15.8	28.7	553	100	100	0	0	76.3	0	0	1600	1600	0	1600	1600	1600	1600	0	0	1419
25/01/05A	15.4	2.4	4.0	10.1	62	63	39	0	0	15.4	0	0	1600	1600	0	631	631	398		233	969	
25/01/05B	0.0	4.7	7.8	19.6	116	100	63	0	0	6.0	0	0	1600	1600	233	1013	1245	1245	1644	0	587	1175
3/2/2005	136.1	0.2	8.0	42.4	4649	100	100	0	0	136.1	2600	0	1600	1600	0	1600	4200	4200	4200	0	0	4119
9/2/2005	176.7	1.7	8.0	30.4	941	100	100	0	0	176.7	0	0	1600	1600	0	1600	1600	1600	1600	0	0	1787
10/2/2005	7.2	1.7	3.0	4.2	46	25	32	0	0	7.2	0	0	1600	1600	0	520	520	32	32	487	1080	

Appendix B Mass Balance Model Calculations

Table B.3 continued.

25/2/2005	26.0	1.0	2.5	10.3	122	65	66	0	0	26.0	0	0	1600	1600	436	1057	1493	242	242	1251	543	161
8/3/2005	261.3	0.4	4.3	12.2	1040	79	100	0	0	261.3	0	0	1600	1600	0	1600	1600	1263	1263	337	0	869
18/3/2005	226.0	4.7	13.8	13.8	152	91	79	0	0	226.0	0	0	1600	1600	32	1262	1295	1181	1181	114	338	1075
15/4/2005	128.3	0.4	2.5	15.2	629	100	100	0	0	128.3	0	0	1600	1600	55	1600	1655	414	414	1242	0	467
28/4/2005	282.3	2.4	4.3	12.6	70	82	43	0	0	282.3	0	0	1600	1600	0	693	693	566	566	127	907	770
13/05/2005A	363.5	9.5	9.3	2.9	12	25	30	12.5	6000	363.5	0	0	1600	6000	0	1800	1800	450		1350	4200	
13/05/2005B	0.0	4.1	5.7	3.8	25	25	30	12.4	6000	0.0	0	0	1600	6000	1350	1800	3150	788	1238	2363	4200	1475
20/5/2005	175.3	1.0	7.8	29.8	831	100	100	0	0	175.3	0	0	1600	1600	706	1600	2306	2306	2306	0	0	2476
15/06/2005A	55.4	3.6	6.8	8.1	60	48	39	0	0	55.4	0	0	1600	1600	0	618	618	297		321	982	
15/06/2005B	0.0	2.8	9.7	23.3	317	100	100	6.6	6000	0.0	0	0	982	6000	321	6000	6321	6321		0	0	
15/06/2005C	0.0	6.4	7.8	2.6	18	25	30	5	6000	0.0	0	0	0	6000	0	1800	1800	450	7068	1350	4200	6713
21/06/2005A	91.2	12.9	21.2	7.3	43	42	32	0	0	91.2	0	0	1600	1600	858	504	1362	573		788	1096	
21/06/2005B	0.0	3.8	4.8	6.9	13	39	30	19.8	6000	0.0	0	0	1096	6000	788	1800	2588	1008		1580	4200	
21/06/2005C	0.0	4.6	7.0	3.8	15	25	30	7.8	6000	0.0	0	0	1600	6000	1580	1800	3380	845	2426	2535	4200	2071
28/6/2005A	198.2	2.5	3.5	4.6	17	25	30	0	0	198.2	0	0	1600	1600	525	480	1005	251		754	1120	
28/6/2005B	0.0	11.6	9.1	3.6	7	25	30	26.4	6000	0.0	0	0	1120	6000	754	1800	2554	638		1915	4200	
28/6/2005C	0.0	3.3	3.4	5.5	22	29	30	14.8	6000	0.0	0	0	1600	6000	1915	1800	3715	1065	1955	2650	4200	1481
29/6/2005A	2.0	2.6	3.1	4.9	21	25	30	0	0	2.0	0	0	1600	1600	2629	480	3109	777		2332	1120	
29/6/2005B	0.0	3.6	21.3	11.9	517	77	100	4	6000	0.0	0	0	1120	6000	2332	6000	8332	6376		1956	0	
29/6/2005C	0.0	3.4	3.4	2.8	11	25	30	7.9	6000	0.0	0	0	0	6000	1956	1800	3756	939	8092	2817	4200	7493
11/9/2005	207.3	1.2	3.8	7.2	98	41	55	0	0	207.3	0	0	1600	1600	481	887	1368	563	563	806	713	
16/9/2005	117.9	2.5	9.3	45.1	894	100	100	0	0	117.9	0	0	1600	1600	426	1600	2026	2026	2026	0	0	
27/9/2005	245.3	0.6	2.3	4.7	74	25	45	0	0	245.3	0	0	1600	1600	0	715	715	45	45	670	886	
30/9/2005	65.2	1.0	2.3	10.7	134	67	71	0	0	65.2	0	0	1600	1600	495	1135	1630	275	275	1355	465	
14/10/2005	313.4	1.8	20.8	36.1	2117	100	100	0	0	313.4	2600	0	1600	1600	0	1600	4200	4200	4200	0	0	3793
17/10/2005A	34.8	5.3	9.4	5.9	40	32	30	0	0	34.8	0	0	1600	1600	0	480	480	154		326	1120	
17/10/2005B	0.0	7.4	14.6	8.7	75	52	45	14.7	6000	0.0	0	0	1120	6000	326	2725	3051	1598		1453	3275	
17/10/2005C	0.0	3.3	5.3	5.0	36	25	30	8.8	6000	0.0	0	0	1600	6000	1453	1800	3253	813	2565	2440	4200	1570

Appendix B Mass Balance Model Calculations

Table B.3 continued.

21/10/2005A	79.1	7.0	16.0	8.0	73	48	44	0	79.1	0	0	1600	1600	1668	710	2378	1135	1243	890		
21/10/2005B	0.0	1.9	15.8	30.2	1328	100	100	0	6.0	2600	0	1600	1600	1243	1600	5443	5443	6578	0	0	
25/10/2005	69.3	2.4	20.3	48.2	2061	100	100	0	69.3	2079	0	1600	1600	0	1600	3679	3679	3679	0	0	3978
26/10/2005	25.8	0.7	8.0	29.8	2479	100	100	0	25.8	774	0	1600	1600	0	1600	2374	2374	2374	0	0	1155
27/10/2005	3.9	1.2	5.0	11.9	232	77	100	0	3.9	0	0	1600	1600	0	1600	1600	1224	1224	376	0	
6/11/2005	84.6	7.7	64.3	72.1	2116	100	100	0	84.6	2600	0	1600	1600	248	1600	4448	4448	4448	0	0	4763
11/11/2005	98.1	2.1	6.3	11.2	114	72	62	0	98.1	0	0	1600	1600	0	999	999	717	717	283	601	
16/11/2005	100.0	2.1	25.3	38.9	2572	100	100	0	100.0	2600	0	1600	1600	170	1600	4370	4370	4370	0	0	4584
2/12/2005A	119.3	3.5	7.5	5.1	63	25	40	0	119.3	0	0	1600	1600	0	642	642	163	479	958		
2/12/2005B	0.0	2.2	8.5	13.1	295	86	100	0	6.0	0	0	1600	1600	479	1600	2079	1778	1941	301	0	3232
17/12/2005	60.4	1.8	12.0	26.3	968	100	100	0	60.4	0	0	1600	1600	228	1600	1828	1828	1828	0	0	2404
4/1/2006	135.4	2.1	7.0	15.7	208	100	100	0	135.4	0	0	1600	1600	0	1600	1600	1600	1600	0	0	1669
5/1/2006A	5.5	1.0	20.2	60.4	7210	100	100	0	5.5	2600	0	1600	1600	0	1600	4200	4200	0	0		
5/1/2006B	0.0	5.9	13.6	7.3	69	42	43	3.1	6000	0.0	0	0	6000	0	2561	2561	1086	5286	1475	3439	3533
6/1/2006	17.3	1.6	5.5	9.6	153	59	79	0	17.3	0	0	1600	1600	1373	1270	2642	1562	1562	1080	330	504
9/1/2006	9.1	3.5	19.0	30.7	764	100	100	0	9.1	0	0	1600	1600	1041	1600	2641	2641	2641	0	0	1996

Appendix C Case Study Calculations

■ Table C.1 Effect of Urban Land Use Type - NCP load calculations for hypothetical Residential catchment

<i>Input Data</i>						
Area (ha)	1.0	Roof 20%	Grass 58%	Bare 0%	Carpark 10%	Road 12%

<i>Storm Rainfall Data</i>		<i>Load Calculations</i>						<i>Runoff Volume Calculations</i>						EMC mg/L
Storm	P mm	Roof L g	Grass L g	Bare L g	Carpark L g	Road L g	Sum L g	Roof R kL	Grass R kL	Bare R kL	Carpark R kL	Road R kL	Sum R kL	
7/12/2004	17.5	324	0	0	436	1948	2708	29	0	0	16	19	65	42
9/12/2004	9.5	72	0	0	95	383	549	17	0	0	8	10	36	15
11/12/2004	48.5	182	3341	0	659	1823	6005	92	84	0	45	56	277	22
26/12/2004	20.25	676	0	0	533	5930	7139	39	0	0	19	23	81	89
28/12/2004	7.25	350	0	0	599	1822	2770	13	0	0	7	7	27	103
7/1/2005	43	360	5290	0	1521	5419	12590	82	106	0	42	50	279	45
17/1/2005	4	184	0	0	615	946	1745	8	0	0	4	3	15	119
18/1/2005	24.5	447	435	0	2419	4978	8279	47	15	0	23	28	112	74
22/1/2005	15.75	297	0	0	175	1702	2175	30	0	0	14	17	62	35
25/1/2005	11.75	127	0	0	954	1410	2490	22	0	0	10	13	45	55
3/2/2005	8	2354	0	0	2604	4943	9902	15	0	0	7	9	31	317
9/2/2005	8	291	0	0	1612	2144	4047	14	0	0	6	8	28	144
10/2/2005	3	79	0	0	74	47	200	5	0	0	2	2	8	24
25/2/2005	2.5	34	0	0	326	194	554	3	0	0	2	1	6	91
8/3/2005	4.25	179	0	0	308	1043	1530	7	0	0	3	4	14	113
18/3/2005	13.75	224	0	0	347	1290	1861	26	0	0	12	15	53	35
15/4/2005	2.5	64	0	0	127	561	752	3	0	0	1	1	6	122
28/4/2005	4.25	99	0	0	257	924	1280	7	0	0	3	4	14	94
13/5/2005	15	65	0	0	455	1771	2290	29	0	0	14	17	59	39
20/5/2005	7.75	133	0	0	380	2972	3484	14	0	0	6	8	28	124
15/6/2005	24.25	226	0	0	790	8056	9072	47	0	0	23	28	98	93

Appendix C Case Study Calculations

Table C.1 continued.

21/6/2005	33	133	376	0	323	2485	3316	65	9	0	32	38	144	23
28/6/2005	16.25	99	0	0	203	1777	2078	30	0	0	14	17	61	34
29/6/2005	28.25	167	2504	0	1337	8992	12999	55	63	0	27	32	178	73
14/10/2005	20.75	2228	131	0	2500	4552	9411	40	3	0	19	23	85	110
17/10/2005	29.25	90	1354	0	174	1884	3501	57	34	0	28	34	153	23
21/10/2005	31.75	138	1713	0	575	7893	10320	62	43	0	30	37	172	60
25/10/2005	20.25	226	59	0	421	4774	5480	39	1	0	19	23	82	67
26/10/2005	8	136	0	0	197	1386	1719	15	0	0	7	8	29	58
6/11/2005	64.25	523	6388	0	1516	5715	14142	128	160	0	63	76	426	33
16/11/2005	25.25	363	778	0	518	5500	7160	49	19	0	24	29	121	59
2/12/2005	16	245	0	0	244	3878	4367	31	0	0	15	18	63	70
17/12/2005	12	502	0	0	1710	2885	5096	22	0	0	11	13	46	110
5/1/2006	33.75	314	2001	0	1394	4239	7949	66	50	0	31	39	186	43
6/1/2006	5.5	184	0	0	175	605	964	9	0	0	5	5	19	50
9/1/2006	19	473	0	0	810	2395	3678	36	0	0	17	21	75	49

■ **Table C.2 Effect of Urban Land Use Type - NCP load calculations for hypothetical Commercial catchment**

Input Data						
Area (ha)	1.0	Roof	Grass	Bare	Carpark	Road
		30%	30%	0%	20%	20%

Storm Rainfall Data		Load Calculations						Runoff Volume Calculations						EMC mg/L
Storm	P mm	Roof L g	Grass L g	Bare L g	Carpark L g	Road L g	Sum L g	Roof R kL	Grass R kL	Bare R kL	Carpark R kL	Road R kL	Sum R kL	
7/12/2004	17.5	486	0	0	872	3246	4604	44	0	0	32	32	108	42
9/12/2004	9.5	108	0	0	189	638	935	26	0	0	16	17	60	16
11/12/2004	48.5	274	1728	0	1317	3038	6357	138	43	0	89	94	365	17
26/12/2004	20.25	1014	0	0	1065	9884	11964	58	0	0	38	38	134	89
28/12/2004	7.25	525	0	0	1197	3036	4759	20	0	0	13	12	45	106
7/1/2005	43	540	2736	0	3042	9032	15350	123	55	0	83	83	344	45
17/1/2005	4	276	0	0	1230	1576	3082	11	0	0	7	6	24	126
18/1/2005	24.5	670	225	0	4838	8297	14030	70	8	0	45	47	169	83
22/1/2005	15.75	446	0	0	351	2837	3634	45	0	0	29	29	103	35
25/1/2005	11.75	191	0	0	1907	2349	4447	33	0	0	21	21	75	59
3/2/2005	8	3531	0	0	5208	8239	16978	23	0	0	15	14	52	327
9/2/2005	8	437	0	0	3224	3573	7235	21	0	0	13	13	47	155
10/2/2005	3	119	0	0	148	78	344	7	0	0	4	3	14	25
25/2/2005	2.5	51	0	0	652	323	1026	5	0	0	4	2	10	101
8/3/2005	4.25	268	0	0	617	1738	2623	10	0	0	6	6	22	117
18/3/2005	13.75	336	0	0	694	2150	3180	39	0	0	25	25	89	36
15/4/2005	2.5	96	0	0	254	935	1284	5	0	0	2	2	10	127
28/4/2005	4.25	149	0	0	514	1540	2203	10	0	0	6	6	22	98
13/5/2005	15	97	0	0	909	2951	3957	43	0	0	27	28	98	40
20/5/2005	7.75	199	0	0	760	4953	5912	21	0	0	13	13	47	127
15/6/2005	24.25	339	0	0	1580	13427	15346	71	0	0	46	46	162	94
21/6/2005	33	199	194	0	645	4141	5180	97	5	0	63	63	229	23

Appendix C Case Study Calculations

Table C.2 continued.

28/6/2005	16.25	148	0	0	405	2962	3515	45	0	0	28	29	102	35
29/6/2005	28.25	250	1295	0	2674	14986	19206	83	32	0	55	54	224	86
14/10/2005	20.75	3342	68	0	5000	7587	15997	60	2	0	38	38	138	116
17/10/2005	29.25	135	700	0	349	3139	4323	86	18	0	56	56	215	20
21/10/2005	31.75	207	886	0	1151	13155	15399	93	22	0	61	62	238	65
25/10/2005	20.25	339	31	0	843	7956	9168	58	1	0	38	38	135	68
26/10/2005	8	204	0	0	394	2309	2908	22	0	0	14	13	49	59
6/11/2005	64.25	784	3304	0	3031	9526	16645	192	83	0	126	126	527	32
16/11/2005	25.25	545	403	0	1036	9167	11151	74	10	0	48	48	179	62
2/12/2005	16	368	0	0	489	6463	7320	46	0	0	29	29	104	70
17/12/2005	12	752	0	0	3419	4808	8980	34	0	0	22	21	77	117
5/1/2006	33.75	471	1035	0	2789	7066	11361	99	26	0	62	65	252	45
6/1/2006	5.5	276	0	0	349	1009	1634	14	0	0	10	8	32	51
9/1/2006	19	709	0	0	1621	3991	6322	54	0	0	35	35	124	51

■ **Table C.3 Effect of Bare Soil Areas - NCP load calculations for hypothetical Residential catchment**

<i>Input Data</i>						
Area (ha)	1.0	Roof 20%	Grass 48%	Bare 10%	Carpark 10%	Road 12%

<i>Storm Rainfall Data</i>		<i>Load Calculations</i>						<i>Runoff Volume Calculations</i>					EMC mg/L	
Storm	P mm	Roof L g	Grass L g	Bare L g	Carpark L g	Road L g	Sum L g	Roof R kL	Grass R kL	Bare R kL	Carpark R kL	Road R kL		Sum R kL
7/12/2004	17.5	324	0	91	436	1948	2799	29	0	1	16	19	66	43
9/12/2004	9.5	72	0	0	95	383	549	17	0	0	8	10	36	15
11/12/2004	48.5	182	2765	12525	659	1823	17954	92	69	19	45	56	281	64
26/12/2004	20.25	676	0	91	533	5930	7230	39	0	1	19	23	81	89
28/12/2004	7.25	350	0	1360	599	1822	4130	13	0	2	7	7	29	144
7/1/2005	43	360	4378	15811	1521	5419	27489	82	87	24	42	50	284	97
17/1/2005	4	184	0	0	615	946	1745	8	0	0	4	3	15	119
18/1/2005	24.5	447	360	5980	2419	4978	14184	47	12	4	23	28	113	125
22/1/2005	15.75	297	0	0	175	1702	2175	30	0	0	14	17	62	35
25/1/2005	11.75	127	0	0	954	1410	2490	22	0	0	10	13	45	55
3/2/2005	8	2354	0	1360	2604	4943	11262	15	0	2	7	9	33	344
9/2/2005	8	291	0	0	1612	2144	4047	14	0	0	6	8	28	144
10/2/2005	3	79	0	0	74	47	200	5	0	0	2	2	8	24
25/2/2005	2.5	34	0	0	326	194	554	3	0	0	2	1	6	91
8/3/2005	4.25	179	0	0	308	1043	1530	7	0	0	3	4	14	113
18/3/2005	13.75	224	0	0	347	1290	1861	26	0	0	12	15	53	35
15/4/2005	2.5	64	0	0	127	561	752	3	0	0	1	1	6	122
28/4/2005	4.25	99	0	0	257	924	1280	7	0	0	3	4	14	94
13/5/2005	15	65	0	0	455	1771	2290	29	0	0	14	17	59	39
20/5/2005	7.75	133	0	0	380	2972	3484	14	0	0	6	8	28	124
15/6/2005	24.25	226	0	0	790	8056	9072	47	0	0	23	28	98	93
21/6/2005	33	133	311	6331	323	2485	9582	65	8	5	32	38	147	65

Appendix C Case Study Calculations

Table C.3 continued.

28/6/2005	16.25	99	0	0	203	1777	2078	30	0	0	14	17	61	34
29/6/2005	28.25	167	2072	9084	1337	8992	21652	55	52	14	27	32	181	120
14/10/2005	20.75	2228	108	209	2500	4552	9598	40	3	0	19	23	85	113
17/10/2005	29.25	90	1120	7375	174	1884	10643	57	28	7	28	34	154	69
21/10/2005	31.75	138	1418	8273	575	7893	18298	62	35	9	30	37	174	105
25/10/2005	20.25	226	49	0	421	4774	5470	39	1	0	19	23	82	67
26/10/2005	8	136	0	0	197	1386	1719	15	0	0	7	8	29	58
6/11/2005	64.25	523	5287	19951	1516	5715	32991	128	132	36	63	76	435	76
16/11/2005	25.25	363	644	5785	518	5500	12811	49	16	4	24	29	122	105
2/12/2005	16	245	0	0	244	3878	4367	31	0	0	15	18	63	70
17/12/2005	12	502	0	0	1710	2885	5096	22	0	0	11	13	46	110
5/1/2006	33.75	314	1656	8992	1394	4239	16596	66	41	11	31	39	188	88
6/1/2006	5.5	184	0	0	175	605	964	9	0	0	5	5	19	50
9/1/2006	19	473	0	0	810	2395	3678	36	0	0	17	21	75	49

■ **Table C.4 Effect of Rainwater Tanks - NCP load calculations for hypothetical Residential catchment**

Input Data						
Area (ha)	1.0	Roof	Grass	Bare	Carpark	Road
		20%	58%	0%	10%	12%

Tank Data	
Sc (kL/ha)	100
U (kl/ha/day)	1.3

Storm Rainfall Data		Load Calculations							Runoff Volume Calculations									EMC mg/L	
Storm	P mm	Roof L g	O'Flow L g	Grass L g	Bare L g	Carpark L g	Road L g	Sum L g	Roof R kL	Sa kL	Si kL	So kL	Ro'flow kL	Grass R kL	Bare R kL	Carpark R kL	Road R kL		Sum R kL
7/12/2004	17.5	324	0	0	0	436	1948	2384	29	0	0	29	0	0	0	16	19	35	67
9/12/2004	9.5	72	0	0	0	95	383	477	17	29	29	46	0	0	0	8	10	18	26
11/12/2004	48.5	182	76	3341	0	659	1823	5898	92	46	46	138	38	84	0	45	56	223	26
26/12/2004	20.25	676	613	0	0	533	5930	7076	39	100	96	135	35	0	0	19	23	77	92
28/12/2004	7.25	350	295	0	0	599	1822	2716	13	100	98	111	11	0	0	7	7	25	109
7/1/2005	43	360	305	5290	0	1521	5419	12535	82	100	87	169	69	106	0	42	50	266	47
17/1/2005	4	184	0	0	0	615	946	1561	8	100	86	94	0	0	0	4	3	7	221
18/1/2005	24.5	447	385	435	0	2419	4978	8218	47	94	94	140	40	15	0	23	28	105	78
22/1/2005	15.75	297	256	0	0	175	1702	2134	30	100	96	126	26	0	0	14	17	58	37
25/1/2005	11.75	127	122	0	0	954	1410	2486	22	100	99	121	21	0	0	10	13	44	56
3/2/2005	8	2354	1212	0	0	2604	4943	8760	15	100	93	108	8	0	0	7	9	24	367
9/2/2005	8	291	91	0	0	1612	2144	3847	14	100	90	104	4	0	0	6	8	19	208
10/2/2005	3	79	72	0	0	74	47	193	5	100	100	104	4	0	0	2	2	8	24
25/2/2005	2.5	34	18	0	0	326	194	538	3	100	99	102	2	0	0	2	1	5	115
8/3/2005	4.25	179	0	0	0	308	1043	1351	7	100	86	93	0	0	0	3	4	7	205
18/3/2005	13.75	224	56	0	0	347	1290	1693	26	93	81	106	6	0	0	12	15	34	50
15/4/2005	2.5	64	0	0	0	127	561	688	3	100	93	97	0	0	0	1	1	3	256
28/4/2005	4.25	99	0	0	0	257	924	1181	7	97	81	88	0	0	0	3	4	7	178
13/5/2005	15	65	0	0	0	455	1771	2225	29	88	68	97	0	0	0	14	17	30	74

Appendix C Case Study Calculations

Table C.4 continued.

20/5/2005	7.75	133	14	0	0	380	2972	3366	14	97	88	101	1	0	0	6	8	16	216
15/6/2005	24.25	226	212	0	0	790	8056	9058	47	100	97	144	44	0	0	23	28	95	96
21/6/2005	33	133	122	376	0	323	2485	3305	65	100	95	160	60	9	0	32	38	139	24
28/6/2005	16.25	99	63	0	0	203	1777	2043	30	100	89	119	19	0	0	14	17	50	41
29/6/2005	28.25	167	166	2504	0	1337	8992	12999	55	100	100	155	55	63	0	27	32	177	73
14/10/2005	20.75	2228	1277	131	0	2500	4552	8460	40	100	83	123	23	3	0	19	23	68	124
17/10/2005	29.25	90	87	1354	0	174	1884	3498	57	100	98	155	55	34	0	28	34	151	23
21/10/2005	31.75	138	130	1713	0	575	7893	10312	62	100	96	158	58	43	0	30	37	169	61
25/10/2005	20.25	226	204	59	0	421	4774	5458	39	100	96	135	35	1	0	19	23	78	70
26/10/2005	8	136	123	0	0	197	1386	1706	15	100	99	113	13	0	0	7	8	28	61
6/11/2005	64.25	523	504	6388	0	1516	5715	14123	128	100	95	223	123	160	0	63	76	422	33
16/11/2005	25.25	363	323	778	0	518	5500	7120	49	100	95	144	44	19	0	24	29	116	62
2/12/2005	16	245	193	0	0	244	3878	4316	31	100	94	124	24	0	0	15	18	56	77
17/12/2005	12	502	138	0	0	1710	2885	4732	22	100	84	106	6	0	0	11	13	30	158
5/1/2006	33.75	314	312	2001	0	1394	4239	7947	66	100	100	166	66	50	0	31	39	186	43
6/1/2006	5.5	184	165	0	0	175	605	945	9	100	99	108	8	0	0	5	5	18	52
9/1/2006	19	473	466	0	0	810	2395	3672	36	100	100	136	36	0	0	17	21	74	49

■ **Table C.5 Effect of Grass Swales - NCP load calculations for Road**

<i>Input Data</i>							
Area (m ²)	450	Max - FPdry	1600	AR -FPdry	2000	LR-RPdrain	100
SVFR	185	Max - FPwet	6000	AR - FPwet	1000	Cp	25%
		Max - DPdry	2600	AR - DPdry	30		

<i>Storm Rainfall Data</i>						<i>Calculations</i>																
Storm	ADP hrs	D hrs	P mm	Peak I mm/hr	∑ I ₆ ² /D	TE drain %	WE FP %	Twet hrs	L FPwet mg/m ²	Tdry hrs	L DPdrain mg/m ²	Dust fall mg/m ²	L FPi mg/m ²	L FPsurf mg/m ²	L RPdrain mg/m ²	L FPdrain mg/m ²	L drain mg/m ²	L mg/m ²	Sum L mg/m ²	L RPdraini mg/m ²	L RPsurf mg/m ²	
7/12/2004	91.4	3.5	17.5	20.7	489	30	100	0	0	91.4	0	0	1600	1600	0	1600	1600	484	484	1116	0	0
9/12/2004	4.6	6.0	9.5	9.8	42	27	31	0	0	4.6	0	0	1600	1600	0	496	496	134	134	362	1104	
11/12/2004	2.8	3.8	48.5	12.9	307	28	100	0	0	2.8	0	0	1600	1600	0	1600	1600	451	451	1149	0	
23/12/2004	41.7	2.6	3.8	4.5	34	24	30	0	0	41.7	0	0	1600	1600	0	480	480	114	114	366	1120	
26/12/2004A	66.9	1.5	8.0	24.4	737	31	100	0	0	66.9	0	0	1600	1600	0	1600	1600	496		1104	0	
26/12/2004B	0.0	4.1	12.2	15.6	181	29	92	1.7	3400	0.0	0	0	0	3400	0	3123	3123	907	1402	2217	277	
28/12/2004	37.9	2.8	7.3	25.5	274	31	100	0	0	37.9	0	0	1600	1600	0	1600	1600	499	499	1101	0	
7/1/2005	232.1	2.3	43.0	46.7	6604	34	100	0	0	232.1	2600	0	1600	1600	0	1600	4200	1419	1419	2781	0	
17/1/2005	256.6	2.5	4.0	14.5	102	29	57	0	0	256.6	0	0	1600	1600	0	917	917	263	263	654	683	
18/1/2005	1.3	1.8	24.5	34.4	1571	32	100	0	0	1.3	2600	0	1600	1600	0	1600	4200	1364	1364	2836	0	
22/1/2005	76.3	4.2	15.8	28.7	553	32	100	0	0	76.3	0	0	1600	1600	0	1600	1600	507	507	1093	0	
25/01/05A	15.4	2.4	4.0	10.1	62	27	39	0	0	15.4	0	0	1600	1600	0	631	631	171		460	969	
25/01/05B	0.0	4.7	7.8	19.6	116	30	63	0	0	6.0	0	0	1600	1600	0	1013	1013	304	475	709	587	
3/2/2005	136.1	0.2	8.0	42.4	4649	33	100	0	0	136.1	2600	0	1600	1600	0	1600	4200	1402	1402	2798	0	
9/2/2005	176.7	1.7	8.0	30.4	941	32	100	0	0	176.7	0	0	1600	1600	0	1600	1600	511	511	1089	0	
10/2/2005	7.2	1.7	3.0	4.2	46	23	32	0	0	7.2	0	0	1600	1600	0	520	520	30	30	489	1080	
25/2/2005	26.0	1.0	2.5	10.3	122	27	66	0	0	26.0	0	0	1600	1600	0	1057	1057	72	72	985	543	
8/3/2005	261.3	0.4	4.3	12.2	1040	28	100	0	0	261.3	0	0	1600	1600	0	1600	1600	447	447	1153	0	

Appendix C Case Study Calculations

Table C.5 continued.

18/3/2005	226.0	4.7	13.8	13.8	152	29	79	0	0	226.0	0	0	1600	1600	0	1262	1262	360	360	903	338
15/4/2005	128.3	0.4	2.5	15.2	629	29	100	0	0	128.3	0	0	1600	1600	0	1600	1600	116	116	1484	0
28/4/2005	282.3	2.4	4.3	12.6	70	28	43	0	0	282.3	0	0	1600	1600	0	693	693	195	195	498	907
13/05/2005A	363.5	9.5	9.3	2.9	12	22	30	12.5	6000	363.5	0	0	1600	6000	0	1800	1800	392		1408	4200
13/05/2005B	0.0	4.1	5.7	3.8	25	23	30	12.4	6000	0.0	0	0	1600	6000	0	1800	1800	412	804	1388	4200
20/5/2005	175.3	1.0	7.8	29.8	831	32	100	0	0	175.3	0	0	1600	1600	0	1600	1600	509	509	1091	0
15/06/2005A	55.4	3.6	6.8	8.1	60	26	39	0	0	55.4	0	0	1600	1600	0	618	618	162		456	982
15/06/2005B	0.0	2.8	9.7	23.3	317	31	100	6.6	6000	0.0	0	0	982	6000	0	6000	6000	1847		4153	0
15/06/2005C	0.0	6.4	7.8	2.6	18	21	30	5	6000	0.0	0	0	0	6000	0	1800	1800	382	2391	1418	4200
21/06/2005A	91.2	12.9	21.2	7.3	43	26	32	0	0	91.2	0	0	1600	1600	0	504	504	130		374	1096
21/06/2005B	0.0	3.8	4.8	6.9	13	25	30	19.8	6000	0.0	0	0	1096	6000	0	1800	1800	458		1342	4200
21/06/2005C	0.0	4.6	7.0	3.8	15	23	30	7.8	6000	0.0	0	0	1600	6000	0	1800	1800	412	1000	1388	4200
28/6/2005A	198.2	2.5	3.5	4.6	17	24	30	0	0	198.2	0	0	1600	1600	0	480	480	114		366	1120
28/6/2005B	0.0	11.6	9.1	3.6	7	23	30	26.4	6000	0.0	0	0	1120	6000	0	1800	1800	407		1393	4200
28/6/2005C	0.0	3.3	3.4	5.5	22	24	30	14.8	6000	0.0	0	0	1600	6000	0	1800	1800	441	962	1359	4200
29/6/2005A	2.0	2.6	3.1	4.9	21	24	30	0	0	2.0	0	0	1600	1600	0	480	480	115		365	1120
29/6/2005B	0.0	3.6	21.3	11.9	517	28	100	4	6000	0.0	0	0	1120	6000	0	6000	6000	1671		4329	0
29/6/2005C	0.0	3.4	3.4	2.8	11	22	30	7.9	6000	0.0	0	0	0	6000	0	1800	1800	388	2174	1412	4200
11/9/2005	207.3	1.2	3.8	7.2	98	26	55	0	0	207.3	0	0	1600	1600	0	887	887	227	227	660	713
16/9/2005	117.9	2.5	9.3	45.1	894	34	100	0	0	117.9	0	0	1600	1600	0	1600	1600	538	538	1062	0
27/9/2005	245.3	0.6	2.3	4.7	74	24	45	0	0	245.3	0	0	1600	1600	0	715	715	43	43	672	886
30/9/2005	65.2	1.0	2.3	10.7	134	27	71	0	0	65.2	0	0	1600	1600	0	1135	1135	78	78	1058	465
14/10/2005	313.4	1.8	20.8	36.1	2117	33	100	0	0	313.4	2600	0	1600	1600	0	1600	4200	1373	1373	2827	0
17/10/2005A	34.8	5.3	9.4	5.9	40	25	30	0	0	34.8	0	0	1600	1600	0	480	480	119		361	1120
17/10/2005B	0.0	7.4	14.6	8.7	75	26	45	14.7	6000	0.0	0	0	1120	6000	0	2725	2725	721		2004	3275
17/10/2005C	0.0	3.3	5.3	5.0	36	24	30	8.8	6000	0.0	0	0	1600	6000	0	1800	1800	433	1273	1367	4200
21/10/2005A	79.1	7.0	16.0	8.0	73	26	44		0	79.1	0	0	1600	1600	0	710	710	186		524	890
21/10/2005B	0.0	1.9	15.8	30.2	1328	32	100	0	0	6.0	2600	0	1600	1600	0	1600	4200	1340	1526	2860	0

Appendix C Case Study Calculations

Table C.5 continued.

25/10/2005	69.3	2.4	20.3	48.2	2061	34	100	0	69.3	2079	0	1600	1600	0	1600	3679	1248	1248	2431	0
26/10/2005	25.8	0.7	8.0	29.8	2479	32	100	0	25.8	774	0	1600	1600	0	1600	2374	756	756	1618	0
27/10/2005	3.9	1.2	5.0	11.9	232	28	100	0	3.9	0	0	1600	1600	0	1600	1600	446	446	1154	0
6/11/2005	84.6	7.7	64.3	72.1	2116	36	100	0	84.6	2600	0	1600	1600	0	1600	4200	1499	1499	2701	0
11/11/2005	98.1	2.1	6.3	11.2	114	28	62	0	98.1	0	0	1600	1600	0	999	999	276	276	723	601
16/11/2005	100.0	2.1	25.3	38.9	2572	33	100	0	100.0	2600	0	1600	1600	0	1600	4200	1386	1386	2814	0
2/12/2005A	119.3	3.5	7.5	5.1	63	24	40	0	119.3	0	0	1600	1600	0	642	642	155		487	958
2/12/2005B	0.0	2.2	8.5	13.1	295	28	100	0	6.0	0	0	1600	1600	0	1600	1600	452	607	1148	0
17/12/2005	60.4	1.8	12.0	26.3	968	31	100	0	60.4	0	0	1600	1600	0	1600	1600	501	501	1099	0
4/1/2006	135.4	2.1	7.0	15.7	208	29	100	0	135.4	0	0	1600	1600	0	1600	1600	465	465	1135	0
5/1/2006A	5.5	1.0	20.2	60.4	7210	35	100	0	5.5	2600	0	1600	1600	0	1600	4200	1466		2734	0
5/1/2006B	0.0	5.9	13.6	7.3	69	26	43	3.1	6000	0.0	0	0	6000	0	2561	2561	659	2126	1902	3439
6/1/2006	17.3	1.6	5.5	9.6	153	27	79	0	17.3	0	0	1600	1600	0	1270	1270	341	341	928	330
9/1/2006	9.1	3.5	19.0	30.7	764	32	100	0	9.1	0	0	1600	1600	0	1600	1600	512	512	1088	0